Cellular immunity in Tanzanian volunteers upon malaria vaccination and controlled human malaria infection

Inauguraldissertation
zur
Erlangung der Würde eines Doktors der Philosophie

vorgelegt der
Philosophisch-Naturwissenschaftlichen Fakultät
der Universität Basel

von

Tobias Rutishauser

von
Langrickenbach TG

Basel, 2018

Genehmigt von der Philosophisch-Naturwissenschaftlichen Fakultät

auf Antrag von

Prof. Dr. Marcel Tanner, Prof. Dr. Claudia Daubenberger, Prof. Dr. François Spertini

Basel, 26. Juni 2018

Prof. Dr. Martin Spiess

Dekan

Summary

Despite considerable efforts and achievements, malaria continues to be one of the most devastating infectious diseases in the world. Clearly, an effective vaccine against malaria would help to reduce disease burden and support elimination programs. This year, the malaria vaccine RTS,S/AS01 will be rolled out in three countries of sub-Saharan Africa, representing a milestone in malaria vaccine development. However, RTS,S induced only partial and short-lived protection when assessed in large-scale clinical trials in infants and children of sub-Saharan Africa, highlighting the need for more effective vaccines. Conversely, it has been known for a long time that sterile protection against malaria can be achieved by administration of large amounts of radiation-attenuated sporozoites. The Sanaria PfSPZ Vaccine consists of radiation-attenuated, aseptic, purified, cryopreserved *Plasmodium falciparum* sporozoites (PfSPZ). This vaccination approach has induced up to 100% protection during clinical trials in malaria-naïve, US volunteers. At the same time, development of the PfSPZ Vaccine also enabled the use of non-attenuated cryopreserved PfSPZ in controlled human malaria infection (CHMI) to assess vaccine efficacy. Together, these tools are not only promising for vaccine development, but also offer a unique opportunity to study the human immune response to *P. falciparum* in a highly controlled setting in sub-Saharan Africans, the population most strongly affected by malaria.

Thus, the aims of this thesis were: First, to study the cellular immune response towards RTS,S, the most advanced subunit malaria vaccine in a paediatric phase III clinical trial in Tanzania. Second, to assess safety, immunogenicity and protective efficacy of the PfSPZ Vaccine, a live-attenuated malaria vaccine, in a phase I clinical trial in adult Tanzanians. Third, to develop an analysis pipeline that allows for unbiased detection of *ex vivo* phenotypic alterations of T-cell subsets measured by multicolour flow cytometry. Fourth, to analyse the immune response of unconventional T cells towards PfSPZ vaccination and CHMI in Tanzanian volunteers in a comprehensive and unbiased approach. These aims led to the generation of data that are presented in the following four manuscripts:

Manuscript 1: RTS,S/AS01E Malaria Vaccine Induces Memory and Polyfunctional T Cell Responses in a Pediatric African Phase III Trial

RTS,S is a subunit vaccine based on the main PfSPZ surface antigen, the circumsporozoite protein (CSP). While RTS,S induces a certain protection against clinical malaria across different populations and age groups, this protection is only partial and short-lived. The reasons for this weak immune response are largely unknown, but clearly, appropriate T-cell help is important for long-lived humoral immunity. Here, we analysed T-cell polyfunctionality and their memory phenotype induced by RTS,S vaccination in children living in sub-Saharan Africa. We found CSP-specific T cells to be more polyfunctional than previously appreciated, expressing not only IFN-γ, but also IL-4, IL-21 and CD40 ligand, implying a possible role in B-cell help. CSP-specific T cells were also found in the memory compartment, which might be important for long-lasting protection. While this study was not designed to assess the effect of those phenotypes on clinical outcome, it highlights the complexity of the cellular immune response towards RTS,S.

Manuscript 2: Safety, immunogenicity and protective efficacy against controlled human malaria infection of PfSPZ Vaccine in Tanzanian adults

In this study, we assessed the safety of the PfSPZ Vaccine and at the same time monitored vaccine efficacy by direct venous inoculation of PfSPZ Challenge for the first time in Africa. The dosage of PfSPZ vaccination was similar to the one that led to 100% protection in malaria-naïve, US volunteers. We found PfSPZ Vaccine and Challenge to be safe and well tolerated. Vaccine efficacy, however, was considerably lower than in US volunteers, at 5% in the low-dose group and 20% in the high-dose group. This effect can only be partially explained by the rigorous mode of CHMI applied in this study for two reasons: first, immunogenicity was also lower than in US volunteers, and second, a cohort in Mali showed similar results. The way forward might be administration of higher doses of PfSPZ, but these findings also highlight our incomplete understanding of the human immune response towards *P. falciparum* and the need for further research.

Manuscript 3: Modulation of bacterial metabolism by the microenvironment controls MAIT cell stimulation

Human mucosal-associated invariant T (MAIT) cells are an abundant T-cell subset recognising microbial metabolites presented by the MHC class I-related molecule MR1. The influence of the gut microenvironment on the generation of MAIT-cell antigens has not been well characterised. In this manuscript, we show that altered bacterial growth conditions lead to differential accumulation of MAIT-cell antigens, inducing distinct T-cell activation patterns. These findings might also be relevant during malaria, as more and more studies show the bidirectional interactions between the composition of the human gut microbiome and malaria infection.

Of note, in this manuscript we developed an unbiased approach to identify phenotypic alterations of T-cell subsets using high dimensional multicolour flow cytometry using dimensionality reduction and clustering algorithms. This analysis pipeline is highly versatile and was used in *Manuscript 4* to detect *ex vivo* phenotypic alterations in unconventional T cells.

Manuscript 4: Unbiased analysis of unconventional T cells in Tanzanian volunteers reveals a personalised Vδ1 T-cell response upon controlled human malaria infection

Here, we used PBMC derived from the clinical trial described in *Manuscript 2* to examine the role of unconventional T cells during PfSPZ vaccination and CHMI. While we could not detect major changes in frequency and surface marker expression upon vaccination, upon CHMI all examined γδ T-cell subsets as well as MAIT cells were expanded and activated in volunteers who developed asexual blood-stage parasitaemia. Remarkably, the Vδ1 and Vδx subsets showed a particularly strongly activated phenotype that was characterised by an expansion of $CD38^{+}PD\text{-}1^{+}$ co-expressing cells. Interestingly, we isolated Vδ1 T-cell clones and showed that a group of clones expressed a functional TCR Vγ10 chain, a gene that so far has been thought to be non-functional in humans. Intriguingly, a data base search revealed that this functional TCRγ chain is unique to Africans and people of recent African descent, and is present at a frequency of 27% in the Tanzanian trial population. Together, our results indicate a highly personalised T-cell response during controlled human malaria infections that encompasses T-cell subsets that so far were not well characterised or even unknown.

Acknowledgements

During the course of my PhD I had the pleasure to work with and learn from a wide range of people without whom this work would not have been possible. I would like to express my gratitude to the following people:

First, my supervisor Claudia Daubenberger, for her constant support during my PhD and for giving me a lot of freedom to explore our interesting sample set.

Marcel Tanner for his support and for agreeing to be my faculty representative, for which I am very grateful.

François Spertini, for taking the time to evaluate my PhD thesis and defence.

Gennaro De Libero for hosting me in his lab during the majority of analyses that I performed. A special thank goes to Marco, from whom I learned a lot during this time. Furthermore, I would like to especially thank Daniela, for her great support, and Mathias and Martin for the constructive scientific discussion. I am also grateful to Cristina, for not giving up during the cloning of the TCR chains.

Stephen Hoffman and the whole Sanaria team without whom none of this work would have been possible.

The IHI team in Bagamoyo for welcoming me to work there. I am especially grateful to the BRTC team, including Jackson, Saidi, Grace and Solomoni for their help and the good times that we shared.

Pascal Mäser, Sergio Wittlin, Christian Scheurer and the Parasite Chemotherapy team for the constant supply of blood-stage parasites and great collaboration.

The Clinical Immunology team, especially Mama D., Dada Anneth, Max, Tobi, Damien and JP for their support and scientific interaction in Bagamoyo and Basel. A very special thank you goes to Isa and Julian for the great time we shared in Bagamoyo and continue to share in Basel.

I am especially grateful to my good friends in Zürich and Basel: Dani, Marc, Beni, Dave and Andi.

A huge thank you goes to my parents and family for their constant support during all of my education.

Table of contents

List of abbreviations

α-gal	Galα1-3Galβ1-4GlcNAc-R
BCG	Bacillus Calmette-Guérin
β2m	Beta-2-microglobulin
BTNL	Butyrophilin-like
BTN3A1	Butyrophilin 3A1
CD40L	CD40 ligand
CDR3	Complementarity-determining region 3
CHMI	Controlled human malaria infection
CM	Central memory
CMV	Cytomegalovirus
CSP	Circumsporozoite protein
CVac	Chemoprophylaxis vaccination
DVI	Direct venous inoculation
EBV	Epstein-Barr virus
EM	Effector memory
EMA	European Medicines Agency
EPCR	Endothelial protein C receptor
EPI	Expanded Programme on Immunization
5-A-RU	5-amino-6-D-ribitylaminouracil
5-OE-RU	5-(2-oxoethylideneamino)-6-D-ribitylaminouracil
5-OP-RU	5-(2-oxopropylideneamino)-6-D-ribitylaminouracil
GAP	Genetically attenuated parasite
GPI	Glycosylphosphatidylinositol
G6PD	Glucose-6-phosphate dehydrogenase
HBsAg	Hepatitis B surface antigen
HIV	Human immunodeficiency virus
HMBPP	(*E*)-4-Hydroxy-3-methyl-but-2-enyl pyrophosphate
ICAM-1	Intercellular adhesion molecule 1
ID	Intradermal / intradermally
IFN-γ	Interferon gamma
IL	Interleukin
IM	Intramuscular / intramuscularly

IPP	Isopentenyl pyrophosphate
LAG-3	Lymphocyte-activation gene 3
MAIT cell	Mucosal-associated invariant T cell
MHC	Major histocompatibility complex
MICA	MHC class I polypeptide-related sequence A
Mo-DC	Monocyte-derived dendritic cell
MPL	3-O-desacyl-4′-monophosphoryl lipid A
MR1	Major histocompatibility complex class I-related
NK cell	Natural killer cell
NKT cell	Natural killer T cell
P. falciparum	*Plasmodium falciparum*
PAMP	Pathogen-associated molecular pattern
PBMC	Peripheral blood mononuclear cell
PCR	Polymerase chain reaction
PD-1	Programmed cell death protein 1
PE	Phycoerythrin
PfRBC	*Plasmodium falciparum*-infected red blood cell
PfSPZ	*Plasmodium falciparum* sporozoite
PRR	Pattern recognition receptor
PV	Parasitophorous vacuole
RNA	Ribonucleic acid
TCR	T-cell receptor
T_{FH} cell	Follicular helper T cell
TLR	Toll-like receptor
TNF	Tumour necrosis factor
uRBC	Uninfected red blood cell
US	United States
WHO	World Health Organization

Chapter 1

Introduction

1.1. Malaria biology, disease burden and pathogenesis

1.1.1. Disease burden

Malaria continues to be one of the most devastating infectious diseases globally. According to the WHO World Malaria Report, in 2016 there were 216 million cases of malaria leading to an estimated 445'000 deaths [1]. Worryingly, earlier trends towards lower malaria incidence and number of deaths are currently stalling and even reverting. Sub-Saharan Africa is especially strongly affected by malaria – about 90% of both cases and deaths occur in this region. The most vulnerable population are children under the age of 5 years, accounting for 70% of all malaria deaths [1].

1.1.2. Malaria transmission and life cycle

1.1.2.1. Pre-erythrocytic stage

Malaria is caused by parasites of the *Plasmodium* genus and is transmitted to humans through bites of infected *Anopheles* mosquitoes [2]. The huge majority of malaria cases and deaths in humans are caused by *P. falciparum*, a species that is particularly prevalent in sub-Saharan Africa. During a blood meal, infected mosquitoes inject a small number of sporozoites into the skin of the human host (see Figure 1) [3], [4]. Most sporozoites will leave the skin through blood or lymph, but recent evidence from mouse models suggests that a fraction of sporozoites can remain in the skin for several days [5]. Sporozoites can move by gliding motility and a part of the injected sporozoites will invade a blood vessel, enter the blood stream and reach the liver. Interaction between sporozoites and human hepatocytes involves circumsporozoite protein (CSP), the main surface protein of sporozoites [6]. The parasites uses cell traversal to escape from the liver sinusoids into the liver parenchyma, where they can traverse several hepatocytes before setting up residence inside a parasitophorous vacuole (PV) within a hepatocyte [7]. There, the sporozoite develops into a spherical liver stage that grows extensively and ultimately gives rise to thousands of merozoites that will then enter the blood stream. For this purpose, the parasite induces cell death of the hepatocyte and manipulates the hepatocyte membrane, leading to formation of parasite-filled vesicles (merosomes) containing hundreds of merozoites [8]. The merosomes are remarkably stable and help the parasite to distribute in the human body until finally the merozoites are released and proceed to invade erythrocytes [9]. The duration of liver-stage development is variable between few days to several weeks in different *Plasmodium* species, but for *P. falciparum*, it takes about 6 days to complete [10].

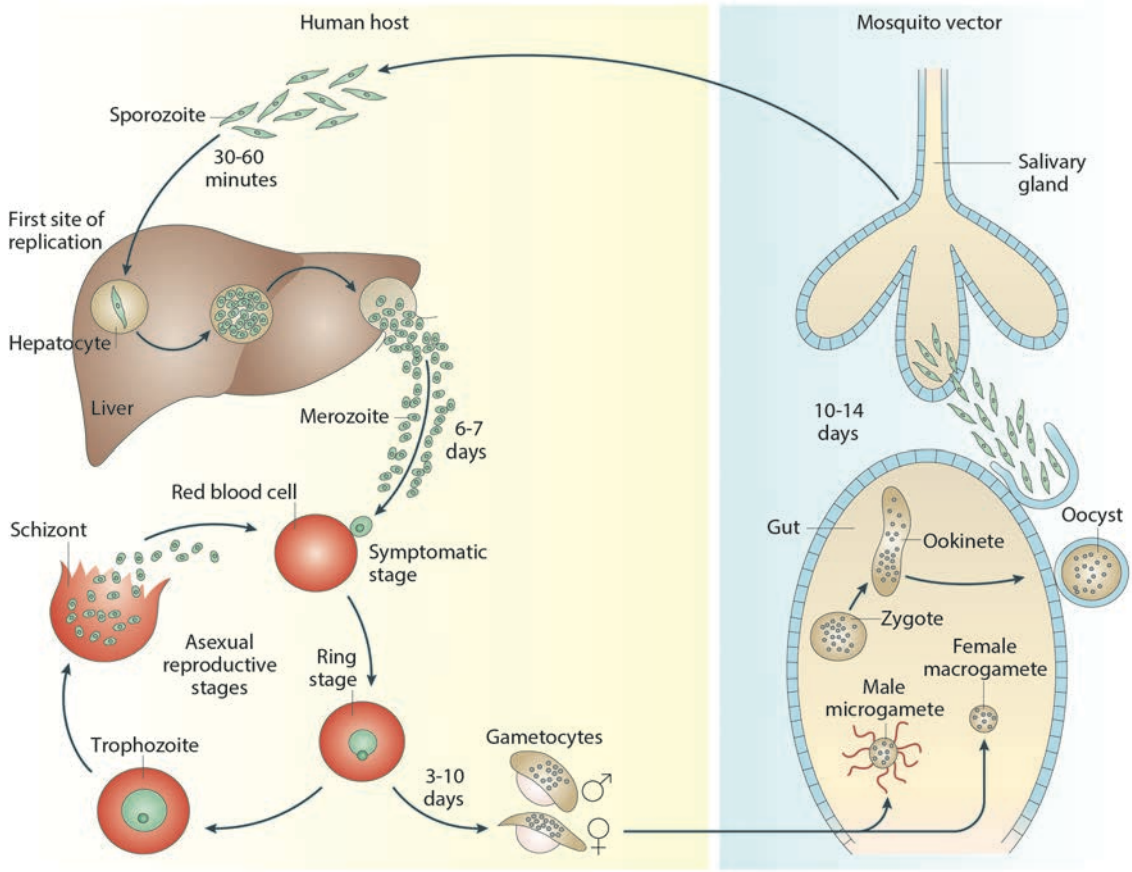

Figure 1 *Plasmodium* life cycle in human and mosquito [11].

1.1.2.2. Blood stage

The erythrocytic stage of development is characterized by repeated cycles of erythrocyte invasion, parasite replication, egress and invasion of other erythrocytes. Invasion of erythrocytes by merozoites is facilitated through specific interaction between parasite proteins and receptors on the erythrocyte surface [12]. Inside an erythrocyte, the parasite sets up residence inside a PV and develops into the ring-stage, while it starts to actively re-model the host cell. It feeds on haemoglobin as well as nutrients from blood plasma and develops into a trophozoite [13]. The trophozoite stage is characterized by extensive parasite growth, sustained by ingestion of large amounts of haemoglobin, leading to accumulation of toxic haem groups, which the parasite converts into the crystalline haemozoin form and stores in its food vacuole [14]. Then, during the schizont stage, the parasite undergoes a few rounds of nuclear divisions, leading to generation of 16-32 merozoites [13]. Finally, the merozoites escape through lysis of the erythrocyte and PV membranes in a protease-dependent process [15]. The free merozoites can then infect other erythrocytes, completing the cyclic erythrocyte development.

1.1.2.3. Sexual stage and mosquito stage

Successful transmission of *Plasmodium* parasites from the human host to a mosquito involves formation of a sexual parasite stage [16]. This involves the formation of male and female gametocytes, a process that only a small fraction of blood-stage parasites undergo. During gametogenesis, the parasite develops through five morphological stages, of which only the last one is detectable in peripheral blood. The other stages occur within erythroid precursor cells in the bone marrow, enabling early gametocytes to avoid splenic clearance [17], [18].

When gametocytes are taken up by a mosquito during a blood meal, they sense a change in temperature, pH and chemical environment, which induces their development into gametes within the mosquito mid-gut [19]. There, male microgametes and female macrogametes fuse to form a short diploid stage, the zygote, that then develops into an ookinete. In the ookinete stage, meiotic recombination occurs, the parasite traverses the epithelial cell layer in the mosquito mid-gut and transforms into an oocyst [20]. Ultimately, the oocyst ruptures, releasing sporozoites into the haemocoel of the mosquito from where they migrate to the salivary glands and are ready to be injected into the human host [21].

1.1.3. Malaria pathogenesis

Malaria is characterised by cyclic episodes of fever that are caused by synchronised rupture of infected erythrocytes, releasing large amounts of parasites and parasite-derived molecules that induce a strong pro-inflammatory response. Most symptoms are relatively unspecific and include chills, headache, nausea, diarrhoea and anaemia [11]. First symptoms of malaria appear 7-10 days after infection, indicating that pre-erythrocytic stages are clinically silent, while most clinical symptoms and complications occur only upon blood-stage parasitaemia [11]. A certain degree of anaemia is induced by rupture and destruction of infected erythrocytes by blood-stage parasites. However, it has become clear that the majority of cleared erythrocytes are uninfected, an effect that is explained by the reduced half-life of all erythrocytes and an increase of splenic clearance [22], [23].

Plasmodium parasites extensively remodel the erythrocyte and its plasma membrane by expressing a range of parasite-encoded proteins on the erythrocyte surface [24]. This leads to increased rigidity of the membrane, binding of infected erythrocytes to endothelial cells as well as formation of aggregates of infected and uninfected erythrocytes (rosetting), which helps the parasite to avoid splenic clearance [25]. Adherence of erythrocytes to the microvasculature leads to obstruction of blood flow, endothelial injury and increased inflammation [26]. When

this sequestration takes place in the brain or placenta, the severe complications of cerebral and placental malaria can occur [27].

In malaria-endemic areas, the most vulnerable population are children under the age of 5 years, including foetuses. Older children and adults usually develop a certain level of protective immunity induced by repeated exposure to the parasite, leading to decreasing disease severity with age [11].

1.2. Unconventional T cells

1.2.1. Overview

The majority of human T cells are reactive to peptides presented by major histocompatibility complex (MHC) molecules. In terms of numbers, the major subsets are $CD4^+$ T cells restricted to MHC class II, and $CD8^+$ T cells restricted to MHC class I. MHC molecules are highly polymorphic and can present peptides derived from a huge range of endogenous and foreign proteins that are recognised by an equally large repertoire of T-cell receptors (TCRs) [28]. This huge diversity of TCRs means that each naïve antigen-specific T cell is very rare and cannot induce a strong immune response. Protective immunity conferred by these adaptive T cells thus requires expansion of rare, antigen-specific T cells and formation of immunological memory.

In contrast, unconventional T cells are generally not restricted to peptide-MHC complexes (see Figure 2). Instead, the major unconventional T-cell subsets are reactive to CD1 (natural killer T cells), MR1 (MAIT cells) or BTN3A1 (Vγ9Vδ2 T cells) [28]. Furthermore, these subsets tend to have a narrow TCR repertoire, localise to tissues rather than circulate in peripheral blood, and have the potential to respond rapidly to antigenic challenge [28]. These characteristics are referred to as innate-like, a fitting term for some unconventional T cells such as NKT cells, MAIT cells, or Vγ9Vδ2 T cells. However, some unconventional T cells show clonal selection upon antigen encounter, have strong proliferative capacity and altered phenotypic and homing properties after antigen encounter, reminiscent of adaptive T cells [29], [30]. Thus, while some unconventional T-cell subsets show innate-like behaviour, there are others that clearly do not fit this paradigm.

In this introduction, I will focus on γδ T cells and MAIT cells due to their abundance in humans and known, but largely unexplored role in human malaria infection (see also section 1.3.3).

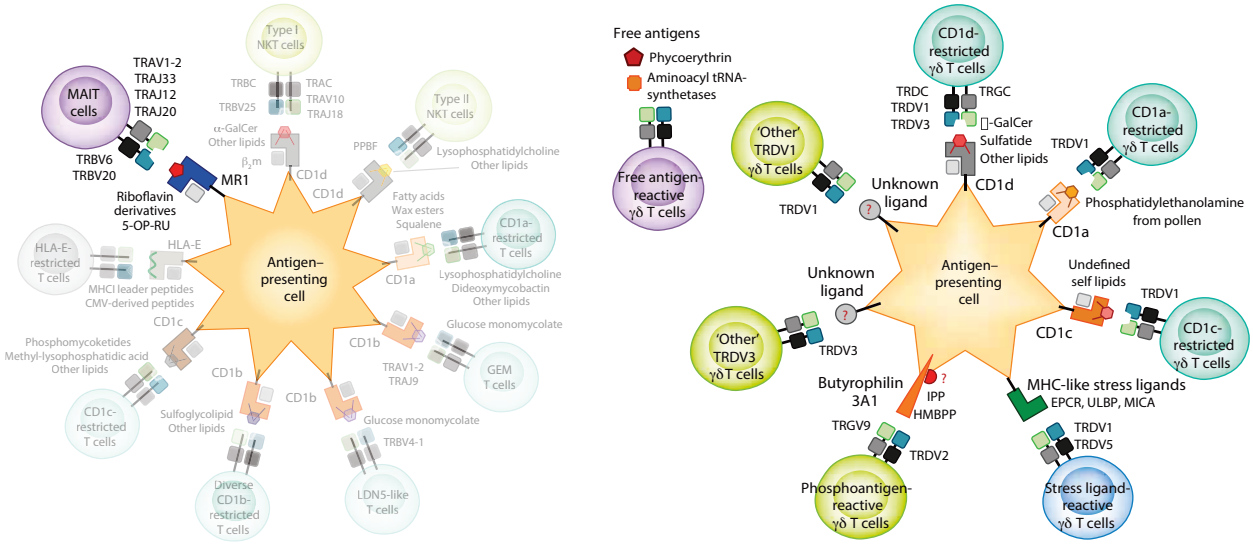

Figure 2 Overview of human unconventional TCRαβ (left) and TCRγδ T cells (right). The T cells of focus in this thesis are highlighted: MAIT cells (left) and γδ T cells (adapted from [28]).

1.2.2. γδ T cells

1.2.2.1. Overview

The TCRγ chain genes were discovered and cloned in the 1980s, which was followed by the chance discovery of the TCRδ locus during examination of the TCRα locus, within which the TCRδ genes are located [31], [32]. γδ T cells have several specialised roles that indicate a non-redundant role of this subset compared to conventional αβ T cells. For example, they develop very early in ontogeny of many different species [33]. Moreover, the length of the complementarity-determining region 3 (CDR3) of the γδ TCR is much less constrained than the one of the αβ TCR, and especially the CDR3 of the TCRδ chain can be significantly longer. This is reminiscent of the CDR3-length distribution of antibodies and it has been implied that γδ T cells recognise antigen in an antibody-like manner [34]. As an example, human γδ T cells can recognise the algae protein phycoerythrin (PE), a known B-cell antigen, independently of an antigen-presenting molecule [35].

A specialised role of γδ T cells is highlighted by the fact that they are enriched in epithelia, where they can fulfil specific roles such as protection against parasitic disease [36]. Some murine subsets of γδ T cells home directly to tissues as has been demonstrated for epidermis, dermis, intestine, lungs or uterus. These tissue-resident γδ T cells often have a limited, tissue-specific TCR diversity and are thought to recognise either self-ligands or pathogen-derived ligands that are abundant in these anatomical sites [28], [37], [38]. A prototypical example of

these subsets are dendritic epidermal γδ T cells that home to the epidermis, express an almost monoclonal TCR repertoire and have been described in several mammalian species, but notably not in humans [39]. Recently, these intra-epithelial subsets of γδ T cells have been shown to be selected by specific butyrophilin-like (BTNL) molecules that are expressed in a tissue-specific manner [40]. Thus, some γδ T-cell subsets show a restricted TCR repertoire, home to defined sites and recognise potentially conserved antigens. This is inconsistent with a conventional adaptive behaviour, involving repeated sampling of antigen in secondary lymphoid organs, followed by expansion of rare, antigen-specific T-cell clones.

On the other hand, γδ T cells have been reported to have adaptive-like behaviour, one example of which are the PE-specific cells mentioned above that upon activation upregulate CD44 and downregulate CD62L, reminiscent of a priming response of αβ T cells [35]. However, the limited clonal expansion and different kinetics upon vaccination with PE highlight marked difference to a canonical response of a naïve conventional T cell [30]. Clearly, γδ T-cell biology cannot be fully explained with the dichotomy of innate versus adaptive immunity.

1.2.2.2. Vγ9Vδ2 T cells

In humans, the most abundant γδ T-cell subset in peripheral blood expresses the combination of Vγ9 and Vδ2 TCR chains. These cells recognise small phosphorylated compounds such as isopentenyl pyrophosphate (IPP) [41], often termed phosphoantigens. IPP is an important intermediate in isoprenoid synthesis, a ubiquitous biochemical pathway present in prokaryotic as well as eukaryotic cells, explaining the wide pattern of reactivity of Vγ9Vδ2 T cells [42]. The IPP-related compound (*E*)-4-Hydroxy-3-methyl-but-2-enyl pyrophosphate (HMBPP) is much more strongly stimulatory than IPP and is derived from a synthetic pathway that is present in eubacteria as well as apicomplexan parasites, but is absent in most eukaryotes [43]. In addition, Vγ9Vδ2 T cells can recognise certain tumour cells in a TCR-mediated manner, possibly through the recognition of tumour-cell-derived IPP that can accumulate upon enhanced cell metabolism [44], [45]. Recent advances have revealed the central role of butyrophilin 3A1 (BTN3A1) in activation of Vγ9Vδ2 T cells. The mechanism of action is intriguingly different from antigen presentation in conventional T cells: phosphorylated compounds bind to the intracellular domain of BTN3A1, an event that is then sensed on the cell surface by the Vγ9Vδ2 TCR [46]. The exact mechanisms remain somewhat mysterious but are thought to involve conformational changes in BTN3A1 as well as recruitment of intracellular binding partners of BTN3A1 [47]. This inside-out signalling makes sense physiologically, allowing a cell to sense metabolic alterations that can occur for example during

transformation. Furthermore, in enables cells to sense pathogen-derived phosphoantigens from intracellular pathogens such as *Mycobacterium tuberculosis* [46]. Thus, the Vγ9Vδ2 TCR acts like a surrogate pattern recognition receptor (PRR) that can sense cell stress through accumulation of both endogenous or pathogen-derived phosphoantigens [48].

1.2.2.3. Non-Vγ9Vδ2 γδ T cells

γδ T cells are sometimes grouped into $V\delta2^{+}$ and $V\delta2^{neg}$ subsets [49]–[51]. However, this classification is not accurate, as a recent characterisation of $V\delta2^{+}$ T cells indicates different features of $V\gamma9^{+}V\delta2^{+}$ and $V\gamma9^{neg}V\delta2^{+}$ T cells, the latter having adaptive-like characteristics [30]. More precise is a characterisation into Vγ9Vδ2 T cells, which are largely innate-like and responsive to phosphoantigens in the context of BTN3A1, and the remainder of γδ T cells that have more adaptive-like features [30].

The majority of this latter group expresses the Vδ1 TCRδ chain – a subset that at birth and in some epithelial tissues is the largest subset of all γδ T cells [52], [53]. These cells have traditionally been considered to act in an innate-like fashion, because of their potent cytokine response, abundant expression of NK receptors and wide range of responsiveness [48]. However, this view is changing as data accumulate that Vδ1 T cells show clonal expansion and a maturation of their phenotype upon antigenic challenge such as cytomegalovirus (CMV) infection [29], [54]. Importantly, these expanded clonotypes can persist over several years, contributing to long-term immune protection [48]. This clonal expansion is accompanied by changes in phenotype and expression of effector molecules. The TCR-diverse, 'naïve' Vδ1 T-cell subset expresses high levels of CD27, which is accompanied by expression of CD28, CD62L and CCR7, markers that were downregulated on clonally expanded Vδ1 T cells – closely resembling phenotypic behaviour of $CD8^{+}$ conventional T cells [29]. Interestingly, this $CD27^{lo}$ subset retained responsiveness to TCR-mediated stimulation, but was not responsive towards IL-12 and IL-18, further indicating an adaptive-like character and setting them apart from Vγ9Vδ2 T cells and MAIT cells [29]. While CMV was shown to be a major driver of clonal expansion, it is not the only stimulus to do so, as also some CMV-negative donors showed expanded Vδ1 clonotypes [48]. Of note, CMV infection did not induce clonal selection within the Vδ1 T-cell subset of all donors, further adding evidence for a personalised, and not innate-like response. This fact could be explained by the lack of CMV-specific Vδ1 clonotypes in some of these donors, or by a compensatory immune response from other subsets [48].

Only few γδ TCR ligands have been identified, but one example that could prove to be characteristic of the non-Vγ9Vδ2 γδ T-cell response is endothelial protein C receptor (EPCR)

[55]. Intriguingly, the corresponding T-cell clone recognised CMV-infected fibroblasts in an EPCR-dependent manner, but EPCR was not upregulated upon infection. Rather, the T cell relied on other, TCR-extrinsic signals, such as interaction with ICAM-1, which is upregulated upon CMV infection [55]. Thus, for full activation, non-Vγ9Vδ2 γδ T cells might rely on integration of several signals, both TCR-mediated and TCR-extrinsic [48]. Consistent with this, in addition to EPCR, other self-encoded ligands have been suggested to be recognised by γδ TCRs [56].

1.2.3. MAIT cells

MAIT cells are characterised by expression of the TCRα chain rearrangement Vα7.2-Jα33 paired with a biased TCRβ repertoire and high surface expression of CD161 [57]–[59]. They are restricted to the MHC class I-related molecule MR1 and depend on the presence of the commensal microbiota for development and activation [60]. The canonical MAIT-cell antigens presented by MR1 were discovered to be vitamin B metabolites derived from microbial biosynthesis pathways [61]. Further characterisation revealed the molecular nature of these antigens – they are derived from 5-amino-6-D-ribitylaminouracil (5-A-RU), an intermediate of the riboflavin biosynthesis pathway present in many microbes. 5-A-RU itself is not a strong antigen, but depends on non-enzymatic condensation with the small molecules glyoxal or methylglyoxal to generate the potent antigens 5-(2-oxoethylideneamino)-6-D-ribitylaminouracil (5-OE-RU) and 5-(2-oxopropylideneamino)-6-D-ribitylaminouracil (5-OP-RU), respectively [62]. These adducts are instable, but can get trapped and stabilised in the antigen-binding pocket of MR1 by formation of a Schiff base with lysine 43 [62]. Recent studies showed that the repertoire of MR1 ligands is larger than expected and could include drugs [63], ligands derived from riboflavin-auxotroph bacteria [64], and ligands derived from mammalian cells [65].

Consistent with recognition of these antigens, MAIT cells are activated by cells infected with bacteria or yeast that are able to synthesize riboflavin, but not by uninfected or virus-infected cells [66]. Thus, MAIT cells contribute to antimicrobial immunity by targeting cells that sense microbial ligands intracellularly [66], an effect reminiscent of Vγ9Vδ2 T cells. Notably, MAIT cells can also be potently activated by IL-12 and IL-18 in a TCR-independent manner, an effect that is conserved across many CD161-expressing T cells [67], [68].

In summary, MAIT cells fit the paradigm of innate-like T cells well in many aspects, having a biased TCR repertoire, fast effector response, shared and conserved antigen specificity and high responsiveness to cytokines.

1.3. The human immune response to *P. falciparum*

1.3.1. Immune response towards the pre-erythrocytic stage

1.3.1.1. Immune response to natural infection

The pre-erythrocytic stage induces only a minimal immune response and therefore, no per-erythrocytic immunity is achieved by natural infection, even after repeated exposure [69]. One reason for this is the low number of sporozoites injected into the host and the short time they spend in the circulation. Furthermore, pre-erythrocytic stages of *Plasmodium* spp. reside mainly in the skin and liver, compartments that are known to be immunomodulatory and do not induce strong immune responses [70]. Data from mouse models also indicate that parasites actively down-modulate the immune response by inducing a regulatory-T-cell response in the skin and suppressing Kupffer cell function in the liver [71], [72]. More recent evidence suggests that hepatocytes can sense *Plasmodium* RNA through a cytoplasmic RNA sensor, leading to a partially protective immune response through release of type I interferons [73].

1.3.1.2. Immune response to high-dose sporozoite administration

In stark contrast to the almost undetectable immune response upon natural infection, pre-erythrocytic immunity can be achieved by administration of attenuated sporozoites. The immunodominant sporozoite antigen is CSP, and antibodies against this protein are readily induced upon exposure to *Plasmodium falciparum* sporozoites (PfSPZ) [74]–[76].

Several studies have also shown a role of $CD8^+$ $TCR\alpha\beta^+$ liver-resident, sporozoite-specific T cells in protection against pre-erythrocytic malaria (see Figure 3) [77], [78]. *Plasmodium*-specific $CD8^+$ T cells can be primed in skin-draining lymph nodes and then migrate to the liver, where they recognise infected hepatocytes [79]. As sporozoites do not infect dendritic cells (DCs), the priming of $CD8^+$ T cells requires cross-presentation of sporozoite-derived antigens. Furthermore, hepatocytes need to present antigen on MHC class I molecules, and this necessitates access of antigen to the cytosol, either upon cell traversal of sporozoites or through release of antigen from the hepatocyte PV [80]. This pathway of antigen presentation might account for the immunodominance of CSP, as sporozoites constantly shed this protein, for example during cell traversal of hepatocytes [81]. The effector functions that leads to the protective effect of $CD8^+$ T cells in the liver have not been elucidated, but probably there is a redundant role of IFN-γ, TNF, Fas ligand, perforin and possibly other effector molecules [82]. In order to reach full protection from malaria, large numbers of parasite-specific T cells are needed, as from a single infected hepatocyte huge numbers of merozoites that can be released,

and thus even the unrecognised development of a single sporozoite could spoil protection [70], [83].

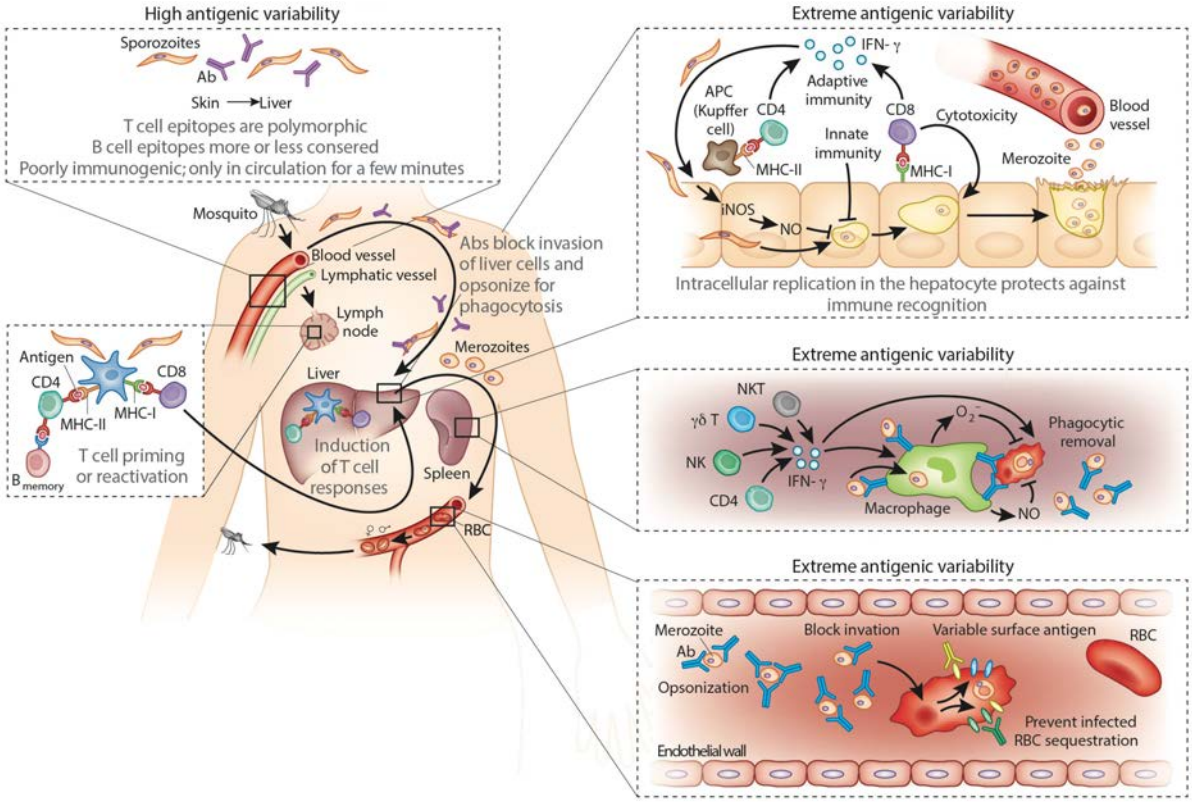

Figure 3 Human immune response to *P. falciparum* (adapted from [84]).

1.3.1.3. Immune response to RTS,S

RTS,S/AS01 (RTS,S) is a recombinant subunit vaccine consisting of recombinant *P. falciparum* CSP in combination with hepatitis B surface antigen (see section 1.4.2). This vaccine is designed to protect through induction of high titres of anti-CSP antibodies and strong T_H1 T-cell responses. Indeed, RTS,S reliably induces anti-CSP antibodies and antibody titres are associated with protection against malaria [85]. However, the majority of vaccination-induced antibodies are short-lived, with an estimated half-life of only 45 days [85]. This is a huge contrast with data from viral vaccines in US volunteers, where vaccination-induced antibodies have half-lives of typically dozens of years [86]. Different schedules of vaccination allowed also to compare the effect of a booster dose of RTS,S, which was beneficial, but antibody levels after boosting did not exceed the levels after primary vaccination [85].

In addition, vaccination induces CSP-specific $CD4^+$ and $CD8^+$ T cells, and the frequency of both subsets have been associated with protection [87], [88]. Studies of T-cell responses in

vaccinated children living in sub-Saharan Africa also indicate an expansion of CSP-specific T_H1 T cells [89]–[91]. To which extent antibodies and T cells contribute to protection and especially what determines the short half-life of antibodies, remains poorly understood and requires further investigation.

Due to the complexity of the *Plasmodium* life cycle and its interaction with the human host, the correlate of protection will probably be an equally complex one [92].

1.3.2. Immune response to the blood stage

Erythrocytes are a formidable choice of host cell by the parasite to minimise detection by the host immune system, as they do not express MHC class I, MHC class II or BTN3A1 [93], [94]. Nevertheless, over repeated natural exposure, protection from clinical malaria develops frequently [95]. In high-transmission areas, children under the age of five are susceptible to life-threatening malaria, adolescents tend to have mild malaria episodes, while adults are often largely protected from clinical malaria [95]. Thus, the human immune system cannot induce sterile protection upon natural exposure, but over frequent encounter of the parasite can develop protection from symptomatic malaria.

Two main immune processes are thought to contribute to the protective immune response against blood-stage infection. One is inflammation, particularly the protective induction of IFN-γ, and the other is the humoral immune response, leading to generation of neutralising antibodies [70].

Blood-stage parasitaemia induces a considerable release of pro-inflammatory cytokines such as IL-1β, IL-6, IL-8, IL-10, IL-12 and TNF [96]. Higher levels of these cytokines correlate with better control of parasitaemia, but also with stronger clinical symptoms, highlighting the dual role of these cytokines [97]. A part of this pro-inflammatory response is induced by recognition of pathogen-associated molecular patterns (PAMPs) by immune cells expressing the corresponding PRR. In the case of *Plasmodium*, the main PAMPs include glycosylphosphatidylinositol (GPI) anchors, haemozoin, and stimulatory nucleic acid motifs [98]. GPI anchors are recognised by macrophages mainly through TLR2, an interaction that depends on the fine-structure of the GPI anchor and leads to release of pro-inflammatory cytokines [99]. Haemozoin activates PRRs by a mechanism that is incompletely understood, but probably involves phagocytosis of haemozoin together with parasite DNA [98]. Inflammation is also enhanced by interactions of parasite-encoded proteins with host receptors, such as PfEMP1 binding to endothelial protein C receptor (EPCR) and inhibiting its protective function [100].

A central player in control of blood-stage parasitaemia are $CD4^+$ T cells, both by their ability to produce protective IFN-γ as well as provide B-cell help [93]. Early models of $CD4^+$ T-cell biology in malaria indicated a T_H1 response during early blood stage and a shift towards T_H2 in late blood stage [101]. However, recent advances have shown that reality is not so simple, but that T cells can exhibit plasticity and multifunctionality. Furthermore, T follicular helper (T_{FH}) cells might play an important role in the cross-talk with humoral immunity, with IL-21 and CD40L being main molecular players [102]. Thus, future studies should include markers for these effector molecules that could be crucial for protective immunity against malaria.

IFN-γ during early blood stage is not only produced by $CD4^+$ T cells, but also involves NK cells and γδ T cells, but the extent to which they contribute to protection has not been conclusively answered [103], [104]. Interestingly, γδ T cells bearing NK receptors, but not NK cells, have been reported to contribute significantly to IFN-γ release upon *in vitro* stimulation with *P. falciparum* parasites [105]. Thus, pro-inflammatory cytokines from various sources are important mediators in a protective immune response against blood-stage parasites, but we are only beginning to understand the complexity that lies beyond.

The humoral immune response also plays an important role in protection against blood-stage malaria as indicated more than 50 years ago when transfer of purified antibodies from malaria-immune individuals to susceptible children led to decreased parasite number and disease severity [106]. However, the parasite is extremely adept at evading antibody-dependent clearance through its huge genetic diversity and the ability to extensively vary the proteins that it expresses on the erythrocyte membrane [107]. Further complicating antibody-based immunity against *P. falciparum* is the fact that the half-life of anti-*Plasmodium* antibodies is extremely short and can drop to undetectable levels within months [108].

1.3.3. Unconventional T cells in malaria

1.3.3.1. Pre-erythrocytic stage

Recent data suggest that γδ T cells are expanded upon PfSPZ vaccination and a role in the protective response has been postulated, but the mechanisms of action remain unclear [76], [109]. The task of examining this further is complicated by the absence of an equivalent of Vγ9Vδ2 T cells in mouse models [110].

In the pre-erythrocytic immune response to *P. yoelii*, NKT cells were found to be recruited to the liver upon innate sensing of parasites in the liver and subsequent release of type I interferons. Furthermore, NKT cells, but not conventional T cells or NK cells were found to be

important in protection against a secondary infection [111]. This indicates that unconventional T cells might play a role in pre-erythrocytic immunity by sensing type I interferons in the liver.

1.3.3.2. Blood stage

Vγ9Vδ2 T cells are expanded upon blood-stage malaria and their frequency has been associated both with improved parasite control and more severe pathogenesis [110], [112]–[114]. This expansion is at least partially attributable to the fact that *P. falciparum*-infected erythrocytes contain phosphoantigens able to stimulate Vγ9Vδ2 T cells [115], [116]. However, erythrocytes do not express the known binding partner of Vγ9Vδ2 T cells, BTN3A1 [94]. Indeed, activation seems to be independent of contact between Vγ9Vδ2 T cells and infected erythrocytes, supporting a model in which phosphoantigens are released upon schizont rupture and can be self-presented by Vγ9Vδ2 T cells that express BTN3A1 [94]. Consistently, free merozoites, but not intra-erythrocytic parasites are targeted by Vγ9Vδ2 T cells, emphasizing the erythrocyte as a niche for parasite development, in which it is also largely protected from Vγ9Vδ2 T cells. The mechanism by which free merozoites are recognised by Vγ9Vδ2 T cells remains unknown [117]. A possible mechanism *in vivo* might be antibody-dependent cytotoxicity, as Vγ9Vδ2 T cells can express the Fc receptor CD16 [118].

Evidence for an involvement of non-Vγ9Vδ2 γδ T cells in malaria remains fragmental. Early work indicated a high frequency of Vδ1 T cells in healthy individuals living in a malaria-endemic region in Ghana as well as rapid, but transient expansion of Vδ1 T cells upon malaria chemotherapy in children [119], [120]. This expansion included the usage of all TCRγ chains, indicating a polyclonal response, but enigmatically, there was an increase of Vδ1 T cells that could not be stained with any of the available anti-TCRγ antibodies [120].

The frequency of MAIT cells was recently found to be dynamically altered during a CHMI clinical trial in Tanzania [121]. On the day of first detectable blood-stage parasitaemia, MAIT cells were decreased in peripheral blood, and expanded afterwards, but the mechanisms of activation remain unclear and might be cytokine-driven, as *P. falciparum* does not possess the ability to produce the canonical MAIT-cell antigens [121], [122].

1.4. Malaria vaccine development

1.4.1. The need for a malaria vaccine

The current malaria control strategy relies on a combination of several measures. This includes indoor residual spraying of insecticides, sleeping under insecticide-treated bed nets, seasonal

chemoprophylaxis as well as targeted diagnostics and treatment. While these measures have proven quite successful, malaria elimination is still difficult to achieve and insecticides as well as anti-malarial drugs are prone to development of resistance [1]. An effective vaccine would complement these malaria control efforts. Current malaria vaccine approaches include pre-erythrocytic vaccines that prevent both disease and transmission, blood-stage vaccines that limit infection, and transmission-blocking vaccines that block the spread of malaria [123]. The optimal vaccine would act during the pre-erythrocytic stage as this could not only prevent clinical disease, but also block transmission of malaria and therefore be useful in elimination campaigns.

1.4.2. RTS,S

The most advanced malaria vaccine, RTS,S/AS01 (RTS,S) received a positive scientific opinion from the European Medicines Agency in 2015 [124] and will be rolled out in 2018 in three countries in sub-Saharan Africa, representing a milestone in malaria vaccine development [125].

RTS,S is based on the two recombinant proteins RTS and S. RTS is a fusion protein between the carboxy-terminal part of *P. falciparum* CSP (RT), containing known B-cell and T-cell epitopes, and HBsAg (S). When RTS and S are expressed concomitantly in yeast cells, they assemble spontaneously into virus-like particles, a structure that is thought to enhance immunogenicity [126]. RTS,S is often formulated with AS01, an adjuvant system containing the two immune-stimulatory molecules MPL and QS-21 [127]. MPL is derived from lipopolysaccharide, is a ligand for TLR4, and can therefore directly stimulate antigen-presenting cells, while QS-21 is a saponin molecule that enhances both antibody and $CD8^+$ T-cell responses [127].

Between 2009 and 2011, RTS,S was tested in a phase III clinical trial in nine sub-Saharan countries in children (age 5-17 months) and infants (age 6-12 weeks). Vaccine efficacy against clinical malaria during a follow up of 36-48 months was 36% and 26% in the two age groups, respectively [128]. This represents a significant decrease over initial results examining a shorter follow-up period, indicating waning immune response during the time of follow up [128], [129]. Vaccine efficacy was found to be consistently lower in infants than in children, which coincided with lower anti-CSP antibody titres. The presence of anti-CSP antibodies before the first vaccination was associated with lower titres post-vaccination, indicating that previous exposure might dampen vaccination-induced immune responses [129].

Although representing a major advance, the RTS,S vaccine efficacy falls far short of the goal of 80% protection from clinical disease established in the 2006 Malaria Vaccine Technology Roadmap [130].

1.4.3. Whole-sporozoite vaccination

1.4.3.1. Radiation-attenuated sporozoites

More than 40 years ago, it was demonstrated that complete protection from malaria can be achieved in humans through administration of large numbers of irradiated sporozoites by mosquito bite [131], [132]. However, it requires the bites of around 1000 infected mosquitoes to induce sterile immunity in humans, which is not feasible for a wide application. Development of techniques to aseptically produce, isolate and cryopreserve *P. falciparum* sporozoites that are radiation-attenuated, pure, metabolically active and non-replicating (the PfSPZ Vaccine) by the biotechnology company Sanaria has overcome these problems [133]. A first clinical trial in 80 volunteers showed that administration of $1.35*10^5$ PfSPZ Vaccine intradermally (ID) or subcutaneously was safe and well tolerated [78]. However, protection was low and immunogenicity was modest and dose-dependent, providing evidence for an immunological threshold that needs to be overcome to reach protection. In the same study, experiments with mice and non-human primates indicated that intravenous administration leads to better protection and immunogenicity [78]. Therefore, the next clinical trial evaluated whether the same holds true for humans. Indeed, intravenous administration of five doses of $1.35*10^5$ PfSPZ Vaccine led to 100% (6 out of 6) protection against homologous controlled human malaria infection (CHMI) by mosquito bite [76].

Currently, several trials are under way to assess safety, efficacy and immunogenicity of the PfSPZ Vaccine in the malaria-endemic regions Tanzania (NCT02132299, NCT03420053), Gabon (NCT03521973), Equatorial Guinea [134], Kenya (NCT02687373), Burkina Faso (NCT02663700) and Mali [135]. Results from the clinical trial in Mali confirmed that the vaccine is safe and well tolerated. Protective efficacy against natural infection was 29% through 24 weeks of follow-up, falling short of the target 80% for use in elimination programs. Antibody responses to CSP and PfSPZ upon vaccination were detectable but low and did not correlate with protection and neither did any measured cellular responses [135].

In the BSPZV1 clinical trial in Bagamoyo, protection was assessed by direct venous inoculation (DVI) of 3200 PfSPZ Challenge, which consists of non-attenuated, fully infectious

PfSPZ. This resulted in 20% protection in the high-dose group that was vaccinated with 5 doses of $1.35*10^5$ PfSPZ Vaccine per injection (see *Chapter 3*; Jongo et al, manuscript in press).

1.4.3.2. Fully infectious sporozoites under chemoprophylaxis

An optimal vaccine based on PfSPZ would allow development of the parasite into late liver stage, allowing for a wider range and higher load of liver-stage antigens to be expressed and thus inducing a stronger immune response, while still preventing clinical disease [136]. However, radiation-attenuated PfSPZ are thought to arrest development early during liver stage [137].

An alternative approach of whole-sporozoite vaccination is the administration of fully infectious PfSPZ and concomitant chemoprophylaxis using e.g. chloroquine. Chloroquine does not affect liver-stage development of *P. falciparum*, but kills blood-stage parasites and thus exposes the immune system to the whole range of pre-erythrocytic as well as early blood-stage antigens, while still avoiding clinical disease [138]. Promisingly, first experiments in mouse models indicated that this regimen can induce sterile protection [139]. Similar results were obtained in human studies in which PfSPZ were administered by mosquito bite under chloroquine treatment leading to 100% protection against homologous mosquito bite challenge [140], [141]. Recently, this approach has been further developed by replacing the mosquito bites with DVI of PfSPZ Challenge, leading to 100% protection in the high-dose group (3 doses of $5.12*10^4$ PfSPZ Challenge) [142]. Currently, this approach (termed PfSPZ-CVac) is being evaluated in clinical trials in Equatorial Guinea (NCT02859350) and Mali (NCT02996695).

1.4.3.3. Genetically attenuated parasites

Genetically attenuated parasites (GAP) can represent promising tools for vaccination, because the stage at which parasite development arrests can potentially be controlled by choosing the genes that are deleted. Initial studies screened for genes that are essential for completion of the liver-stage development in the rodent malaria parasite *P. berghei* and knockout of these genes indeed led to attenuation and inhibition of blood-stage parasitaemia and induced a protective immune response [143], [144].

First evaluation of GAP in humans involved *P. falciparum* parasites deficient for the proteins P52 and P36, two related proteins important for liver-stage development. Administration to humans by mosquito bite showed strong, but surprisingly only incomplete attenuation, leading to blood-stage infection in one volunteer after 200 bites of infected mosquitoes [145]. To increase safety of these GAP, a third gene, *sap1*, was knocked out leading to a triple-knockout

GAP showing complete attenuation in a humanized mouse model carrying human hepatocytes [146]. These GAP have been recently tested in humans and proven to be completely attenuated and able to induce functional anti-sporozoite antibodies [147]. However, the GAP that are currently being evaluated in humans arrest early in liver-stage development, highlighting the delicate balance between safety and immunogenicity in this system [147].

1.4.4. Controlled human malaria infection

Historically, controlled human malaria infection (CHMI) has been evaluated as treatment for neurosyphilis [148] and even HIV [149]. Nowadays, it is a valuable tool to assess malaria drug and vaccine efficacy as well as an approach for vaccination when co-administered with malaria chemoprophylaxis (see section 1.4.3.2) [150]. Most of the early studies used bites of infected mosquitoes as a means of administration of sporozoites [151]. More recently, technology was developed to generate the aseptic, purified, cryopreserved, fully infectious PfSPZ Challenge, allowing for more controlled conditions and lower infrastructural requirements than CHMI by mosquito bite [152]. The first clinical trial was performed in Dutch volunteers by ID administration of PfSPZ Challenge and resulted in 83% infectivity, independently of the administered dose (2'500-25'000 PfSPZ Challenge), while adverse events were comparable to the ones observed in mosquito bite challenge [152]. In a next step, the ID administration route was compared with intramuscular (IM) administration, indicating a higher infectivity through the ID route [153].

The PfSPZ Challenge given ID was then tested in Tanzanian adults and revealed a similar infection rates as in the malaria-naïve, Dutch cohort [154]. Further optimisation of the protocol indicated a more than 20-fold higher efficiency when the challenge was administered by DVI as compared with the IM route, leading to 100% of infected volunteers after injection of 3'200 PfSPZ Challenge by DVI [155], [156]. Therefore, this standard of CHMI was used in the BSPZV1 clinical trial (see *Chapter 3*).

1.5. Aims of the thesis

As described in section 1.4.2, the most advanced malaria vaccine RTS,S will start to be rolled out in 2018. The first aim of this thesis (see *Chapter 2*) was to assess the T-cell response induced by RTS,S vaccination in a cohort of children living in sub-Saharan Africa. In particular, the goal was to measure a wide range of effector molecules including IL-4, IL-21

and CD154 that are important for the cross-talk between T cells and B cells and thus, for efficient formation of a humoral immune response.

Currently, several whole, purified *P. falciparum* sporozoite-based vaccination approaches are under evaluation in clinical trials, as described in section 1.4.3. The second aim of the thesis was the assessment of safety, immunogenicity and protective efficacy of the PfSPZ Vaccine during a phase I clinical trial in healthy, male Tanzanian adults (see *Chapter 3*). For the first time in Africa, vaccine efficacy was to be assessed by homologous CHMI via DVI.

The human immune response towards malaria infection involves a wide range of immune cells, including unconventional T cells. Recently, MAIT cells have been described to be altered during a CHMI in Tanzania [121]. The third aim of this thesis was to examine how MAIT cells can sense alterations in bacterial metabolism induced by different growth conditions (see *Chapter 4*). At the same time, the goal was to develop a novel, unbiased analysis pipeline to detect phenotypic alterations in T cells measured by multicolour flow cytometry.

The forth aim of this thesis was to dissect the immune response of unconventional T cells towards PfSPZ vaccination and CHMI (see *Chapter 5*). This should be done using an unbiased analysis approach using the methodology developed in *Chapter 4*. We hypothesised that using this approach, we could identify subsets of unconventional T cells that have been previously overlooked in the immune response during malaria. After identification of interesting subsets using an *ex vivo* flow cytometry approach, the goal was to characterise these T-cell subsets using complementary *in vitro* assays.

Chapter 2

RTS,S/AS01E Malaria Vaccine Induces Memory and Polyfunctional T Cell Responses in a Pediatric African Phase III Trial

This chapter contains the following publication:

Moncunill, G., Rosa, D., C, S., Ayestaran, A., Nhabomba, A.J., Mpina, M., Cohen, K.W., Jairoce, C., **Rutishauser, T**., Campo, J.J., Harezlak, J., Sanz, H., Díez-Padrisa, N., Williams, N.A., Morris, D., Aponte, J.J., Valim, C., Daubenberger, C., Dobaño, C., McElrath, M.J., 2017. RTS,S/AS01E Malaria Vaccine Induces Memory and Polyfunctional T Cell Responses in a Pediatric African Phase III Trial. Front Immunol 8.

https://doi.org/10.3389/fimmu.2017.01008

frontiers in Immunology

ORIGINAL RESEARCH
published: 23 August 2017
doi: 10.3389/fimmu.2017.01008

RTS,S/AS01E Malaria Vaccine Induces Memory and Polyfunctional T Cell Responses in a Pediatric African Phase III Trial

Gemma Moncunill[1,2,3†], Stephen C. De Rosa[2,4†], Aintzane Ayestaran[1], Augusto J. Nhabomba[3], Maximillian Mpina[5], Kristen W. Cohen[2], Chenjerai Jairoce[3], Tobias Rutishauser[6,7], Joseph J. Campo[1,3], Jaroslaw Harezlak[8], Héctor Sanz[1], Núria Díez-Padrisa[1], Nana Aba Williams[1], Daryl Morris[2], John J. Aponte[1], Clarissa Valim[9,10], Claudia Daubenberger[6,7], Carlota Dobaño[1,3†] and M. Juliana McElrath[2,11†]*

[1] ISGlobal, Barcelona Ctr. Int. Health Res. (CRESIB), Hospital Clínic – Universitat de Barcelona, Barcelona, Spain, [2] Vaccine and Infectious Disease Division, Fred Hutchinson Cancer Research Center, Seattle, WA, United States, [3] Centro de Investigação em Saúde de Manhiça (CISM), Maputo, Mozambique, [4] Department of Laboratory Medicine, University of Washington, Seattle, WA, United States, [5] Ifakara Health Institute, Bagamoyo Research and Training Centre, Bagamoyo, Tanzania, [6] Swiss Tropical and Public Health Institute, Basel, Switzerland, [7] University of Basel, Basel, Switzerland, [8] Department of Epidemiology and Biostatistics, School of Public Health-Bloomington, Indiana University, Bloomington, IN, United States, [9] Department of Osteopathic Medical Specialties, Michigan State University, East Lansing, MI, United States, [10] Department of Immunology and Infectious Diseases, Harvard T.H. Chen School of Public Health, Boston, MA, United States, [11] Department of Medicine, University of Washington, Seattle, WA, United States

Comprehensive assessment of cellular responses to the RTS,S/AS01E vaccine is needed to understand potential correlates and ultimately mechanisms of protection against malaria disease. Cellular responses recognizing the RTS,S/AS01E-containing circumsporozoite protein (CSP) and Hepatitis B surface antigen (HBsAg) were assessed before and 1 month after primary vaccination by intracellular cytokine staining and 16-color flow cytometry in 105 RTS,S/AS01-vaccinated and 74 rabies-vaccinated participants (controls) in a pediatric phase III trial in Africa. RTS,S/AS01E-vaccinated children had significantly higher frequencies of CSP- and HBsAg-specific $CD4^+$ T cells producing IL-2, TNF-α, and CD40L and HBsAg-specific $CD4^+$ T producing IFN-γ and IL-17 than baseline and the control group. Vaccine-induced responses were identified in both central and effector memory (EM) compartments. EM $CD4^+$ T cells expressing IL-4 and IL-21 were detected recognizing both vaccine antigens. Consistently higher response rates to both antigens in RTS,S/AS01E-vaccinated than comparator-vaccinated children were observed. RTS,S/AS01E induced polyfunctional CSP- and HBsAg-specific $CD4^+$ T cells, with a greater degree of polyfunctionality in HBsAg responses. In conclusion, RTS,S/AS01E vaccine induces T cells of higher functional heterogeneity and polyfunctionality than previously characterized. Responses detected in memory $CD4^+$ T cell compartments may provide correlates of RTS,S/AS01-induced immunity and duration of protection in future correlates of immunity studies.

Keywords: malaria, *Plasmodium falciparum*, vaccine, cellular immune responses, T cells, intracellular cytokine staining, flow cytometry

OPEN ACCESS

Edited by:
Urszula Krzych, Walter Reed Army Institute of Research, United States

Reviewed by:
Stephen M. Todryk, Northumbria University, United Kingdom
Noah Butler, University of Iowa, United States

***Correspondence:**
Gemma Moncunill
gemma.moncunill@isglobal.org

†Shared authorships.

Specialty section:
This article was submitted to Vaccines and Molecular Therapeutics, a section of the journal Frontiers in Immunology

Received: *28 June 2017*
Accepted: *07 August 2017*
Published: *23 August 2017*

Citation:
Moncunill G, De Rosa SC, Ayestaran A, Nhabomba AJ, Mpina M, Cohen KW, Jairoce C, Rutishauser T, Campo JJ, Harezlak J, Sanz H, Díez-Padrisa N, Williams NA, Morris D, Aponte JJ, Valim C, Daubenberger C, Dobaño C and McElrath MJ (2017) RTS,S/AS01E Malaria Vaccine Induces Memory and Polyfunctional T Cell Responses in a Pediatric African Phase III Trial. Front. Immunol. 8:1008. doi: 10.3389/fimmu.2017.01008

INTRODUCTION

A highly efficacious vaccine can substantially contribute to control and eventual elimination of malaria. This life-threatening disease caused an estimated 429,000 deaths in 2015 (1), mainly among sub-Saharan African children. In 2009–2014, the RTS,S/AS01E malaria vaccine was evaluated in a pediatric Phase III trial in Africa (2–4). Vaccine efficacy (VE) against clinical malaria over 1 year post-immunization was moderate (56%) in children enrolled at age 5–17 months and low (31%) in infants enrolled at age 6–12 weeks. Importantly, the protective effects waned quickly over time. To better understand why the RTS,S/AS01E vaccine induced only partial and short-lived protection against malaria, a thorough examination of the immune responses elicited, including different effector functions and memory phenotypes, using qualified or validated assays to ensure appropriate assay sensitivity and specificity to detect small frequencies of antigen-specific cells is needed.

RTS,S is a vaccine based on the circumsporozoite protein (CSP) of *Plasmodium falciparum*, targeting the sporozoite and liver stages of infection. This self-assembling virus-like particle consists of a recombinant protein containing part of CSP fused to the hepatitis B surface antigen (HBsAg) and it is coexpressed with HBsAg alone. In the Phase III trial, RTS,S was formulated with AS01E liposomal adjuvant containing monophosphoryl lipid A and QS21 and was designed to induce strong anti-CSP antibody and T helper (T_H) 1 cell responses. Accordingly, in past clinical trials in endemic areas, RTS,S consistently induced high anti-CSP IgG titers (5–11) and moderate T_H1 $CD4^+$ T cell responses (5–10). IgG titers have been recently shown to correlate with vaccine-induced protection in secondary analysis of Phase III trial data (12, 13). However, IgG responses do not explain why RTS,S/AS01E VE is moderate or short-lived.

Regarding the cellular responses, $CD4^+$ T cells expressing IL-2, TNF-α, and IFN-γ (and CD40L in naïve adults) have been detected by intracellular cytokine staining (ICS) or ELISpot (5–11, 14, 15) upon vaccination. In vaccinated naïve adults challenged with *P. falciparum*-infected mosquitoes, CSP-specific $CD4^+$ T cells and IFN-γ measured by ELISPot were associated with protection (11, 14, 15). One study evaluating RTS,S/AS02D in African children less than 1 year old did not find any association with protection (5), whereas in another one with RTS,S/AS01E in children 5–17 months old observed CSP-specific TNF-α^+ $CD4^+$ T cell responses to be associated with a reduced risk of clinical malaria independently of anti-CSP IgG titers (8). Polyfunctional analysis of the ICS data of the later study showed that IFN-γ IL-2^-TNF-α^+ $CD4^+$ T cells independently predicted reduced risk of clinical malaria, although the response was also detected in control vaccinees, and found a synergistic interaction with anti-CSP IgG titers (9). $CD8^+$ T cell responses were only detected in humans in two studies, one in infants in whom the responses were not correlated with protection and the other in naïve adults (5, 14). Interestingly, NK cells were found to be the main producers of IFN-γ in one field trial, but its association with protection was not assessed (10). Overall, no clear cellular correlates of protection have been demonstrated in African trials although only a limited number of assays restricted to a few immune variables have been studied. There has been no assessment of other cell effector functions, such as T_H2 or follicular helper T cells (T_{FH}), or memory phenotypes that may be induced by RTS,S/AS01E and could be correlated with antibody responses and involved in vaccine-induced protection. Interestingly, in the Phase III trial, we detected T_H1 responses in supernatants of CSP-stimulated cells associated with protection in RTS,S/AS01E vaccinees, whereas a T_H2 cytokine, IL-5, was associated with increased risk for malaria (16). To our knowledge, T_H2 responses had only been examined in one previous study in humans, where IL-4 was found elevated in culture supernatants from RTS,S/AS02D-vaccinated infants (5). Lastly, memory T cell subsets have only been examined in a study with malaria-naïve adults who underwent a challenge with *P. falciparum*-infected mosquitoes after RTS,S vaccination. In that study, central memory T (T_{CM}) cells and effector/effector memory T cells from RTS,S-vaccinated adults produced IL-2 after *ex vivo* CSP stimulation and frequencies were higher in protected vs. non-protected subjects (15).

Assessing the memory phenotype, the polyfunctionality degree and other relevant functions besides T_H1 responses, such as T_H2, T_H17, cytotoxic, or immunoregulatory responses, may be key to identify functionally complex responses to RTS,S/AS01E and unravel its mode of action. In fact, complexity of the immune response to malaria and the partial and short-lived protection induced by RTS,S/AS01E stresses the need to expand the breadth of immunological profiling to T_H2- and regulatory-type markers. This may be particularly relevant in infants in African settings, as they are exposed to prenatal and environmental factors that may modulate immune response to vaccines.

The aim of this study was to analyze RTS,S/AS01E cellular immunogenicity after primary vaccination using two qualified 16-color multiparametric ICS assays that allow the assessment of memory cell subsets and regulatory, cytotoxic, T_H1, T_H2, T_H17, T_{FH} effector functions, most of them never assessed before, and to identify and establish a baseline of cell phenotypes and functional responses to be evaluated in studies of immune correlates of protection elicited by the vaccine. To this end, we analyzed the CSP- and HBsAg-specific cells *ex vivo* using previously cryopreserved peripheral blood mononuclear cells (PBMC) isolated from a subset of children aged 5–17 months at enrollment from Tanzania and Mozambique and following receipt of either the RTS,S/AS01E vaccine or a comparator rabies vaccine.

MATERIALS AND METHODS

Study Population and Study Design

We performed a study on a subset of 179 children aged 5–17 months from the RTS,S/AS01E Phase III trial (ClinicalTrials.gov NCT00866619), described elsewhere (4): 105 children received RTS,S/AS01E and 74 children received the rabies vaccine as a comparator at study months zero (M0), one, and two. PBMC were collected at M0 before vaccination and approximately 30 days after the third vaccination dose (M3). RTS,S/AS01E-vaccinated and rabies-vaccinated children were randomly selected for this

study among participants with no reported malaria episodes defined by observation of *P. falciparum* parasites on blood smears, identified through passive case detection during 18 months of follow-up after third vaccination dose. Of note, PBMC samples from children who had malaria cases were reserved for future correlates analyses to test the selected markers identified in this study. Samples were collected in two different African centers: Manhiça Health Research Center, Fundação Manhiça (FM-CISM, Mozambique; 120 children), and Ifakara Health Institute and Bagamoyo Research and Training Centre (IHI-BRTC, Tanzania; 59 children). The two sites had low-medium malaria transmission intensity at the time of the study (2–4). Investigators conducted all assays blinded to vaccination status.

Sample Collection

Blood was collected in 5 ml sodium citrate (BD Vacutainer® CPT™) tubes. PBMCs were isolated by density gradient centrifugation, cryopreserved and shipped to the Fred Hutchinson Cancer Research Center where the PBMC were thawed and stained (see Methods in Supplementary Material).

PBMC Stimulations

Thawed PBMC were rested in a 37°C, 5% CO_2 incubator overnight. The resting step increases the sensitivity of the assay (data not shown), probably by decreasing the stress and activation of PBMC due to the thawing process and exposure to the toxic cryopreservation agent. PBMC were stimulated with peptide pools covering the HBsAg or the CSP antigen present in the RTS,S vaccine (Table S1 in Supplementary Material). Negative controls contained 0.5% DMSO, the diluent for peptide pools, and Staphylococcal enterotoxin B was used as positive control stimulation at 1 μg/ml. Cultures were incubated 6 h at 37°C, 5% CO_2. This short incubation time increases the sensitivity and specificity of the assay to detect antigen-specific cells, avoiding non-specific and secondary immune responses. Further details are found in Supplementary Material.

Intracellular Cytokine Staining

Peripheral blood mononuclear cells were stained with one of two 16-color ICS panels that were designed for the study and that had previously undergone assay qualification with a formerly validated panel (17, 18). Cell staining was performed as described (17) (Supplementary Material). Antibody details can be found in Tables S2 and S3 in Supplementary Material. Data were acquired using a BD LSR II flow cytometer (BD Biosciences) directly from the plates using a high throughput sampler. We found some toxicity of HBsAg peptides, but since we could exclude dead cells, data were considered acceptable for analysis. We noted some spillover from CD154 to CXCR5 and therefore, T_{FH}-like cells were excluded from the analysis. Flow cytometry analysis was performed using FlowJo software (Version 9.9 Tree Star). Gating strategies for both panels are shown in Figures S1 and S2 in Supplementary Material.

Statistical Analysis

The raw FCS files and manual gates were imported into the R environment (19) using the OpenCyto framework (20) and cell counts for the cell gates of interest were obtained for all stimulations and subjects.

For the analysis of the effect of vaccination on the frequencies of cells expressing the functional markers, a multivariate linear mixed effect model was fitted using logarithm-10 transformed cell frequencies (cells expressing the functional marker/total number of cells within each cell subset) as an outcome. These models are commonly used (21–24) and allow to model jointly the different cell stimulations that each subject sample underwent using random effects. The model included a random intercept for the subject effect nested within stimulation and a random slope for timepoint. In these models, observations generated by different subjects (biological replicates) are assumed to be independent. We included the following predictors in the regression models (as fixed effects): stimulation (CSP, DMSO, or HBsAg and DMSO, as appropriate), time of visit (pre- vs. post-vaccination), and vaccination status (RTS,S/AS01E vs. comparator vaccine), as well as all interactions between the three factors to allow variations of responses across subgroups of vaccinees and time. Linear combination of coefficients in these models allowed addressing specific study questions (details in Supplementary Material). Through these models, we estimated the % change in cell frequencies in RTS,S/AS01E vs. comparator vaccinees at each timepoint, the % change from M0 to M3 in each vaccine group, and the % change in RTS,S/AS01E vs. comparator vaccinees accounting for both timepoints. Statistical significance of comparisons was based on likelihood ratio tests. Antigen-specific responses were analyzed accounting for background, i.e., DMSO stimulation.

To define positivity of responses in each cell subset and subject, we identified the functional markers that were differentially expressed between the antigen (CSP or HBsAg) stimulations and their corresponding background (DMSO control stimulation) for each cell subset, subject, and at each timepoint. Thus, the proportion of cells expressing that marker was compared between the two stimulation conditions for each subject and timepoint. The statistical method used was mixture models for single-cell assays (MIMOSA) (25), using the default algorithm (Expectation–Maximization algorithm) and a false-discovery rate of 0.05%. This method was chosen because it has higher sensitivity and specificity than alternative methods such as Fisher's exact test (25). A separate model for each functional marker, cell subset, and stimulation was fitted. Once we had defined the positivity or negativity for each functional marker, cell subset, subject, and timepoint, then the proportion of children with positive responses between vaccine groups at baseline or 1-month post-vaccination was compared using two-sided Fisher's exact test.

Polyfunctional responses (cell subsets that express multiple functional markers) were analyzed using combinatorial polyfunctionality analysis of antigen-specific T cell subsets (COMPASS) (26). COMPASS models all cell subsets expressing functional markers simultaneously and selects the subsets most likely to have a positive antigen-specific response. The antigen-specific response is quantified by the probability of having a positive response. COMPASS functionality and polyfunctionality scores, summarizing each subject's polyfunctional profile, were compared

between vaccine groups using Wilcoxon test. The functionality score is the estimated proportion of antigen-specific cell subsets detected among all possible ones, whereas the polyfunctionality score is similar but weighted by the degree of polyfunctionality.

In addition, COMPASS generates heatmaps that show the posterior probabilities for each modeled cell subset for each subject. CD107a marker was eliminated from MIMOSA and COMPASS analysis, because peptide pool stimulation was associated with a

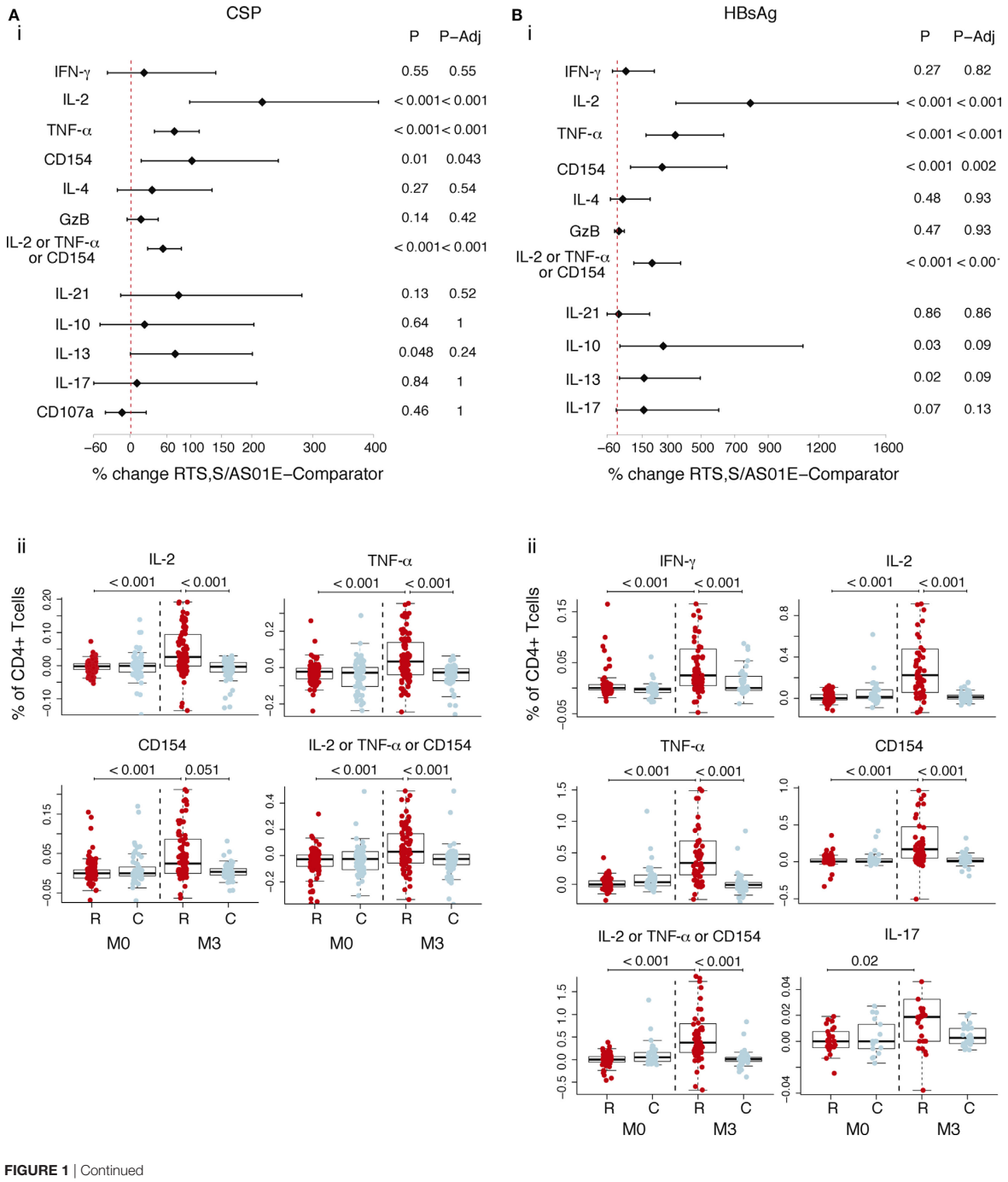

FIGURE 1 | Continued

FIGURE 1 | Continued
CSP- and hepatitis B surface antigen (HBsAg)-specific CD4+ T cell responses induced by RTS,S/AS01E. CSP- **(A)** and HBsAg- **(B)** specific CD4+ T cells expressing the common functional markers of both intracellular cytokine staining panels. (i) Forest plot showing the overall effect of RTS,S/AS01E (R) vaccination from baseline (M0) to 1 month post-third immunization (M3) taking into account the M0–M3 changes in comparator (C) vaccinees. The % change between RTS,S/AS01E and comparator vaccinees taking into account M0–M3 changes and 95% confidence intervals shown were obtained with a multivariate linear mixed effect model. *P* values (P) were obtained through likelihood ratio test and were adjusted for multiple testing (P-Adj) through Holm's approach. (ii) Box plots showing the frequencies of CD4+ T cells expressing the functional markers after background subtraction found to be statistically significant in (i). Boxplots illustrate the medians and the 25th and 75th quartiles, and whiskers display 1.5 times interquartile ranges, outliers are not shown to facilitate visualization of the differences between comparison groups. Differences between vaccine groups at M0 and at M3 and differences from M0 to M3 within each vaccine group were computed through a multivariate linear mixed effect model and *P* values obtained through likelihood ratio test and were adjusted for multiple testing through Holm approach. Only significant *P* values adjusted for multiple testing are shown. Sample size in **(A)**, for markers detected by both staining panels *N* = 100 RTS,S/AS01E and 65 comparator at M0, 100 RTS,S/AS01E and 70 comparator at M3. For comparisons including M0 and M3, only subjects that had samples at both timepoints are included (*N* = 156 for markers detected by both panels, *N* = 83 for markers detected by panel 1, *N* = 73 for markers detected by panel 2). Sample size in **(B)** *N* = 62 RTS,S/AS01E and 36 comparator at M0, 67 RTS,S/AS01E and 50 comparator at M3. For IL-17 (detected by panel 2) *N* = 30 RTS,S/AS01E and 18 comparator at M0, 37 RTS,S/AS01E and 27 comparator at M3. For comparisons including M0 and M3, only subjects that had samples at both timepoints are included (*N* = 71 for markers detected by both panels, *N* = 35 for markers detected by panel 1, *N* = 36 for markers detected by panel 2).

non-specific increase in CD107a compared to background, and response positivity could not be defined.

Statistical tests were considered significant at 0.05 α-level. Adjustments for multiple testing were done using Holm (27) and Benjamini–Hochberg (28) approaches. All analyses were conducted using R software. See Supplementary Material for detailed descriptions.

RESULTS

Study Population

We used two different multiparameter ICS panels to assess cellular immune responses specific to the RTS,S/AS01E vaccine antigens. PBMC from 55 RTS,S and 41 comparator vaccinees, and 50 RTS,S and 33 comparator vaccinees were stained with antibody panel 1 (P1) and panel 2 (P2), respectively. The two panels had the same set of core markers, which allowed the exclusion of dead cells, monocytes (CD14), identification of CD4+ and CD8+ T cells (CD4, CD8 and CD3), NK and NK-T cells (CD56), the T_H1 cytokines IFN-γ, IL-2, and TNF-α, the T_H2 cytokine IL-4, the costimulatory molecule CD154 (CD40L), and the cytotoxic marker granzyme B (Figures S1 and S2 in Supplementary Material; Tables S2 and S3 in Supplementary Material). P1 additionally had CD45RA and CCR7 markers that allowed the identification of memory cell subsets, and IL-21, a cytokine related to T_{FH}. Panel 2 (P2) included γδ TCR for the identification of γδ T cells and several functional markers: the regulatory cytokine IL-10, the T_H2 cytokine IL-13, the T_H17 cytokine IL-17, and cytotoxicity marker CD107a. The gating strategy is detailed in Figures S1 and S2 in Supplementary Material. The common set of core markers (lineage and functional markers) allowed the pooled analysis for these markers. Males and females were similarly represented in both study sites and vaccine groups, with a proportion of 59 and 56.8% females in the RTS,S/AS01E and comparator groups, respectively.

Frequencies of CSP- and HBsAg-Specific CD4+ T Cells Induced by RTS,S/AS01E

We compared frequencies of CSP- or HBsAg-specific T cells expressing functional markers in RTS,S- and rabies-vaccinated children, accounting for the pre-vaccination frequencies in a multivariate model. RTS,S/AS01E-vaccinated children had a statistically significant increase of CSP-specific CD4+ T cells expressing IL-2 (217% increase), TNF-α (72.3%), and CD154 (101.4%) from baseline to post-vaccination in contrast to the rabies vaccinees (**Figure 1A**, i). We observed larger increases over time of HBsAg-specific CD4+ T cells expressing IL-2 (732.2%), TNF-α (346%), and CD154 (268.3%) (**Figure 1B**, i) in RTS,S/AS01E than in rabies vaccinees.

Figure 1A (ii) and **Figure 1B** (ii) show the frequencies of CSP- and HBsAg-specific CD4+ T cells after background subtraction. Higher frequencies of CSP- and HBsAg-specific CD4+ T cells expressing the above markers, and additionally HBsAg-specific CD4+ T cells expressing IFN-γ and IL-17 cells, were observed in RTS,S/AS01E vaccinees at post-vaccination compared to baseline and to comparators. No differences were detected between the two vaccine groups at baseline, or from baseline to post-vaccination in comparator vaccinees, the latter suggesting that there was no effect of naturally acquired immunity on cellular responses.

Antigen-specific T cells in memory subsets, defined by CD45RA and CCR7, were analyzed following vaccination. CD4+ T_{CM} (CD45RA− CCR7+) and CD4+ T_{EM} (CD45RA− CCR7−) cells recognized both vaccine antigens. After accounting for baseline frequencies, RTS,S/AS01E vaccinees had more CSP-specific CD4+ T_{EM} cells producing IL-2 and TNF-α, respectively, than comparator vaccinees (**Figure 2A**, i). Comparisons between vaccine groups at post-vaccination and from baseline to post-vaccination revealed additional responses: higher frequencies of CD4+ T_{CM} expressing IL-2 and TNF-α and CD4+ T_{EM} cells expressing CD154, IL-4 and IL-21, in RTS,S/AS01E than comparator vaccinees (**Figure 2A**, ii). Regarding HBsAg-specific responses, RTS,S/AS01E vaccinees had increased frequencies of CD4+ T_{CM} producing IL-2, TNF-α and CD154 and CD4+ T_{EM} producing IL-2, TNF-α, CD154 and IL-21 than comparator vaccinees (**Figure 2B**, i).

Therefore, RTS,S/AS01E vaccination induced CSP and HBsAg-specific CD4+ T_{CM} and CD4+ T_{EM} with T_H1, and additional T_H2, and T_{FH} functions. No overall effect of RTS,S vaccination was detected on the frequencies of terminally differentiated CD4+ T cells (CD45RA+ CCR7−), naïve CD4+ T cells (CD45RA+

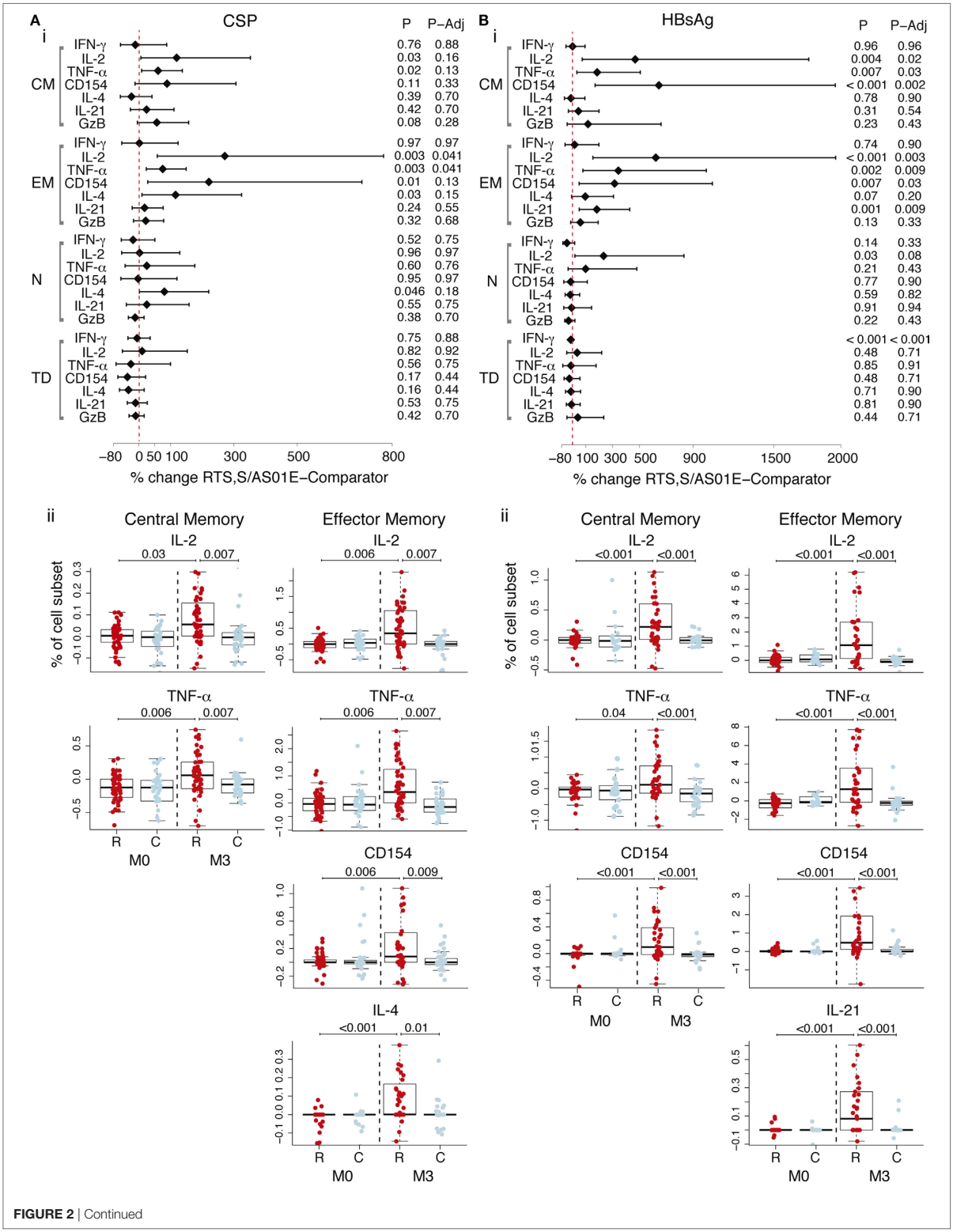

FIGURE 2 | Continued

FIGURE 2 | Continued
CSP- and hepatitis B surface antigen (HBsAg)-specific CD4+ T cell memory responses induced by RTS,S/AS01E. CSP- **(A)** and HBsAg- **(B)** specific memory CD4+ T cell subsets [central memory (CM); effector memory (EM); naive (N); terminally differentiated (TD)] expressing functional markers measured in the intracellular cytokine staining panels panel 1. (i) Forest plot showing the overall effect of RTS,S/AS01E (R) vaccination from baseline (M0) to 1 month post-third immunization (M3) taking into account the M0–M3 changes in comparator (C) vaccinees. The % change between RTS,S/AS01E and comparator vaccinees and 95% confidence intervals shown were obtained with a multivariate linear mixed effect model. *P* values (P) were obtained through likelihood ratio test and were adjusted for multiple testing (P-Adj) through Benjamini–Hochberg approach. (ii) Box plots showing the frequencies of CD4+ T_{CM} and CD4+ T_{EM} cells expressing selected functional markers after background subtraction. Boxplots illustrate the medians and the 25th and 75th quartiles, and whiskers display 1.5 times interquartile ranges, outliers are not shown to facilitate visualization of the differences between comparison groups. Differences between vaccine groups at M0 and at M3 and differences from M0 to M3 within each vaccine group were computed through a multivariate linear mixed effect model and *P* values obtained through likelihood ratio test and were adjusted for multiple testing through Holm approach. Only significant *P* values adjusted for multiple testing are shown. Sample size in **(A)** For *N* = 53 RTS,S/AS01E and 35 comparator at M0, 52 RTS,S/AS01E and 39 comparator at M3. For comparisons including M0 and M3, only subjects that had samples at both timepoints are included (*N* = 83). Sample size in **(B)** *N* = 32 RTS,S/AS01E and 18 comparator at M0, 37 RTS,S/AS01E and 27 comparator at M3. For comparisons including M0 and M3, only subjects that had samples at both timepoints are included (*N* = 35).

CCR7+), other analyzed cell subsets (NK, NK-T like, γδ T, CD8+ T cells) or on other functional markers (Tables S5 and S6 in Supplementary Material).

Non-Specific CD4+ T Cell and CD8+ T Cell Responses Induced by RTS,S/AS01E Vaccination

Analysis of frequencies of cell subsets expressing functional markers in the background (DMSO, serving as the unstimulated control) revealed non-specific responses (i.e., not specific for CSP or HBsAg) upon RTS,S/AS01E vaccination (**Figure 3**). Accounting for baseline and responses in comparator vaccinees, RTS,S/AS01E vaccination increased the frequencies of CD4+ T cells producing IL-2 or TNF-α or CD154, IL-4, and CD107a (**Figure 3A**, i). In comparator vaccinees, a decrease in these two subsets from baseline to post-vaccination was detected. Interestingly, RTS,S/AS01E vaccination also increased the frequencies of CD8+ T cells producing IL-4 and CD107a (**Figure 3B**, i).

Since we detected an effect of RTS,S/AS01E vaccination in the background, we looked at the *ex vivo* antigen stimulations when not accounting for background. RTS,S/AS01E-vaccinated children had CD4+ T cells and CD8+ T cells expressing IL-4 and CD107a, as was observed for the background alone and, thus, likely reflecting non-specific responses (Figure S3 in Supplementary Material). Additionally, RTS,S/AS01E vaccination increased the frequencies of CD4+ T cells expressing IL-13 and CD8+ T cells expressing CD154 and IL-2 or TNF-α or CD154 following CSP stimulation when not taking background into account (Figure S3 in Supplementary Material). These additional responses in RTS,S/AS01E-vaccinated children were no longer significant when taking into account the background and likely reflect a non-specific effect of RTS,S/AS01E vaccination.

Higher Proportion of Positive CD4+ T Cell Responses Defined by MIMOSA in RTS,S/AS01E than Comparators

To assess the vaccine specificity of the antigen-specific T cell responses detected and the rate of responders to the RTS,S/AS01E vaccine (participants whose T-cells responded to stimulation), we determined the positivity of the responses for each subject comparing the frequencies of T cells expressing a functional marker in the antigen-stimulated and unstimulated control conditions for each participant using the MIMOSA statistical method. If a response is truly vaccine specific, one would expect to detect it after vaccination but not at baseline or in the comparator vaccinees. We found a significantly higher proportion of IL-2+, TNF-α+, and CD154+ CD4+ T cell positive CSP-specific responses in RTS,S/AS01E than in comparator vaccinees post-vaccination (**Table 1**). Response rates for these markers ranged from 24 to 30% in RTS,S/AS01E vaccinees; whereas for comparator vaccinees, there were none or very few responses (**Table 1**). Similarly, CSP-specific positive responses were absent or very low at baseline, supporting the specificity of the definition of positivity (Table S7 in Supplementary Material).

For HBsAg, we additionally detected more IFN-γ+ and IL-17+ CD4+ T cell positive responses in RTS,S/AS01E than comparator vaccinees at post-vaccination. Rates of HBsAg responders ranged from 26.7 to 76.1% in RTS,S/AS01E vaccinees (**Table 1**). However, a proportion of comparator vaccinees at post-vaccination and all vaccinees at M0 were also positive (**Table 1**; Table S7 in Supplementary Material), likely due to the fact that these children received the hepatitis B vaccine during the Expanded Program of Immunization (EPI) before the study. Most of the CSP responders were also HBsAg responders (Figure S4 in Supplementary Material).

When looking at CD4+ T_{CM} and CD4+ T_{EM} cell subsets, we found a significantly higher proportion of CSP responders in RTS,S/AS01E than in comparator vaccinees for IL-2, TNF-α, and CD154 (**Table 2**). Regarding HBsAg responses, RTS,S/AS01E vaccinees had higher rates of IL-2 and CD154 responses in CD4+ T_{CM} cells and IFN-γ, IL-2, TNF-α, CD154 and IL-21 responses in CD4+ T_{EM} than comparator vaccinees. Very few positive responses to CSP and HBsAg were detected in comparator vaccinees or at baseline (**Table 2**; Table S8 in Supplementary Material). Almost no positive responses were found in the other cell subsets analyzed (CD4+ T_{TD}, CD4+ T_N, NK, NK-T like, γδ T, CD8+ T cells, and memory CD8+ T cell subsets), and no significant differences were detected between vaccination groups for any of the two vaccine antigens (Tables S9–S11 in Supplementary Material).

CSP- and HBsAg-Specific Polyfunctional CD4⁺ T Cell Responses Induced by RTS,S/AS01E

When analyzing the pooled data for the functional markers included in both panels, RTS,S/AS01 vaccinees had significantly higher functionality and polyfunctionality scores for CSP- and HBsAg-specific CD4⁺ T cells than comparator vaccinees (**Figures 4A,B**). Heatmaps of posterior probabilities of responses showed CSP-specific CD4⁺ T cell responses among subsets coexpressing three markers (IL-2, TNF-α, and CD154), and two markers (TNF-α and CD154; IL-2 and TNF-α) in RTS,S/

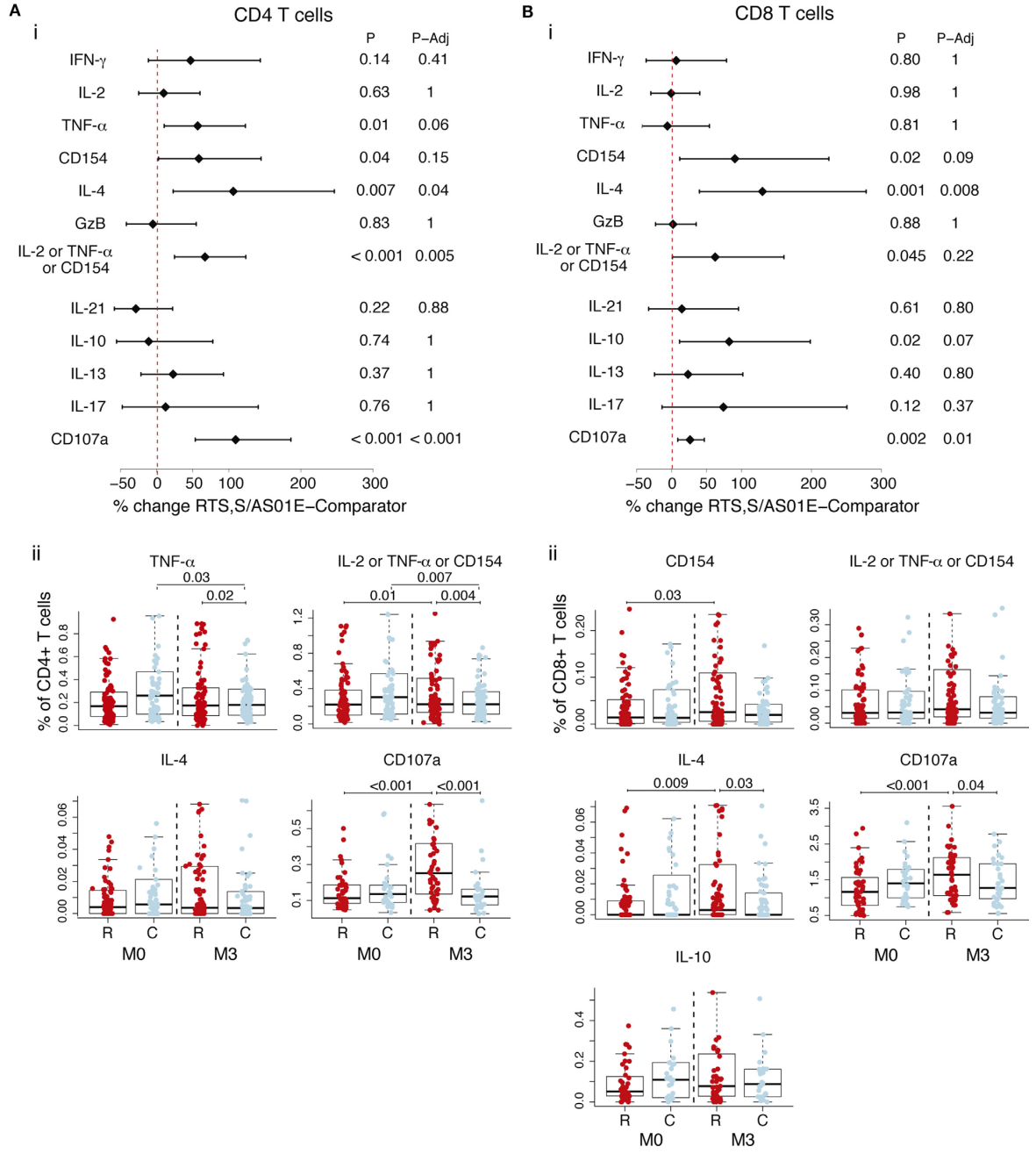

FIGURE 3 | Continued

FIGURE 3 | Continued
Non-specific CD4+ T and CD8+ T cell responses induced by RTS,S/AS01E as determined by the difference between M0 and M3 for the control stimulation. Frequencies in control stimulations (stimulation with the peptide diluent, DMSO, considered background) of CD4+ T cells **(A)** and CD8+ T cells **(B)** expressing the common functional markers of both intracellular cytokine staining panels and also functional markers measured separately in each panel. (i) Forest plot showing the overall effect of RTS,S/AS01E (R) vaccination from baseline (M0) to 1 month post-third immunization (M3) taking into account the M0–M3 changes in comparator (C) vaccinees. The % change between RTS,S/AS01E and comparator vaccinees and 95% confidence intervals shown were obtained with a multivariate linear mixed effect model. *P* values (P) were obtained through likelihood ratio test and were adjusted for multiple testing (P-Adj) through Holm approach. (ii) Box plots showing the frequencies of T cells expressing functional markers when significant differences were detected. Boxplots illustrate the medians and the 25th and 75th quartiles, and whiskers display 1.5 times interquartile ranges, outliers are not shown to facilitate visualization of the differences between comparison groups. Differences between vaccine groups at M0 and at M3 and differences from M0 to M3 within each vaccine group were computed through a multivariate linear mixed effect model and *P* values obtained through likelihood ratio test and were adjusted for multiple testing through Holm approach. Only significant *P* values adjusted for multiple testing are shown. Sample size in **(A)** for markers detected by both staining panels *N* = 100 RTS,S/AS01E and 65 comparator at M0, 101 RTS,S/AS01E and 70 comparator at M3. For CD107a (detected by panel 2), *N* = 47 RTS,S/AS01E and 30 comparator at M0, 49 RTS,S/AS01E and 31 comparator at M3. For comparisons, including M0 and M3, only subjects that had samples at both timepoints are included (*N* = 157 for markers detected by both panels, *N* = 83 for markers detected by panel 1 and *N* = 74 for markers detected by panel 2). Sample size in **(B)** for markers common from both staining panels *N* = 100 RTS,S/AS01E and 64 comparator at M0, 99 RTS,S/AS01E and 69 comparator at M3. For CD107a *N* = 47 RTS,S/AS01E and 30 comparator at M0, 47 RTS,S/AS01E and 31 comparator at M3. For comparisons including M0 and M3, only subjects that had samples at both timepoints are included (*N* = 154 for markers detected by both panels, *N* = 82 for markers detected by panel 1 and *N* = 742 for markers detected by panel 2).

TABLE 1 | Comparison of proportion of positive CD4+ T cell responses to CSP and hepatitis B surface antigen (HBsAg) between RTS,S/AS01E and comparator vaccinees 1-month post-third vaccination.

		CSP				HBsAg			
		RTS,S/AS01E	Comparator	*P*-value		RTS,S/AS01E	Comparator	*P*-value	
Functional marker[a]	**Intracellular cytokine staining panel**[b]	**Positive/total (%)**	**Positive/total (%)**	**Raw *P*[c]**	**Adj *P*[d]**	**Positive/total (%)**	**Positive/total (%)**	**Raw *P*[c]**	**Adj *P*[d]**
IFN-γ	P1 and P2	1/100 (1%)	0/70 (0%)	1	1	**34/67 (50.75%)**	**9/50 (18%)**	**<0.001**	**0.001**
IL-2	P1 and P2	**30/100 (30%)**	**0/70 (0%)**	**<0.001**	**<0.001**	**49/67 (73.13%)**	**9/50 (18%)**	**<0.001**	**<0.001**
TNF-α	P1 and P2	**24/100 (24%)**	**0/70 (0%)**	**<0.001**	**<0.001**	**48/67 (71.64%)**	**4/50 (8%)**	**<0.001**	**<0.001**
CD154	P1 and P2	**29/100 (29%)**	**5/70 (7.14%)**	**<0.001**	**0.002**	**51/67 (76.12%)**	**15/50 (30%)**	**<0.001**	**<0.001**
IL-4	P1 and P2	0/100 (0%)	2/70 (2.86%)	0.17	0.5	17/67 (25.37%)	6/50 (12%)	0.1	0.2
IL-2 or TNF-α or CD154	P1 and P2	**21/100 (21%)**	**0/70 (0%)**	**<0.001**	**<0.001**	**46/67 (68.66%)**	**2/50 (4%)**	**<0.001**	**<0.001**
IL-21	P1	2/52 (3.85%)	0/39 (0%)	0.5	1	20/37 (54.05%)	12/27 (44.44%)	0.61	1
IL-10	P2	0/48 (0%)	0/31 (0%)	1	1	3/30 (10%)	2/23 (8.7%)	1	1
IL-13	P2	5/48 (10.42%)	1/31 (3.23%)	0.39	1	**20/30 (66.67%)**	**8/23 (34.78%)**	**0.03**	0.11
IL-17	P2	1/48 (2.08%)	0/31 (0%)	1	1	**8/30 (26.67%)**	**0/23 (0%)**	**0.007**	**0.03**

Bold font indicates differences with p-values <0.05.
[a]*Granzyme B was included in the analysis, but not shown because it is constitutively expressed independently of cell stimulation and activation.*
[b]*Data from markers detected by both staining panels, P1 and P2, are combined.*
[c]*Raw P, original P-value computed based on two-sided Fisher's exact test.*
[d]*Adj P, P values adjusted for multiple testing through Holm's approach.*

AS01E vaccinees, whereas almost no responses were detected in comparator vaccinees or at baseline (**Figure 4A**, ii). For HBsAg responses, more CD4+ T cell subsets with positive responses and with higher degree of polyfunctionality were detected in RTS,S/AS01E vaccinees (**Figure 4B**, ii). Besides the same triple- and double-positive CD4+ T cell responses recognizing CSP antigen, we also detected CD154+ IL-2+ TNF-α+ IFN-γ+ CD4+ T cells and CD154+ IL-2+ TNF-α+ IL4+ CD4+ T cells. By contrast, comparator vaccinees or all vaccinees at baseline had none or weak responses in these subsets that could be explained by background responses to previous malaria exposure or hepatitis B vaccination. Therefore, RTS,S/AS01E induced polyfunctional CD4+ T cells to both vaccine antigens, with a higher degree of polyfunctionality for HBsAg that included T_H1 and T_H2 responses.

When the COMPASS analysis was performed using all the functional makers included in each antibody panel separately, we identified additional highly polyfunctional CD4+ T cell subsets coexpressing IL-13 (for both vaccine antigens) or IL-21 (for HBsAg) in addition to IL-2, TNF-α and CD154 (Figure S5 in Supplementary Material). This further highlights the induction of highly polyfunctional CD4+ T cell subsets with a T_H2 and T_{FH} functions by RTS,S/AS01E. No polyfunctional responses were detected in CD8+ T cells for either vaccine antigen.

DISCUSSION

We provide a detailed characterization of the *ex vivo* antigen-specific T cell response induced by RTS,S/AS01E vaccination in a pediatric Phase III trial (2–4). In addition to previously described IL-2- and TNF-α-expressing CD4+ T cell responses (5–10), we have identified for the first time in a pediatric field trial T_H2 effector functions and IL-21 in RTS,S vaccinees, attributed the responses to the central memory (CM) and effector memory (EM) compartments, and observed polyfunctional CD4+ T cell

TABLE 2 | Comparison of proportion of positive responses to CSP and hepatitis B surface antigen (HBsAg) in memory CD4+ T cell subsets between RTS,S/AS01E and comparator vaccinees 1-month post-third vaccination.

		CSP				HBsAg			
		RTS,S/AS01E	Comparator	*P*-value		RTS,S/AS01E	Comparator	*P*-value	
Memory subset	**Functional marker[a]**	**Positive/total (%)**	**Positive/total (%)**	**Raw *P*[b]**	**Adj *P*[c]**	**Positive/total (%)**	**Positive/total (%)**	**Raw *P*[b]**	**Adj *P*[c]**
CM	IFN-γ	1/52 (1.92%)	0/39 (0%)	1	1	1/37 (2.7%)	0/27 (0%)	1	1
	IL-2	**12/52 (23.08%)**	**0/39 (0%)**	**<0.001**	**0.009**	**14/37 (37.84%)**	**0/27 (0%)**	**<0.001**	**0.001**
	TNF-α	**8/52 (15.38%)**	**0/39 (0%)**	**0.01**	**0.049**	**8/37 (21.62%)**	**0/27 (0%)**	**0.02**	0.058
	CD154	**11/52 (21.15%)**	**0/39 (0%)**	**0.002**	**0.01**	**12/37 (32.43%)**	**1/27 (3.7%)**	**0.005**	**0.02**
	IL-4	0/52 (0%)	0/39 (0%)	1	1	2/37 (5.41%)	0/27 (0%)	0.5	1
	IL-21	0/52 (0%)	0/39 (0%)	1	1	0/37 (0%)	0/27 (0%)	1	1
EM	IFN-γ	1/52 (1.92%)	0/39 (0%)	1	1	**9/37 (24.32%)**	**0/27 (0%)**	**0.008**	**0.03**
	IL-2	**21/52 (40.38%)**	**0/39 (0%)**	**<0.001**	**<0.001**	**23/37 (62.16%)**	**1/27 (3.7%)**	**<0.001**	**<0.001**
	TNF-α	**12/52 (23.08%)**	**0/39 (0%)**	**<0.001**	**0.009**	**18/37 (48.65%)**	**0/27 (0%)**	**<0.001**	**<0.001**
	CD154	**14/52 (26.92%)**	**2/39 (5.13%)**	**0.01**	**0.049**	**21/37 (56.76%)**	**1/27 (3.7%)**	**<0.001**	**<0.001**
	IL-4	4/52 (7.69%)	0/39 (0%)	0.13	0.46	8/37 (21.62%)	1/27 (3.7%)	0.07	0.19
	IL-21	**7/52 (13.46%)**	**0/39 (0%)**	**0.02**	0.07	**16/37 (43.24%)**	**2/27 (7.41%)**	**0.002**	**0.01**
TD	IFN-γ	0/52 (0%)	0/39 (0%)	1	1	0/37 (0%)	0/27 (0%)	1	1
	IL-2	0/52 (0%)	0/39 (0%)	1	1	0/37 (0%)	0/27 (0%)	1	1
	TNF-α	0/52 (0%)	0/39 (0%)	1	1	0/37 (0%)	0/27 (0%)	1	1
	CD154	0/52 (0%)	0/39 (0%)	1	1	0/37 (0%)	0/27 (0%)	1	1
	IL-4	0/52 (0%)	0/39 (0%)	1	1	0/37 (0%)	0/27 (0%)	1	1
	IL-21	0/52 (0%)	0/39 (0%)	1	1	0/37 (0%)	0/27 (0%)	1	1
Naive	IFN-γ	0/52 (0%)	0/39 (0%)	1	1	1/37 (2.7%)	2/27 (7.41%)	0.57	1
	IL-2	0/52 (0%)	0/39 (0%)	1	1	4/37 (10.81%)	2/27 (7.41%)	1	1
	TNF-α	0/52 (0%)	0/39 (0%)	1	1	5/37 (13.51%)	0/27 (0%)	0.07	0.19
	CD154	0/52 (0%)	0/39 (0%)	1	1	1/37 (2.7%)	0/27 (0%)	1	1
	IL-4	0/52 (0%)	0/39 (0%)	1	1	0/37 (0%)	0/27 (0%)	1	1
	IL-21	0/52 (0%)	0/39 (0%)	1	1	14/37 (37.84%)	11/27 (40.74%)	1	1

Bold font indicates differences with p-values <0.05.

CM, central memory (CD45RA⁻ CCR7⁺); EM, effector memory (CD45RA⁻ CCR7⁻); TD, terminally differentiated (CD45RA⁺ CCR7⁻).

[a]*Granzyme B was included in the analysis, but not shown because it is constitutively expressed independently of cell stimulation and activation.*

[b]*Raw P, original P-value computed based on two-sided Fisher's exact test.*

[c]*Adj P, P values adjusted for multiple testing through Benjamini–Hochberg approach.*

responses, which may be a key feature of a protective response. Although this analysis was limited to vaccine recipients who did not become infected with *P. falciparum*, this study has identified key immune responses that can be examined in a larger case-control study within this trial.

RTS,S/AS01E vaccination induced distinct antigen-specific CD4+ T cell populations in a subset of children: CSP-specific IL-2, TNF-α, and CD154 CD4+ T cell responses and HBsAg-specific IFN-γ, IL-2, TNF-α, CD154, and IL-17 CD4+ T cell responses. Frequencies of cytokine-positive CD4+ T cells were consistent with the frequencies of IL-2 and TNF-α CSP-specific responses reported previously in RTS,S Phase II trials in endemic areas (5–10). Although no clear associations of TNF-α and IL-2 responses with protection were found in past field studies, they could contribute in RTS,S-induced protection (8, 9). TNF-α is an effector cytokine that may mediate mechanisms of *P. falciparum* pre-erythrocytic protection (29–31) and IL-2 induces proliferation of T cells and amplifies effector functions. CD4+ T cells producing IL-2 may contribute to the memory pool of CD4+ T cells with effector functions since they can be maintained during long periods of time and can develop into IFN-γ-producing T cells following subsequent stimulation (32). Of note, rates of IL-2 CSP responders (23–40% depending on the CD4+ T cell subset) were similar to the estimated VE in the Phase III trial (50% after a year of follow-up or 28% till study end) (4). IL-2 expression can also induce NK activation and secretion of IFN-γ (10, 33, 34), a key effector cytokine involved in malaria protection (35). Contrary to previous findings, we did not detect IFN-γ expression in CD4+ T cells or NK cells *ex vivo* following CSP stimulation (5, 7, 8, 10, 14). This is probably due to the short stimulation time in our study compared to longer times in whole blood assays from previous studies, which allowed bystander activation of CD4+ T cells and NK cells through IL-2 (10). Remarkably, we detected CD40L expression in antigen-specific CD4+ T cells, in contrast to previous field studies (6, 7).

Importantly, CD4+ T cell responses were detected in CM and EM compartments. Memory phenotypes are relevant to define high-quality and long-lasting responses, for instance, the higher proliferative potential of CM cells has been associated with protection from infection (32, 36–38). CD4+ T_{CM} responses could, therefore, be involved in long-lasting protection, whereas the CD4+ T_{EM} responses could be associated with the short protection observed in the trial. IL2+, CD154+, and TNF-α+ CD4+ T_{CM} cells were detected, whereas CD4+ T_{EM} cells had additional effector functions, in accordance with the different cytokine profiles associated with these memory T cell subsets (32, 39, 40)

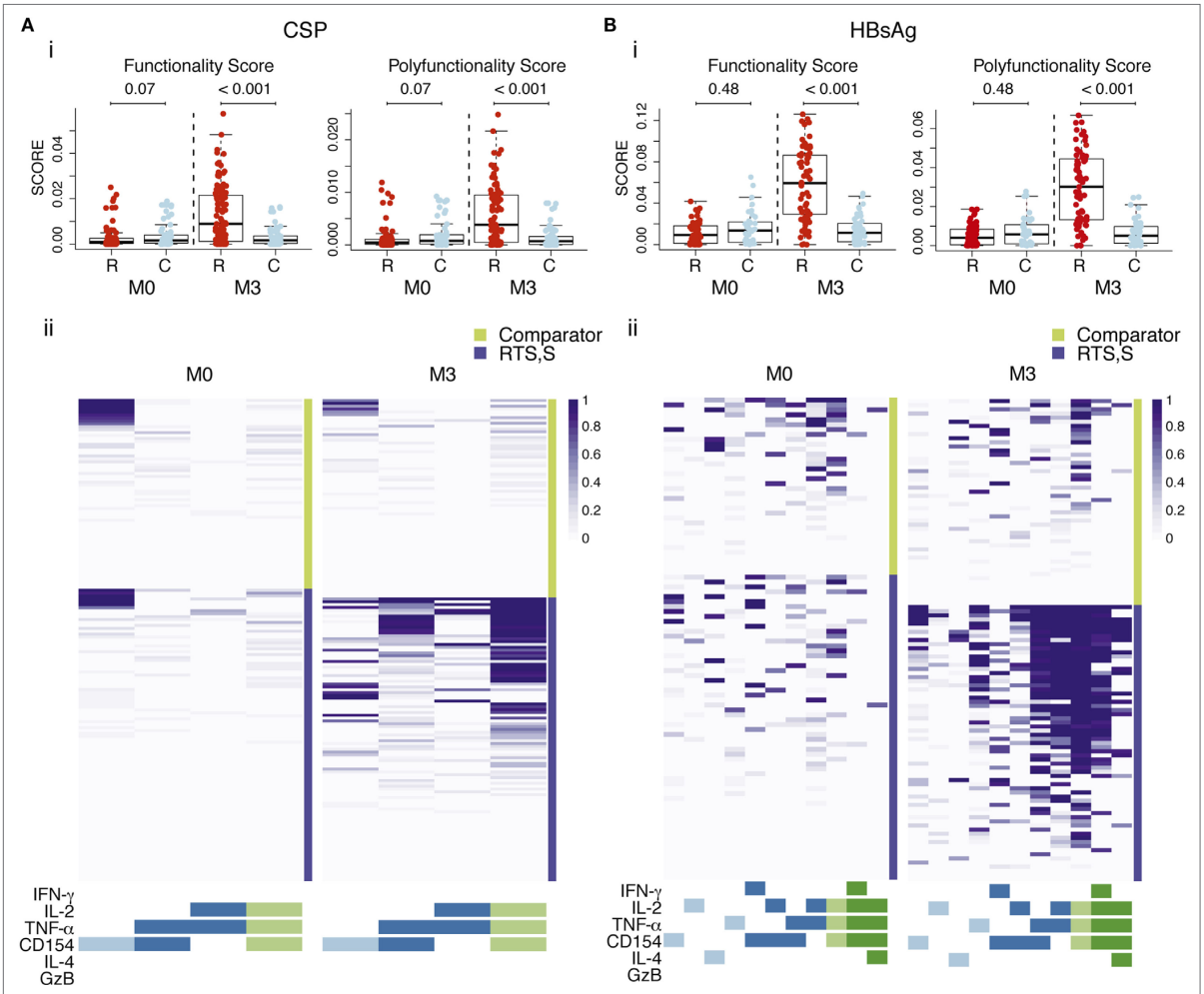

FIGURE 4 | CSP- **(A)** and hepatitis B surface antigen (HBsAg)-specific **(B)** CD4⁺ T cell polyfunctional responses. (i) Box plots of functionality and polyfunctionality scores calculated by combinatorial polyfunctionality analysis of antigen-specific T cell subsets (COMPASS), stratified by vaccine group and timepoint. The functionality score represents the estimated proportion of cell subsets showing positive responses among all possible cell subsets expressing any functional marker, whereas the polyfunctional score is similar but it is weighted by the degree of polyfunctionality. Boxplots illustrate the medians and the 25th and 75th quartiles, and whiskers display 1.5 times interquartile ranges. COMPASS analysis was performed using the common markers of both panels and all subjects with data (IL-4, IFN-γ, granzyme B (GzB), IL-2, TNF-α, CD154, 64 possible subsets). *P* values computed through Wilcoxon tests and adjusted for multiple testing through Holm approach separately for CSP and HBsAg antigens are shown. (ii) Heatmap of COMPASS posterior probabilities showing CD4⁺ T cell responses to CSP and HBsAg in RTS,S/AS01E and comparator vaccinees at pre-vaccination (M0) and 1 month post-third vaccination (M3). Columns represent functional cell subsets with detectable antigen-specific responses, color coded by the number of functional markers they express and are ordered by increasing degree of polyfunctionality. Rows represent study children, which are stratified by vaccine status, at the top the comparator vaccinees and at the bottom the RTS,S/AS01E vaccinees. Each cell shows the probability (color coded by purple intensity) that the corresponding child shows an antigen-specific response in the corresponding cell subset. Sample size in **(A)** *N* = 100 RTS,S/AS01E and 65 comparator at M0, 100 RTS,S/AS01E and 70 comparator at M3; **(B)** *N* = 62 RTS,S/AS01E and 36 comparator at M0, 67 RTS,S/AS01E and 50 comparator at M3.

and studies reporting CD4⁺ T_{EM} cells as the main producers of effector cytokines (32, 40). Higher frequencies of CD4⁺ T_{EM} cells expressing IL-4, and IL-21 for both vaccine antigens, and IFN-γ for HBsAg, were detected in RTS,S/AS01E-vaccinated children compared to baseline frequencies or comparator vaccinees. T_H2 (IL-4) and T_{FH} (IL-21) effector functions together with CD40L could provide help to B cells for humoral responses and may correlate with antibody responses (41–44). No responses were detected in CD4⁺ T_{TD} cells, a cell subset with high IFN-γ effector function, with no long-term memory potential and fated for death (32).

RTS,S/AS01E vaccination induced polyfunctional CSP- and HBsAg-specific CD4⁺ T cells. This finding is particularly important since multifunctional T cells have been associated with higher

quality responses and risk (26) or protection from infections (45, 46). Most CSP and HBsAg positive responses were found in the triple functional marker $CD4^+$ T cell subset coexpressing IL-2, TNF-α, and CD154, although we also observed responses in a 4-function subset coexpressing IL-13. For HBsAg, we also found numerous responses in $CD4^+$ T cells subsets simultaneously producing four functional markers: IL-2, TNF-α, CD154 plus IL-21 or IFN-γ or IL-4, reflecting T_{FH}, T_H1 and T_H2 distinct differentiation of these effector cell subsets.

Overall, HBsAg-specific responses were of higher magnitude, effector breadth and polyfunctionality than CSP-specific responses, suggesting a higher quality of response probably due to a booster effect since children should have been previously vaccinated with hepatitis B, or a higher immunogenicity of HBsAg compared to CSP due to the higher proportion of HBsAg than CSP in RTS,S (4:1).

RTS,S/AS01E may have a non-specific effect since higher background $CD4^+$ T cell and $CD8^+$ T cell responses were detected after vaccination compared with baseline. Since these responses included IL-4 and CD107a, it could be indicating a bias to a T_H2 status and higher cytolytic potential of T cells in RTS,S/AS01E-vaccinated children. There is increasing evidence of non-specific effect of vaccines (47, 48), but a non-specific effect of RTS,S/AS01E may still have an impact on the response against *P. falciparum* infection. The significance of these responses may be worth noting in the context of the future correlates analyses. This finding of a non-specific effect highlights the importance of correcting for the background (by subtracting background) in order to assess antigen-specific effects.

In this study, we only included children without experiencing a documented malaria episode during the 18 months of follow-up; therefore, the clinical relevance of our findings will be assessed in future correlates studies. The exclusion of malaria cases is unlikely to bias results and affect study conclusions since malaria transmission intensity was low at that time in Manhiça and Bagamoyo and lack of malaria is not likely to be due solely to vaccine-induced protection, but also to lack of exposure to the mosquito-bearing parasite. Another potential limitation of our study relates to the toxicity of HBsAg peptide concentration used. Although this could impact cellular responsiveness, we did exclude dead and dying cells in the analysis, and it is likely that any impact would affect both vaccine groups.

The breadth of functions, patterns, and variability of responses to CSP, together with memory phenotypes of responding cell subsets described in our study, reflects a complex response to the RTS,S/AS01 vaccine. These responses, together with anti-CSP IgG data, may provide insights into the lack of protection in a substantial proportion of vaccinees, and may be key in providing correlates for VE and duration of protection.

ETHICS STATEMENT

Approval for the study protocol was obtained from the Ethical Committee of the Hospital Clínic in Barcelona (CEIC, Spain), the National Health and Bioethics Committee (CNBS, Mozambique), the Ethikkommission Beider Basel (EKBB, Switzerland), the National Institutional Review Board (NIMR, Tanzania), the Ifakara Health Institute IRB (IHIIRB, Tanzania), and the PATH's Research Ethics Committee (REC, USA). Written informed consent was obtained from parents or guardians of participating children in accordance with the Declaration of Helsinki.

AUTHOR CONTRIBUTIONS

Substantial contributions to the conception or design of the work: GM, SR, CDa, CDo, and MJM. Acquisition of samples/data: GM, AN, MM, CJ, TR, JC, CDa, and CDo. Supervision analysis of samples: SR, KC. Analysis of data: GM, AA, JH, JA, DM, and CV. Data management: HS. Project management and coordination: ND-P and NW. Interpretation of data for the work and drafting the manuscript: GM, SR, CDo. Revising it critically for important intellectual content; final approval of the version to be published; and agreement to be accountable for all aspects of the work in ensuring that questions related to the accuracy or integrity of any part of the work are appropriately investigated and resolved: GM, SR, AA, AN, MM, KC, CJ, TR, JC, JH, HS, ND-P, NW, DM, JA, CV, CDa, CDo, MJM.

ACKNOWLEDGMENTS

We wish to thank all the participants of the study and their families. We thank the MAL055 clinical team, the field and laboratory personnel from the CISM, ISGlobal, and IHI-Bagamoyo research and training center, in particular Laura Puyol, Bendita Zavale, Lázaro Quimice, Nelito Ernesto José, Anneth Tumbo, and Helder Bulo, Carole Amroune, and Claudia Hernández for their administrative and management support. We are very grateful to the Fred Hutch research technologists, in particular, Terry Stewart, Paul Newling, and Kevin Hawkins for their work performing the PBMC stimulations, ICS assays and FlowJo gating. Thanks also to Carol Marty and David Chambliss for their logistic laboratory support. We are also grateful to the members of the MAL067 Vaccine Immunology Workgroup and its Working Groups (Statistical and Cellular). We would like to thank Marc Lievens for his help in the selection of samples. We also thank GSK Vaccines and PATH Malaria Vaccine Initiative (MVI) for their support in the conduct of the MAL067 Study. ISGlobal is a member of the CERCA Programme, Generalitat de Catalunya.

FUNDING

Supported in part by the PATH Malaria Vaccine Initiative (MVI), and grants from the National Institutes of Health (NIH)—National Institute of Allergy and Infectious Diseases (NIAID), grant number R01AI095789; the HIV Vaccine Trials Network Laboratory Center (HVTN, National Institute of Allergy and Infectious Diseases), grant number UM1 AI068618; the Human Immunology Project Consortium (HIPC, National Institute of Allergy and Infectious Diseases), grant number P30 AI027757; the Instituto de Salud Carlos III, grant number PS11/00423; and

the Agència de Gestió d'Ajuts Universitaris i de Recerca AGAUR, grant number 2014SGR991. CD was recipient of a Ramon y Cajal Contract from the Ministerio de Economía y Competitividad (RYC-2008-02631). GM was recipient of a Sara Borrell – ISCIII fellowship (CD010/00156).

SUPPLEMENTARY MATERIAL

The Supplementary Material for this article can be found online at http://journal.frontiersin.org/article/10.3389/fimmu.2017.01008/full#supplementary-material.

REFERENCES

1. WHO. *World Malaria Report 2016*. Geneva: WHO (2016).
2. RTS,S Clinical Trials Partnership, Agnandji ST, Lell B, Fernandes JF, Abossolo BP, Methogo BG, et al. A phase 3 trial of RTS,S/AS01 malaria vaccine in African infants. *N Engl J Med* (2012) 367:2284–95. doi:10.1056/NEJMoa1208394
3. Agnandji ST, Lell B, Soulanoudjingar SS, Fernandes JF, Abossolo BP, Conzelmann C, et al. First results of phase 3 trial of RTS,S/AS01 malaria vaccine in African children. *N Engl J Med* (2011) 365:1863–75. doi:10.1056/NEJMoa1102287
4. RTS,S Clinical Trials Partnership. Efficacy and safety of RTS,S/AS01 malaria vaccine with or without a booster dose in infants and children in Africa: final results of a phase 3, individually randomised, controlled trial. *Lancet* (2015) 386:31–45. doi:10.1016/S0140-6736(15)60721-8
5. Barbosa A, Naniche D, Aponte JJ, Manaca MN, Mandomando I, Aide P, et al. *Plasmodium falciparum*-specific cellular immune responses after immunization with the RTS,S/AS02D candidate malaria vaccine in infants living in an area of high endemicity in Mozambique. *Infect Immun* (2009) 77:4502–9. doi:10.1128/IAI.00442-09
6. Agnandji ST, Fendel R, Mestré M, Janssens M, Vekemans J, Held J, et al. Induction of *Plasmodium falciparum*-specific CD4+ T cells and memory B cells in Gabonese children vaccinated with RTS,S/AS01(E) and RTS,S/AS02(D). *PLoS One* (2011) 6:e18559. doi:10.1371/journal.pone.0018559
7. Ansong D, Asante KP, Vekemans J, Owusu SK, Owusu R, Brobby NAW, et al. T cell responses to the RTS,S/AS01(E) and RTS,S/AS02(D) malaria candidate vaccines administered according to different schedules to Ghanaian children. *PLoS One* (2011) 6:e18891. doi:10.1371/journal.pone.0018891
8. Olotu A, Moris P, Mwacharo J, Vekemans J, Kimani D, Janssens M, et al. Circumsporozoite-specific T cell responses in children vaccinated with RTS,S/AS01E and protection against *P. falciparum* clinical malaria. *PLoS One* (2011) 6:e25786. doi:10.1371/journal.pone.0025786
9. Ndungu FM, Mwacharo J, Kimani D, Kai O, Moris P, Jongert E, et al. A statistical interaction between circumsporozoite protein-specific T cell and antibody responses and risk of clinical malaria episodes following vaccination with RTS,S/AS01E. *PLoS One* (2012) 7:e52870. doi:10.1371/journal.pone.0052870
10. Horowitz A, Hafalla JCR, King E, Lusingu J, Dekker D, Leach A, et al. Antigen-specific IL-2 secretion correlates with NK cell responses after immunization of Tanzanian children with the RTS,S/AS01 malaria vaccine. *J Immunol* (2012) 188:5054–62. doi:10.4049/jimmunol.1102710
11. Kester K, Cummings JF, Ofori-Anyinam O, Ockenhouse CF, Krzych U, Moris P, et al. Randomized, double-blind, phase 2a trial of falciparum malaria vaccines RTS,S/AS01B and RTS,S/AS02A in malaria-naive adults: safety, efficacy, and immunologic associates of protection. *J Infect Dis* (2009) 200:337–46. doi:10.1086/600120
12. RTS,S Clinical Trials Partnership. Efficacy and safety of the RTS,S/AS01 malaria vaccine during 18 months after vaccination: a phase 3 randomized, controlled trial in children and young infants at 11 African sites. *PLoS Med* (2014) 11:e1001685. doi:10.1371/journal.pmed.1001685
13. White MT, Verity R, Griffin JT, Asante KP, Owusu-Agyei S, Greenwood B, et al. Immunogenicity of the RTS,S/AS01 malaria vaccine and implications for duration of vaccine efficacy: secondary analysis of data from a phase 3 randomised controlled trial. *Lancet Infect Dis* (2015) 3099:1–9. doi:10.1016/S1473-3099(15)00239-X
14. Sun P, Schwenk R, White K, Stoute JA, Cohen J, Ballou WR, et al. Protective immunity induced with malaria vaccine, RTS,S, is linked to *Plasmodium falciparum* circumsporozoite protein-specific CD4+ and CD8+ T cells producing IFN-gamma. *J Immunol* (2003) 171:6961–7. doi:10.4049/jimmunol.171.12.6961
15. Lumsden JM, Schwenk RJ, Rein LE, Moris P, Janssens M, Ofori-Anyinam O, et al. Protective immunity induced with the RTS,S/as vaccine is associated with IL-2 and TNF-α producing effector and central memory CD4 T cells. *PLoS One* (2011) 6:e20775. doi:10.1371/journal.pone.0020775
16. Moncunill G, Mpina M, Nhabomba AJ, Aguilar R, Ayestaran A, Sanz H, et al. Distinct TH1 and TH2 cellular responses associated with malaria protection and risk in RTS,S/AS01E vaccinees. *Clin Infect Dis* (2017). doi:10.1093/cid/cix429
17. Moncunill G, Dobaño C, McElrath MJ, De Rosa SC. OMIP-025: evaluation of human T- and NK-cell responses including memory and follicular helper phenotype by intracellular cytokine staining. *Cytometry A* (2015) 87:289–92. doi:10.1002/cyto.a.22590
18. De Rosa SC, Carter DK, McElrath MJ. OMIP-014: validated multifunctional characterization of antigen-specific human T cells by intracellular cytokine staining. *Cytometry A* (2012) 81:1019–21. doi:10.1002/cyto.a.22218
19. R Core Team. *R: A Language and Environment for Statistical Computing*. (2015). Available from: http://www.r-project.org/
20. Finak G, Frelinger J, Jiang W, Newell EW, Ramey J, Davis MM, et al. OpenCyto: an open source infrastructure for scalable, robust, reproducible, and automated, end-to-end flow cytometry data analysis. *PLoS Comput Biol* (2014) 10:e1003806. doi:10.1371/journal.pcbi.1003806
21. Fitzmaurice GM, Laird NM, Ware JH. *Applied Longitudinal Analysis*. Hoboken, NJ: Wiley (2011).
22. Betts MR, Krowka JF, Kepler TB, Davidian M, Christopherson C, Kwok S, et al. Human immunodeficiency virus type 1-specific cytotoxic T lymphocyte activity is inversely correlated with HIV type 1 viral load in HIV type 1-infected long-term survivors. *AIDS Res Hum Retroviruses* (1999) 15:1219–28. doi:10.1089/088922299310313
23. Burton BK, Thorup AAE, Jepsen JR, Poulsen G, Ellersgaard D, Spang KS, et al. Impairments of motor function among children with a familial risk of schizophrenia or bipolar disorder at 7 years old in Denmark: an observational cohort study. *Lancet Psychiatry* (2017) 4:400–8. doi:10.1016/S2215-0366(17)30103-7
24. Doody RS, Raman R, Farlow M, Iwatsubo T, Vellas B, Joffe S, et al. A phase 3 trial of semagacestat for treatment of Alzheimer's disease. *N Engl J Med* (2013) 369:341–50. doi:10.1056/NEJMoa1210951
25. Finak G, Mcdavid A, Chattopadhyay P, Dominguez M, De Rosa S, Roederer M, et al. Mixture models for single-cell assays with applications to vaccine studies. *Biostatistics* (2014) 15:87–101. doi:10.1093/biostatistics/kxt024
26. Lin L, Finak G, Ushey K, Seshadri C, Hawn TR, Frahm N, et al. COMPASS identifies T-cell subsets correlated with clinical outcomes. *Nat Biotechnol* (2015) 33:610–6. doi:10.1038/nbt.3187
27. Holm S. A simple sequentially rejective multiple test procedure. *Scand J Stat* (1979) 6:65–70. doi:10.2307/4615733
28. Benjamini Y, Hochberg Y, Benjamini Y, Hochberg Y. Controlling the false discovery rate: a practical and powerful approach to multiple testing. *J R Stat Soc B* (1995) 57:289–300. doi:10.2307/2346101
29. Depinay N, Franetich JF, Grüner AC, Mauduit M, Chavatte J-MM, Luty AJF, et al. Inhibitory effect of TNF-α on malaria pre-erythrocytic stage development: influence of host hepatocyte/parasite combinations. *PLoS One* (2011) 6:e17464. doi:10.1371/journal.pone.0017464
30. Mazier D, Rénia L, Nussler A, Pied S, Marussig M, Goma J, et al. Hepatic phase of malaria is the target of cellular mechanisms induced by the previous and the subsequent stages. A crucial role for liver nonparenchymal cells. *Immunol Lett* (1990) 25:65–70. doi:10.1016/0165-2478(90)90093-6

31. Korten S, Anderson RJ, Hannan CM, Sheu EG, Sinden R, Gadola S, et al. Invariant Valpha14 chain NKT cells promote *Plasmodium berghei* circumsporozoite protein-specific gamma interferon- and tumor necrosis factor alpha-producing CD8+ T cells in the liver after poxvirus vaccination of mice. *Infect Immun* (2005) 73:849–58. doi:10.1128/IAI.73.2.849-858.2005
32. Seder RA, Darrah PA, Roederer M. T-cell quality in memory and protection: implications for vaccine design. *Nat Rev Immunol* (2008) 8:247–58. doi:10.1038/nri2274
33. Horowitz A, Behrens RH, Okell L, Fooks AR, Riley EM. NK cells as effectors of acquired immune responses: effector CD4+ T cell-dependent activation of NK cells following vaccination. *J Immunol* (2010) 185:2808–18. doi:10.4049/jimmunol.1000844
34. Horowitz A, Newman KC, Evans JH, Korbel DS, Davis DM, Riley EM. Cross-talk between T cells and NK cells generates rapid effector responses to *Plasmodium falciparum*-infected erythrocytes. *J Immunol* (2010) 184:6043–52. doi:10.4049/jimmunol.1000106
35. Crompton PD, Moebius J, Portugal S, Waisberg M, Hart G, Garver LS, et al. Malaria immunity in man and mosquito: insights into unsolved mysteries of a deadly infectious disease. *Annu Rev Immunol* (2014) 32:157–87. doi:10.1146/annurev-immunol-032713-120220
36. Vogelzang A, Perdomo C, Zedler U, Kuhlmann S, Hurwitz R, Gengenbacher M, et al. Central memory CD4$^+$ T cells are responsible for the recombinant bacillus Calmette-Guérin ΔureC:hly vaccine's superior protection against tuberculosis. *J Infect Dis* (2014) 210:1928–37. doi:10.1093/infdis/jiu347
37. Reece WHH, Pinder M, Gothard PK, Milligan P, Bojang K, Doherty T, et al. A CD4 + T-cell immune response to a conserved epitope in the circumsporozoite protein correlates with protection from natural *Plasmodium falciparum* infection and disease. *Nat Med* (2004) 10:406–10. doi:10.1038/nm1009
38. Zaph C, Uzonna J, Beverley SM, Scott P. Central memory T cells mediate long-term immunity to *Leishmania major* in the absence of persistent parasites. *Nat Med* (2004) 10:1104–10. doi:10.1038/nm1108
39. Sallusto F, Geginat J, Lanzavecchia A. Central memory and effector memory T cell subsets: function, generation, and maintenance. *Annu Rev Immunol* (2004) 22:745–63. doi:10.1146/annurev.immunol.22.012703.104702
40. Sallusto F, Lenig D, Förster R, Lipp M, Lanzavecchia A. Two subsets of memory T lymphocytes with distinct homing potentials and effector functions. *Nature* (1999) 401:708–12. doi:10.1038/44385
41. Crotty S. Follicular helper CD4 T cells (TFH). *Annu Rev Immunol* (2011) 29:621–63. doi:10.1146/annurev-immunol-031210-101400
42. Spensieri F, Borgogni E, Zedda L, Bardelli M, Buricchi F, Volpini G, et al. Human circulating influenza-CD4+ ICOS1+IL-21+ T cells expand after vaccination, exert helper function, and predict antibody responses. *Proc Natl Acad Sci U S A* (2013) 110:14330–5. doi:10.1073/pnas.1311998110
43. van Kooten C, Banchereau J. CD40-CD40 ligand. *J Leukoc Biol* (2000) 67:2–17.
44. McGuire HM, Vogelzang A, Warren J, Loetsch C, Natividad KD, Chan TD, et al. IL-21 and IL-4 collaborate to shape T-dependent antibody responses. *J Immunol* (2015) 195:5123–35. doi:10.4049/jimmunol.1501463
45. Darrah PA, Patel DT, De Luca PM, Lindsay RWB, Davey DF, Flynn BJ, et al. Multifunctional TH1 cells define a correlate of vaccine-mediated protection against *Leishmania major*. *Nat Med* (2007) 13:843–50. doi:10.1038/nm1592
46. Kannanganat S, Ibegbu C, Chennareddi L, Robinson HL, Amara RR. Multiple-cytokine-producing antiviral CD4 T cells are functionally superior to single-cytokine-producing cells. *J Virol* (2007) 81:8468–76. doi:10.1128/JVI.00228-07
47. Shann F. Nonspecific effects of vaccines and the reduction of mortality in children. *Clin Ther* (2013) 35:109–14. doi:10.1016/j.clinthera.2013.01.007
48. Kleinnijenhuis J, Quintin J, Preijers F, Joosten LAB, Ifrim DC, Saeed S, et al. Bacille Calmette-Guerin induces NOD2-dependent nonspecific protection from reinfection via epigenetic reprogramming of monocytes. *Proc Natl Acad Sci U S A* (2012) 109:17537–42. doi:10.1073/pnas.1202870109

Conflict of Interest Statement: The authors declare that the research was conducted in the absence of any commercial or financial relationships that could be construed as a potential conflict of interest.

Chapter 3

Safety, Immunogenicity, and Protective Efficacy against Controlled Human Malaria Infection of *Plasmodium falciparum* Sporozoite Vaccine in Tanzanian Adults

This chapter contains the following manuscript (accepted for publication in The American Journal of Tropical Medicine and Hygiene)

Said A. Jongo, Seif A. Shekalage, L. W. Preston Church, Adam J. Ruben, Tobias Schindler, Isabelle Zenklusen, **Tobias Rutishauser**, Julian Rothen, Anneth Tumbo,1 Catherine Mkindi, Maxmilian Mpina, Ali T. Mtoro, Andrew S. Ishizuka, Kassim Kamaka Ramadhani, Florence A. Milando, Munira Qassim, Omar A. Juma, Solomon Mwakasungula, Beatus Simon, Eric R. James, Yonas Abebe, Natasha K. C., Sumana Chakravarty, Elizabeth Saverino, Bakari M. Bakari, Peter F. Billingsley, Robert A. Seder, Claudia Daubenberger, B. Kim Lee Sim, Thomas L. Richie, Marcel Tanner, Salim Abdulla, and Stephen L. Hoffman, 2018. Safety, Immunogenicity, and Protective Efficacy against Controlled Human Malaria Infection of *Plasmodium falciparum* Sporozoite Vaccine in Tanzanian Adults. Am. J. Trop. Med. Hyg.

https://doi.org/10.4269/ajtmh.17-1014

Am. J. Trop. Med. Hyg., 99(2), 2018, pp. 338–349
doi:10.4269/ajtmh.17-1014

Safety, Immunogenicity, and Protective Efficacy against Controlled Human Malaria Infection of *Plasmodium falciparum* Sporozoite Vaccine in Tanzanian Adults

Said A. Jongo,[1]† Seif A. Shekalaghe,[1]† L. W. Preston Church,[2] Adam J. Ruben,[2] Tobias Schindler,[3,4] Isabelle Zenklusen,[3,4] Tobias Rutishauser,[3,4] Julian Rothen,[3,4] Anneth Tumbo,[1] Catherine Mkindi,[1] Maximillian Mpina,[1] Ali T. Mtoro,[1] Andrew S. Ishizuka,[5] Kamaka Ramadhani Kassim,[1] Florence A. Milando,[1] Munira Qassim,[1] Omar A. Juma,[1] Solomon Mwakasungula,[1] Beatus Simon,[1] Eric R. James,[2] Yonas Abebe,[2] Natasha KC,[2] Sumana Chakravarty,[2] Elizabeth Saverino,[2] Bakari M. Bakari,[1] Peter F. Billingsley,[2] Robert A. Seder,[5] Claudia Daubenberger,[3,4] B. Kim Lee Sim,[2,6] Thomas L. Richie,[2] Marcel Tanner,[3,4] Salim Abdulla,[1]† and Stephen L. Hoffman[2]*†

[1]*Bagamoyo Research and Training Centre, Ifakara Health Institute, Bagamoyo, Tanzania;* [2]*Sanaria Inc., Rockville, Maryland;* [3]*Swiss Tropical and Public Health Institute (Swiss TPH), Basel, Switzerland;* [4]*University of Basel, Basel, Switzerland;* [5]*Vaccine Research Center (VRC), National Institute of Allergy and Infectious Diseases, National Institutes of Health, Bethesda, Maryland;* [6]*Protein Potential LLC, Rockville, Maryland*

Abstract. We are using controlled human malaria infection (CHMI) by direct venous inoculation (DVI) of cryopreserved, infectious *Plasmodium falciparum* (Pf) sporozoites (SPZ) (PfSPZ Challenge) to try to reduce time and costs of developing PfSPZ Vaccine to prevent malaria in Africa. Immunization with five doses at 0, 4, 8, 12, and 20 weeks of 2.7×10^5 PfSPZ of PfSPZ Vaccine gave 65% vaccine efficacy (VE) at 24 weeks against mosquito bite CHMI in U.S. adults and 52% (time to event) or 29% (proportional) VE over 24 weeks against naturally transmitted Pf in Malian adults. We assessed the identical regimen in Tanzanians for VE against PfSPZ Challenge. Twenty- to thirty-year-old men were randomized to receive five doses normal saline or PfSPZ Vaccine in a double-blind trial. Vaccine efficacy was assessed 3 and 24 weeks later. Adverse events were similar in vaccinees and controls. Antibody responses to Pf circumsporozoite protein were significantly lower than in malaria-naïve Americans, but significantly higher than in Malians. All 18 controls developed Pf parasitemia after CHMI. Four of 20 (20%) vaccinees remained uninfected after 3 week CHMI ($P = 0.015$ by time to event, $P = 0.543$ by proportional analysis) and all four (100%) were uninfected after repeat 24 week CHMI ($P = 0.005$ by proportional, $P = 0.004$ by time to event analysis). *Plasmodium falciparum* SPZ Vaccine was safe, well tolerated, and induced durable VE in four subjects. Controlled human malaria infection by DVI of PfSPZ Challenge appeared more stringent over 24 weeks than mosquito bite CHMI in United States or natural exposure in Malian adults, thereby providing a rigorous test of VE in Africa.

INTRODUCTION

In 2015 and in 2016, there were an estimated 429,000–730,500 deaths caused by malaria.[1–3] *Plasmodium falciparum* (Pf) is the cause of > 98% of malaria deaths and > 80% of malaria cases in sub-Saharan Africa. Our goal is to field a vaccine that will prevent infection with Pf and thereby prevent all manifestations of Pf malaria and parasite transmission from humans to mosquitoes.[4]

Plasmodium falciparum sporozoites (SPZ) are the only immunogens that have ever prevented Pf infection in > 90% of subjects.[5–7] Sanaria® PfSPZ Vaccine (Sanaria Inc., Rockville, MD) is composed of radiation-attenuated, aseptic, purified, cryopreserved PfSPZ.[8,9] When administered by rapid intravenous injection, PfSPZ Vaccine protected 100% (6/6) of malaria-naïve subjects in the United States against mosquito bite–controlled human malaria infection (CHMI) with Pf parasites similar to those in the vaccine (homologous) 3 weeks after the last immunization,[10] and 65% at 24 weeks.[11] Protection was durable against homologous mosquito bite CHMI for at least 59 weeks[12] and heterologous (parasites different than in vaccine) mosquito bite CHMI for at least 33 weeks.[13] PfSPZ Vaccine also prevented naturally transmitted heterogeneous Pf in adults in Mali for at least 24 weeks (vaccine efficacy [VE] 52% by time to event and 29% by proportional analysis).[14]

We used the same dosage regimen as in the United States and Mali to evaluate the tolerability, safety, immunogenicity, and VE of PfSPZ Vaccine in young adult male Tanzanians. Previously, we had conducted the first modern CHMI in Africa and showed that injection of aseptic, purified, cryopreserved PfSPZ, Sanaria® PfSPZ Challenge, consistently infected Tanzanian volunteers and subsequently repeated in multiple other countries.[15–21] In this study, we took advantage of this capability to assess VE of PfSPZ Vaccine by CHMI with PfSPZ Challenge (NF54). The same PfSPZ Vaccine dosage regimen was less immunogenic and protective in Tanzanians than in Americans,[11] and VE against homologous CHMI in Tanzania was lower (or similar) to VE against intense field exposure to heterogeneous Pf parasites in Mali.[14]

MATERIAL AND METHODS

Study design and population. This double-blind, randomized, controlled trial was conducted in Bagamoyo, Tanzania, between April 2014 and August 2015. Sixty-seven healthy male volunteers of 18–35 years of age were recruited from higher learning institutions in Dar es Salaam. After initial screening, prospective volunteers were invited to the Bagamoyo Clinical Trial Unit of the Ifakara Health Institute (IHI) to complete informed consent and screening.

All had to complete a 20-question assessment of trial understanding with a 100% correct response rate on the first or second attempt (Supplemental Table 1) to be eligible. Volunteers were screened using predetermined inclusion and exclusion criteria (Supplemental Tables 2 and 3). History of malaria in the previous 5 years or antibodies to Pf exported protein 1 (PfEXP1) by an enzyme-linked immunosorbent assay (ELISA) above a level associated with a single, recent Pf infection by CHMI[19] (see the Antibody assays section) were the exclusion criteria. Hematology, biochemistry, and parasitology testing, including malaria thick blood smear (TBS), stool,

* Address correspondence to Stephen L. Hoffman, Sanaria Inc., 9800 Medical Center Dr., Suite A209, Rockville, MD 20850. E-mail: slhoffman@sanaria.com
† These authors contributed equally to this study.

and urine by microscopy was carried out. Tests for human immunodeficiency virus and hepatitis B and C were performed after counseling; volunteers were excluded if positive and referred for evaluation and management by appropriate local physicians. Volunteers were excluded if they had significant abnormalities on electrocardiograms.

The trial was performed in accordance with Good Clinical Practices. The protocol was approved by institutional review boards (IRBs) of the IHI (Ref. No. IHI/IRB/No:02-2014), the National Institute for Medical Research Tanzania (NIMR/HQ/R.8a/Vol.IX/1691), the Ethikkommission Nordwest-und Zentralschweiz, Basel, Switzerland (reference number 261/13), and by the Tanzania Food and Drug Authority (Ref. No. TFDA 13/CTR/0003); registered at Clinical Trials.gov (NCT02132299); and conducted under U.S. FDA IND application.

Investigational products (IPs). The IPs were Sanaria® PfSPZ Vaccine[8–14] and Sanaria® PfSPZ Challenge.[15–20] PfSPZ Vaccine consists of aseptic, purified, vialed, metabolically active, nonreplicating (radiation attenuated), cryopreserved PfSPZ (NF54 strain). It was stored, thawed, diluted, and administered by direct venous inoculation (DVI) in 0.5 mL through a 25-gauge needle.[11,14,18,20] PfSPZ Challenge is identical to PfSPZ Vaccine except it is not radiation attenuated. It was handled and administered like PfSPZ Vaccine. Preparation of IPs was supervised by the study pharmacist. After labeling the syringe, the pharmacist handed it to the clinical team through a window.

Allocation and randomization. Volunteers were allocated to five groups (Table 1; Figure 1). Forty-nine received PfSPZ Vaccine and eight normal saline (NS). Ten were additional infectivity controls. The clinical team and volunteers were blinded to assignment to vaccine or NS until study end.

Group 1. Three volunteers received consecutive doses of 3×10^4, 1.35×10^5, and 2.7×10^5 PfSPZ of PfSPZ Vaccine at 4-week intervals to assess safety (Group 1).

Groups 2 and 3. Volunteers were randomized to receive 1.35×10^5 PfSPZ of PfSPZ Vaccine ($N = 20$) or NS ($N = 4$) (Group 2), or 2.7×10^5 PfSPZ of PfSPZ Vaccine ($N = 20$) or NS ($N = 4$) (Group 3) at 0, 4, 8, 12, and 20 weeks.

Group 4. Six volunteers were immunized with 2.7×10^5 PfSPZ of PfSPZ Vaccine on the same schedule as Group 3.

Group 5. Ten volunteers served as unblinded infectivity controls during CHMIs (see in the following paragraph): two with CHMI #1, two with CHMI #2, and six with CHMI #3.

Vaccine efficacy. *Controlled human malaria infection.* Vaccine efficacy was assessed by CHMI by DVI of 3.2×10^3 PfSPZ of PfSPZ Challenge. Controlled human malaria infection #1 was 3 weeks after the last immunization in Group 2. Controlled human malaria infection #2 was 3 weeks after the last immunization in Group 3. Controlled human malaria infection #3 was 24 weeks after the last immunization in Groups 3 and 4 and included the four volunteers in Group 3 who did not develop parasitemia after CHMI #2 and the six Group 4 volunteers. Volunteers were inpatients from day 9 after PfSPZ Challenge injection for observation until diagnosed and treated for malaria or until day 21; daily outpatient monitoring for TBS-negative volunteers continued until day 28. Thick blood smears were obtained every 12 hours on days 9–14 after CHMI and daily on days 15–21 until positive or until day 21. Thick blood smears could be performed more frequently, if volunteers had symptoms/signs consistent with malaria. After initiation of treatment, TBSs were assessed until two consecutive daily TBSs were negative and on day 28.

Detection of Pf parasites and parasite DNA. Slide preparation and reading for TBSs were performed as described.[19] Sensitivity was 2 parasites/μL blood unless the volunteer was symptomatic, in which case four times as many fields were read. Parasitemia was also determined by quantitative polymerase chain reaction (qPCR) with sensitivity of 0.1 parasites/μL blood based on a multiplex assay detecting *Plasmodium* spp. 18S genes and the human RNaseP gene as endogenous control.[22] A second, more sensitive qPCR assay with a sensitivity of 0.05 parasites/μL blood and targeting the Pf-specific telomere-associated repetitive element 2[23] was used to reanalyze all samples that were negative by 18S-based qPCR. After the start of CHMI, the time of first blood sample positivity by qPCR was used to determine infection status and for the calculation of prepatent period. Volunteers were continuously monitored by qPCR until malaria treatment based on TBS positivity. The World Health Organization International Standard for Pf DNA Nucleic Acid Amplification Techniques (NIBSC, Hertfordshire, United Kingdom) was used as standard for calculation of parasite densities. DNA was extracted from 100 μL whole blood and eluted with 50 μL Elution Buffer using Quick-gDNA Blood MicroPrep Kit (Zymo Research, Irvine, CA). Blood samples were analyzed retrospectively by qPCR after storing at −80°C after the conclusion of CHMIs. To exclude field strain infections, parasite genotyping was performed on samples randomly chosen as described.[24] In all cases in which TBS was negative and qPCR was considered positive, two consecutive samples were positive by qPCR.

Adverse events (AEs). Volunteers were observed as inpatients for 48 hours after administration of IP and discharged with diaries and thermometers for recording AEs and temperatures and followed with daily telephone calls. Symptoms and signs (solicited and unsolicited) were recorded and graded by physicians: mild (easily tolerated), moderate (interfere with normal activity), severe (prevents normal activity),

TABLE 1
Demographic characteristics of volunteers

	Vaccinees	Normal saline controls	Infectivity controls
Number of volunteers	49	8	10
Percentage males	100%	100%	100%
Mean age in years (range)	24 (20, 30)	23 (20, 28)	25 (21, 28)
Percentage Africans	100%	100%	100%
Mean body mass index (range)	22.33 (18.00, 29.70)	21.91 (19.00, 24.20)	21.68 (18.40, 24.30)
Number (%) heterozygous for alpha thalassemia	22 (44.9%)	4 (50%)	5 (50%)
Number (%) with LTBI* (QuantiFERON positive)	17 (34.7%)	3 (36.5%)	1 (10%)
Number (%) positive on screening of urine or stool for parasitic infection	0 (0%)	1 (12.5%)	0 (0%)
Number (%) students	49 (100%)	8 (100%)	10 (100%)

* Latent tuberculosis infection.

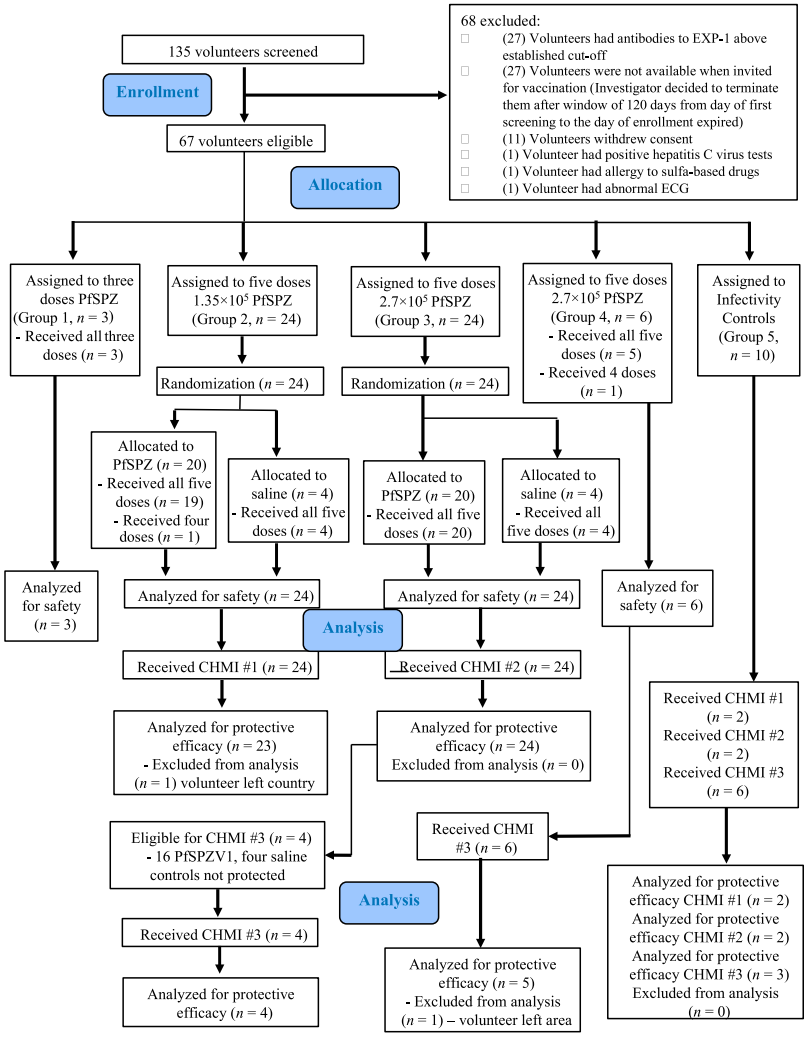

FIGURE 1. Volunteer participation (CONSORT 2010 diagram). This figure appears in color at www.ajtmh.org.

or life threatening. Axillary temperature was grade 1 (> 37.5–38.0°C), grade 2 (> 38.0–39.0°C), grade 3 (> 39.0–40.0°C), or grade 4 (> 40.0°C). Hematological and biochemical abnormalities were also assessed using standard clinical assays.

During the first 7 days after injection of IPs, prespecified local (site of injection) and systemic AEs were solicited. Open-ended questioning was used to identify unsolicited AEs through day 28 (Supplemental Table 4). All AEs were assessed for severity and relatedness to IP administration. Adverse events were classified as definitely related, probably related, possibly related, unlikely to be related, and not related. Definitely, probably, and possibly were considered to be related. Unlikely to be related and not related were considered to be unrelated. For CHMIs, volunteers returned on day 9 for admission to the ward for diagnosis and treatment of malaria. Events during the 8–28 day period were assessed for relationship to Pf infection and considered related if the event was within 3 days before and 7 days after TBS was first positive.

Antibody assays. Sera were assessed for antibodies by ELISA, immunofluorescence assay (aIFA), and inhibition of sporozoite invasion (ISI) assay as described (see Supplemental Table 5).[25] For ELISAs, the results are reported as the serum dilution at which the optical density (OD) was 1.0. Enzyme-linked immunosorbent assay for PfEXP1 was used to screen volunteers for possible malaria exposure (Supplemental Table 6). Any subject with an OD 1.0 of ≥ 600 was excluded. This was because we had previously determined in Tanzanians who underwent CHMI[19] that antibodies to PfEXP1 at this level were a sensitive indicator of recent Pf infection (unpublished).

T-cell assays. T-cell responses in cryopreserved peripheral blood mononuclear cells (PBMC) were measured by flow cytometry in a single batch after the study as described.[12] After stimulation, cells were stained as described.[26] The staining panels are in Supplemental Table 7 and antibody clones and manufacturers are in Supplemental Table 8. All antigen-specific frequencies are reported after background

subtraction of identical gates from the same sample incubated with control antigen. Data were analyzed with FlowJo v9.9.3 (TreeStar, Ashland, OR) and graphed in Prism v7.0a (GraphPad, San Diego, CA).

Statistical analysis. Comparisons of categorical variables between groups were analyzed using 2-tailed Fisher's exact test. Comparisons of continuous variables between groups were analyzed by 2-tailed nonparametric tests. For multiple group comparisons, the Kruskal–Wallis test was used. Time to event was assessed by the Kaplan–Meier curves and log-rank test. Vaccine efficacy by time to event was quantified using Cox proportional hazards ratios. Time to event data were analyzed from CHMI injection until positive TBS result or positive qPCR result. Controlled human malaria infection follow-up period lasted until day 28 after CHMI injection. Analyses of immunological data are described with the data.

Role of the funding source. The funders were involved in study design, study management, data collection, data analysis, data interpretation, and writing the report. Salim Abdulla and Stephen L. Hoffman had full access to all data in the study and final responsibility for decision to submit for publication.

RESULTS

Study population and experience with DVI. Fifty-seven Tanzanian men (Table 1; Figure 1) met the criteria (Supplemental Tables 2 and 3) and received PfSPZ Vaccine ($N = 49$) or NS ($N = 8$). All volunteers had AA hemoglobin and normal G6PD activity. Thirty-one volunteers (46%) were heterozygous for α-thalassemia; 21 had evidence of latent tuberculosis infection by Quantiferon testing, but showed no evidence of active tuberculosis. One volunteer (group 2, NS) had *Strongyloides stercoralis* on screening and was successfully treated before vaccination (Table 1).

Of 237 immunizations with PfSPZ Vaccine, 234 were completed with a single injection (98.7%). Two hundred and thirty injections (97.0%) were considered painless by the volunteer. For NS subjects, 39 of 40 immunizations (97.5%) were completed in a single injection and 39 of 40 (97.5%) considered painless by the volunteer. The nurse performing immunizations considered the procedure to be simple in 265 of 273 single injections (97.1%).

One subject in Group 2 received four immunizations. The third immunization was withheld while the subject was evaluated for what was diagnosed as benign ethnic neutropenia.[27,28] One subject in Group 4 missed his second immunization when he left town. All other subjects (other than Group 1 and added infectivity controls) received five immunizations.

Safety. Among 49 volunteers who received 237 doses of PfSPZ Vaccine, there were 17 solicited AEs possibly related to IP (17/237 = 7.2%) in 10 of the 49 vaccinees (20.4%) (Table 2). Among eight volunteers who received 40 doses of NS, there were two solicited AEs possibly related to IP (2/40 = 5.0%) in one of the eight controls (12.5%) (Table 2). There were no AEs considered by the clinicians to be probably or definitely related to IP. There were no local or serious AEs. One episode each of headache and fever were grade 2; all other solicited AEs were grade 1. None of the comparisons of AEs between vaccinees and controls or between Group 2 (1.35×10^5 PfSPZ) and Groups 3 and 4 (2.7×10^5 PfSPZ) showed statistically significant differences (Table 2). Twenty-six of 49 vaccinees (53.1%) experienced 43 unsolicited AEs (0.88/individual) in the 28 days following injections #1–#4 and the 21 days before CHMI after injection #5. Seven of eight controls (87.5%) experienced 14 unsolicited AEs (2/individual) during this period. None of these unsolicited AEs recorded within 28 days of an immunization was considered related to IP.

Laboratory abnormalities occurred at roughly equal rates comparing PfSPZ Vaccine recipients and controls, except for leukocytosis and eosinophilia, which were more frequent in controls (Table 3). There was no apparent explanation for these differences. A cyclic variation in total bilirubin following

TABLE 2

Solicited AEs by group considered possibly* related to administration of the investigational product during the first 7 days post immunization

	Group 1 (dose escalation)	Group 2 (1.35×10^5 PfSPZ)	Group 3 (2.7×10^5 PfSPZ)	Group 4 (2.7×10^5 PfSPZ)	Total PfSPZ vaccine	NS controls
Number of volunteers	3	20	20	6	49	8
Total number of injections	9	99	100	29	237	40
Number of local AEs	0	0	0	0	0	0
Numbers of systemic AEs (% of total immunizations)						
All	1 (11%)	10 (10.1%)	6 (6%)	0	17 (7.2%)	2 (5.0%)
Headache*	1 (11%)	7 (7%)†	2 (2%)	0	10 (4.2%)	1 (2.5%)
Abdominal pain	0	2 (2%)	1 (1%)	0	3 (1.3%)	0
Chills	0	0	1 (1%)	0	1 (0.4%)	0
Fever	0	0	2 (2%)	0	2 (0.8%)	0
Diarrhea	0	0	0	0	0	1 (2.5%)
Chest pain	0	1 (1%)	0	0	1 (0.4%)	0
Other	0	0	0	0	0	0
Systemic AEs - no. volunteers with ≥ 1 event (% of volunteers)						
Any	1 (33%)	7 (35%)	2 (10%)	0	10 (20.4%)	1 (13%)
Headache	1 (33%)	6 (30%)	2 (10%)	0	9 (18.4%)	1 (13%)
Abdominal pain	0	2 (10%)	1 (5%)	0	3 (6.1%)	0
Chills	0	0	1 (5%)	0	1 (2.0%)	0
Fever	0	0	2 (10%)	0	2 (4.1%)	0
Diarrhea	0	0	0	0	0	1 (13%)
Chest pain	0	1 (5%)	0	0	1 (2.0%)	0
All other	0	0	0	0	0	0

AEs = adverse events; PfSPZ = *Plasmodium falciparum* sporozoites. There were no significant differences between vaccinees as compared with normal saline (NS) controls for any or all AEs. All AEs were grade 1, except one headache and one fever. Local solicited AEs: injection site pain, tenderness, erythema, swelling, or induration. Systemic solicited AEs: allergic reaction (rash, pruritus, wheezing, shortness of breath, bronchospasm, allergy-related edema/angioedema, hypotension, and anaphylaxis), abdominal pain, arthralgia, chest pain/discomfort, chills, diarrhea, fatigue, fever, headache, malaise, myalgia, nausea, pain (other), palpitations, shortness of breath, and vomiting.

* All AEs were considered possibly related. None were considered probably or definitely related.

† 4/7 episodes of headache occurred after the third vaccine dose and did not recur with fourth or fifth doses. No factor was identified to account for this apparent clustering of headache.

each immunization was observed equally in volunteers receiving vaccine or NS that was attributed to enriched diet, as the volunteers were transported to Bagamoyo from Dar es Salaam during the periods of immunization and CHMI and were amply fed (see Supplemental Figure 1). In Dar es Salaam, malaria transmission is low. No volunteer had malaria during screening or during the trial other than from CHMI.

Tolerability, safety, and VE during CHMI. Forty-six vaccinees, eight NS controls, and 10 added infectivity controls underwent homologous CHMI. All subjects were negative by TBS and qPCR for Pf infection on the day of CHMI. Two volunteers were excluded from primary analysis—a Group 2 volunteer who left the area 2 days after administration of PfSPZ Challenge and a Group 4 volunteer who left 9 days after. Both volunteers were located and treated preemptively.

Tolerability and safety of administration of PfSPZ challenge. Controlled human malaria infection was well tolerated with no local solicited AEs and three systemic solicited AEs (grade 1 headache in Group 3, grade 2 headache in Group 4, and grade 1 arthralgia in an infectivity control) in the 7 days post-administration of PfSPZ Challenge.

Parasitemia. Controls. The 18 NS and infectivity controls developed Pf infection after CHMI (16 TBS and qPCR positive and two TBS negative and qPCR positive) (Figure 2A–D and Supplemental Table 9). These included four NS and two infectivity controls in CHMI #1, the same in CHMI #2, and six infectivity controls in CHMI #3. All received the same lot of PfSPZ Challenge. One isolate of those positive from CHMI #1, one from CHMI #2, and four from CHMI #3 were genotyped,[24] and all parasites tested were PfNF54. Vaccine efficacy was calculated based on the results of qPCR assays from the six controls in CHMI #1, CHMI #2, and CHMI #3 individually (Figure 2D).

Group 2 (1.35×10^5 PfSPZ). Seventeen of 18 volunteers who received five doses and 1/1 volunteer who received four doses developed parasitemia (Figure 2A), 15 positive by TBS and qPCR, and 3 by qPCR only (CHMI #1) (Supplemental Table 10). One volunteer was negative through day 28 by TBS and qPCR. Vaccine efficacy by proportional analysis was 5.56% (95% confidence interval [CI]: 3.61%, 14.73%; $P > 0.99$, Fisher's exact test, 2-tailed). There was no significant delay in parasitemia by qPCR in the vaccinees as compared with controls ($P = 0.4481$ by log rank).

Group 3 (2.7×10^5 PfSPZ). First CHMI at 3 weeks (CHMI #2): 16/20 volunteers who received five doses developed parasitemia (Figure 2B), all positive by TBS and qPCR; four volunteers were negative through day 28 by TBS and qPCR. Vaccine efficacy by proportional analysis was 20% (95% CI: 4.62%, 35.38%; $P = 0.543$). There was a delay in the onset of parasitemia in vaccinees as compared with controls ($P = 0.015$ by log rank).

Second CHMI at 24 weeks (CHMI #3): The four uninfected volunteers from the first CHMI underwent a second CHMI 24 weeks after the last vaccine dose (Figure 2C). Three were negative by TBS and qPCR through day 28 day. The fourth volunteer, who was asymptomatic, was reported to have a positive TBS on day 12 and treated. The sample with positive TBS was negative by retrospective qPCR. Reevaluation of the TBS indicated an error in slide reading (false-positive). Vaccine efficacy by proportional analysis at this time point was 100% (for 3/3 and 4/4 protected: 95% CI: 43.8%, 100%, and 51.01%, 100%; $P = 0.012$ and 0.005, respectively). However, given the 20% VE at 3 weeks by proportional analysis, overall VE by proportional analysis was considered to be 20%.

Group 4 (2.7×10^5 PfSPZ). First CHMI at 24 weeks after the last vaccine dose (CHMI #3): 4/5 vaccinees developed parasitemia by TBS and qPCR. The fifth was negative by TBS, but positive by qPCR (see Supplemental Table 10). There was one excluded volunteer (see the previous paragraph). Vaccine efficacy by proportional analysis was 0% ($P > 0.99$%). There was a significant delay in the onset of parasitemia by qPCR in vaccinees as compared with controls ($P = 0.001$ by log rank).

α-thalassemia. Volunteers heterozygous for α-thalassemia were no more likely to be TBS negative and qPCR positive than volunteers without α-thalassemia (three of 27 versus three of 34, $P = 1.0$). Protection from CHMI did not correlate with α-thalassemia status; 3/37 with normal hemoglobin and 2/29 heterozygous for α-thalassemia were protected.

TABLE 3
Summary of abnormal laboratory values and severity grades

Laboratory parameter	Vaccinees in Group 2 (1.35×10^5 PfSPZ) ($N = 20$)		Vaccinees in groups 3 and 4 (2.7×10^5 PfSPZ) ($N = 26$)		NS controls ($N = 8$)		P values: vaccinees ($N = 46$) vs. controls ($N = 8$)
	No.	%	No.	%	No.	%	
Leukocytosis	1	5	2	7.7	3	37.5	0.0358
Leukopenia	6	30	7	27	1	12.5	> 0.05
Neutropenia	6	30	5	19	2	25	> 0.05
Lymphopenia	3	15	3	11.5	2	25	> 0.05
Eosinophilia	0	0	2	7.7	3	37.5	0.0194
Decreased hemoglobin	1	5	0	0	0	0	> 0.05
Thrombocytopenia	1	5	0	0	0	0	> 0.05
Elevated creatinine	2	10	4	15.4	2	25	> 0.05
Low total bilirubin	4	20	7	27	1	12.5	> 0.05
Elevated total bilirubin	2	10	2	7.7	2	25	> 0.05
Elevated alkaline phosphatase	1	5	2	7.7	0	0	> 0.05
Elevated alanine aminotransferase	3	15	5	19	2	25	> 0.05
Elevated aspartate aminotransferase	0	0	3	11.5	0	0	> 0.05

PfSPZ = *Plasmodium falciparum* sporozoites. *P* values calculated using Fisher's exact test (2-tailed). One volunteer who received saline developed Grade 3 eosinophilia attributed to *Strongyloides stercoralis* infection, which improved with anthelminthic therapy. This volunteer had a baseline of mild eosinophilia, which persisted throughout the clinical trial. All other laboratory abnormalities were Grade 2 or less. There was no association between laboratory abnormalities and time after a dose or increasing number of doses. Three abnormalities during immunization were deemed clinically significant or Grade 3. One was diagnosed as benign ethnic neutropenia, one was lymphopenia associated with an infected foot laceration, and one was eosinophilia associated with *Fasciolopsis buski* and *S. stercoralis* infection. Lymphopenia and eosinophilia resolved with treatment. Two Group 4 volunteers had asymptomatic hookworm infections diagnosed before controlled human malaria infection; one was coinfected with *Enterobius vermicularis*.

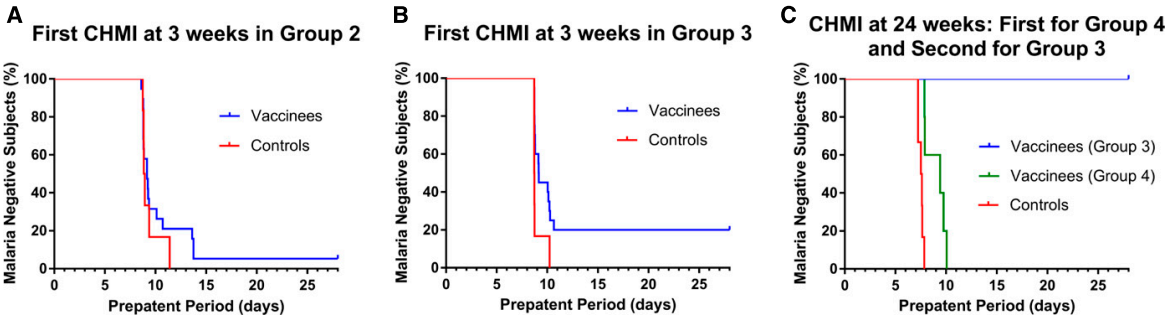

D

Group	Timing of CHMI	Number protected/ Number underwent CHMI	Vaccine efficacy by proportional analysis	Vaccine efficacy by proportional analysis 95% CI	Vaccine efficacy by proportional analysis *P* value (Fisher's Exact Test, 2-tailed)	Median prepatent period by qPCR of positive vaccinees (days)****	Median prepatent period by qPCR of controls (days)****	Log rank test
2 (1.35×10^5 PfSPZ)	3 weeks after fifth immunization	1/18	5.56%	(-3.61%, 14.73%)	> 0.999	9.2	8.9	0.45
3 (2.7×10^5 PfSPZ)	3 weeks after fifth immunization	4/20	20%	(4.62%, 35.38%)	0.543	9.0	8.7	**0.02**
3 (2.7×10^5 PfSPZ)	24 weeks after fifth immunization*	3/3 or 4/4**	100% (20% overall)	(43.85%, 100%) or (51.01%, 100%)***	**0.012 or 0.005****	not applicable	7.6	**0.01 or 0.004****
4 (2.7×10^5 PfSPZ)	24 weeks after fifth immunization	0/5	0%	(0.00%, 25.88%)***	> 0.999	8.7	7.6	**< 0.001**

FIGURE 2. Kaplan–Meier survival curves in immunized volunteers vs. controls as assessed by quantitative polymerase chain reaction (qPCR). Kaplan–Meier curves in volunteers undergoing controlled human malaria infection (CHMI) 3 weeks after the last of five doses with 1.35×10^5 (Group 2) (**A**) or 2.7×10^5 (Group 3) (**B**) *Plasmodium falciparum* Sporozoites (PfSPZ) of PfSPZ Vaccine. Panel (**C**) volunteers undergoing either first (Group 4) or second (Group 3) CHMI 24 weeks after the fifth immunization with 2.7×10^5 PfSPZ of PfSPZ Vaccine. (**D**) Vaccine efficacy and prepatent period results. *This was the second CHMI for the 4 volunteers in Group 3 who were protected after the first CHMI at 3 weeks. **One volunteer was inappropriately treated on day 13 for a false positive TBS. Without this volunteer, 3/3 protected. With this volunteer 4/4 were protected. ***Confidence intervals were calculated using Wilson's score interval. ****Volunteers in CHMI #1 and #2 (3 week CHMI in Groups 2 and 3) had specimens first acquired on day9. Volunteers in CHMI #3 (24 week CHMI in Groups 3 and 4) had specimens first acquired on day 8. This figure appears in color at www.ajtmh.org.

Prepatent periods and parasite densities. Although the median prepatent periods by TBS in controls in each CHMI group (12.5, 13.0, and 12.0, respectively) were shorter than in the vaccinees in Groups 2–4 (14.0, 14.0, and 15.3 days, respectively), these differences did not reach the level of statistical significance ($P = 0.486$, $P = 0.491$, and $P = 0.333$, respectively) (Supplemental Table 9). The prepatent periods by qPCR in vaccineees in Group 3 (3 and 24 week CHMIs) and Group 4 (24 week CHMI) were significantly longer than in the respective controls (Figure 2D). The parasite densities by qPCR and TBS at the time of diagnosis for each individual are in Supplemental Table 10. The median parasite density in controls versus vaccinees at the time of first positivity were 0.5 versus 0.4 parasites/μL for qPCR ($P = 0.5714$) and 11.2 versus 15.0 parasites/μL for TBS ($P = 0.1492$).

Tolerability and safety of parasitemia during CHMI. Controls. Sixteen controls developed parasitemia by TBS; 9 (56%) never had symptoms (Supplemental Table 11). Headache occurred in 7/7 symptomatic individuals. One of two control volunteers only positive by qPCR did not have any symptoms; the second had headache 8 days after qPCR spontaneously reverted to negative. No volunteer had symptoms at the time of first positive qPCR.

Vaccinees. Thirty-five immunized volunteers developed parasitemia by TBS; 20 (57%) never had symptoms. Three volunteers had temperature > 39.0°C; all other clinical manifestations were grade 1 or 2. Fever (28.6%) and headache (31.4%) were most common. Compared with controls, elevated temperature was more common in vaccinees with positive TBSs (9/35 versus 0/16, $P = 0.043$). There was no significant difference in the frequency of headache between controls and vaccinees. In the three volunteers in Group 2 who were qPCR positive and TBS negative, one developed headache 3 days after qPCR positivity. No volunteer had symptoms at the time of first positive qPCR.

Clinical laboratories. No unexpected changes were observed following CHMI. Declines in lymphocyte counts were observed in TBS positive controls and vaccinees (mean decline 1,110 ± 720 cells/μL and 1,180 ± 680 cells/μL, respectively) on day of first positive TBS. Absolute lymphocyte

counts less than 1,000 cells/μL were observed in 8/16 and 16/35 TBS positive controls and vaccinees. All lymphocyte counts returned to the baseline by day 28. There were mild decreases in platelet counts in TBS positive subjects, but all platelet counts were > 100 × 10^3 cells/μL.

Treatment. Volunteers with positive TBSs were treated with either atovaquone/proguanil (*N* = 43) or artemether/lumefantrine (*N* = 8) within 24 hours of first positive TBS. Normal saline and infectivity controls who were TBS negative (*N* = 2) were treated at day 28.

Immunogenicity. *Antibody responses.* Pf circumsporozoite protein (PfCSP) and PfSPZ. Antibodies against PfCSP by ELISA 1), PfSPZ by aIFA 2), and PfSPZ by ISI 3) in sera taken 2 weeks after the last vaccine dose and just before CHMI (20–23 days after the last dose) for Groups 2 (CHMI #1) and 3 (CHMI #2) are in Figure 3A–C. The median responses and those uninfected and infected by qPCR are shown.

For all three assays, median antibody responses before first CHMI were higher in uninfected than in infected vaccinees. There was a significant difference in median net aIFA

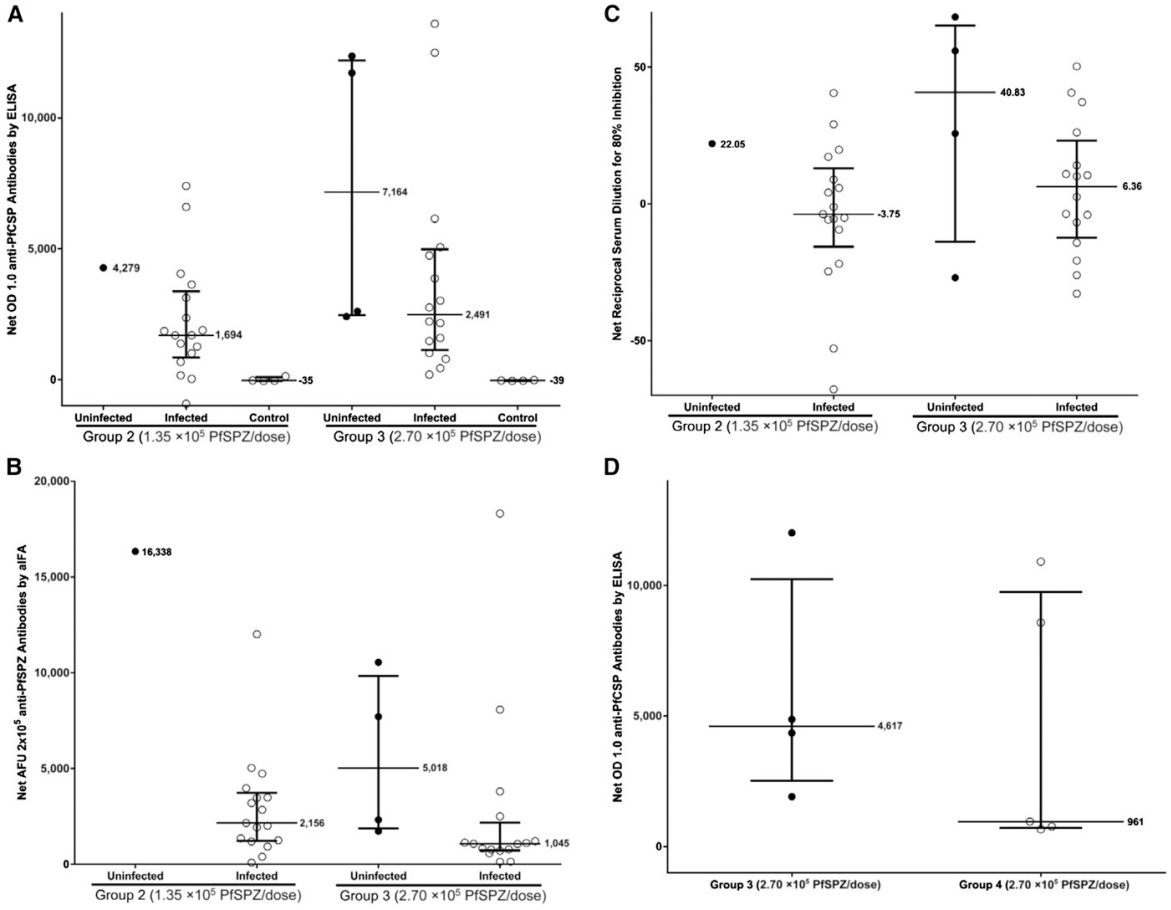

FIGURE 3. Antibody responses to *Plasmodium falciparum* Sporozoites (PfSPZ) and PfCSP before controlled human malaria infection (CHMI). For all assays, uninfected subjects are shown as filled (black) circles and infected subjects are open circles. For each of the defined subject groups, the interquartile ranges and the median values of response of subjects in each group are shown. Assessment of antibodies was performed in sera from subjects before immunization and before CHMI #1 (~2 weeks after the last dose of PfSPZ Vaccine or normal saline [NS]) and/or CHMI #2 (~24 weeks after last dose of PfSPZ or NS) (**A**, **D**). Antibodies to PfCSP by ELISA are reported as net optical density (OD) 1.0 (the difference in OD 1.0 between pre-CHMI and preimmunization sera). (**B**, **E**) Antibodies to PfSPZ by aIFA are reported as net AFU 2 × 10^5, the reciprocal serum dilution at which the fluorescent units were 2 × 10^5 (AFU 2 × 10^5) in pre-CHMI minus preimmunization sera. (**C**, **F**) Results of inhibition of sporozoite invasion (ISI) assay are reported as serum dilution at which there was 80% reduction of the number of PfSPZ that invaded a human hepatocyte line (HC-04) in the presence of pre-CHMI as compared with preimmunization sera from the same subject. Panels **A–C** show groups 2 (five doses of 1.35 × 10^5 PfSPZ) and 3 (five doses of 2.7 × 10^5 PfSPZ) before short-term CHMI (2 weeks after the last dose of PfSPZ or NS) and panels **D–F** show those volunteers in Groups 3 (five doses of 2.7 × 10^5 PfSPZ) and 4 (five doses of 2.7 × 10^5 PfSPZ) who underwent long-term CHMI (24 weeks after the last dose of PfSPZ). Panel **G** shows net optical density (OD) 1.0 anti-PfCSP antibodies by an enzyme-linked immunosorbent assay (ELISA) comparing vaccinated Tanzanian volunteers to volunteers in other trials receiving the same regimen. After five doses of 2.70 × 10^5 PfSPZ/dose, volunteers in bagamoyo sporozoite vaccine 1 (BSPZV1) (*N* = 25) had a 4.3-fold lower median net OD 1.0 than those in the U.S.-based clinical trial Walter Reed Army Institute of Research (WRAIR) 2080 (*N* = 26) but a 6.6-fold higher median OD 1.0 than volunteers in 14-I-N010 in Bamako, Mali (*N* = 42), where malaria transmission rates are higher. There was a significant difference between the results for WRAIR 2080 vs. BSPZV1 (*P* = 0.0012), WRAIR 2080 vs. 14-I-N010 (*P* < 0.0001), and even 14-I-N010 vs. BSPZV1 (*P* = 0.002) (two-tailed *t*-test). AFU = arbitrary fluorescence units; aIFA = antibodies by immunofluorescence assay.

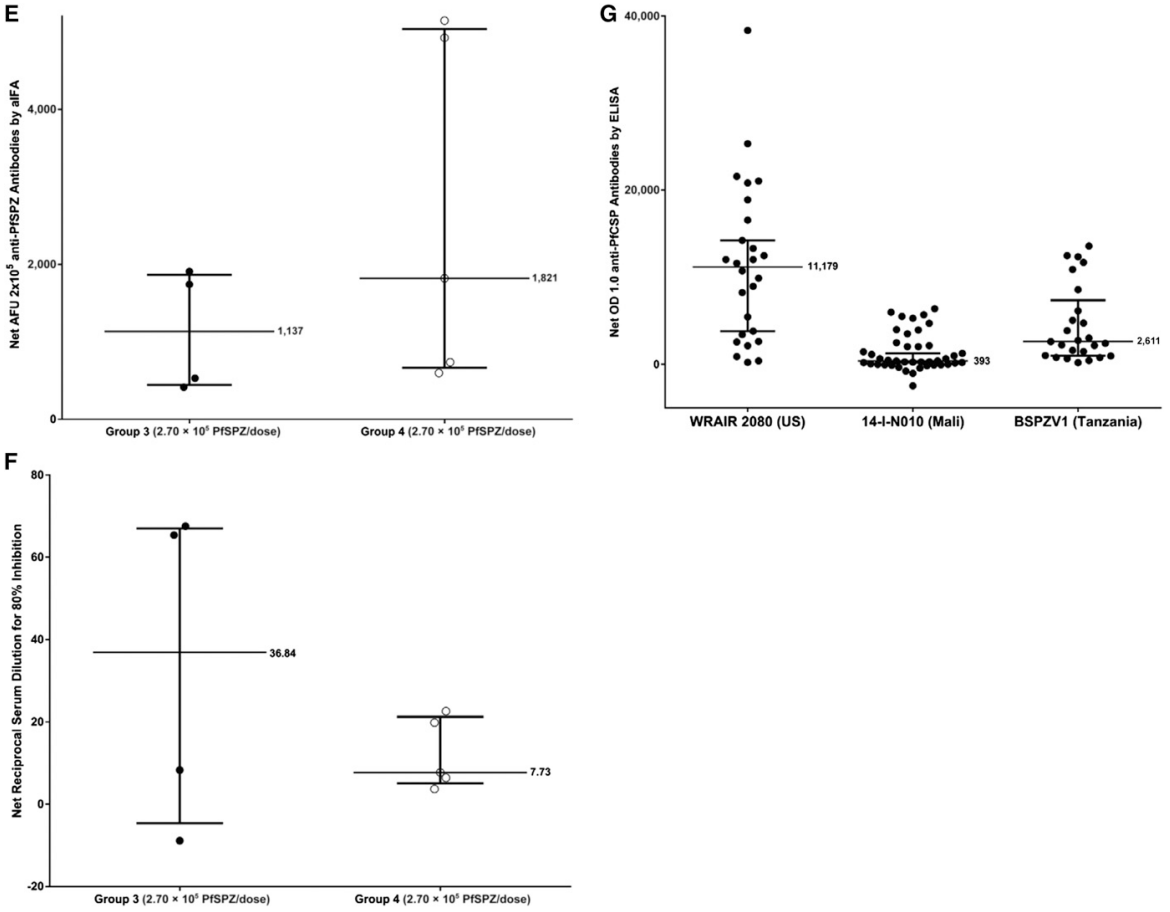

FIGURE 3. (*Continued*)

responses between infected and uninfected volunteers in Group 3 before CHMI #1 ($P = 0.0499$, Wilcoxon Rank-Sum Test), but not PfCSP ($P = 0.290$) or for ISI ($P = 0.249$).

In sera collected before CHMI #3 (170–171 days after the last vaccine dose), antibodies by the three assays for Group 4 and for the four volunteers in Group 3 uninfected in CHMI #1 who underwent CHMI #2 are in Figure 3D–F. All data appear in Supplemental Table 12.

After the fifth dose, in the PfCSP ELISA, volunteers were considered to have seroconverted if their net OD 1.0 and OD 1.0 ratio calculated, respectively, by subtracting or dividing by the prevaccination antibody OD 1.0, were ≥ 50 and ≥ 3.0. By these criteria, 15/18 volunteers (83%) in Group 2, 20/20 (100%) in Group 3, and 5/5 (100%) in Group 4 seroconverted, median net OD 1.0 of positives of 1,189, 2,685, and 961, and median OD 1.0 ratio of positives of 11.50, 21.15, and 37.83, respectively (Supplemental Table 13). In the aIFA, volunteers with a net arbitrary fluorescence unit (AFU) 2×10^5 of ≥ 150 and a ratio of post- to pre-AFU 2×10^5 of ≥ 3.0 were considered positive (Supplemental Table 13). By these criteria, 17/18 volunteers (94%) in Group 2, 18/20 (90%) in Group 3, and 5/5 (100%) in Group 4 seroconverted, median net OD 1.0 of positives of 2,844, 1,165, and 1,820, and median OD 1.0 ratio of positives of 1,193.00, 552.88, and 224.86, respectively (Supplemental Table 13). For the ISI, volunteers with a net ISI activity of ≥ 10% and a ratio of post- to pre-ISI activity of ≥ 3.0 were considered positive. By these criteria, 3/18 volunteers (17%) in Group 2, 8/20 (40%) in Group 3, and 3/5 (60%) in Group 4 were positive, median net OD 1.0 of positives of 22.05, 38.92, and 12.44, and median OD 1.0 ratio of positives of 19.79, 12.53, and 13.44, respectively (Supplemental Table 13).

Other antigens. Two weeks after the fifth dose in Group 2 (1.35×10^5 PfSPZ) and groups 3 and 4 (2.7×10^5 PfSPZ), there were antibodies to PfCSP in 15/18 and 25/25 subjects, respectively. Ten of 25 volunteers immunized with 2.7×10^5 PfSPZ made antibodies to Pf apical membrane antigen 1 and 4–16% responded to PfCelTOS, PfMSP5, PfMSP1, or Pf erythrocyte binding antigen 175 (PfEBA175) (Supplemental Table 14). The presence of antibodies, albeit at low incidence, against proteins first expressed in late liver stages (PfMSP1 and PfEBA175) was unexpected; results were confirmed by repeating the assays. No antibody responses were associated with protection.

T-cell responses. T cells against liver-stage malaria parasites in mice and nonhuman primates immunized with

radiation-attenuated SPZ mediate protection[9,29–31] and it is likely this is the case in humans.[12] CD8 and CD4 T-cell responses generally peak after the first vaccination with PfSPZ Vaccine.[13] In this trial, T-cell responses were measured before immunization, 2 weeks after the first and 2 weeks after the final immunization in Group 2 (1.35×10^5 PfSPZ). For technical reasons (loss of viability), the other groups could not be studied.

After the first vaccination, the percent of Pf red blood cell (PfRBC)-specific and PfSPZ-specific cytokine-producing memory CD4 T-cell responses increased by 0.25 ± 0.06 (mean ± SEM) and 0.24 ± 0.04, respectively (Figure 4A, B). Throughout, "naïve T cell" refers to cells that co-express CCR7 and CD45RA, and "memory T cell" refers to all other T cells. After the final vaccination, at week 22, the CD4 T-cell responses were above prevaccine responses by 0.17 ± 0.05 and 0.18 ± 0.05% points, respectively. These responses were lower than after the same immunization regimen in malaria-naïve U.S. adults.[10]

PfRBC-specific CD8 T cells were not significantly above the prevaccine levels, and PfSPZ-specific CD8 T cells were slightly above background (Figure 4C, D); responses were lower than in U.S. adults.[10,12]

In contrast to other PfSPZ Vaccine trials,[10,12–14] there was negligible change in the frequency of circulating γδ T cells (Figure 4E) or activation as measured by change in expression of the activation markers HLA-DR and CD38 following immunization (Figure 4F). To identify potential explanations for lower cellular immune responses in Tanzanians, we examined frequency of T regulatory (Treg) cells ($CD4^+Foxp3^+CD25^+CD127^-$) expressing the activation marker CD137 (also known as 4-1BB)[32] after stimulation with PfRBC. There was no difference in prevaccine frequency of PfRBC-specific Tregs in the Tanzanians as compared with Americans[10] (Figure 4G). Consistent with CD4 and CD8 T-cell responses, PfRBC-specific Tregs were highest after first immunization (Figure 4H). Last, the prevaccine frequency of total memory T cells relative to total naïve T cells was significantly higher than in Americans (Figure 4I).

DISCUSSION

To our knowledge, this was the first assessment of the VE of a malaria vaccine in Africa against CHMI. *Plasmodium falciparum* SPZ Vaccine was well tolerated and safe but less immunogenic and protective in Tanzanian men than in U.S. volunteers.

In our studies, all 18 controls became infected. Four of 20 (20%) recipients of five doses of 2.7×10^5 PfSPZ did not become infected after homologous CHMI by DVI 3 weeks after the last immunization. By contrast, 12/13 (92.3%) volunteers in the United States who received five doses of 2.7×10^5 PfSPZ were protected after homologous CHMI by mosquito bite 3 weeks after the last vaccine dose.[11] When the four uninfected Tanzanian volunteers underwent repeat homologous CHMI at 24 weeks after the last dose, all four (100%) were protected. In the United States, Seven of 10 previously protected volunteers were protected when they underwent homologous CHMI at 24 weeks[11] and all five volunteers in the United States who were protected at 21 weeks after the last immunization (four doses of 2.7×10^5 PfSPZ) were protected against repeat mosquito-administered CHMI at 59 weeks.[12] This could be due to boosting by the small numbers of PfSPZ administered during the CHMI, or is more likely due to the fact that in these protected individuals, the protective immune responses induced by immunization were sustained.

The same exact immunization regimen was assessed for VE against intense field transmission of heterogeneous Pf in Mali. Vaccine efficacy against infection with Pf on TBS was 52% by time to event and 29% by proportional analysis during 24 weeks after the last vaccine dose.[14] This was higher than the VE by proportional analysis against homologous CHMI in Tanzania. In Tanzania, there was a significant delay in the onset of parasitemia after CHMI at 3 and 24 weeks in subjects who received five doses of 2.7×10^5 PfSPZ and were not fully protected (Figure 2B–D). Nonetheless, the proportional analysis suggests that homologous CHMI by DVI of a 100% infectious dose of homologous PfSPZ Challenge is at least as rigorous as a test of VE and potentially more rigorous than intense field transmission of heterogeneous Pf.

Vaccine-induced antibody and T-cell responses in the Tanzanians were lower than in malaria-naïve Americans who received the exact same dosage regimen. Two weeks after the last dose, the median antibody responses to PfCSP, the major protein on the surface of PfSPZ, were 4.3 times lower in the Tanzanians than those in Americans ($P = 0.0012$, Student's *t*-test, 2-tailed),[11] but significantly higher than in Malians who received the same immunization regimen ($P = 0.002$)[14] (Figure 3G).

The T-cell responses were also lower than in Americans[10,12] (Figure 4), but this could only be assessed in PBMCs from individuals who received the lower dose (five doses of 1.35×10^5 PfSPZ), not in the individuals who received the higher dose (five doses of 2.7×10^5 PfSPZ), the group that had sustained protection for 24 weeks. Thus, it is possible that had PBMCs from the higher dose group been assessed, responses would have been comparable to the responses in nonimmune Americans. The Tanzanians who were assessed had a significantly higher proportion of total memory T cells compared with total naïve T cells at the baseline than did the Americans. This higher frequency of memory cells compared with naïve cells may explain the lower immunogenicity due to less available naïve cells for expansion during the vaccinations. Moreover, the greater frequency of non-Pf–specific memory T cells may compete for infected cell contacts during pathogen surveillance.[33] These data suggest that PfSPZ Vaccine immunogenicity may be dependent on cumulative history of Pf exposure. Another explanation is that an activated immune microenvironment in the Tanzanians as compared with the Americans reduced immune responses.[34] Helminth infections have been associated with reduced immune responses to malaria[35]; however, the paucity of helminth infections in this population does not support helminth infection as a cause of the reduced immune responses.

There were no differences between vaccine and NS placebo recipients in regard to vaccine tolerability or AEs; 97.1% of the DVI administrations were rated painless and no volunteer experienced any local AE. Systemic AEs, most commonly headache, were mild, infrequent, and of short duration, with a similar frequency in NS controls as in vaccinees (no statistically significant differences in rates).

Among the controls, 16 of 18 were positive for Pf by TBS after CHMI. However, all 18 were positive by qPCR. This is consistent with findings in Gabon after CHMI.[21] It is likely that preexisting asexual blood stage immunity limits Pf replication in some individuals. Thus, they never reach the threshold for detection by

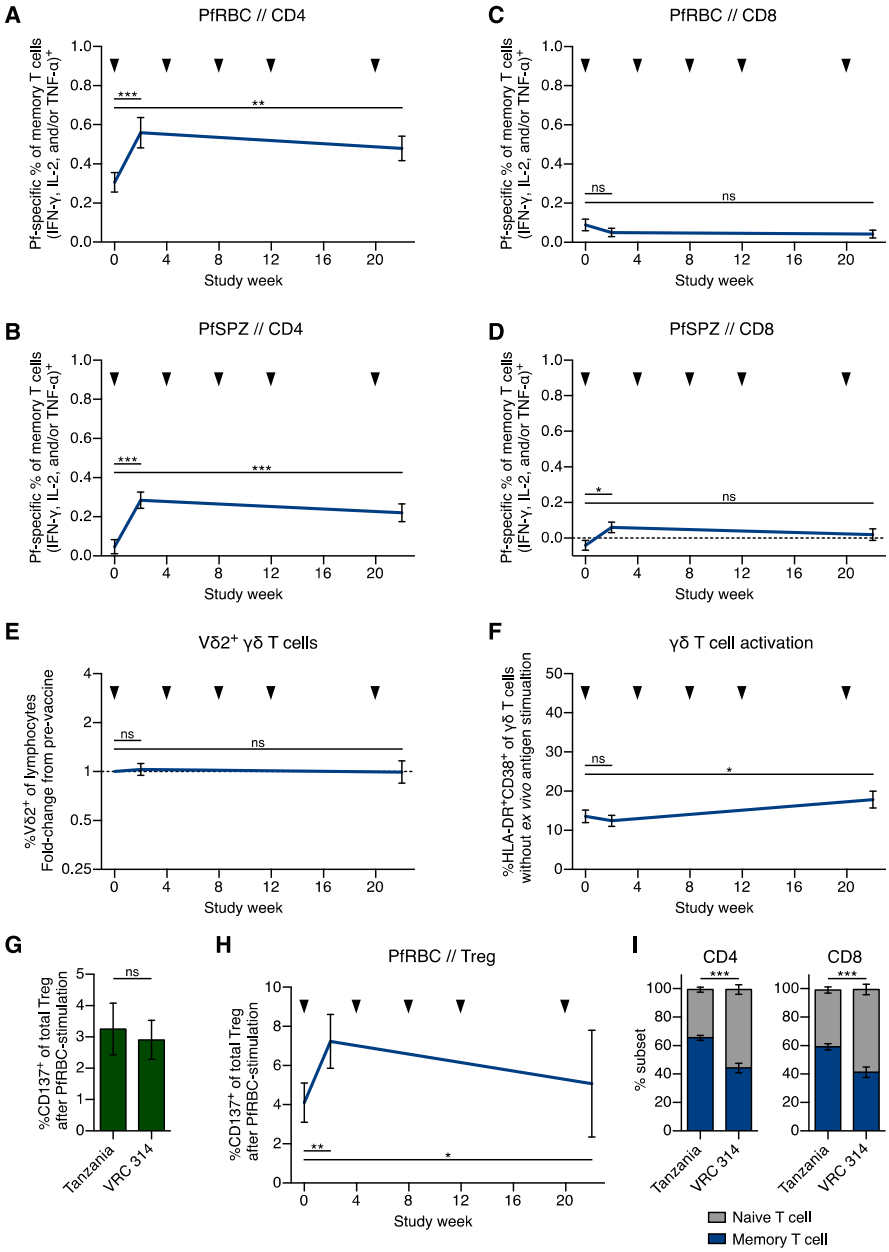

FIGURE 4. *Plasmodium falciparum* Sporozoites (PfSPZ)–specific T-cell responses in vaccine recipients receiving 1.35×10^5 PfSPZ. (**A–D**) PfSPZ-specific T-cell responses. Frequency of cytokine-producing memory CD4 T cells responding to (**A**) PfRBC or (**B**) PfSPZ. Throughout, "naïve T cell" refers to cells that co-express CCR7 and CD45RA, and "memory T cell" refers to all other T cells. Frequency of cytokine-producing memory CD8 T cells responding to (**C**) PfRBC or (**D**) PfSPZ. Results are the percentage of memory T cells producing interferon gamma, interleukin 2, and/or tumor necrosis factor alpha following stimulation minus the percentage of cells following control stimulation. (**E**) Frequency of the $V\delta2^+$ subfamily of γδ T cells of total lymphocytes. Results are expressed as fold-change from the prevaccine frequency. (**F**) γδ T-cell activation in vivo. Data are the percentage of memory γδ T cells expressing HLA-DR and CD38 as measured on PBMCs following incubation with control stimulation (vaccine diluent). (**G**) Prevaccine frequency of PfRBC-specific Tregs in Tanzania compared with malaria-naïve U.S. subjects from the Vaccine Research Center (VRC) 314 study. (**H**) Frequency of PfRBC-specific Treg. Results are the percentage of $CD4^+Foxp3^+CD25^+CD127^-$ T cells expressing CD137 (also known as 4-1BB) after stimulation with Pf red blood cell (PfRBC) minus the percentage of cells following stimulation with uninfected RBC. (**I**) Percentage of total CD4 (left) or CD8 (right) T cells that are naïve (gray bar; $CCR7^+CD45RA^+$) or memory (blue bar; not $CCR7^+CD45RA^+$) phenotype assessed prevaccination in all 48 subjects vaccinated in Tanzania or in 14 healthy U.S. subjects from the VRC 314 study.[13] For **A–F** and **H**, $N = 24$, and statistical difference was measured by using the Wilcoxon matched-pairs signed rank test. For **G** and **I**, statistical difference was measured by using the Mann–Whitney *U* test. *P* values are reported as not significant (ns), < 0.05 (*), < 0.01 (**), or < 0.001 (***). Data are mean ± SEM. Time points are prevaccine, 2 weeks after the first vaccination, and 2 weeks after the final vaccination. Black arrowhead designates PfSPZ Vaccine administration. This figure appears in color at www.ajtmh.org.

TBS. In our CHMI studies in Bagamoyo, we now use qPCR to confirm positive TBS, and retrospectively or in real time, assess parasitemia in all volunteers by qPCR.

We propose that increasing the numbers of PfSPZ per dose and altering intervals between doses will lead to overcoming the downregulation of humoral and cell-mediated immunity most likely because of previous exposure to Pf and thereby increase immune responses to PfSPZ Vaccine and VE. We also hypothesize that immune responses in younger, less malaria-exposed individuals will be of greater magnitude than those in adults.

Received December 27, 2017. Accepted for publication April 19, 2018.

Published online June 25, 2018.

Note: Supplemental tables and figure appear at www.ajtmh.org.

Acknowledgments: We would like to thank the study volunteers for their participation in the study. We also thank the entire study team at the Bagamoyo branch of the Ifakara Health Institute and the manufacturing, quality control, regulatory, clinical, and statistical teams at Sanaria, Inc. for their contributions to the conduct of this trial. We would also like to thank the members of the Safety Monitoring Committee, Kent Kester (chair), Peter Kisenge (safety monitor), and Alan Cross, for their thoughtful oversight. Clinicaltrials.gov Registration: NCT02132299.

Financial support: This clinical trial was supported by the Tanzanian Commission on Science and Technology (COSTECH), the Ifakara Health Institute, and the Swiss Tropical Public Health Institute. The development, manufacturing, and quality control release and stability studies of PfSPZ Vaccine and PfSPZ Challenge were supported in part by National Institute of Allergy and Infectious Diseases Small Business Innovation Research grant 5R44AI055229. Sanaria supported transport of PfSPZ Vaccine and PfSPZ Challenge to the study site and syringe preparation.

Disclosures: Sanaria Inc. manufactured PfSPZ Vaccine and PfSPZ Challenge, and Protein Potential LLC is affiliated with Sanaria. Thus, all authors associated with Sanaria or Protein Potential have potential conflicts of interest. There are no other conflicts of interest.

Authors' addresses: Said A. Jongo, Anneth Tumbo, Catherine Mkindi, Maxmillian Mpina, Ali T. Mtoro, Kamaka Ramadhani Kassim, Florence A. Milando, Munira Qassim, Omar A. Juma, Solomon Mwakasungula, Beatus Simon, Bakari M. Bakari, and Salim Abdulla, Bagamoyo Research and Training Centre, Ifakara Health Institute, Bagamoyo, Tanzania, E-mails: sjongo@ihi.or.tz, atumbo@ihi.or.tz, cmkindi@ihi.or.tz, mmpina@ihi.or.tz, amtoro@ihi.or.tz, kramadhani@ihi.or.tz, fmilando@ihi.or.tz, mqassim@ihi.or.tz, ojuma@ihi.or.tz, smwakasungula@ihi.or.tz, bbongole@ihi.or.tz, bbakari@ihi.or.tz, and sabdulla@ihi.or.tz. Seif A. Shekalaghe, District Commissioner, Maswa District, Simiyu, Tanzania, E-mail: sshekalaghe@yahoo.com. L. W. Preston Church, Adam J. Ruben, Eric R. James, Yonas Abebe, Natasha KC, Sumana Chakravarty, Elizabeth Saverino, Peter F. Billingsley, Thomas L. Richie, and Stephen L. Hoffman, Sanaria Inc., Rockville, MD, E-mails: lwpchurch@sanaria.com, aruben@sanaria.com, ejames@sanaria.com, yabebe@sanaria.com, nkc@sanaria.com, schakravarty@sanaria.com, esaverino@sanaria.com, pbillingsley@sanaria.com, trichie@sanaria.com, and slhoffman@sanaria.com. Tobias Schindler, Isabelle Zenklusen, Tobias Rutishauser, Julian Rothen, Claudia Daubenberger, and Marcel Tanner, Swiss Tropical and Public Health Institute (Swiss TPH), Basel, Switzerland, and University of Basel, Basel, Switzerland, E-mails: tobias.schindler@unibas.ch, isabelle.zenklusen@gmail.com, tobias.rutishauser@unibas.ch, julian.rothen@unibas.ch, claudia.daubenberger@unibas.ch, and marcel.tanner@unibas.ch. Andrew S. Ishizuka and Robert A. Seder, Vaccine Research Center (VRC), National Institute of Allergy and Infectious Diseases, National Institutes of Health, Bethesda, MD, E-mails: andrew.ishizuka@nih.gov and rseder@mail.nih.gov. B. Kim Lee Sim, Sanaria Inc., Rockville, MD, and Protein Potential LLC, Rockville, MD, E-mail: ksim@protpot.com.

REFERENCES

1. WHO, 2017. *World Malaria Report 2017*. Geneva, Switzerland: World Health Organization.
2. GBD 2015 Mortality and Causes of Death Collaborators, 2016. Global, regional, and national life expectancy, all-cause mortality, and cause-specific mortality for 249 causes of death, 1980–2015: a systematic analysis for the Global Burden of Disease Study 2015. *Lancet 388:* 1459–1544.
3. Gething PW et al., 2016. Mapping *Plasmodium falciparum* mortality in Africa between 1990 and 2015. *N Engl J Med 375:* 2435–2445.
4. Richie TL et al., 2015. Progress with *Plasmodium falciparum* sporozoite (PfSPZ)-based malaria vaccines. *Vaccine 33:* 7452–7461.
5. Clyde DF, Most H, McCarthy VC, Vanderberg JP, 1973. Immunization of man against sporozoite-induced falciparum malaria. *Am J Med Sci 266:* 169–177.
6. Rieckmann KH, Carson PE, Beaudoin RL, Cassells JS, Sell KW, 1974. Sporozoite induced immunity in man against an Ethiopian strain of *Plasmodium falciparum*. *Trans R Soc Trop Med Hyg 68:* 258–259.
7. Hoffman SL et al., 2002. Protection of humans against malaria by immunization with radiation-attenuated *Plasmodium falciparum* sporozoites. *J Infect Dis 185:* 1155–1164.
8. Hoffman SL et al., 2010. Development of a metabolically active, non-replicating sporozoite vaccine to prevent *Plasmodium falciparum* malaria. *Hum Vaccin 6:* 97–106.
9. Epstein JE et al., 2011. Live attenuated malaria vaccine designed to protect through hepatic $CD8^+$ T cell immunity. *Science 334:* 475–480.
10. Seder RA et al.; VRC 312 Study Team, 2013. Protection against malaria by intravenous immunization with a nonreplicating sporozoite vaccine. *Science 341:* 1359–1365.
11. Epstein JE et al., 2017. Protection against *Plasmodium falciparum* malaria by PfSPZ vaccine. *JCI Insight 2:* e89154.
12. Ishizuka AS et al., 2016. Protection against malaria at 1 year and immune correlates following PfSPZ vaccination. *Nat Med 22:* 614–623.
13. Lyke KE et al., 2017. Attenuated PfSPZ vaccine induces strain-transcending T cells and durable protection against heterologous controlled human malaria infection. *Proc Natl Acad Sci USA 114:* 2711–2716.
14. Sissoko MS et al., 2017. Safety and efficacy of PfSPZ vaccine against *Plasmodium falciparum* via direct venous inoculation in healthy malaria-exposed adults in Mali: a randomised, double-blind phase 1 trial. *Lancet Infect Dis 17:* 498–509.
15. Roestenberg M et al., 2013. Controlled human malaria infections by intradermal injection of cryopreserved *Plasmodium falciparum* sporozoites. *Am J Trop Med Hyg 88:* 5–13.
16. Sheehy SH et al., 2013. Optimising controlled human malaria infection studies using cryopreserved *P. falciparum* parasites administered by needle and syringe. *PLoS One 8:* e65960.
17. Hodgson SH et al., 2014. Evaluating controlled human malaria infection in Kenyan adults with varying degrees of prior exposure to *Plasmodium falciparum* using sporozoites administered by intramuscular injection. *Front Microbiol 5:* 686.
18. Mordmüller B et al., 2015. Direct venous inoculation of *Plasmodium falciparum* sporozoites for controlled human malaria infection: a dose-finding trial in two centres. *Malar J 14:* 117.
19. Shekalaghe S et al., 2014. Controlled human malaria infection of Tanzanians by intradermal injection of aseptic, purified, cryopreserved *Plasmodium falciparum* sporozoites. *Am J Trop Med Hyg 91:* 471–480.
20. Gomez-Perez GP et al., 2015. Controlled human malaria infection by intramuscular and direct venous inoculation of cryopreserved *Plasmodium falciparum* sporozoites in malaria-naive volunteers: effect of injection volume and dose on infectivity rates. *Malar J 14:* 306.
21. Lell B et al., 2018. Impact of sickle cell trait and naturally acquired immunity on uncomplicated malaria after controlled human malaria infection in adults in Gabon. *Am J Trop Med Hyg 98:* 508–515.
22. Kamau E, Alemayehu S, Feghali KC, Saunders D, Ockenhouse CF, 2013. Multiplex qPCR for detection and absolute quantification of malaria. *PLoS One 8:* e71539.

23. Hofmann N, Mwingira F, Shekalaghe S, Robinson LJ, Mueller I, Felger I, 2015. Ultra-sensitive detection of *Plasmodium falciparum* by amplification of multi-copy subtelomeric targets. *PLoS Med 12:* e1001788.
24. Anderson TJ, Su XZ, Bockarie M, Lagog M, Day KP, 1999. Twelve microsatellite markers for characterization of *Plasmodium falciparum* from finger-prick blood samples. *Parasitology 119:* 113–125.
25. Mordmuller B et al., 2017. Sterile protection against human malaria by chemoattenuated PfSPZ vaccine. *Nature 542:* 445–449.
26. Lamoreaux L, Roederer M, Koup R, 2006. Intracellular cytokine optimization and standard operating procedure. *Nat Protoc 1:* 1507–1516.
27. Haddy TB, Rana SR, Castro O, 1999. Benign ethnic neutropenia: what is a normal absolute neutrophil count? *J Lab Clin Med 133:* 15–22.
28. Hammerschmidt DE, 1999. It's as simple as black and white! Race and ethnicity as categorical variables. *J Lab Clin Med 133:* 10–12.
29. Schofield L, Villaquiran J, Ferreira A, Schellekens H, Nussenzweig RS, Nussenzweig V, 1987. Gamma interferon, CD8+ T cells and antibodies required for immunity to malaria sporozoites. *Nature 330:* 664–666.
30. Weiss WR, Sedegah M, Beaudoin RL, Miller LH, Good MF, 1988. CD8+ T cells (cytotoxic/suppressors) are required for protection in mice immunized with malaria sporozoites. *Proc Natl Acad Sci USA 85:* 573–576.
31. Weiss WR, Jiang CG, 2012. Protective CD8+ T lymphocytes in primates immunized with malaria sporozoites. *PLoS One 7:* e31247.
32. Schoenbrunn A et al., 2012. A converse 4-1BB and CD40 ligand expression pattern delineates activated regulatory T cells (Treg) and conventional T cells enabling direct isolation of alloantigen-reactive natural Foxp3+ Treg. *J Immunol 189:* 5985–5994.
33. Fernandez-Ruiz D et al., 2016. Liver-resident memory CD8+ T cells form a front-line defense against malaria liver-stage infection. *Immunity 45:* 889–902.
34. Muyanja E et al., 2014. Immune activation alters cellular and humoral responses to yellow fever 17D vaccine. *J Clin Invest 124:* 3147–3158.
35. Hartgers FC, Yazdanbakhsh M, 2006. Co-infection of helminths and malaria: modulation of the immune responses to malaria. *Parasite Immunol 28:* 497–506.
36. Purkins L, Love ER, Eve MD, Wooldridge CL, Cowan C, Smart TS, Johnson PJ, Rapeport WG, 2004. The influence of diet upon liver function tests and serum lipids in healthy male volunteers resident in a phase I unit. *Br J Clin Pharmacol 57:* 199–208.

Chapter 4

Modulation of Bacterial Metabolism by the Microenvironment Controls MAIT Cell Stimulation

This chapter contains the following publication:

Schmaler, M., Colone, A., Spagnuolo, J., Zimmermann, M., Lepore, M., Kalinichenko, A., Bhatia, S., Cottier, F., **Rutishauser, T**., Pavelka, N., Egli, A., Azzali, E., Pieroni, M., Costantino, G., Hruz, P., Sauer, U., Mori, L., Libero, G.D., 2018. Modulation of bacterial metabolism by the microenvironment controls MAIT cell stimulation. Mucosal Immunology 1.

https://doi.org/10.1038/s41385-018-0020-9

MucosalImmunology www.nature.com/mi

ARTICLE

Modulation of bacterial metabolism by the microenvironment controls MAIT cell stimulation

Mathias Schmaler[1], Alessia Colone[2], Julian Spagnuolo[1], Michael Zimmermann[3,4], Marco Lepore[1], Artem Kalinichenko[1], Sumedha Bhatia[2], Fabien Cottier[2], Tobias Rutishauser[1], Norman Pavelka[2], Adrian Egli[5,6], Elisa Azzali[7], Marco Pieroni[7], Gabriele Costantino[7], Petr Hruz[8], Uwe Sauer[3], Lucia Mori[1,2] and Gennaro De Libero[1,2]

Mucosal-associated invariant T (MAIT) cells are abundant innate-like T lymphocytes in mucosal tissues and recognize a variety of riboflavin-related metabolites produced by the microbial flora. Relevant issues are whether MAIT cells are heterogeneous in the colon, and whether the local environment influences microbial metabolism thereby shaping MAIT cell phenotypes and responses. We found discrete MAIT cell populations in human colon, characterized by the diverse expression of transcription factors, cytokines and surface markers, indicative of activated and precisely controlled lymphocyte populations. Similar phenotypes were rare among circulating MAIT cells and appeared when circulating MAIT cells were stimulated with the synthetic antigens 5-(2-oxoethylideneamino)-6-D-ribitylaminouracil, and 5-(2-oxopropylideneamino)-6-D-ribitylaminouracil. Furthermore, bacteria grown in colon-resembling conditions with low oxygen tension and harvested at stationary growth phase, potently activated human MAIT cells. The increased activation correlated with accumulation of the above antigenic metabolites as indicated by mass spectrometry. Thus, the colon environment contributes to mucosal immunity by directly affecting bacterial metabolism, and indirectly controlling the stimulation and differentiation of MAIT cells.

Mucosal Immunology _####################_ https://doi.org/10.1038/s41385-018-0020-9

INTRODUCTION

Mucosal-associated invariant T (MAIT) cells are a unique subset of evolutionary-conserved innate-like T lymphocytes found in blood and mucosae. MAIT cells express a semi-invariant TCR[1] with marked TCR oligoclonality.[2] In humans, MAIT TCR is composed of three TCRα chains in which TRAV1-2 is rearranged to TRAJ33, TRAJ20, or TRAJ12 and paired with TCRβ chains mostly belonging to the TRBV6 and TRBV20 families.[2–4] MAIT cells responding to diverse pathogens including *Mycobacterium smegmatis*, *Salmonella typhimurium*, and *Candida albicans* displayed pathogen-specific differences in their TCRβ usage.[5] These findings support substantial heterogeneity across the MAIT cell repertoire and suggested the presence of adaptive-like responses within some MAIT cell populations.[4–6]

MAIT cells comprise 1–5% of T cells in the periphery and are present at ~2% and 10–30% of tissue resident T cells in mucosal sites and in the liver, respectively, in humans and mice.[1,6–8] They develop in the thymus upon interaction with MHC class I-related protein (MR1) expressed on $CD4^+CD8^+$ thymocytes.[9] Mature MAIT cells exit the thymus as naïve cells, seed bone marrow[3] and require commensal flora and B cells for acquisition of effector/memory phenotype.[1,10] The probable role of B cells is to present antigens to MAIT cells in defined niches, whereas that of commensal flora is to release antigenic molecules that stimulate MAIT TCR.[11,12] Indeed, only infections with bacteria, which produce the stimulatory antigens, activate MAIT cells in vivo.[13] In some instances MAIT cells are stimulated by an array of cytokines independently from TCR engagement.[8,14,15]

Metabolites generated in the riboflavin (vitamin B2) pathway stimulate MAIT cells.[16–19] The key molecule is the intermediate metabolite 5-amino-6-(1-D-ribitylamino)uracil (5-A-RU), which gives rise to structurally related antigens. The first antigen is the enzymatically generated 6,7-dimethyl-8-(D-ribityl)lumazine[16] (RL-6,7-diMe), the immediate precursor of riboflavin.[20] This compound also gives rise to 7-hydroxy-6-methyl-8-D-ribityllumazine and to reduced 6-hydroxymethyl-8-D-ribityllumazine, which both stimulate MAIT cells.[16]

Other two antigens are pyrimidine-like molecules, namely 5-(2-oxoethylideneamino)-6-D-ribitylaminouracil (5-OE-RU) and 5-(2-oxopropylideneamino)-6-D-ribitylaminouracil (5-OP-RU).[18] These compounds result from non-enzymatic condensation of 5-A-RU with the dialdehyde glyoxal or the ketoaldehyde methylglyoxal[18] (MG), respectively, and thus are adducts representing chemical side reactions of the pathway not required for riboflavin synthesis.

Both 5-OP-RU and 5-OE-RU, but not RL-6,7-diMe, make a Schiff base with Lys43 of MR1, generating highly stable complexes with MR1 and stabilizing it in a MAIT cell-stimulatory conformation.[18] Increased expression of MR1 on the surface of antigen-presenting

[1]Experimental Immunology, Department of Biomedicine, University and University Hospital Basel, 4031 Basel, Switzerland; [2]Singapore Immunology Network (SIgN), Agency for Science, Technology and Research, Singapore 138648, Singapore; [3]Institute of Molecular Systems Biology, Eidgenössische Technische Hochschule (ETH) Zurich, Zurich, Switzerland; [4]Department of Microbial Pathogenesis, Yale University School of Medicine, New Haven, CT 06510, USA; [5]Applied Microbiology Research, Department of Biomedicine, University and University Hospital Basel, 4031 Basel, Switzerland; [6]Clinical Microbiology, University Hospital Basel, 4031 Basel, Switzerland; [7]Department of Food and Drug, University of Parma, Parma, Italy and [8]Department of Gastroenterology, University Hospital, Basel, Switzerland
Correspondence: Lucia Mori (lucia.mori@unibas.ch) or Gennaro De Libero (gennaro.delibero@unibas.ch)

Received: 4 October 2017 Revised: 18 January 2018 Accepted: 19 February 2018
Published online: 09 May 2018

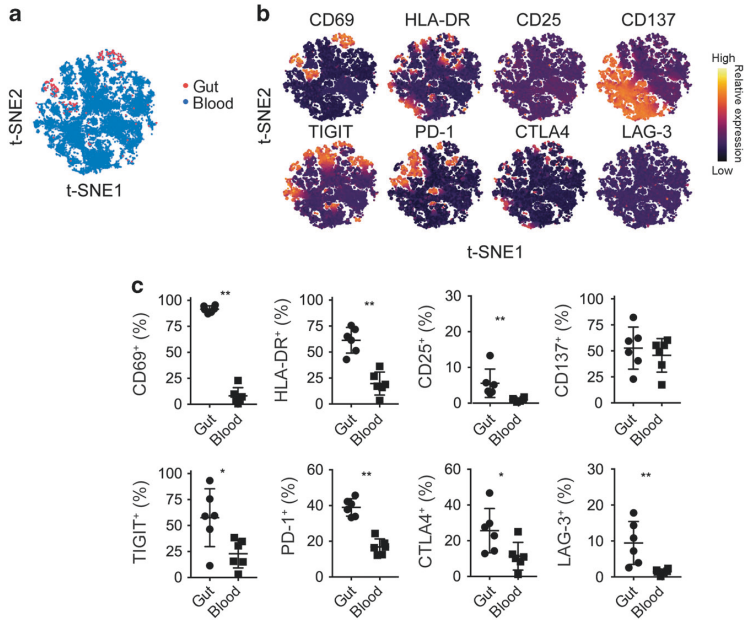

Fig. 1 Intestinal MAIT cells are phenotypically homogeneous and cluster differentially from MAIT cells in blood. **a** t-SNE plots of flow cytometry-analyzed gut (red) and blood (blue) $CD3^+CD161^+$MR1-5-OP-RU tetramer$^+$ MAIT cells. t-SNE analysis was performed after down-sampling and concatenation of all samples (paired blood and gut from six healthy donors). **b** t-SNE plots as in **a** showing relative expression of the indicated markers according to the color scale. **c** Percentage of MAIT cells expressing the indicated surface markers in gut vs. blood ($n = 6$). Horizontal bars represent mean ± sd. *$P < 0.05$ by Wilcoxon-rank test

cells (APCs) pulsed with these antigens is a consequence of this stabilization.[21,22] In contrast, RL-6,7-diMe binds weakly to MR1 and refolds inefficiently with recombinant MR1.[17] MAIT cell activation is strongly influenced by the mode of ligand binding to MR1 and the chemical structure of the stimulatory metabolites. For example, 5-OP-RU has a very short half-life, and becomes stable only after binding MR1.[22] Thus, the physiological relevance of 5-OP-RU is determined by immediate formation of a Schiff base with MR1. The variety of MAIT cell antigens raises questions about the nature of stimulatory metabolites produced under physiological conditions, and specificities of their effects on MAIT cell response.

The metabolism of commensal and opportunistic microbes in the gut constantly adapts to changing host conditions.[23–27] Whether the mucosal physiological conditions affect the relative abundance of MAIT-stimulatory metabolites, thus influencing the type of MAIT cell activation, has not yet been investigated. Here we show that diverse metabolite antigens induce differential MAIT cell responses. In addition, we found that growth conditions affect the relative abundance of these MAIT cell-stimulatory compounds in bacteria, thereby influencing MAIT responses.

RESULTS

MAIT cells freshly isolated from normal human colon exhibit activation signature

To characterize the heterogeneity of colon-resident MAIT cells, we profiled normal colon biopsies and matching blood samples from six individuals using multicolor flow cytometry. Each sample was analyzed with a panel of 13 monoclonal antibodies including those specific for activation and immunomodulatory markers (e.g., CD137, CD69, CD25, HLA-DR, PD-1, LAG-3, CTLA4, TIGIT, CD38, and CD244, see Supplementary Table 1 online). t-SNE analysis revealed that MR1-5-OP-RU-tetramer-positive MAIT cell populations in biopsies clustered only in three main regions. MAIT cells in these regions were rare in the blood indicating important phenotypic differences between mucosal and circulating MAIT cells (Fig. 1a and Supplementary Figure 1).

Gut-resident MAIT cells differed from blood MAIT cells according to the expression patterns of activation and immunomodulatory markers (Fig. 1b). A larger number of intestinal MAIT cells showed expression of CD69, HLA-DR, CD25, TIGIT, PD-1, CTLA4, and LAG-3 as compared with blood-derived MAIT cells (Fig. 1c and Supplementary Figure 1).

Next, we analyzed the expression of transcription factors T-bet and RORγt, together with those of granzyme B, IFNγ, IL-17, IL-22, and TNFα after PMA stimulation of paired gut-resident and circulating MAIT cells from seven donors (Fig. 2 and Supplementary Table 2). Gut-resident MAIT cells distributed into distinct subpopulations, which minimally overlapped with blood-derived MAIT cells (Fig. 2a), indicating that, like the activation markers, the expression of cytokines and transcription factors was also distributed differently compared to circulating cells. About 9% of gut-resident MAIT cells expressed RORγt, and 65% were T-bet-positive, while in blood they were 1.5% and 40%, respectively. The percentage of gut-resident MAIT cells positive for all tested cytokines and granzyme B was significantly increased compared to that of blood (Fig. 2c). Unsupervised cluster analysis using DBSCAN identified 25 populations of MAIT cells (Fig. 2d). Populations 11, 12, 14, 20, and 25 contained higher frequencies of gut-derived MAIT cells (Supplementary Figure 2), whereas populations 2, 18, 19, 21, and 24 were more abundant in blood-derived MAIT cells. Populations 11, 12, and 14 in the gut showed high production of IL-17 and TNFα (Fig. 2e), while populations 11 and 12 also produced IFNγ. Population 20 mostly produced TNFα, while population 25 produced both TNFα and IFNγ. The populations significantly more abundant in the blood (2, 18, 19, 21, and 24, Supplementary Figure 2) instead produced very low amounts or no IFNγ, TNFα, IL-17, and IL-22 (Fig. 2e). These findings

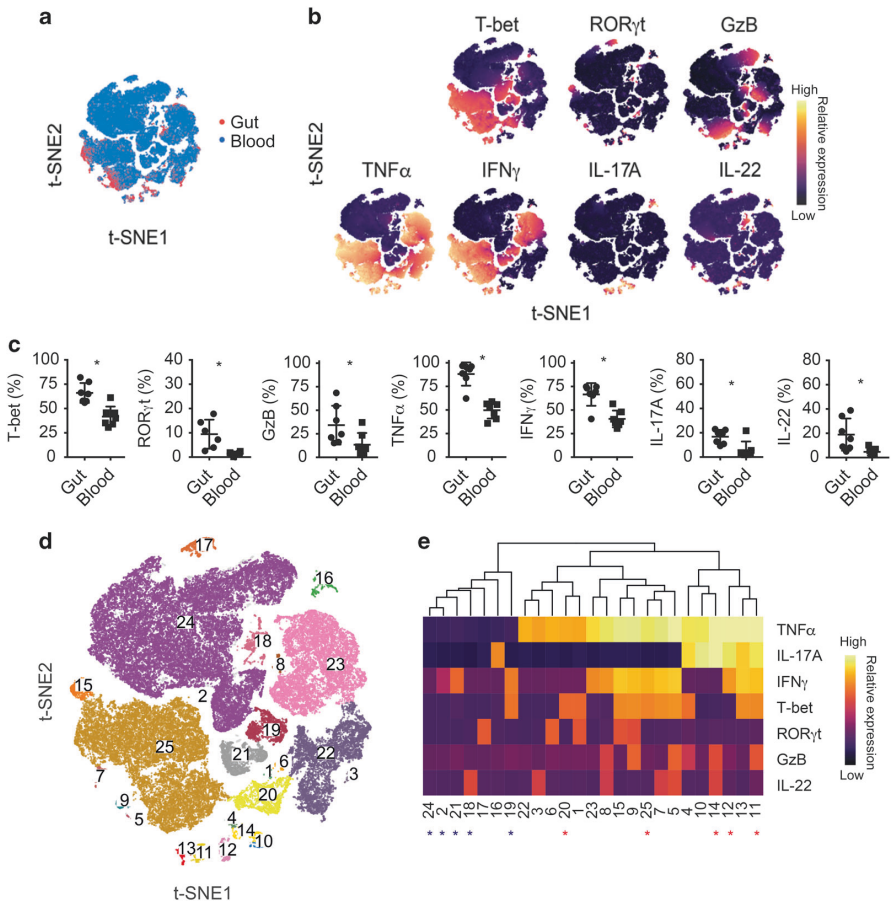

Fig. 2 Intestinal MAIT cells are functionally homogeneous and cluster differentially from MAIT cells in blood. **a** t-SNE plots of flow cytometry-analyzed gut (red) and blood (blue) $CD3^+CD161^+MR1\text{-}5\text{-}OP\text{-}RU$ tetramer$^+$ MAIT cells. t-SNE analysis was performed after down-sampling and concatenation of all samples (paired blood and gut from seven healthy donors). **b** t-SNE plots as in **a** showing relative expression of the indicated markers according to the color scale. **c** Percentage of MAIT cells expressing the indicated intracellular marker in gut vs. blood ($n = 7$). Horizontal bars represent mean ± sd. **d** Semi-automated clustering using DBSCAN to identify MAIT cell populations (1–25) and **e** heatmap of their relative expression of the indicated markers in individual MAIT cell populations in gut vs. blood ($n = 7$). *$P < 0.05$ by Wilcoxon-rank test. The red asterisks denote populations significantly increased in gut vs. blood, the blue ones those decreased

Table 1. Hierarchy of MAIT cell antigen potencies

EC_{50} values (M)				
MAIT cells	TRBV	5-OP-RU	5-OE-RU	RL-6,7-diMe
SMC3[a]	20-1	5.329e−14	1.45e−10	4.603e−08
MRC25[a]	6-1	8.757e−13	2.731e−09	2.332e−06
Donor 7[b]	Polyclonal	3.083e−10	1.030e−08	2.618e−05
Donor 8[b]	Polyclonal	3.027e−10	8.920e−09	3.267e−05
Donor 9[b]	Polyclonal	1.888e−11	7.558e−10	1.970e−05
Donor 10[b]	Polyclonal	2.949e−10	2.501e−09	1.887e−05
Donor 11[b]	Polyclonal	1.864e−10	nd	8.189e−06

nd not done
[a] EC_{50} calculated by IFNγ response
[b] EC_{50} calculated by TCR Vα7.2 downmodulation at 24 h

suggest that in the colon, MAIT cells express activation markers (Fig. 1) and are primed for production of pro-inflammatory cytokines in large amounts.

These phenotypes and functions probably reflect constant stimulation by metabolites derived from commensal and opportunistic microflora. The expression of inhibitory molecules might provide a suitable mechanism to balance local continuous antigen stimulation. These observations suggest that the microflora and probably the gut microenvironment have important effects on tissue resident MAIT cells.

Potency hierarchy of MAIT cell-stimulatory metabolites

We then sought to determine whether the bacterial metabolites, which stimulate MAIT cells with different potencies,[28] have different effects on MAIT cells. We used synthetic 5-OE-RU, 5-OP-RU, and RL-6,7-diMe presented by engineered A375 cells lacking functional MHC class I and class I-like molecules, transduced with a hybrid β2M-human MR1 gene (A375.MR1)

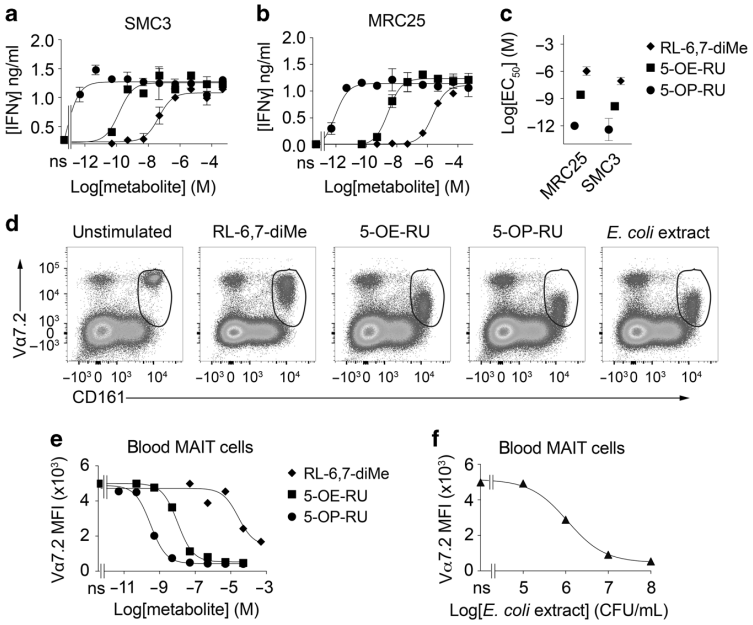

Fig. 3 Bacterial riboflavin-related synthetic antigens activate MAIT cells in a dose-dependent manner. **a**, **b** Dose-dependent IFNγ response of the MAIT cell clone (**a**) SMC3 and (**b**) MRC25 after stimulation with A375.MR1 cells and RL-6,7-diMe (diamonds), 5-OP-RU (circles), 5-OE-RU (squares), or in the absence of antigen (ns, not stimulated). **c** $Log_{10}EC_{50}$ values of RL-6,7-diMe (diamonds), 5-OE-RU (squares), and 5-OP-RU (circles) inducing half maximum IFNγ release by MAIT cell clones as in **a**, **b**. Data show mean ± sd of duplicates and are representative of two independent experiments. **d** Flow cytometry assessing TCR downregulation on MAIT cells ($CD3^+Vα7.2^+CD161^{hi}$) present in PBMCs of a representative donor after co-culture with A375.MR1 and RL-6,7-diMe (50 µM), 5-OE-RU (0.5 µM), 5-OP-RU (5 nM) or *E. coli* extract (5×10^7 CFU/mL). **e**, **f** Median fluorescence intensity (MFI) of the TCR on MAIT cells ($Vα7.2^+CD161^{hi}$ as in **d** of another donor in response to varying doses of **e** 5-OP-RU (circles), 5-OE-RU (squares), RL-6,7-diMe (diamonds) or **f** *E. coli* extract. One representative out of five experiments is shown

(ref. [29] and Supplementary Figure 3). These APCs were engineered in order to limit alloreactive stimulation and prevent the effects of MHC class-I-binding inhibitory molecules potentially expressed by MAIT cells.

All three synthetic MAIT cell antigens increased MR1 surface expression (Supplementary Figure 3a), thereby confirming the stabilization capacity of these molecules.[30] In this assay, RL-6,7-diMe induced MR1 upregulation less efficiently than the other compounds (Supplementary Figure 3b). At high concentrations (50–500 µM), 5-OP-RU was more effective than the other compounds (Supplementary Figure 3b).

To examine the potencies of the three synthetic antigens in stimulating MAIT cells, we selected two human MR1-restricted MAIT cell clones, MRC25 and SMC3, which express canonical TRAV1.2–TRAJ33 TCRα chains paired to different TCRβ chains (Table 1) and respond to *E. coli*-infected APCs.[2,29] The release of IFNγ by MAIT cell clones upon antigen recognition was used to measure the potency (effective concentration for half-maximum response, EC_{50}) of each tested compound. 5-OP-RU and 5-OE-RU were highly stimulatory to both clones, whereas RL-6,7-diMe displayed lower potency (Fig. 3a, b). SMC3 was slightly more sensitive than MRC25 (Fig. 3c) and each compound showed comparable EC_{50} values in each of the two clones (Fig. 3c and Table 1). The stimulatory capacity of these antigens displayed a consistent potency hierarchy of 5-OP-RU > 5-OE-RU > RL-6,7-diMe.

We next compared the three synthetic antigens and *E. coli* cell extract for their capacity to stimulate MAIT cells present in freshly isolated PBMC. Due to the TCR heterogeneity of circulating MAIT cells, the antigen-induced downregulation of the TCR in polyclonal MAIT cell populations was used to determine the EC_{50} of each compound; one such example is shown in Fig. 3d. Dose response curves confirmed the hierarchy of potencies observed with MAIT clones, (Fig. 3e, f and Table 1). Despite inter-donor variability, 5-OP-RU at EC_{50} doses induced upregulation of CD69 in stimulated circulating MAIT cells from five healthy donors, and CD25 and CD137 in three out of five donors (Supplementary Figure 4). In contrast, EC_{50} doses of 5-OE-RU and RL-6,7-diMe did not induce comparable MAIT cell activation in the majority of donors (Supplementary Figure 4). These findings are in line with other studies conducted with T cells engineered with TCR genes from one MAIT clone and indicating 5-OP-RU as a potent antigen.[16,18]

We next assessed whether the same hierarchy was observed in the presence of APCs expressing physiological levels of MR1 as those present in blood. PBMCs from healthy individuals were exposed for a short time to synthetic antigens without the addition of exogenous APCs. The downregulation of the TCR and concomitant upregulation of the activation markers CD69, CD25, and CD137 on MAIT cells was analyzed by flow cytometry (Supplementary Figure 5a,b). Also under these experimental conditions, the previously observed potency hierarchy was observed. However, the efficiency of stimulation was much lower; the EC_{50} concentrations calculated from TCR downregulation were ~10^2–10^3 times higher than those observed in the presence of MR1-transfected APCs (EC_{50} 5-OP-RU, 43.2 nM; EC_{50} 5-OE-RU, 3.21 µM), and even at high concentrations (500 µM) of RL-6,7-diMe, TCR downregulation was barely detectable.

Phenotypic changes of MAIT cells after activation by synthetic antigens

To analyze the antigen-induced phenotypic changes, circulating MAIT cells were stimulated for 24 h with A375.MR1 cells and three

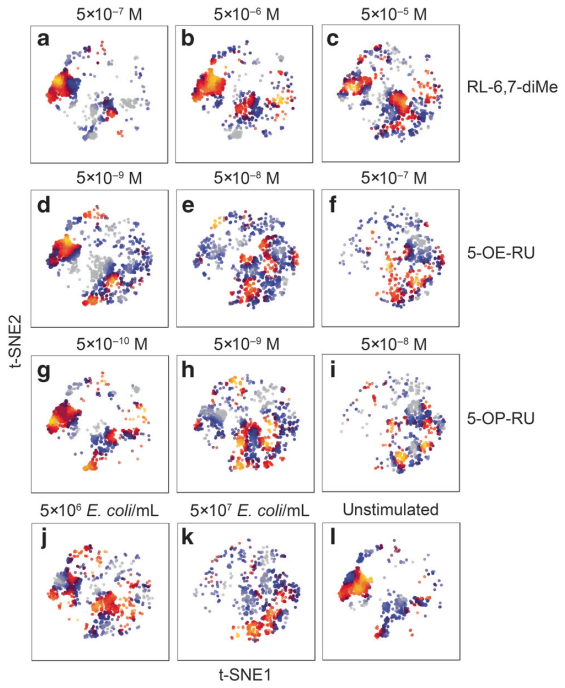

Fig. 4 Multiple populations of *ex vivo* MAIT cells respond to riboflavin-related antigens. MAIT cell response of one healthy donor after PBMC stimulation for 24 h with A375.MR1 cells and **a**–**c** RL-6,7-diMe, **d**–**f** 5-OE-RU, **g**–**i** 5-OP-RU, **j**, **k** *E. coli* extract or **l** medium (unstimulated). The response to EC_{50} and ED_{50} doses of each antigen are presented in the middle panels (**b**, **e**, **h**, **k**). t-SNE analysis of $CD3^{+}V\alpha7.2^{+}CD161^{hi}$ MAIT cells after down-sampling and concatenation of all conditions. Warm color regions of the t-SNE map depict regions of higher cell density. Experiments were performed twice with comparable results in two different donors

doses each of the three synthetic antigens and two concentrations of *E. coli* extract (Fig. 4). The activation and immunomodulatory markers that were investigated are described in Supplementary Table 1.

Unstimulated MAIT cells (Fig. 4l) and those stimulated by RL-6,7-diMe clustered in two major overlapping areas (Fig. 4a–c). RL-6,7-diMe was active only at the highest dose tested, confirming the weak antigenicity of this metabolite. At low concentrations, 5-OE-RU and 5-OP-RU induced minor but clear changes in cluster distribution when compared to unstimulated MAIT cells (Fig. 4d, g vs. l). At higher doses, both 5-OE-RU and 5-OP-RU induced the appearance of novel clusters (Fig. 4e, f, h, i), distinct from those observed after stimulation with RL-6,7-diMe. The main cluster of resting cells observed in the unstimulated condition (Fig. 4l) disappeared after stimulation with 50 nM 5-OE-RU and with 5 nM 5-OP-RU, confirming the differential potency of these two antigens.

The unpurified antigens present in *E. coli* extracts induced a dose-dependent response with the appearance of clusters very similar to those induced by 5-OE-RU and 5-OP-RU (Fig. 4j, k vs. e, f and h, i).

When circulating MAIT cells were stimulated for 72 h with A375.MR1 cells and the EC_{50} of each antigen, the expression of each marker was different from that observed after 24 h (Supplementary Figure 6), indicating that continuous stimulation induces further phenotypic changes.

These data indicated that freshly isolated MAIT cells respond to synthetic antigens by differential modulation of surface markers involved in T-cell activation and regulation.

MAIT cells split into different groups upon stimulation with different antigens

To further investigate the differential MAIT cell response to weak (RL-6,7-diMe), intermediate (5-OE-RU), and strong (5-OP-RU) antigens, PBMCs were stimulated with A375.MR1 and with each of these synthetic analogs at concentrations inducing TCR downregulation. The analysis of flow-cytometry data was performed at two time-points (24 and 72 h after stimulation) using FlowSOM, a semi-supervised clustering and dimensional reduction algorithm.[31] MAIT cells were fit to the best matching node according to the expression of surface markers. Nodes 5, 8, 11, 17, 19, 20, 21, 22, 23, 24, and 25 are shown in Fig. 5a, while all the other nodes are shown in Supplementary Figure 7a. As illustrated by the node size, the majority of MAIT cells stimulated with RL-6,7-diMe for 24 h distributed in the self-organizing map similarly to unstimulated cells, and expressed low levels or none of the investigated markers (Fig. 5b, node 5). In contrast, cells stimulated by 5-OE-RU or 5-OP-RU were fit to three similar nodes (20, 23, and 25) with different phenotypes (Fig. 5b). Nodes 23 and 25 contained MAIT cells expressing the activation markers CD137, CD69, CD25, and the regulatory molecules PD-1 and LAG-3 (Fig. 5b). Cells in nodes 23 and 25 were different because they expressed different levels of investigated marker. For instance, MAIT cells in node 25, but not in node 23, displayed low-surface expression of CD3, indicating a strong response to antigen of these cells (Fig. 5b).

MAIT cells activated by *E. coli* extracts were more similar to that induced by 5-OE-RU than to the activation observed in response to RL-6,7-diMe (Fig. 5b and Supplementary Figure 7b). This analysis revealed MAIT cell responsiveness can be classified into discrete steps, uniquely depicting their response to weak, intermediate, and strong antigens.

MAIT cells analyzed 72 h after stimulation did not show down-modulation of Vα7.2 TCR chain and CD3 (Fig. 5c and Supplementary Figure 7c), independently of the stimulating antigen, confirming the transient nature of CD3–TCR complex down-regulation following antigen recognition.[32]

Cells responsive to the weak antigen RL-6,7-diMe were dispersed across nodes 9–11. MAIT cells in node 9 and 10 expressed PD-1, and those in node 9 co-expressed CD38 and low levels of LAG-3 and HLA-DR (Supplementary Figure 7c). Thus, the analysis of MAIT cells 72 h after stimulation with the weak RL-6,7-diMe antigen clearly displayed differences to unstimulated cells.

After 72 h, MAIT cells stimulated with 5-OE-RU, 5-OE-RU, and *E. coli* extract fit to nodes 22 and 24, and expressed the activation markers CD25, CD69, and CD38, together with the immunomodulatory molecules LAG-3 and PD-1 (Fig. 5c). Cells in node 24 also expressed two additional activation markers; HLA-DR and CD137, thus indicating a higher level of activation in this MAIT cell population than that of node 22 (Fig. 5c). Collectively, these data suggest that the potency of MR1-ligands strongly influences MAIT cell expression of activation and immunomodulatory markers whose differential combinations distinguish responsive MAIT cell populations.

Bacterial cell culture conditions modulate MAIT cell-stimulating capacity

Bacterial growth conditions exert important effects on microbial metabolism and intestinal environmental conditions shape the development and composition of the adaptive immunity.[33] According to this paradigm, we investigated whether *E. coli* adapted to grow in gut-related conditions acquire unique capacities to induce MAIT cell activation and phenotypic changes.

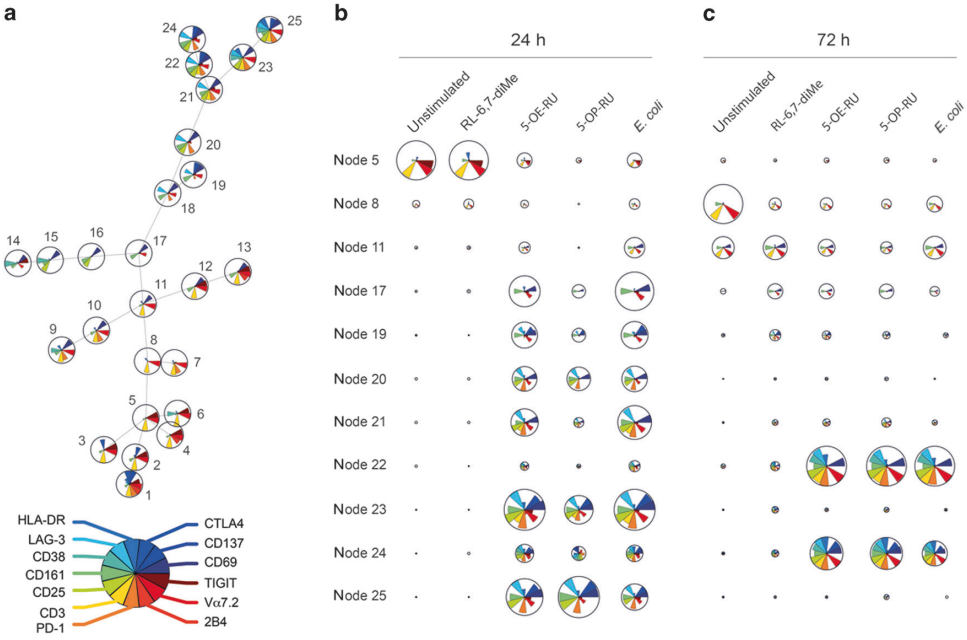

Fig. 5 Clusters of ex vivo-stimulated MAIT cells according to their phenotypic profile. FlowSOM analysis of MAIT cells from one healthy donor after PBMC stimulation with A375.MR1 cells and RL-6,7-diMe, 5-OE-RU, 5-OP-RU, (EC_{50} concentrations), and *E. coli* extract (10^7 CFU/mL, ED_{50}), or medium (unstimulated) for 24 h and 72 h. **a** Minimal spanning tree illustrating 25 nodes containing MAIT cells stimulated with various doses of antigens and *E. coli* extract. Radar charts show expression of markers defining each node. **b**, **c** Expression of indicated surface markers on unstimulated and antigen stimulated MAIT cells after **b** 24 and **c** 72 h in the main node is shown. Minor nodes are shown in Supplementary Fig. 6. Numbers indicate main nodes defined by the semi-supervised FlowSOM algorithm in **a**. Pie charts indicate the median fluorescence intensity of markers and node size corresponds to the number of MAIT cells in each population. Experiments were performed twice with comparable results in three healthy donors

Bacterial metabolites were extracted from *E. coli* grown in different conditions including altered carbon sources and concentrations, various oxygen tensions, or various starting pH values. Bacterial extracts, normalized for their optical density and expressed as CFU/mL were assessed for the capacity to induce IFNγ release by MAIT cell clones. By comparing the half-maximal effective dose response (ED_{50}) to bacterial extract, we assessed the antigenic potency of *E. coli* harvested during exponential or stationary phase, when grown in nutrient-rich LB medium or in minimal M9 medium. The ED_{50} stimulating SMC3 cells was significantly lower with extracts from *E. coli* harvested in stationary vs. exponential phase (Fig. 6a, b), suggesting accumulating antigens are a product of secondary metabolism, active during stationary phase growth. The rich nutrient composition of LB medium also favored stimulation and the ED_{50} calculated for LB and M9 were $10^{5.18 \pm 0.16}$ and $10^{7.44 \pm 0.09}$ (mean ± sd), respectively, for cells harvested during their exponential growth, and $10^{4.51 \pm 0.07}$ and $10^{5.93 \pm 0.06}$, respectively, for cells grown at stationary phase (Fig. 6a, b). When stationary phase *E. coli* were grown in M9 medium with a starting pH ranging from 6.0 to 7.5 (the physiological pH range within the distal intestinal tract[34]), all extracts had similar potency (Fig. 6c), indicating that tested pH conditions do not significantly modulate the bacterial stimulatory ability.

To test whether oxygen modulates the production and accumulation of MAIT antigens, we compared the stimulatory capacity of bacterial extracts obtained from *E. coli* grown under aerobic or anaerobic conditions. Extracts from anaerobically grown stationary phase *E. coli* were more stimulatory than those from aerobically grown *E. coli* (Fig. 6d), suggesting that oxygen limitation enhances the capacity of *E. coli* to activate MAIT cells.

Finally, we assessed the impact of carbon sources during stationary growth of *E. coli* on their MAIT-stimulatory capacity. As indicated by low ED_{50} values, extracts from *E. coli* grown with 40 mM glucose were more potent than those from *E. coli* grown with 4 mM glucose (Fig. 6e and Supplementary Figure 8a). Supplementing M9 medium with a variety of sole carbon sources at 40 mM and comparing the ED_{50} obtained with the same concentration of glucose, we observed that extracts from *E. coli* grown with xylose showed a comparable ED_{50}, while extracts from bacteria grown with ribose were more potent (Fig. 6e and Supplementary Figure 8b,c). In contrast, extracts from *E. coli* grown with sodium pyruvate showed reduced stimulatory capacity (Fig. 6e and Supplementary Figure 8d). When non-fermentable carbon sources like glycerol, lactate and acetate were added as sole carbon source, *E. coli* extracts were less efficient than extracts from bacteria grown in 40 mM glucose (Fig. 6f and Supplementary Figure 8e-g). Taken together these results indicate that growth phase, oxygen tension and carbon sources, but not pH, influence MAIT cell antigenicity of *E. coli* lysates.

Accumulation of stimulatory metabolites in different bacterial growth conditions

To gain insight into the bacterial physiology that underlies the observed culture-dependent alteration of MAIT cell stimulation, we performed untargeted metabolome analysis of *E. coli* grown in defined media with seven different sole carbon sources (glucose, xylose, ribose, pyruvate, glycerol, lactate, and acetate) and at four different pH values (6.0, 6.5, 7.0, and 7.5) for glucose. The identical bacterial lysates were also used to stimulate MAIT cells and determine their ED_{50}. To assess how the 573 detected metabolites changed between growth conditions, we performed a pair-wise

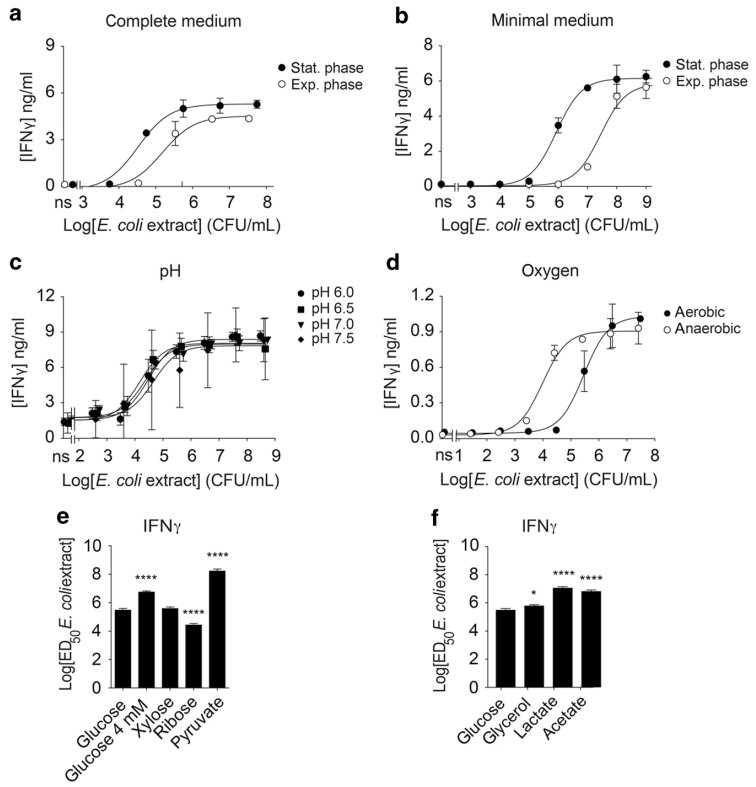

Fig. 6 Bacterial culture conditions influence the response of MAIT cells. Response of the MAIT cell clone SMC3 to A375.MR1 cells in the presence of titrated extracts from *E. coli* grown in exponential (open circles) and stationary (closed circles) phases in **a** complete LB medium and **b** synthetic M9 medium. **c**, **d** Response of SMC3 cells to A375.MR1 stimulated with titrated extracts from *E. coli* grown at stationary phase in **c** synthetic medium with different starting pH and **d** LB medium in aerobic (closed circles) and anaerobic (open circles) conditions. **a–d** Results are expressed as mean ± sd of IFNγ release of triplicate cultures. **e**, **f** ED_{50} values of *E. coli* extracts inducing IFNγ release by SMC3 cells in response to A375.MR1 cells incubated with extracts of *E. coli* grown at stationary phase in M9 medium supplemented with 40 mM of the indicated sole carbon sources or with 4 mM glucose. Log_{10} ED_{50} values were calculated based on the response to titrating amounts of bacterial extracts equivalent to 10^3–10^9 CFU/mL. Results are expressed as mean + sd of IFNγ release of triplicate cultures. *$P \leq 0.05$, ****$P \leq 0.0001$, analyzed using one-way ANOVA with Dunnett's multiple comparison test against values obtained with standard 40 mM glucose. Data show triplicates measured as technical replicas and are representative of two independent experiments

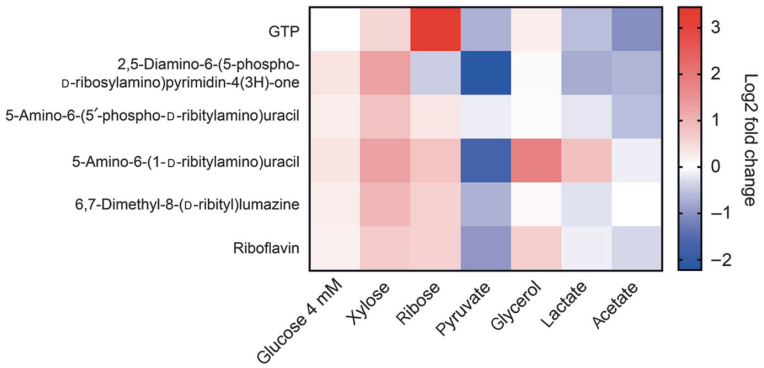

Fig. 7 Accumulation of riboflavin and precursor metabolites in *E. coli* depending on carbon source. Log_2 fold change in the abundance of riboflavin-precursor metabolites in *E. coli* extracts grown in M9 medium supplemented by the indicated sole carbon sources (40 mM) or glucose at 4 mM, relative to that obtained with M9 supplemented by 40 mM glucose ($n = 4$). Metabolite amounts were determined by mass spectrometry. Log_2 fold changes of metabolites are color coded

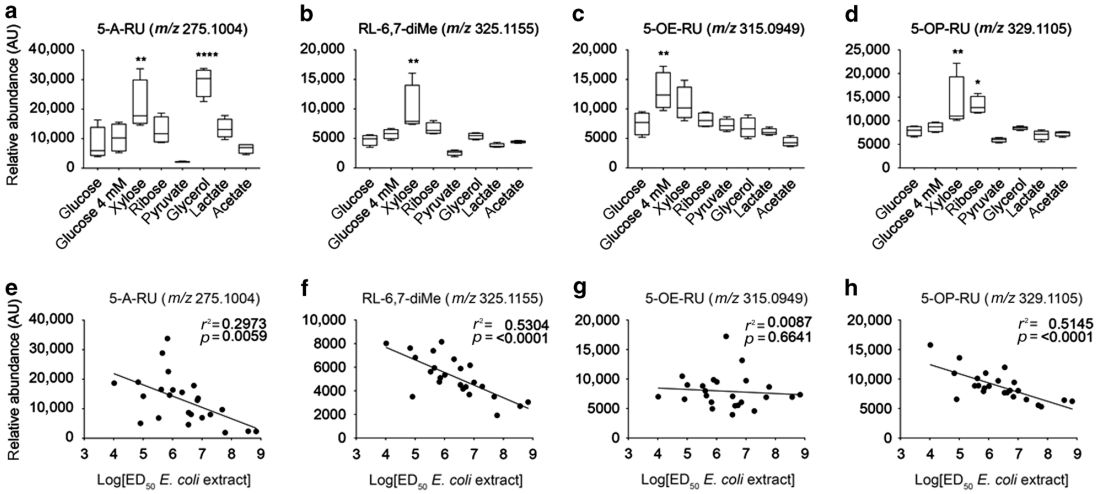

Fig. 8 Abundance of riboflavin-precursor antigens in *E. coli* is modulated by carbon sources and their concentration. **a**–**d** Relative abundance expressed as arbitrary units (AU) of indicated pyrimidines and ribityllumazines in extracts of *E. coli* grown in M9 medium supplemented by the indicated sole carbon sources. **e**–**h** Correlation of the metabolite levels with the *E. coli* Log_{10} ED_{50} of MAIT cell stimulation (as in Fig. 5e, f). **a**, **e** 5-A-RU (*m/z* 275.1004), **b**, **f** RL-6,7-diMe (*m/z* 325.1155), **c**, **g** 5-OE-RU (*m/z* 315.0949), and **d**, **h** 5-OP-RU (*m/z* 329.1105). In this type of analysis, 5-OP-RU cannot not be distinguished from reduced 6-hydroxymethyl-8-D-ribityllumazine (rRL-6-CH_2OH,) as they have identical masses and fragment spectra.[16,18,19] *$P \le 0.05$, **$P \le 0.01$, ****$P \le 0.001$, analyzed using Kruskal–Wallis test with Dunnett's multiple comparison test against values obtained with standard 40 mM glucose. Data show triplicates measured as technical replicas and are representative of two independent experiments

comparison (*t*-test) using glucose (pH 7) as the reference condition (Supplementary Table 3). To relate metabolite changes to actual pathways, we performed a metabolite set enrichment analysis on significantly altered metabolites (log_2 fold change) using the pathway definitions in the KEGG database.[35,36] *E. coli* grown in ribose led to the strongest stimulation amongst all conditions (Fig. 6e), coinciding with metabolites enriched in purine and folate metabolism (Supplementary Figure 9a). In contrast, pyruvate and lactate conditions that poorly stimulated MAIT cells (Fig. 6e, f) showed reduced abundance of purine metabolites, illustrated by pathway enrichment of decreasing metabolites (Supplementary Figure 9b). Both purine and folate pathways are directly connected to the riboflavin pathway[20] and are thus potentially linked to the generation of MAIT cell antigens.[16,18] Hence, these findings support our hypothesis that altered bacterial growth conditions affect the production of riboflavin precursors and correlate with the altered capacity of bacteria to stimulate MAIT cells.

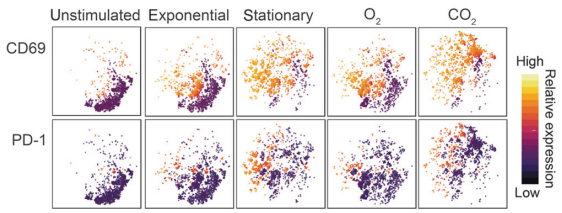

Fig. 9 Ex vivo MAIT cell responses are affected by *E. coli* growth conditions. t-SNE analysis performed on $CD3^+V\alpha7.2^+CD161^{hi}$ MAIT cells after PBMC stimulation in co-culture with A375.MR1 and *E. coli* extracts from the indicated growth conditions. Extracts were normalized to their OD_{600} (as in Fig. 5b, d). MAIT cells from one healthy donor were analyzed after down-sampling and concatenation of all conditions. Colors indicate cell expression levels of CD69 (upper panels) and PD-1 (lower panels). Experiments were performed twice with comparable results in two different donors

To further investigate this possibility, we focused on the abundance of metabolites in the riboflavin pathway. Compared to glucose as a sole carbon source, *E. coli* grown with ribose, xylose, and glycerol showed an increase in abundance of several riboflavin precursors including; GTP, the first metabolite in the pathway; 2,5-diamino-6-(5-phospho-D-ribosylamino)pyrimidin-4(3H)-one; 5-amino-6-(5′-phospho-D-ribitylamino)uracil; 5-A-RU, and RL-6,7-diMe (Fig. 7). In contrast, the levels of these metabolites were unchanged or reduced in the weakly stimulating acetate, lactate or pyruvate conditions (Fig. 7). These findings consolidated our hypothesis that *E. coli* growth conditions facilitating MAIT cell stimulation coincide with an increased abundance of riboflavin biosynthesis intermediates.

Next, we analyzed the levels of the riboflavin-derived antigens 5-OE-RU, 5-OP-RU, RL-6,7-diMe, and their precursor 5-A-RU. Compared to glucose at 40 mM, 5-A-RU was significantly increased in xylose and glycerol (Fig. 8a), RL-6,7-diMe was increased in xylose (Fig. 8b), and 5-OE-RU in 4 mM glucose (Fig. 8c). The potent MAIT cell stimulator 5-OP-RU was increased in xylose and ribose conditions (Fig. 8d). Taken together, these results show hexose, pentose and glycerol conditions, but not pyruvate, lactate, and acetate conditions increased production of MAIT antigens and the abundance of 5-A-RU. In agreement with the unchanged MAIT cell-stimulating capacity of bacterial extracts derived from pH-adjusted bacterial cultures, the abundance of riboflavin-related antigens was also stable (Supplementary Figure 10a-d). Significant correlations between the abundance of these metabolites and the ED_{50} of the corresponding extracts were observed for all investigated molecules (Fig. 8e, f, h), except 5-OE-RU (Fig. 8g). Overall, these findings suggest a link between accumulation of riboflavin-related metabolites and the potential of bacteria to stimulate MAIT cells.

In conclusion, the abundance of MAIT cell-stimulating metabolites significantly varies in *E. coli* depending on growth conditions and by extension on the local host-environment. Growth with hexose, pentose or glycerol maximized the presence of such antigenic metabolites, whereas acetate, lactate, and pyruvate

conditions reduced their abundances. Thus, adaptation of the microflora to gut-related physiological growth conditions impacts on the abundance and type of stimulatory metabolites, which in turn may modulate MAIT cell activation and heterogeneity.

MAIT cells sense bacterial growth conditions

The correlation observed between accumulation of MAIT cell antigenic metabolites depending on *E. coli* growth conditions and capacity to stimulate MAIT cells prompted us to investigate the phenotype of MAIT cells responding to bacteria exposed to diverse gut-related growth conditions.

Flow cytometric analysis of blood MAIT cells stimulated with *E. coli* extracts from exponential phase revealed low levels expression of CD69 and PD-1 (Fig. 9), while those stimulated with stationary phase *E. coli* showed high CD69, PD-1, CD25, and LAG-3 expression (Fig. 9 and Supplementary Figure 11). Growth of *E. coli* under anaerobic conditions also led to significant activation of freshly isolated MAIT cells (Fig. 9 and Supplementary Figure 11), confirming the data obtained with stimulation of a MAIT clone (Fig. 6). In contrast, bacteria grown in aerobic conditions or harvested during exponential growth phase induced weaker expression of these activation markers resulting in a t-SNE map more similar to the unstimulated control (Fig. 9 and Supplementary Figure 11).

In conclusion, bacterial growth conditions directly modulate the accumulation of MAIT cell-stimulating metabolites and indirectly control their activation and expression of inhibitory receptors. This mechanism allows a fine regulation of MAIT cell response in the gut.

DISCUSSION

The human gut has been defined as an anaerobic bioreactor, which maintains a local flora composed of a few divisions of bacteria[37] and with slow microbial growth dynamics.[38] The metabolic repertoire of gut microorganisms is a key factor in shaping the phenotype, composition, and functions of resident immune cells.[39] These effects are mediated through the release of small metabolites that influence a cascade of metabolic events within host cells.[40] Some bacterial metabolites serve as antigens presented by MR1 and stimulating MAIT cells.[16,18,19,41] The contribution of bacterial metabolites produced in tissues to MAIT cell activation and phenotypic differentiation remains poorly investigated.

Our studies showed that MAIT cells in human intestinal mucosa are distributed in a few distinct populations, which represent a minority of cells in the circulating pool. MAIT cells in gut biopsies expressed different combinations of HLA-DR, CD25, CD69, and CD137, suggesting variable states of activation. In particular, about 50% of MAIT cells were $CD137^+$, a marker of recently activated T cells.[42] This finding is in accordance with the known capacity of intestinal bacterial flora to stimulate immune cells.[43,44] Some MAIT cell populations expressed inhibitory receptors, including TIGIT, PD-1, CTLA4, and LAG-3. About 50% of MAIT cells in the gut were $TIGIT^+$ or $PD\text{-}1^+$; however, only a minor percentage of cells co-expressed these two markers, while most of $TIGIT^+$ cells were LAG-3- and CTLA4-negative. These findings indicate that active stimulation occurs in the gut and that MAIT cells rely on different inhibitory mechanisms to dampen their responsiveness to antigen. Most of the MAIT cells observed in colon biopsies express T-bet and only some RORγt transcription factors distinctive of T_{H1} and T_{H17} functional phenotypes, respectively. Accordingly, we found that they produce large amounts of pro-inflammatory cytokines and granzyme B when compared to circulating MAIT cells. The expression of activation markers together with that of inhibitory molecules and the efficient cytokine production suggests that MAIT cells in the colon are primed T cells that might either (i) become readily reactivated, (those not expressing inhibitory receptors) or (ii) remain non-responsive after antigen stimulation (being regulated by inhibitory receptors). The proper balance between these cell populations might be relevant to local immunity.

Notably, a large number of MAIT cells responded to extracts from *E. coli* grown under conditions simulating key features of the colon microenvironment (carbon sources, oxygen tension, and growth phase) by expressing TIGIT or PD-1, while a few cells expressed LAG-3 and CTLA4. Although similar phenotypes were observed in MAIT cells from gut biopsies, it is not possible to conclude that the observed ex vivo phenotypes is a consequence of the same stimulation applied in vitro.

In agreement with published work,[16,18,22] the activity of 5-OP-RU was very potent as low picomolar concentrations induced IFNγ release in MAIT cell clones and TCR downregulation in freshly isolated polyclonal MAIT cells. In contrast, 5-OE-RU and RL-6,7-diMe, respectively, were 10^2–10^3 and 5×10^5–10^9 fold less potent than 5-OP-RU in TCR downregulation. The same potency hierarchy was observed with APC displaying low physiological levels of MR1, although TCR down modulation and high expression of CD25, CD69, and CD137 markers required higher antigen doses. Using such APC, RL-6,7-diMe was poorly stimulatory, even at high doses, thus implicating the importance of MR1 protein levels on the surface of APC in defining the contribution of each antigen to activation.

Stimulation with 5-OP-RU and 5-OE-RU also induced the expression of surface markers found in ex vivo analyzed gut-derived MAIT cells. The weak RL-6,7-diMe antigen did not induce the same upregulation of activation and inhibitory markers at either high doses or after prolonged stimulation. Similar observations were found with the FlowSOM self-organizing map algorithm. This analysis also showed that the investigated markers appeared on stimulated cells in discrete steps, characterized by early appearance of activation markers followed by the inhibitory ones. At a 72 h time point, most cells grouped in two major nodes after stimulation with 5-OP-RU and 5-OE-RU and *E. coli*, but not with RL-6,7-diMe. Thus, different antigens induce different phenotypic changes in MAIT cells.

Having characterized the stimulating capacity of each antigen, we compared their levels in bacteria grown under different conditions. Bacterial metabolism is influenced by environmental cues including nutrient and metabolite concentrations, pH, oxygen tension, as well as microbial cell replication time, and host immune responses.[23–27] By altering in vitro culture conditions we identified several factors, also present in the gut, capable of modulating the capacity of *E. coli* to activate MAIT cells. *E. coli* grown in stationary phase and slowly replicating, as occurs in human gut,[38] stimulated MAIT cells more efficiently than bacteria grown in nutrient-rich media and in exponential phase. Moreover, the absence or low tension of oxygen during bacterial growth enhanced MAIT cell stimulation. Probably, stationary phase and anaerobiosis enhance MAIT cell stimulation by multiple mechanisms with accumulation of MAIT stimulating metabolites providing a critical contribution. In addition, the possibility exists that the relative abundance of non-stimulatory MR1-binding metabolites might affect stimulation.

Metabolomics analysis of extracts from bacteria grown with a sole carbon source indicated a correlation between the increase of purine, vitamin B9 (folic acid) and B2 (riboflavin) pathways, and stimulatory capacity. Metabolites from the three pathways were abundant in *E. coli* grown in defined media supplemented with ribose, which induced the strongest stimulation of MAIT cells. Furthermore, metabolites of the riboflavin pathway showed high levels in the ribose-supplemented condition, and a significant correlation was observed between low EC_{50} (high potency) and increased levels of 5-OP-RU, RL-6,7-diMe, and its precursor 5-A-RU.

Extracts of *E. coli* grown with low oxygen and in stationary phase also induced expression of surface markers on MAIT cells

resembling the markers present on ex vivo investigated colon MAIT cells. These similarities indicate that stimulation occurs inside the gut, possibly facilitated by the local accumulation of potent microbial antigens.

Open issues are: (i) how the steep oxygen gradients are in the gut[45] and (ii) how the precise localization of bacteria in the colon directly affects MAIT cell stimulation. The half-lives of 5-OP-RU and 5-A-RU are very short,[22] and when produced by bacteria located in the central part of the gut lumen they are unlikely to stimulate MAIT cells located in intraepithelial space and lamina propria as they must pass through the glycocalyx that forms a thick bi-layered structure in the colon.[33] In contrast, 5-OP-RU and 5-A-RU released by bacteria growing in the microaereophilic zone adjacent to epithelial cells are more available for presentation by MR1. Since the latter bacteria are directly affected by local immune responses, a reciprocal influence can be envisaged. Therefore, the balance between local microbial surveillance and bacterial riboflavin metabolism might be relevant to MAIT cell activation.

In conclusion, these studies showed that different populations of MAIT cells in the gut exhibit phenotypes of cells with recent antigen experience either ready for further responses or regulated by inhibitory receptors. Similar phenotypes are induced by metabolite antigens that accumulate under low oxygen conditions and during slow bacterial growth. Thus, MAIT cells represent an innate-like population of T cells with the capacity to sense the metabolic state of enteric bacteria.

METHODS

Human samples and cell lines

Colon biopsies and paired blood samples were obtained from the Gastroenterology Unit, University Hospital Basel, Switzerland. Samples were from patients under colon cancer screening and were normal at histological evaluation. The study was approved by the Swiss ethics commission (no. 139-13) and written informed consent was obtained from all subjects. For further details and description of T-cell isolation from biopsies, and used cell lines, see Supplementary Methods.

Functional assays

For description of T-cell stimulation, flow cytometry, multidimensional analyses, metabolite synthesis, extraction of bacterial metabolites, metabolomics methods, and statistical analyses, see Supplementary Methods.

ACKNOWLEDGEMENTS

We thank Shivani Koolarina, Zi-Xin Wong, Lena Angman, Sebastiano Sansano, Anouk Lehmann, Emmanuel Traunecker, and Danny Labes for technical support, Paula Cullen and Thérèse Resink for reading of the manuscript. The MR1-tetramer technology was developed jointly by James McCluskey, Jamie Rossjohn, and David Fairlie, and the material was produced by the NIH Tetramer Core Facility as permitted to be distributed by the University of Melbourne. This work was supported by the core funds of the Department of Biomedicine and SIgN and by the Swiss National Science Foundation (310030-149571 and -173240 to G.D.L.).

AUTHOR CONTRIBUTIONS

M.S., L.M., and G.D.L. conceived and designed experiments. M.S., A.C., M.Z., J.S., and S. B. performed experiments and analyzed data. T.R. contributed to data analysis. M.L. and A.K. provided cells, P.H. provided clinical samples, A.E., F.C., and N.P. provided bacterial samples, E.A., M.P., and G.C. provided synthetic compounds. U.S. supervised metabolomics analysis, L.M. and G.D.L. supervised the work. M.S., L.M., and G.D.L. wrote the manuscript.

ADDITIONAL INFORMATION

The online version of this article (https://doi.org/10.1038/s41385-018-0020-9) contains supplementary material, which is available to authorized users.

Competing interests: The authors declare no competing interests.

REFERENCES

1. Treiner, E. et al. Selection of evolutionarily conserved mucosal-associated invariant T cells by MR1. *Nature* **422**, 164–169 (2003).
2. Lepore, M. et al. Parallel T-cell cloning and deep sequencing of human MAIT cells reveal stable oligoclonal TCRbeta repertoire. *Nat. Commun.* **5**, 3866 (2014).
3. Walker, L. J. et al. Human MAIT and CD8alphaalpha cells develop from a pool of type-17 precommitted CD8+T cells. *Blood* **119**, 422–433 (2012).
4. Reantragoon, R. et al. Antigen-loaded MR1 tetramers define T cell receptor heterogeneity in mucosal-associated invariant T cells. *J. Exp. Med.* **210**, 2305–2320 (2013).
5. Gold, M. C. et al. MR1-restricted MAIT cells display ligand discrimination and pathogen selectivity through distinct T cell receptor usage. *J. Exp. Med.* **211**, 1601–1610 (2014).
6. Dias, J., Leeansyah, E. & Sandberg, J. K. Multiple layers of heterogeneity and subset diversity in human MAIT cell responses to distinct microorganisms and to innate cytokines. *Proc. Natl Acad. Sci. USA* **114**, E5434–E5443 (2017).
7. Dusseaux, M. et al. Human MAIT cells are xenobiotic-resistant, tissue-targeted, CD161hi IL-17-secreting T cells. *Blood* **117**, 1250–1259 (2011).
8. Tang, X. Z. et al. IL-7 licenses activation of human liver intrasinusoidal mucosal-associated invariant T cells. *J. Immunol.* **190**, 3142–3152 (2013).
9. Seach, N. et al. Double-positive thymocytes select mucosal-associated invariant T cells. *J. Immunol.* **191**, 6002–6009 (2013).
10. Koay, H. F. et al. A three-stage intrathymic development pathway for the mucosal-associated invariant T cell lineage. *Nat. Immunol.* **17**, 1300–1311 (2016).
11. Gold, M. C. et al. Human mucosal associated invariant T cells detect bacterially infected cells. *PLoS Biol.* **8**, e1000407 (2010).
12. Le Bourhis, L. et al. Antimicrobial activity of mucosal-associated invariant T cells. *Nat. Immunol.* **11**, 701–708 (2010).
13. Chen Z., et al. Mucosal-associated invariant T-cell activation and accumulation after in vivo infection depends on microbial riboflavin synthesis and co-stimulatory signals. *Mucosal Immunol.* **10**, 58–68 (2016).
14. Ussher, J. E. et al. CD161++CD8+ T cells, including the MAIT cell subset, are specifically activated by IL-12+IL-18 in a TCR-independent manner. *Eur. J. Immunol.* **44**, 195–203 (2014).
15. Jo, J. et al. Toll-like receptor 8 agonist and bacteria trigger potent activation of innate immune cells in human liver. *PLoS Pathog.* **10**, e1004210 (2014).
16. Kjer-Nielsen, L. et al. MR1 presents microbial vitamin B metabolites to MAIT cells. *Nature* **491**, 717–723 (2012).
17. Patel, O. et al. Recognition of vitamin B metabolites by mucosal-associated invariant T cells. *Nat. Commun.* **4**, 2142 (2013).
18. Corbett, A. J. et al. T-cell activation by transitory neo-antigens derived from distinct microbial pathways. *Nature* **509**, 361–365 (2014).
19. Lopez-Sagaseta, J. et al. MAIT recognition of a stimulatory bacterial antigen bound to MR1. *J. Immunol.* **191**, 5268–5277 (2013).
20. Bacher, A., Eberhardt, S., Fischer, M., Kis, K. & Richter, G. Biosynthesis of vitaminb2 (riboflavin). *Annu. Rev. Nutr.* **20**, 153–167 (2000).
21. McWilliam, H. E. et al. The intracellular pathway for the presentation of vitamin B-related antigens by the antigen-presenting molecule MR1. *Nat. Immunol.* **17**, 531–537 (2016).
22. Mak, J. Y. et al. Stabilizing short-lived Schiff base derivatives of 5-aminouracils that activate mucosal-associated invariant T cells. *Nat. Commun.* **8**, 14599 (2017).
23. Louis, P., Scott, K. P., Duncan, S. H. & Flint, H. J. Understanding the effects of diet on bacterial metabolism in the large intestine. *J. Appl. Microbiol.* **102**, 1197–1208 (2007).
24. Spor, A., Koren, O. & Ley, R. Unravelling the effects of the environment and host genotype on the gut microbiome. *Nat. Rev. Microbiol.* **9**, 279–290 (2011).
25. Guarner, F. & Malagelada, J. R. Gut flora in health and disease. *Lancet* **361**, 512–519 (2003).
26. Ley, R. E., Peterson, D. A. & Gordon, J. I. Ecological and evolutionary forces shaping microbial diversity in the human intestine. *Cell* **124**, 837–848 (2006).
27. Hooper, L. V. & Macpherson, A. J. Immune adaptations that maintain homeostasis with the intestinal microbiota. *Nat. Rev. Immunol.* **10**, 159–169 (2010).
28. Birkinshaw, R. W., Kjer-Nielsen, L., Eckle, S. B., McCluskey, J. & Rossjohn, J. MAITs, MR1 and vitamin B metabolites. *Curr. Opin. Immunol.* **26**, 7–13 (2014).
29. Lepore, M., et al. Functionally diverse human T cells recognize non-microbial antigens presented by MR1. *Elife* **6**, e24476 (2017).

30. Mondot, S., Boudinot, P. & Lantz, O. MAIT, MR1, microbes and riboflavin: a paradigm for the co-evolution of invariant TCRs and restricting MHCI-like molecules? *Immunogenetics* **68**, 537–548 (2016).
31. Young, M. H. et al. MAIT cell recognition of MR1 on bacterially infected and uninfected cells. *PLoS ONE* **8**, e53789 (2013).
32. Liu, H., Rhodes, M., Wiest, D. L. & Vignali, D. A. On the dynamics of TCR:CD3 complex cell surface expression and downmodulation. *Immunity* **13**, 665–675 (2000).
33. Agace, W. W. & McCoy, K. D. Regionalized development and maintenance of the intestinal adaptive immune landscape. *Immunity* **46**, 532–548 (2017).
34. Fallingborg, J. Intraluminal pH of the human gastrointestinal tract. *Dan. Med. Bull.* **46**, 183–196 (1999).
35. Kanehisa, M. & Goto, S. KEGG: kyoto encyclopedia of genes and genomes. *Nucleic Acids Res.* **28**, 27–30 (2000).
36. Subramanian, A. et al. Gene set enrichment analysis: a knowledge-based approach for interpreting genome-wide expression profiles. *Proc. Natl Acad. Sci. USA* **102**, 15545–15550 (2005).
37. Backhed, F., Ley, R. E., Sonnenburg, J. L., Peterson, D. A. & Gordon, J. I. Host-bacterial mutualism in the human intestine. *Science* **307**, 1915–1920 (2005).
38. Korem, T. et al. Growth dynamics of gut microbiota in health and disease inferred from single metagenomic samples. *Science* **349**, 1101–1106 (2015).
39. Brestoff, J. R. & Artis, D. Commensal bacteria at the interface of host metabolism and the immune system. *Nat. Immunol.* **14**, 676–684 (2013).
40. Koh, A., De Vadder, F., Kovatcheva-Datchary, P. & Backhed, F. From dietary fiber to host physiology: short-chain fatty acids as key bacterial metabolites. *Cell* **165**, 1332–1345 (2016).
41. Soudais, C. et al. In vitro and in vivo analysis of the Gram-negative bacteria-derived riboflavin precursor derivatives activating mouse MAIT cells. *J. Immunol.* **194**, 4641–4649 (2015).
42. Sanchez-Paulete, A. R. et al. Deciphering CD137 (4-1BB) signaling in T-cell costimulation for translation into successful cancer immunotherapy. *Eur. J. Immunol.* **46**, 513–522 (2016).
43. Round, J. L. & Mazmanian, S. K. The gut microbiota shapes intestinal immune responses during health and disease. *Nat. Rev. Immunol.* **9**, 313–323 (2009).
44. Atarashi, K. et al. Induction of colonic regulatory T cells by indigenous Clostridium species. *Science* **331**, 337–341 (2011).
45. Espey, M. G. Role of oxygen gradients in shaping redox relationships between the human intestine and its microbiota. *Free Radic. Biol. Med.* **55**, 130–140 (2013).

Chapter 5

Unbiased Analysis of Unconventional T Cells in Tanzanian Volunteers Reveals a Personalised Vδ1 T-Cell Response upon Controlled Human Malaria Infection

This chapter is a working manuscript, to be submitted to Nature Communications

Tobias Rutishauser[1,2,3], Daniela Di Blasi[3], Marco Lepore[3], Cristina Tocchini[3], Salim Abdulla[4], Said Jongo[4], Kamaka Ramadhani[4], B. Kim Lee Sim[5], Stephen L. Hoffman[5], Marcel Tanner[1,2], Claudia Daubenberger[1,2,+*], Gennaro De Libero[3+,*]

[1]Swiss Tropical and Public Health Institute, Basel, Switzerland; [2]University of Basel, Basel, Switzerland; [3]Experimental Immunology, Department of Biomedicine, University and University Hospital Basel, Basel, Switzerland; [4]Bagamoyo Research and Training Centre, Ifakara Health Institute, Bagamoyo, Tanzania; [5]Sanaria Inc., Rockville, Maryland
[+]both authors contributed equally;[*]corresponding authors

ABSTRACT

An effective malaria vaccine against *Plasmodium falciparum* would greatly help to reduce disease burden and assist elimination campaigns. However, our understanding of the human immune response to malaria infection remains incomplete. Clinical trials using whole-sporozoite-based vaccination approaches such as the PfSPZ Vaccine followed by controlled human malaria infection to assess vaccine efficacy offer a unique opportunity to study the human immune response to malaria in a highly controlled setting.

Unconventional T cells, especially γδ T cells, have been implied in having a protective role against *Plasmodium* infection, but most work has focussed on Vγ9Vδ2 T cells, the most abundant subset in human peripheral blood. Here, we dissected the human immune response of γδ T cells and mucosal-associated invariant T (MAIT) cells towards PfSPZ vaccination and controlled human malaria infection using an unbiased analysis pipeline. We made several noteworthy findings: First, no major *ex vivo* alterations were detectable upon PfSPZ vaccination, but all four subsets expanded after CHMI. Second, Vδ1 T cells show an especially strongly activated phenotype upon CHMI, but with large inter-individual differences, indicating a personalised immune response against malaria infection. Third, our analyses led to the identification of a functional allele of the human TCRγ chain Vγ10 that has been thought to be non-functional in humans. Vγ10 has only low amino acid similarity with the other TCRγ chains and thus might contribute to the formation of TCRs with unique antigen recognition properties.

INTRODUCTION

Compared to the year 2010, global malaria disease burden has decreased significantly. In recent years, however, this trend is stalling and in some regions even reversing. In 2016, 216 million cases of malaria were reported, leading to 445'000 deaths worldwide [1].

A valuable tool to fight malaria would be an effective vaccine that leads to long-lasting protection. RTS,S, the most advanced and only malaria vaccine having received a positive regulation assessment from the European Medicines Agency (EMA) is being rolled out in Ghana, Kenya and Malawi starting in 2018 [2]. RTS,S/AS01 provided 36% and 26% protection against clinical malaria episodes in African children and infants, respectively, when assessed during a large multi-center phase III clinical study [3]. Recently, the Sanaria PfSPZ Vaccine that is based on direct venous inoculation of cryopreserved, purified, metabolically active, whole, live, radiation-attenuated *P. falciparum* sporozoites (PfSPZ) has led to more promising results in European and US volunteers, inducing up to 100% protection against homologous and heterologous controlled human malaria infection (CHMI) [4], [5]. Alternative PfSPZ vaccination approaches are based on genetically attenuated PfSPZ (GAP) or non-attenuated sporozoites administered to humans under chemoprophylaxis (CVac) [4], [6], [7]. First results from clinical trials in sub-Saharan Africa indicate a considerably lower vaccine efficacy than the one observed in European or US volunteers using similar vaccination regimen [8]. This is accompanied by lower circumsporozoite-protein specific antibody responses and only low changes in NK cells and T cells ([8] and Jongo et al, manuscript in press). The reasons for this difference remain obscure, demonstrating our incomplete understanding of the interactions between malaria pre-exposure, malaria vaccination and vaccination outcome.

The human immune response to *Plasmodium* spp. is parasite-stage-dependent and involves myeloid cells, NK cells, B cells and T cells [9]. Many studies of T-cell biology in malaria have focused on conventional $CD4^+$ or $CD8^+$ T cells bearing an αβ T-cell receptor (TCR), or Vγ9Vδ2 γδ T cells [4]. However, γδ T cells other than the Vγ9Vδ2 T-cell subset are uniquely suited to play an important part in the malaria immune response due to their abundance in tissues and demonstrated role in stress surveillance [10].

Upon human malaria infection, polyclonal expansion of γδ T cells has been observed in several studies [11]–[13]. Early studies focused on the $V\delta1^+$ subset, but since then, the focus has shifted more towards the Vδ2 T cells. Vγ9Vδ2 T cells are the most abundant γδ T cells in

peripheral blood recognizing small, phosphorylated compounds, including *P. falciparum*-derived phosphoantigens that are able to stimulate Vγ9Vδ2 T cells [14]. Additionally, Vγ9Vδ2 cells have also been implied as a possible correlate of protection after PfSPZ vaccination [4], [15].

Recently, mucosal-associated invariant T (MAIT) cells have been shown to expand upon controlled human malaria infection [16]. MAIT cells are a semi-invariant T-cell subset that recognizes microbial-derived riboflavin metabolites presented by the MHC class I-like molecule MR1 [17].

Thus, a role of unconventional T cells in human malaria infection has been firmly established, but the diversity of study designs, differences in the examined populations and analyses performed make it difficult to get a better understanding of their function.

Here, we used the highly controlled setting of a PfSPZ Vaccine clinical trial in Tanzania (clinical trial BSPZV1; NCT02132299; Jongo et al, manuscript in press) that included a controlled human malaria infection (CHMI). Peripheral blood mononuclear cells (PBMC) were analyzed by flow cytometry in combination with an unbiased analysis pipeline to dissect the response of unconventional T cells to human malaria infection. Our results show that unconventional T-cell subsets are distinctly activated upon CHMI. In particular, we provide evidence that Vδ1 T cells are activated upon CHMI in a donor-dependent manner, indicating a personal response. Furthermore, our analyses led to the first description of a T-cell clone bearing a functional Vγ10Vδ1 TCR.

RESULTS

γδ T cells and MAIT cells expand significantly upon human malaria infection

First, we assessed the frequency of four groups of unconventional T cells upon PfSPZ vaccination and CHMI using multicolour flow cytometry in a group of 24 adult, male, healthy Tanzanian volunteers. We grouped the γδ T cells according to their expression of the TCRδ chain into Vδ1 T cells, Vδ2 T cells, and $Vδ1^{neg}Vδ2^{neg}$ (Vδx) T cells. MAIT cells were identified by the expression of TCR Vα7.2 and high levels of CD161.

Between the baseline visit and two weeks post last vaccination, there were no major changes detected in frequency of unconventional T cells within PBMC. The only difference we found was a minor decrease of Vδx T cells upon vaccination (Fig. 1A). However, in PBMC collected 28 days after initiation of CHMI, Vδ2 T cells and MAIT cells expanded strongly (Fig. 1B). Vδ1 T cells as well as Vδx T cells expanded significantly, albeit less strongly (mean fold-change between post-vaccination and post-challenge: Vδ2 T cells and MAIT cells 1.9-fold, Vδ1 T cells 1.3-fold and Vδx T cells 1.2-fold) (Fig. 1B).

Vδ1 T cells and Vδx T cells show a distinct, strongly activated phenotype upon CHMI

Next, we examined phenotypic alterations within each unconventional T-cell subset upon PfSPZ vaccination and CHMI. For this purpose, we designed a multicolour flow cytometry panel including antibodies against NK receptors as well as markers for activation and exhaustion (CD38, CD69, CD94, CD161, HLA-DR, LAG-3, NKp80, PD-1). We used an unbiased approach to identify significant phenotypic changes upon PfSPZ vaccination and asexual blood-stage infection. To reduce the multi-dimensional flow cytometry data to two dimensions, we used the t-SNE algorithm. Then, clusters of phenotypically similar T cells were identified using the clustering algorithm DBSCAN and the cell frequency within each cluster was calculated. Consistent with the absence of expansion upon PfSPZ vaccination (Fig. 1A), we did not discover any significant vaccination-induced phenotypic changes (see Fig. 2B, 3B, S1B, S2B). However, upon asexual blood-stage malaria, several clusters of T cells were significantly increased in all subsets. The most prominent common feature of all unconventional T cells was an increase of CD38 expression after CHMI. A more detailed analysis revealed distinct patterns of surface marker expression in the different T-cell subsets. Within the Vδ1 T cells, we identified five clusters that were increased after malaria infection (Fig. 2B, C). Notably, these clusters expanded across all 20 volunteers who developed blood-stage parasitaemia after CHMI, but there was no such trend in the four volunteers who were

protected from blood-stage infection (Fig. 2D). All clusters showed expression of CD38 and PD-1, and some clusters additionally LAG-3 or HLA-DR, indicative of strong activation (Fig. 2E). This observation was in marked contrast with the phenotype of expanded Vδ2 T cells and MAIT cells, in which expression of inhibitory receptors was completely absent (Fig. S1E and Fig. S2E).

We performed the same analysis on the Vδx subset and found two main groups of cells to be expanded: one was phenotypically similar to the expanded Vδ1 T cells, expressing CD38 and PD-1, but little CD161. The other group of cells expressed CD161 and CD38, but not PD-1 (Fig. 3E). Thus, the mutually exclusive expression of PD-1 and CD161 divides the Vδx subset in two major subsets.

We aimed to confirm the differences in frequency of $CD38^{+}PD\text{-}1^{+}$ cells across the four subsets of unconventional T cells using conventional flow cytometry analysis based on the same data set (Fig. 4). Although there was considerable inter-donor variability, Vδ1 T cells clearly showed the strongest expansion of $CD38^{+}PD\text{-}1^{+}$ cells upon blood-stage malaria. Consistent with the t-SNE analysis, the Vδx T-cell subset showed a lower, but significant increase in $CD38^{+}PD\text{-}1^{+}$ cells, while no significant changes were detectable in Vδ2 T cells and MAIT cells upon CHMI (Fig. 4).

Vδ1 T cells proliferate extensively *in vitro* in response to asexual blood-stage parasites

We hypothesized that the increased *ex vivo* frequency of $CD38^{+}PD\text{-}1^{+}$ Vδ1 T cells after asexual blood-stage parasitaemia could be due to antigen-dependent stimulation of these cells. Thus, we aimed to identify the parasite-responsive cells using an *in vitro* stimulation assay. We differentiated autologous monocyte-derived dendritic cells (Mo-DC) from four BSPZV1 donors and stimulated PBMC using either uninfected erythrocytes (uRBC) or *P. falciparum*-infected erythrocytes (PfRBC). PfRBC were infected with the *P. falciparum* strain NF54, which is also used in the PfSPZ vaccine. Expectedly, we found robust proliferation of $CD4^{+}$ T cells as well as Vδ2 T cells after PfRBC stimulation for 6 days. Interestingly, marked proliferation was also observed in Vδ1 T cells as well as Vδx T cells (Fig. 5A). Reminiscent of the *ex vivo* phenotype observed after CHMI, the proliferating cells showed high expression of CD38 and PD-1, particularly Vδ1 T cells, Vδx T cells as well as $CD4^{+}$ αβ T cells (Fig. 5B).

Vδ1 T-cell clones are strongly autoreactive

Next, we aimed to functionally characterise the proliferating Vδ1 T cells by establishing T-cell lines. We selected a BSPZV1 donor with a strong increase of $CD38^{+}PD\text{-}1^{+}$ Vδ1 T cells *ex vivo* after CHMI and stimulated PBMC from day 28 post-CHMI with autologous Mo-DC and PfRBC for 6 days. We sorted the proliferating $\gamma\delta^{+}$ $V\delta2^{neg}$ T cells and established a T-cell line. This T-cell line, upon stimulation with autologous Mo-DC and PfRBC, showed increased expression of CD137 on Vδ1 T cells, indicative of antigen-dependent stimulation (Fig. S3A). Additionally, $CD4^{+}$ T cells in the same line were strongly activated (Fig. S3B).

In order to further characterize these PfRBC-responsive T cells, we generated T-cell clones from Vδ1 T cells as well as $CD4^{+}$ αβ T cells. These clones were then screened for activation in response to Mo-DC and PfRBC. The $CD4^{+}$ T-cell clones showed a consistent increase of CD137 expression upon stimulation with PfRBC, proving the validity of our approach to isolate *P. falciparum*-responsive T-cell clones (Fig. 6A). In the Vδ1 T-cell clones, no consistent trend towards increased parasite-dependent activation was detectable. However, the Vδ1 T-cell clones showed a high expression of CD137 when co-cultured with homologous Mo-DC and uRBC, independently of the presence of blood-stage parasites. In fact, many Vδ1 T-cell clones expressed higher levels of CD137 in the control condition (Mo-DC with uRBC) than the PfRBC-specific $CD4^{+}$ T cells upon encounter of their cognate ligand (Fig. 6A).

We further evaluated the reactivity of Vδ1 T-cell clones by screening the response towards a panel of cell lines derived from monocytes (U937, THP-1), myeloid cells (K562), B cells (721.221), liver (HC-04) and cervix (HeLa). Co-culture experiments of five selected Vδ1 T-cell clones with these cell lines revealed two clusters of clones differing in their pattern of IFN-γ release assessed by ELISA (Fig. 6B). The clone PfC45 was responsive only to HeLa cells, but not the other lines tested. A cluster of four clones showed stronger reactivity, especially towards the hepatoma cell lines HC-04 and HuH-7. Activation was shown to be independent of β2-microglobulin (β2m), as IFN-γ secretion was not decreased in HC-04 cells lacking β2m, indicating that activation is independent of MHC class I and class I-related molecules.

To analyse if activation of the T-cell clones is TCR-mediated, we amplified the TCRγ and TCRδ chains of the representative clones PfC45 and PfB67 by PCR and transferred them into SKW-3 cells using a lentiviral vector. Both TCRs were abundantly expressed on the surface,

but surprisingly, the PfB67 Vδ1 TCR induced strong up-regulation of CD69 in the SKW-3 cell lines without addition of external stimuli, an effect that was not observed in SKW-3 expressing the PfC45 TCR (Fig. 6C, D). This could indicate that the unidentified ligand of the PfB67 TCR might also be expressed on SKW-3 cells. We confirmed that this PfB67 TCR activation is independent of β2m expression by transferring the PfB67 TCR onto SKW-3 cells that lack β2m (Fig. 6C, bottom right panel).

Next, we assessed whether this strong reactivity of Vδ1 T cells towards cell lines can also be detected *ex vivo*. For this aim, we used PBMC from three BSPZV1 donors collected pre-vaccination, post-vaccination and post-challenge. Proliferation and activation markers were assessed after six days of co-culture with the cell lines THP-1, HC-04 and HeLa. Vδ1 T cells proliferated extensively and up-regulated the activation markers CD38 and PD-1, an effect that was almost absent in the Vδ2 T-cell subset (Fig. 7A, B). Additionally, Vδ1 T cells expressed increased levels of CD137 after co-culture (Fig. 7C). While all tested cell lines induced some degree of proliferation and activation, the strongest response was induced by the hepatocyte cell line HC-04, reminiscent of the activity pattern of T-cell clone PfB67.

The Vδ1 T-cell clone PfB67 expresses a functional Vγ10Vδ1 TCR

We analysed the TCR sequences from the Vδ1 clones and found that PfB67 expresses a functionally rearranged and fully spliced TRGV10 gene in combination with Vδ1. Up to now, TRGV10 was thought to be non-functional, due to lack of an intact splice donor site in the leader intron [18]. However, when we sequenced the TCR of PfB67, we found the majority of transcripts to be correctly spliced. Sequencing of a cDNA from a rare, incompletely spliced transcript revealed an intact splice donor site with the canonical splice donor motif GURAGU (Fig. 8A; allele TRGV10*novel).

We aimed to confirm the presence of this functional allele and determine its frequency in the 24 BSPZV1 volunteers by PCR amplification and sequencing. Two volunteers were homozygous for TRGV10*novel, nine heterozygous and 13 lacked the TRGV10*novel allele. Thus, allele frequency of TRGV10*novel within our population is 13/48 = 27% (Fig. 8B).

Next, we determined the frequency of the TRGV10*novel allele in humans across the world using data from the 1000 genomes project [19]. Allele frequency in the sub-Saharan African populations ranged between 15.7% (Kenya; LWK) and 27.1% (Sierra Leone; MSL). Strikingly, this allele was completely absent in Asians and almost undetectable in Europeans

(0.1%) and Americans (1.3%) (Fig. 8C). Populations of African ancestry living in Barbados (ACB) or the Southwest of the United States (ASW) show a similar allele frequency as sub-Saharan Africans. Thus, these data strongly indicate that the functional TRGV10*novel allele is exclusive to sub-Saharan Africans or people of recent African descent.

Alignment of the canonical human TRGV10 sequences with sequences from other primates indicates that TRGV10*novel, at least in terms of the splice donor site, represents the ancestral allele (Fig. 8D) [20]. Remarkably, TRGV10 is the sole member of the TCR gamma chain subgroup VγIII, with only low amino acid sequence similarity to the other subgroups VγI (TRGV1-8) and VγII (TRGV9) [21], and could therefore represent a functionally distinct γδ T-cell subset with unknown, possibly novel antigen-specificity.

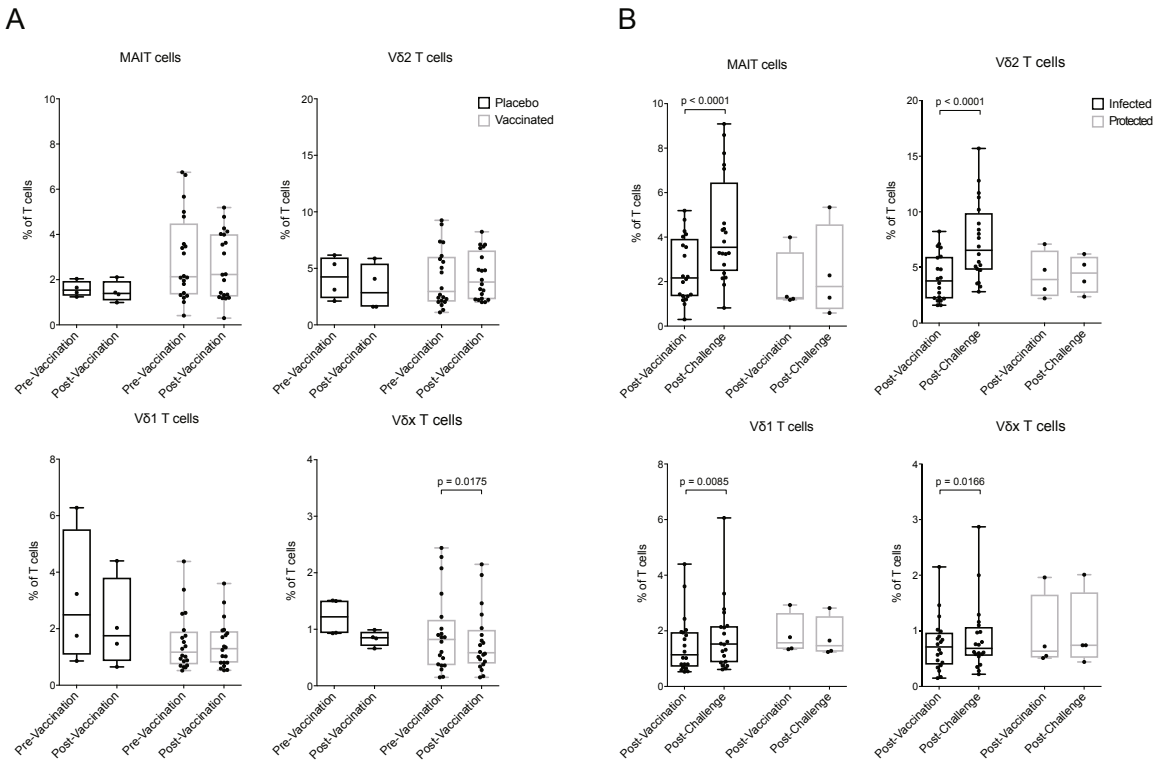

Figure 1 (A) The frequency of unconventional T cells in PBMC is almost unchanged upon vaccination, the only change is a slight decrease in Vδx frequency. (B) All examined unconventional T-cell subsets are significantly expanded in the volunteers who developed blood-stage parasitaemia after CHMI (infected), but not in the ones who were protected from blood-stage parasitaemia (protected).

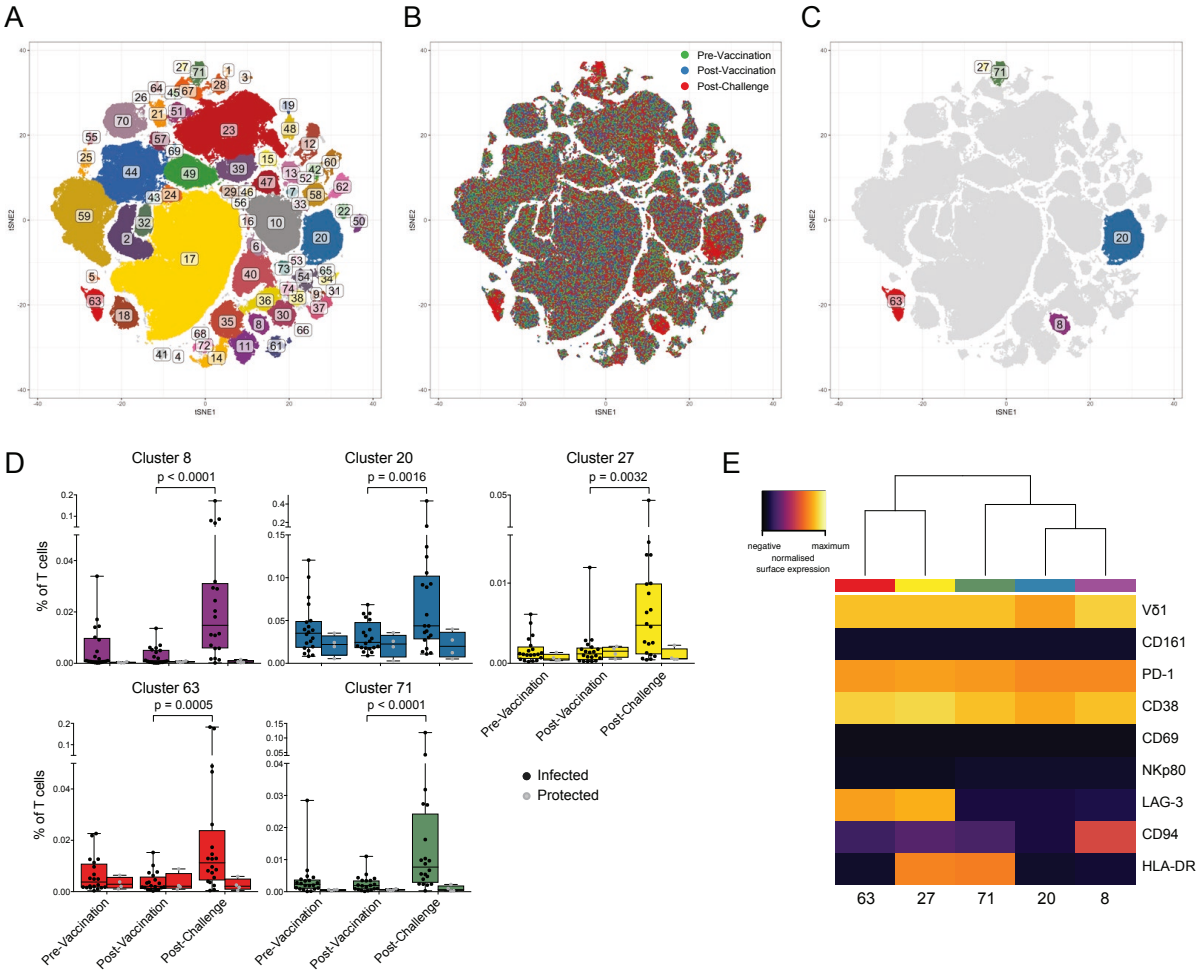

Figure 2 | Subsets of Vδ1 T cells are activated upon controlled human malaria infection. (A) viSNE map after clustering indicates hetereogeneity within Vδ1 T cells. (B) Comparison of Vδ1 T cells at baseline (green dots), after PfSPZ vaccination (blue dots) and after CHMI (red dots). Regions with increased cell frequencies after CHMI appear in red. (C) Significantly altered clusters after CHMI are highlighted and color-coded. Clusters are considered significant with $p < 0.05$ (Wilcoxon signed-rank test adjusted with the Benjamini & Hochberg method) and at least 2.5-fold change of the mean. (D) The five significant clusters are increased only in volunteers who developed blood-stage parasitemia after CHMI (infected; black dots), but remain unchanged in those who did not develop blood-stage parasitemia after CHMI (protected; grey dots). (E) Significantly expanded populations invariably express CD38 and PD-1.

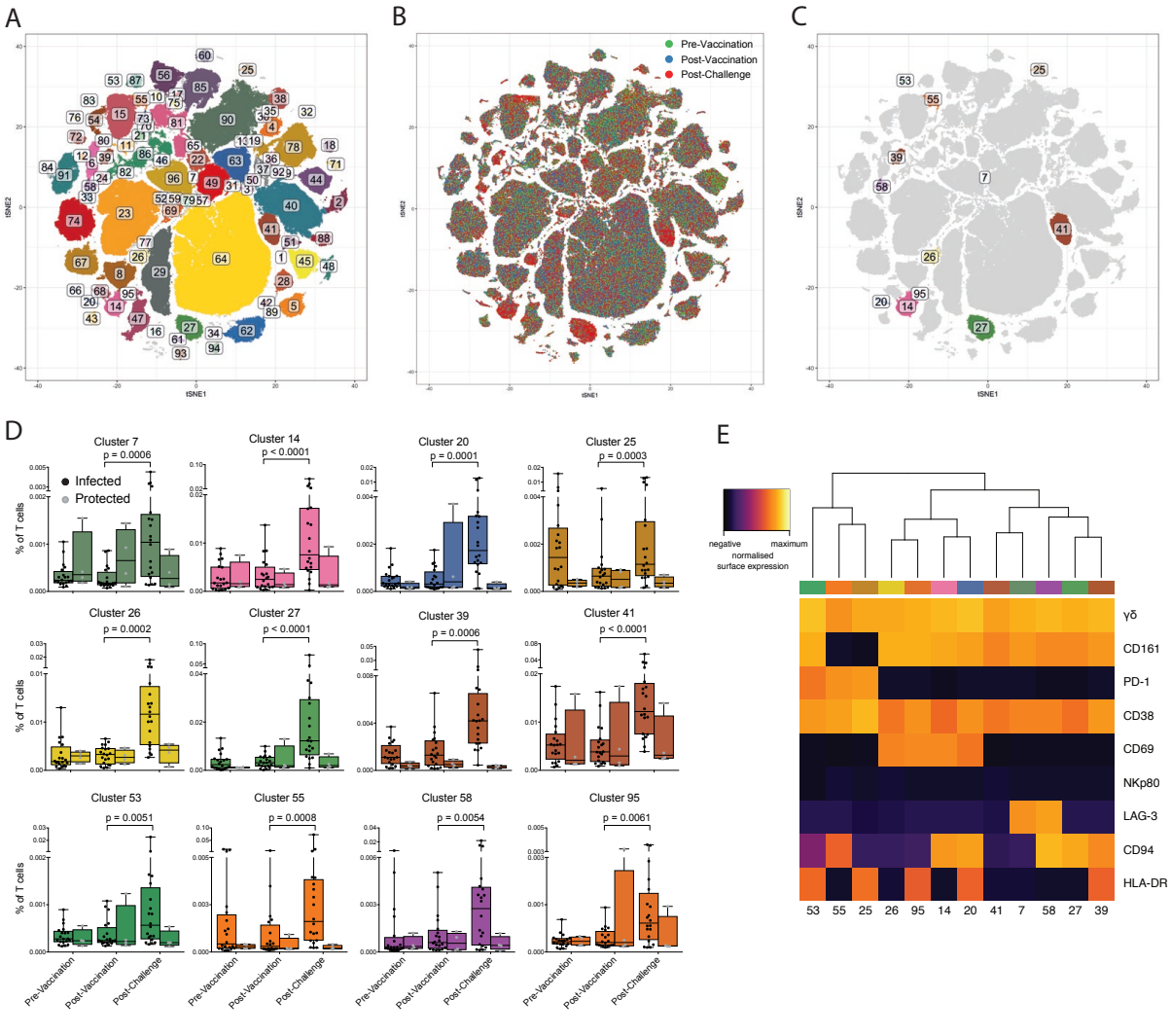

Figure 3 | Subsets of Vδx T cells are activated upon controlled human malaria infection. (A) viSNE map followed by clustering indicates phenotypic heterogeneity within Vδx T cells. (B) Comparison of Vδx T cells at baseline (green dots), after PfSPZ vaccination (blue dots) and after CHMI (red dots). Regions with increased cell frequencies after CHMI appear in red. (C) Significantly altered clusters after CHMI are highlighted and color-coded. Clusters are considered significant with $p < 0.05$ (Wilcoxon signed-rank test adjusted with the Benjamini & Hochberg method) and at least 2.5-fold change of the mean. (D) The 12 significant clusters are increased only in volunteers who developed blood-stage parasitemia after CHMI (infected; black dots), but remain unchanged in those who did not develop blood-stage parasitemia after CHMI (protected; grey dots). (E) Two main groups are expanded after CHMI: one is characterised by expression of CD38 and PD-1, while the other expresses CD38 and CD161, but no PD-1.

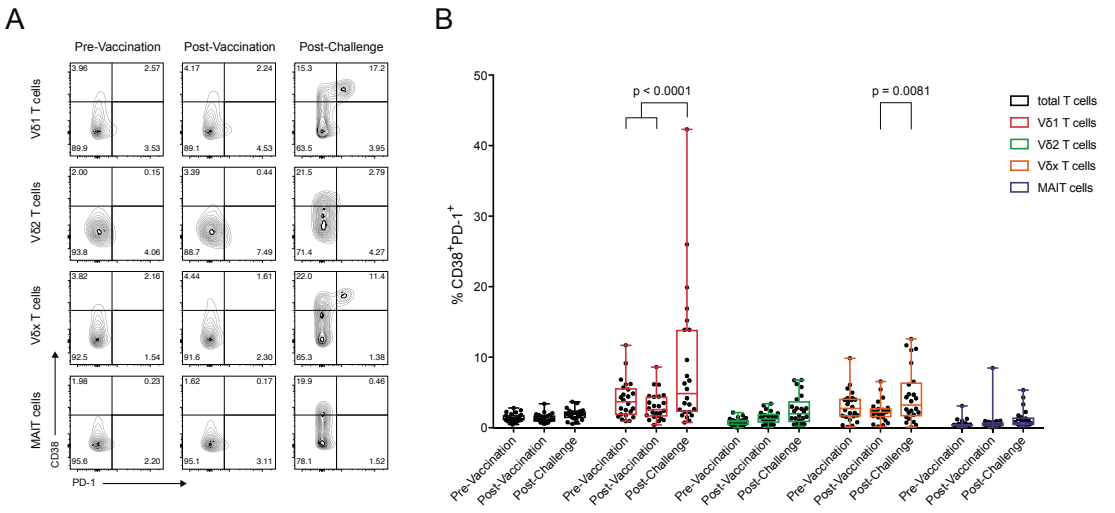

Figure 4 | Vδ1 T cells and Vδx T cells show an increased frequency of CD38$^+$PD-1$^+$ cells after CHMI.
(A) Contour plot of the four examined unconventional T-cell subsets at baseline, post-vaccination and post-challenge in a representative volunteer. (B) Vδ1 and Vδx T-cell subsets show a significantly increased frequency of CD38$^+$PD-1$^+$ cells after CHMI across all volunteers (n = 24). Two-way ANOVA corrected for multiple comparisons using Tukey's range test. While an increase is detectable in most volunteers, the extent of this increase varies considerably between donors, indicating a personalised immune response.

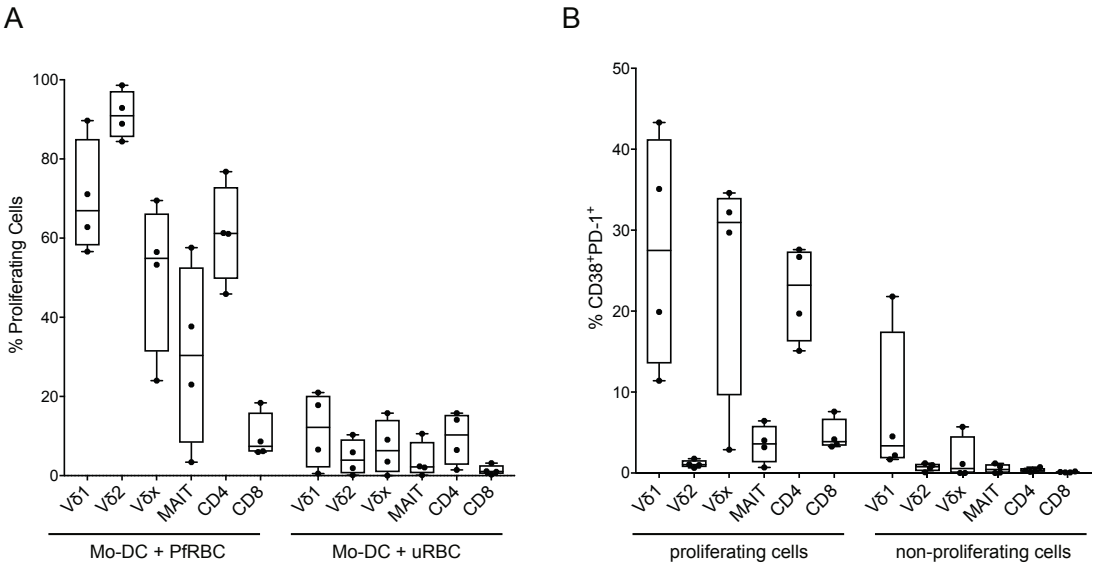

Figure 5 | Vδ1 T cells proliferate extensively upon stimulation with autologous monocyte-derived dendritic cells and blood stage *P. falciparum* parasites.
(A) Proliferation assay of PBMC in response to autologous monocyte-derived dendritic cells (Mo-DC) and *P. falciparum*-infected erythrocytes (PfRBC) or uninfected erythrocytes (uRBC). Vδ1 T cells proliferate to a similar extent as conventional $CD4^+$ T cells. Proliferation was assessed after 6 days of co-culture (n=4). (B) Frequency of $CD38^+PD\text{-}1^+$ double positive cells in proliferating and non-proliferating cells after co-culture with Mo-DC and PfRBC. Proliferating cells are enriched in expression of CD38 and PD-1. Vδ1 and Vδx T cells express higher levels of CD38 and PD-1 than MAIT cells and Vδ2 cells, reminiscent of the ex vivo phenotype after CHMI.

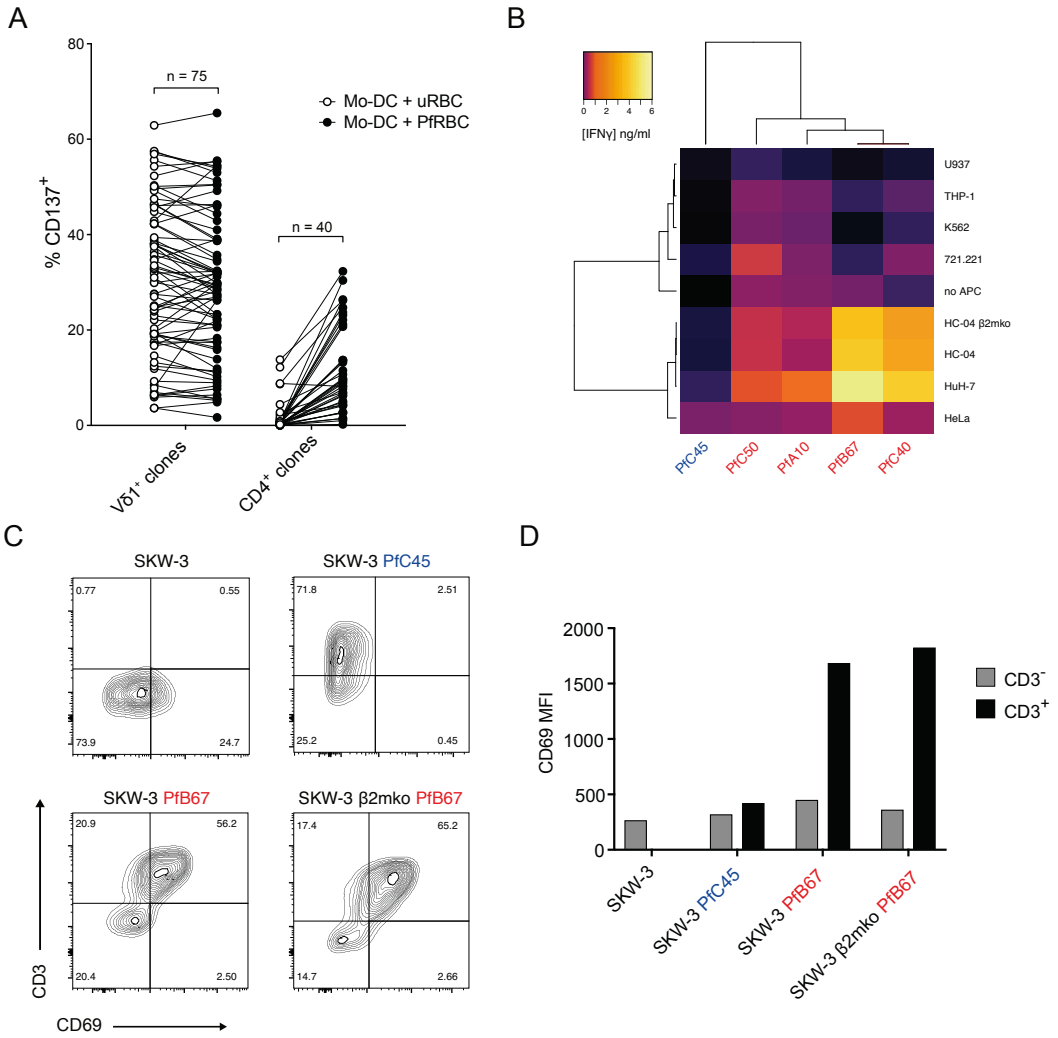

Figure 6 | Vδ1 T-cell clones are strongly autoreactive. (A) The majority of Vδ1 T-cell clones (n=75) are autoreactive towards autologous monocyte-derived DC (Mo-DC) and uninfected RBC (uRBC), but not responsive to *P. falciparum*-infected RBC (PfRBC). $CD4^+$ T-cell clones (n=44) in contrast are only slightly autoreactive, but clearly respond to autologous Mo-DC and PfRBC. (B) Five selected Vδ1 T-cell clones are reactive towards different cell lines as determined by IFN-γ release. Two main clusters of reactivity are detected (highlighted in blue and red). The red cluster is highly autoreactive, especially to hepatocyte-derived cell lines, an effect that is independent of β2-microglobulin expression. PfC45, the sole member of the blue cluster is only slightly autoreactive (towards HeLa cells). (C) Transduction of the PfC45 and PfB67 TCRs into SKW-3 cells. Surface expression of CD3 confirms functional expression and pairing of the two TCRs. Furthermore, the PfB67 TCR, but not PfC45 induces activation in absence of additional cells. The same effect is observed in SKW-3 lacking β2m, confirming that activation is independent of MHC class I and class I-related molecules. (D) Quantification of the median flurorescent intensity (MFI) of CD69 as described in (C).

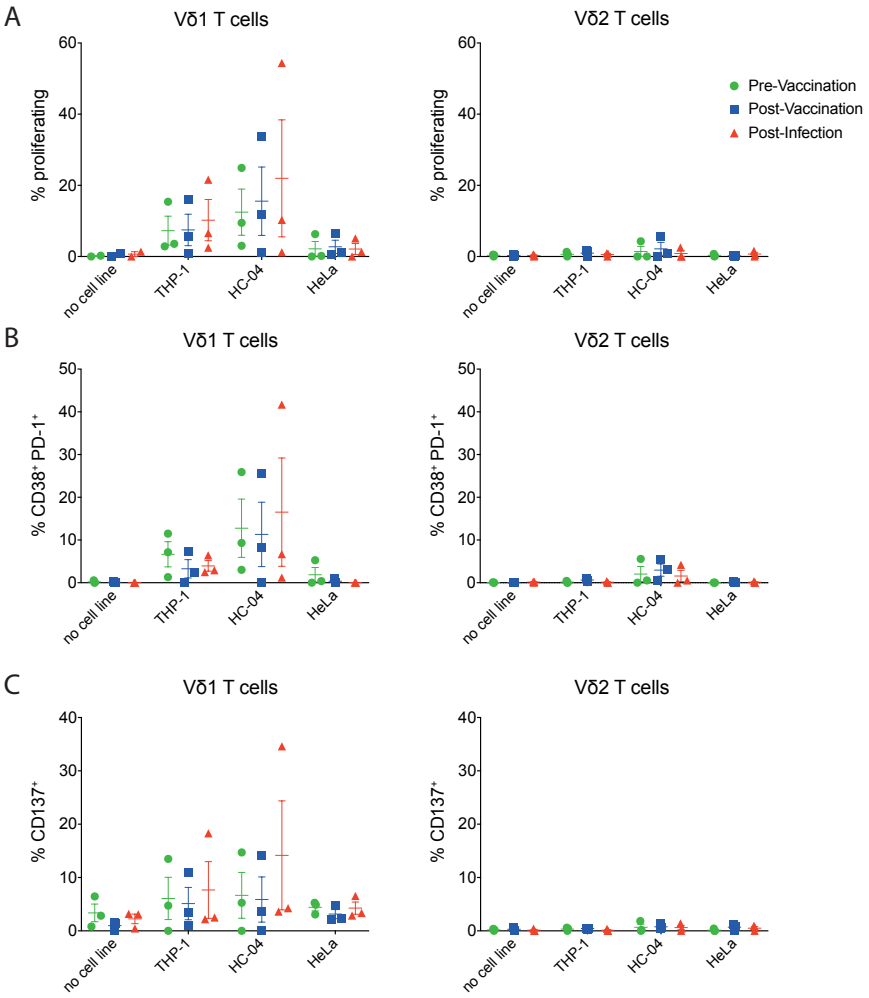

Figure 7 | Polyclonal Vδ1 T cells are activated upon co-culture with cell lines. PBMC from three donors, and three different visits, were co-cultured with the cell lines THP-1, HC-04 and HeLa, and proliferation and activation status was assessedand after 6 days of co-culture. (A) Vδ1 T cells proliferate strongly upon co-culture with cell lines, an effect that is absent in Vδ2 T cells. (B) Vδ1 T cells express increased levels of CD38 and PD-1 after co-culture. (C) Co-culture induces expression of CD137 on Vδ1 T cells, indicating strong, possibly TCR-mediated activation. This effect is specific for the Vδ1 subset and almost undetectable in Vδ2 T cells.

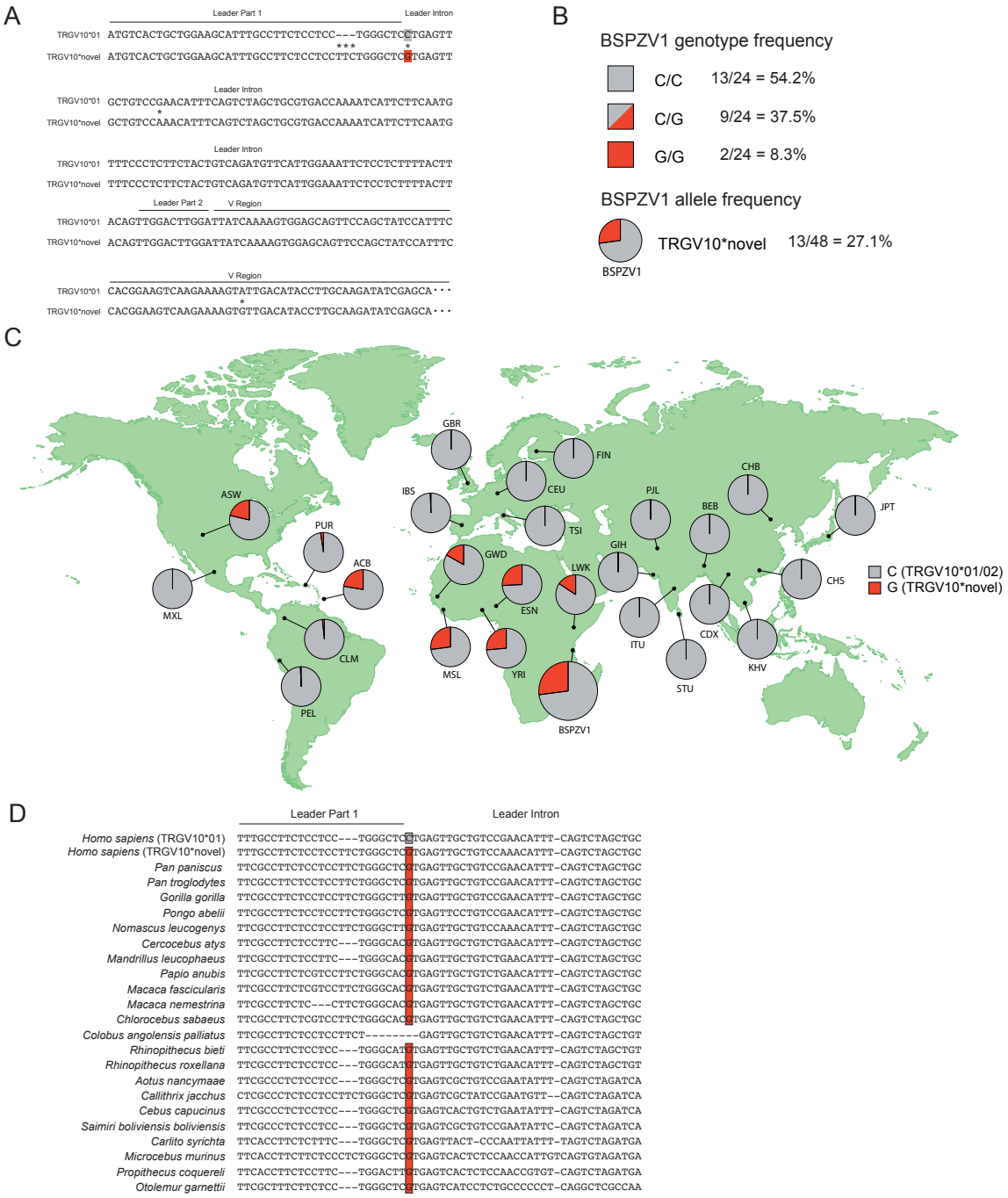

Figure 8 | The functional TRGV10*novel allele is almost exclusive to the African population. (A) Alignment of the leader sequence and the beginning of the V region of the TRGV10*01 with the newly described TRGV10*novel allele. Differences in the sequences are highlighted with asterisks and the intact splice donor guanosine residue of TRGV10*novel is highlighted in red. (B) Genotype and allele frequency from BSPZV1. Allele frequency in our cohort is 27.1%. (C) Distribution of the indicated SNP across the world – the intact splice donor (G) is almost exclusive to Africans or people of recent African descent. ACB: African Carribean in Barbados, ASW: African ancestry in Southwest US. (D) The canonical splice donor site is highly conserved in primate TRGV10 homologues.

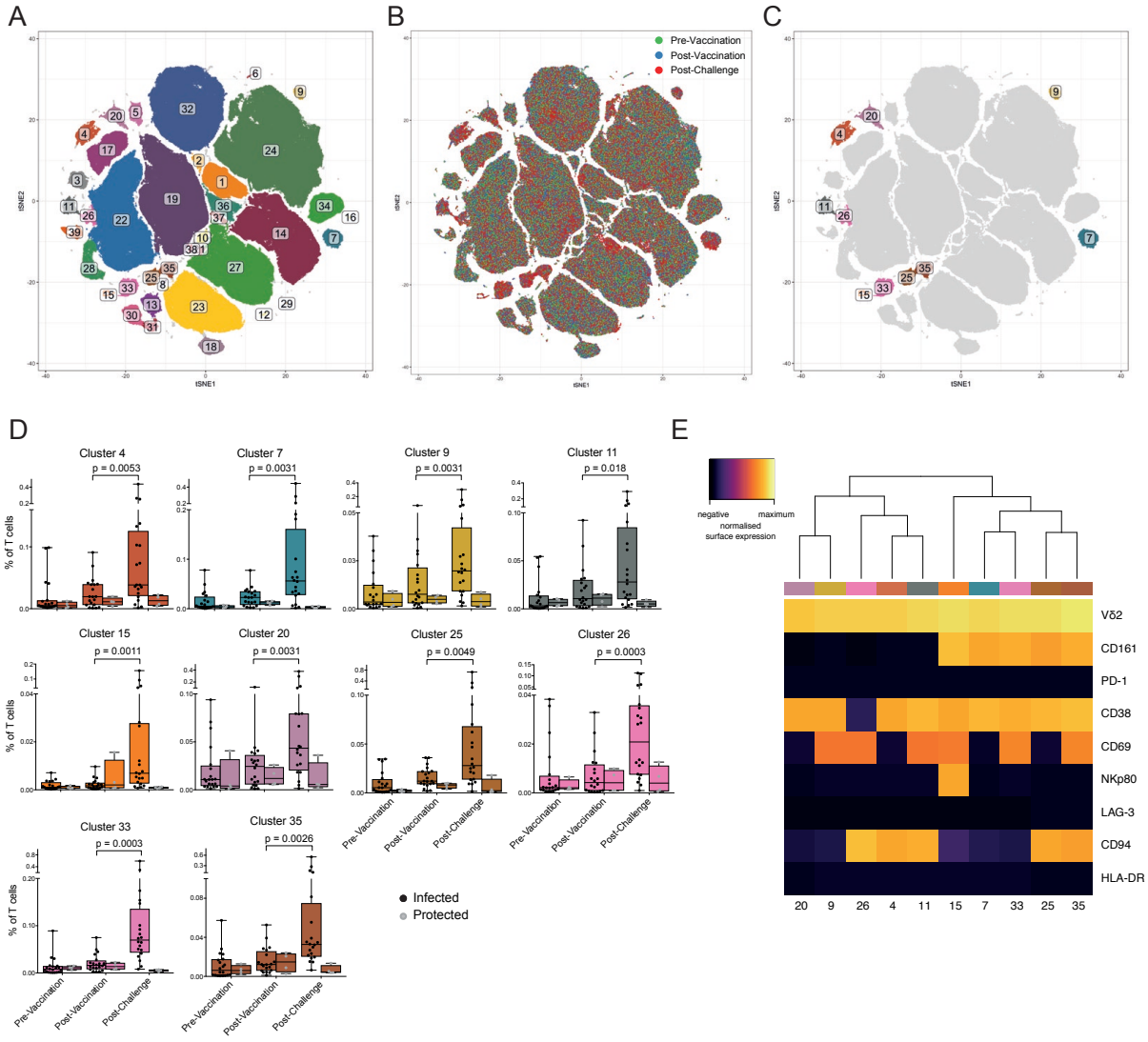

Figure S1 | Vδ2 T cells are activated upon malaria infection. (A) viSNE map followed by clustering. (B) Comparison of Vδ2 T cells at baseline (green dots), after PfSPZ vaccination (blue dots) and after CHMI (red dots). Regions with increased cell frequencies after CHMI appear in red. (C) Significantly altered clusters after CHMI are highlighted and color-coded. Clusters are considered significant with $p < 0.05$ (Wilcoxon signed-rank test adjusted with the Benjamini & Hochberg method) and at least 2.5-fold change of the mean. (D) The 10 significant clusters are increased only in volunteers who developed blood-stage parasitemia after CHMI (infected; black dots), but remain unchanged in those who did not develop blood-stage parasitemia after CHMI (protected; grey dots). (E) Almost all significantly expanded populations express CD38, but no co-inhibitory receptors.

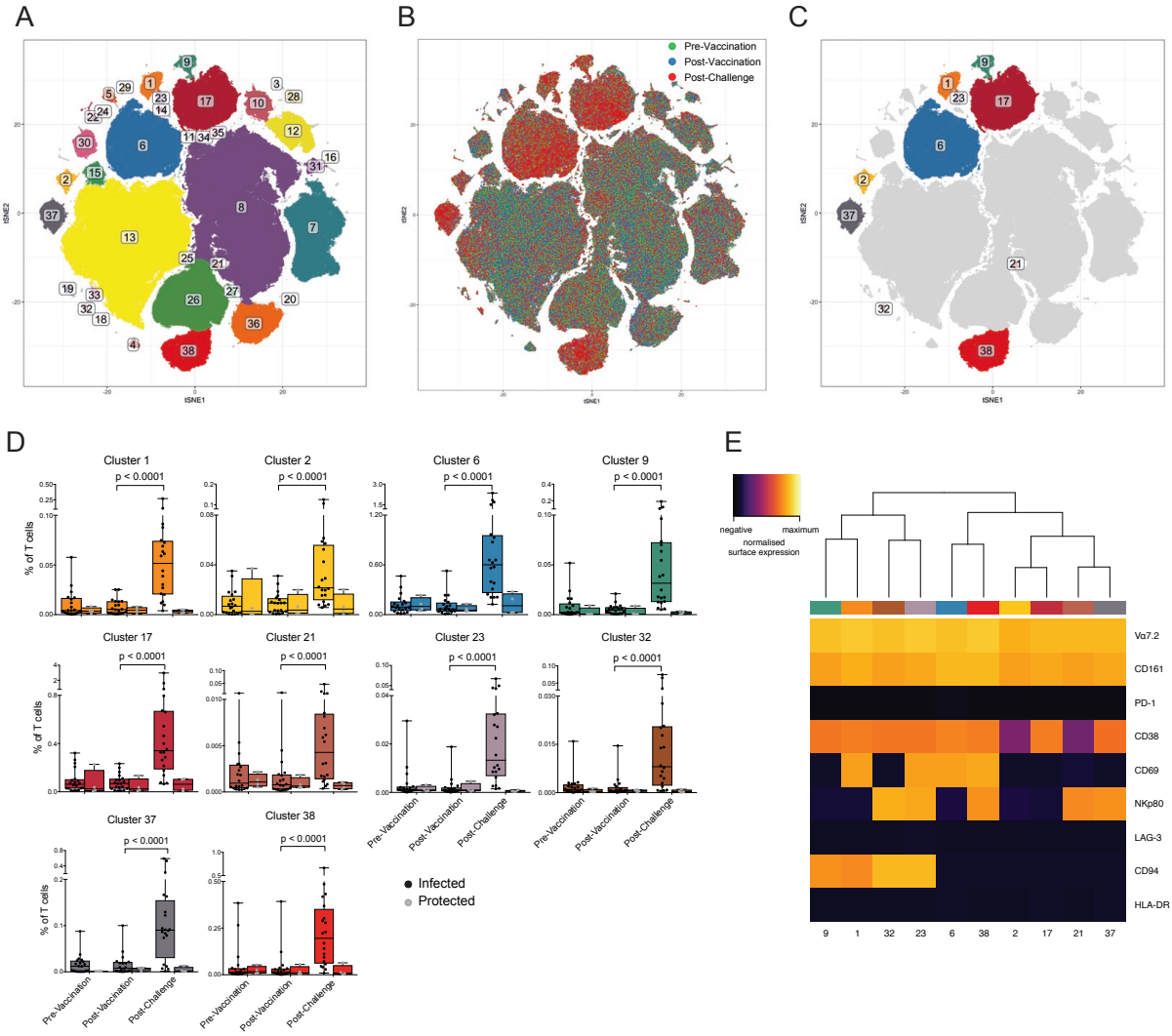

Figure S2 | MAIT cells are activated upon controlled human malaria infection. (A) viSNE map followed by clustering. (B) Comparison of MAIT cells at baseline (green dots), after PfSPZ vaccination (blue dots) and after CHMI (red dots). Regions with increased cell frequencies after CHMI appear in red. (C) Significantly altered clusters after CHMI are highlighted and color-coded. Clusters are considered significant with $p < 0.05$ (Wilcoxon signed-rank test adjusted with the Benjamini & Hochberg method) and at least 2.5-fold change of the mean. (D) The 10 significant clusters are increased only in volunteers who developed blood-stage parasitemia after CHMI (infected; black dots), but remain unchanged in those who did not develop blood-stage parasitemia after CHMI (protected; grey dots). (E) All significantly expanded populations show increased expression of CD38, but no co-inhibitory receptors.

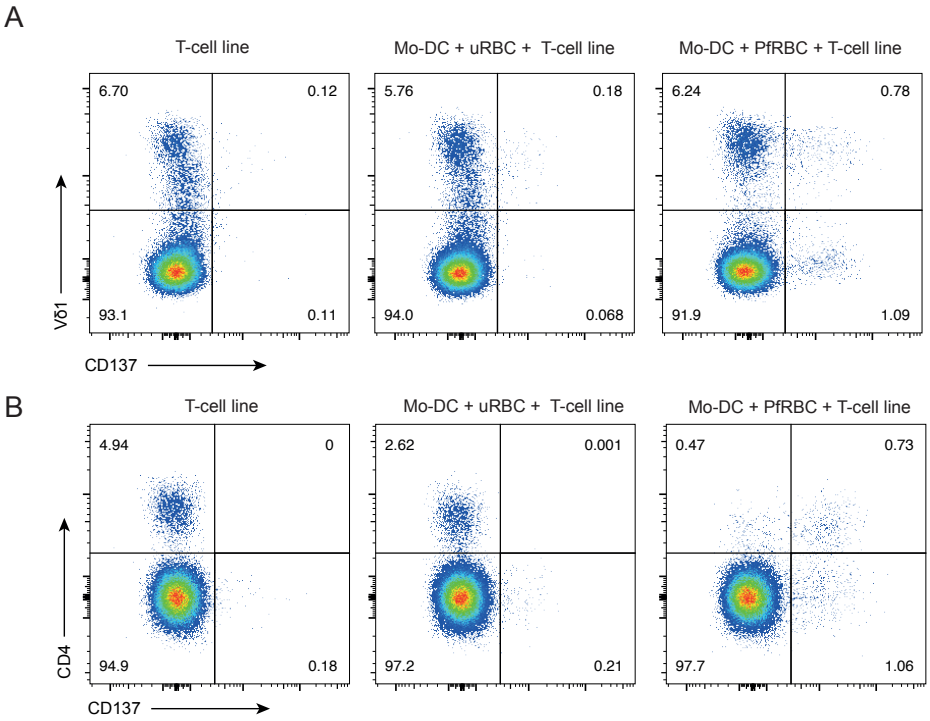

Figure S3 | Vδ1 T cells and CD4$^+$ T cells are activated in a parasite-dependent manner. (A) Vδ1 T cells within a T-cell line are activated upon stimulation with autologous monocyte-derived dendritic cells (Mo-DC) and *Plasmodium falciparum*-infected RBC (PfRBC) as indicated by CD137 expression. (B) CD4$^+$ T cells within the same T-cell line are activated by Mo-DC and PfRBC.

DISCUSSION

CHMI conducted in malaria pre-exposed populations is an essential tool to dissect malaria parasite–host interactions under highly defined conditions [22]. During our CHMI studies in Bagamoyo, we injected 3'200 purified, metabolically active, non-attenuated PfSPZ (strain NF54) intravenously to male, adult volunteers with limited malaria pre-exposure (Jongo et al., manuscript in press). We have analysed here for the first time in detail the frequency and phenotypic changes of MAIT cells and γδ T-cell subsets during CHMI. γδ T cells have been described three decades ago, but the biological functions apart from the Vγ9Vδ2 subset are not very well delineated in humans [23].

Our findings confirm that Vδ2 T cells expand upon asexual blood stage parasitaemia in malaria pre-exposed volunteers [24]. Less is known about the Vδ1 and Vδx T cell subsets in general in humans and in malaria in particular [12]. Therefore, we compared the frequencies and phenotypic changes of Vδ1 and Vδx T-cell subpopulations before and after CHMI using an unbiased approach [25]. Clearly, CD38 was the surface marker across all subsets that increased significantly. However, only distinct subsets of Vδ1 and Vδx T cells co-expressed inhibitory receptors, especially PD-1 and to a lesser extent LAG-3, which were strikingly absent on expanded Vδ2 T cells and MAIT cells. This implies a qualitatively distinct activation of a fraction of Vδ1 T cells and Vδx T cells upon CHMI. PD-1 is known to be particularly upregulated on antigen-specific T cells, not only in cancer but also in chronic infectious diseases [26], [27]. Thus, we speculate that PD-1 expression on Vδ1 and Vδx T cells marks antigen-dependent, TCR-mediated stimulation of those cells. In line with this, the degree of increase in $CD38^{+}PD\text{-}1^{+}$ expression on Vδ1 T cells is highly variable between donors and points towards a personalised response similar to the clonal expansion observed in the response of Vδ1 T cells towards cytomegalovirus infection [28].

Within the expanded Vδx T cells, we found mutually exclusive expression of CD161 and PD-1. Interestingly, in both αβ and γδ T cells, CD161 has been associated with high responsiveness to stimulation by IL-12 and IL-18 [29]. This cytokine-mediated activation is likely to occur during asexual blood-stage malaria, which is known to strongly induce pro-inflammatory cytokines such as IL-1β, IL-6, IL-8, IL-12, IFN-γ, and TNF [9].

Together, our *ex vivo* analysis clearly shows, to our knowledge for the first time, the activation of phenotypically distinct Vδ1 and Vδx T-cell subsets upon CHMI. The cellular subsets expressing PD-1 might have been activated in a strong, possibly TCR-mediated manner whereas the $CD161^{+}$ group could be responsive to cytokine stimulation. Clearly, our

data show that an expansion of Vδ1 and Vδx T-cell populations marked by high levels of CD38 and PD1 expression occurred exclusively in volunteers experiencing a recent asexual blood-stage infection. Volunteers from the same cohort that remained negative for asexual blood-stage parasitaemia did not show this change. Of note, several other infectious diseases have been linked with the expansion of Vδ1 or Vδx T cells in peripheral blood including HIV [30], Epstein-Barr virus (EBV) [31] and CMV [28], with possibly protective immune function.

An interesting finding is the preferential reactivity of a group of Vδ1 T-cell clones towards hepatocyte cell lines. Given the high number of Vδ1 T cells in liver parenchyma [32], one might speculate that these liver-cell-reactive T cells are involved in liver stress surveillance through recognition of an unknown ligand expressed on altered hepatocytes. This would make those T cells ideally suited to play a protective role during malaria liver stage or in response to blood-stage parasitaemia, in which the liver also plays an important role [33]. Our unpublished, preliminary results of CVac-based vaccination of malaria pre-exposed volunteers in Equatorial Guinea during the EGSPZV2 trial indicate that liver-resident, malaria specific immunity might be induced under natural conditions (Olotu et al., manuscript in preparation). Furthermore, data from mouse models suggest that the pre-erythrocytic stage is not immunologically silent but that the liver can sense *Plasmodium* infection through recognition of *Plasmodium* RNA and respond with release of type I interferons [34].

Recent evidence shows that Vδ1 T cells are undergoing clonal selection and differentiation from a naïve T cell repertoire in peripheral blood, with chronic CMV infection being potentially a major driver [35]. Interestingly, Vδ1 T cells are abundant in human liver, where they represent about 50% of all γδ T cells and show a phenotype of effector memory T cells including $CD27^{lo}$ and $CD45RA^{lo}$ [32]. Next-generation sequencing approaches showed that the liver-resident Vδ1 TCR repertoire is highly clonally focussed, private (not shared between individuals), shows complex Vγ segment usage and differs from the peripheral-blood Vδ1 TCR repertoire [32].

The few restricting elements known for human Vδ1 TCRs include MHC class I chain-related proteins A and B (MICA and MICB) and CD1 molecules [10]. While identification of the ligand is beyond the scope of this manuscript, activation of our T-cell clones was unchanged when stimulated with genetically engineered HC-04 cells that lack β2m expression, leading

to absence of surface expression of MHC class I and class I-like molecules. In particular, this indicates that activation is independent of CD1 molecules, which require β2m to be expressed on the cell surface [36].

We established for the first time a γδ T-cell clone expressing a full-length, functional TCR Vγ10 chain in combination with Vδ1. So far, it was believed that Vγ10 is non-functional in humans, although a possible functionality in non-Caucasian populations has been suggested [18]. Evolutionarily, the TCR γ locus shows an interesting dichotomy: the region encoding Vγ1-Vγ8 is rapidly evolving, while the Vγ9-Vγ11 region is highly conserved throughout evolution in primates [37]. This includes Vγ10, which shows a strong selection of synonymous mutations, indicating purifying selection [37]. In line with this strong evolutionary conservation, the mutation in the splice donor site seems to be of recent evolutionary origin and within primates has only arisen in the human lineage [20].

Based on their nucleotide sequence similarity, the TCRγ variable genes have been categorised into four subgroups: Vγ2, 3, 4, 5, and 8 (subgroup VγI), Vγ9 (subgroup VγII), Vγ10 (subgroup VγIII) and Vγ11 (subgroup VγIV) [21]. Therefore, due to its low sequence similarity with the other TCR γ V genes, Vγ10 represents the only member of the subgroup VγIII [21]. Thus, Vγ10 might fulfil a unique function, analogous to Vγ9 that is crucial for the generation of the well-studied and specialised Vγ9Vδ2 TCR that senses stress-induced phosphorylated antigens.

We confirmed the presence of this functional allele and determine its frequency in the 24 BSPZV1 volunteers examined in this study, which was found to be 27.1% (Fig. 7B). In the 1000 human genome project, allele frequency in African populations was between 15.7% (Kenya; LWK) and 27.1% (Sierra Leone; MSL), while the allele was completely absent in Asians and almost undetectable in Europeans (0.1%) and Americans (1.3%) (Fig. 7C). Populations of African ancestry living in Barbados (ACB) or the Southwest of the United States (ASW) show a similar allele frequency as the one found in African populations. Thus, the functional TRGV10 allele is exclusive to Africans or people of recent African descent.

Intriguingly, a study in Ghana had already reported the presence of Vδ1 T cells that remained unlabelled when PBMC were stained with a cocktail of antibodies against all functionally expressed Vγ chains known at that time [12]. This $V\gamma2\text{-}9^{neg}V\delta1^{+}$ population was specifically increased to around 15% of Vδ1 T cells in children who were hospitalized for uncomplicated or cerebral malaria, but not in healthy children from the same area [12]. We speculate that this undefined population might encompass the Vγ10Vδ1 T-cell subset, adding independent

evidence for expansion of Vγ10Vδ1 T cells upon malaria infection in another geographical area and age group.

Further studies are necessary to reveal the tissue distribution, TCR repertoire and functional properties of Vγ10-expressing T cells, but our data indicate a role of Vγ10Vδ1 T cells in human malaria infection and our findings pave the way for further studies of this novel T-cell subset that might only be present in people of recent African descent.

METHODS

Cells and cell culture

The HC-04 human hepatocyte cell line was obtained from BEI Resources. The human cell lines THP-1 (monocytic leukaemia), U937 (histiocytic lymphoma), A375 (melanoma), K562 (erythroleukaemia), HEK 293 (embryonic kidney), 721.221 (B cell), HuH-7 (hepatoma), HeLa (cervical cancer) were obtained from American Type Culture Collection. SKW-3 cells (TCR -deficient T-cell leukaemia) were obtained from the Leibniz-Institute DSMZ. β2m knock out in the HC-04 cell lines was performed using a crispr Cas9 system according to standard protocols.

PBMC were isolated from participants of the BSPZV1 clinical trial (ClinicalTrials.gov Identifier: NCT02132299). Details are published in (Jongo et al., manuscript in press). All participants were healthy, male Tanzanians between 18 and 35 years of age. Samples analysed in this manuscript were derived from the high-dose group that received $2.7*10^5$ PfSPZ of PfSPZ Vaccine per injection. Controlled human malaria infection consisted of 3'200 PfSPZ of PfSPZ Challenge administered by direct venous inoculation.

Monocytes were isolated using a Human CD14 Positive Selection Kit (STEMCELL Technologies) according to the manufacturer's instructions. Mo-DC were generated by culturing CD14 positively selected monocytes in the presence of human recombinant IL-4 and GM-CSF (BioLegend) for five days. Differentiation was controlled through cell surface staining of CD209 (DC-SIGN).
T-cell lines and clones were established as previously described [38].

Flow cytometry and antibodies

Flow cytometry stainings, analyses and cell sortings were performed using standard protocols. The following antibodies were obtained from BioLegend: CD3 (fluorochrome BV650, clone OKT3), CD4 (Alexa700, OKT4), CD38 (APC/Cy7, HB-7), CD69 (PE/Dazzle, HNK-1), CD94 (PerCP/Cy5.5, DX22), CD161 (BV605, HP-3G10), CD209 (PE, 9E9A8), CD294 (BV421, BM16), HLA-DR (Alexy700, L243), NKp80 (APC, 5D12), pan-γδ (PE, B1), PD-1 (BV785, EH12.2H7), Vα7.2 (BV510, 3C10), Vδ2 (BV711, B6). Anti-LAG-3 (PE/Cy7, 3DS223H) was obtained from eBioscience, Vδ1 (FITC, TS8.2) from GeneTex, and CD8 (BUV496, RPA-T8) from BD Biosciences. Cell proliferation was assessed *in vitro*

using the CellTrace Violet proliferation kit (ThermoFisher) according to the manufacturer's instructions.

Data analysis and software

Standard flow cytometry analyses were performed using FlowJo (TreeStar). Dimensionality reduction and semi-automated clustering was performed using a custom R script. Briefly, flow cytometry data were gated and the subsets of interest exported from FlowJo and imported into R. Fluorescent parameters were transformed using an individually centred inverse hyperbolic sine function for each fluorochrome. t-SNE dimensionality reduction [25] was performed using the Rtsne package. Clustering was performed by multiple rounds of DBSCAN with custom parameters using the dbscan package in R. Then, cell frequencies for each cluster were calculated for each sample and statistical analyses performed.

T-cell activation assays

In activation assays with cell lines, $5*10^4$ T cells were co-cultured with cell lines at an effector:target ratio of 1:1 in a final volume of 200µl. Adherent cells were plated and allowed to adhere for 2h before addition of T cells. T cells and target cells were co-cultured for 16h.
For proliferation assays, $2*10^5$ Mo-DC were co-cultured with 10^6 PBMC and $2*10^5$ uRBC or PfRBC and proliferation was assessed after 6 days.

TCR sequencing and transfer

RNA from T-cell clones was extracted using the NucleoSpin RNA kit (Macherey Nagel). cDNA was generated with SuperScript III reverse transcriptase (Invitrogen). TCR γ and δ genes were then PCR amplified using specific primers and sequenced.
For TCR transfer into SKW-3 cells, the corresponding TCR-γ and δ cDNA were cloned into a modified pFUGW lentiviral vector. Lentiviral particles were produced in HEK 293 cells and the SKW-3 cell transduced with supernatant containing the lentiviral particles. Successful transduction was assessed by staining for surface expression of CD3.

Blood stage parasite enrichment

P. falciparum parasites strain NF54 from fresh cultures were enriched using MACS magnetic columns as published [39]. Briefly, fresh parasite cultures were passed on top of the MACS magnetic column and eluted using RMPI 1640 after removing the column from the magnetic

stand. Enrichment of infected erythrocytes was assessed by Giemsa staining. Typical parasitaemia after enrichment was around 90%.

REFERENCES

[1] World Health Organization, *World Malaria Report 2017*. S.l.: World Health Organization, 2017.

[2] "Malaria vaccine: WHO position paper, January 2016 – Recommendations," *Vaccine*, vol. 36, no. 25, pp. 3576–3577, Jun. 2018.

[3] RTS,S Clinical Trials Partnership, "Efficacy and safety of RTS,S/AS01 malaria vaccine with or without a booster dose in infants and children in Africa: final results of a phase 3, individually randomised, controlled trial," *The Lancet*, vol. 386, no. 9988, pp. 31–45, Jul. 2015.

[4] R. A. Seder *et al.*, "Protection Against Malaria by Intravenous Immunization with a Nonreplicating Sporozoite Vaccine," *Science*, vol. 341, no. 6152, pp. 1359–1365, Sep. 2013.

[5] K. E. Lyke *et al.*, "Attenuated PfSPZ Vaccine induces strain-transcending T cells and durable protection against heterologous controlled human malaria infection," *PNAS*, vol. 114, no. 10, pp. 2711–2716, Mar. 2017.

[6] J. G. Kublin *et al.*, "Complete attenuation of genetically engineered *Plasmodium falciparum* sporozoites in human subjects," *Sci Transl Med*, vol. 9, no. 371, p. eaad9099, Jan. 2017.

[7] B. Mordmüller *et al.*, "Sterile protection against human malaria by chemoattenuated PfSPZ vaccine," *Nature*, vol. 542, no. 7642, pp. 445–449, Feb. 2017.

[8] M. S. Sissoko *et al.*, "Safety and efficacy of PfSPZ Vaccine against *Plasmodium falciparum* via direct venous inoculation in healthy malaria-exposed adults in Mali: a randomised, double-blind phase 1 trial," *Lancet Infect Dis*, vol. 17, no. 5, pp. 498–509, May 2017.

[9] P. D. Crompton *et al.*, "Malaria Immunity in Man and Mosquito: Insights into Unsolved Mysteries of a Deadly Infectious Disease," *Annu Rev Immunol*, vol. 32, no. 1, pp. 157–187, 2014.

[10] P. Vantourout and A. Hayday, "Six-of-the-best: unique contributions of γδ T cells to immunology," *Nat Rev Immunol*, vol. 13, no. 2, pp. 88–100, Feb. 2013.

[11] C. Roussilhon, M. Agrapart, P. Guglielmi, A. Bensussan, P. Brasseur, and J. J. Ballet, "Human TcRγδ+ lymphocyte response on primary exposure to *Plasmodium falciparum*," *Clin Exp Immunol*, vol. 95, no. 1, pp. 91–97, Jan. 1994.

[12] L. Hviid *et al.*, "Perturbation and Proinflammatory Type Activation of Vδ1+ γδ T Cells in African Children with *Plasmodium falciparum* Malaria," *Infect. Immun.*, vol. 69, no. 5, pp. 3190–3196, May 2001.

[13] M. Ho *et al.*, "Polyclonal expansion of peripheral gamma delta T cells in human *Plasmodium falciparum* malaria.," *Infect. Immun.*, vol. 62, no. 3, pp. 855–862, Mar. 1994.

[14] C. Behr *et al.*, "*Plasmodium falciparum* stimuli for human gammadelta T cells are related to phosphorylated antigens of mycobacteria.," *Infect Immun*, vol. 64, no. 8, pp. 2892–2896, Aug. 1996.

[15] I. Zaidi *et al.*, "γδ T Cells Are Required for the Induction of Sterile Immunity during Irradiated Sporozoite Vaccinations," *J Immunol*, vol. 199, no. 11, pp. 3781–3788, Dec. 2017.

[16] M. Mpina *et al.*, "Controlled Human Malaria Infection Leads to Long-Lasting Changes in Innate and Innate-like Lymphocyte Populations," *J Immunol*, vol. 199, no. 1, pp. 107–118, Jul. 2017.

[17] A. N. Keller, A. J. Corbett, J. M. Wubben, J. McCluskey, and J. Rossjohn, "MAIT cells and MR1-antigen recognition," *Current Opinion in Immunology*, vol. 46, pp. 66–74, Jun. 2017.

[18] X.-M. Zhang, C. Tonnelle, M.-P. Lefranc, and S. Huck, “T cell receptor γ cDNA in human fetal liver and thymus: Variable regions of γ chains are restricted to VγI or V9, due to the absence of splicing of the V10 and V11 leader intron,” *Eur. J. Immunol.*, vol. 24, no. 3, pp. 571–578, Mar. 1994.
[19] The 1000 Genomes Project Consortium, “A global reference for human genetic variation,” *Nature*, vol. 526, no. 7571, pp. 68–74, Oct. 2015.
[20] X.-M. Zhang, G. Cathala, Z. Soua, M.-P. Lefranc, and S. Huck, “The human T-cell receptor gamma variable pseudogene V10 is a distinctive marker of human speciation,” *Immunogenetics*, p. 8, Jul. 1996.
[21] A. Forster, S. Huck, N. Ghanem, M. P. Lefranc, and T. H. Rabbitts, “New subgroups in the human T cell rearranging V gamma gene locus.,” *EMBO J*, vol. 6, no. 7, pp. 1945–1950, Jul. 1987.
[22] D. I. Stanisic, J. S. McCarthy, and M. F. Good, “Controlled Human Malaria Infection: Applications, Advances, and Challenges,” *Infect. Immun.*, vol. 86, no. 1, pp. e00479-17, Jan. 2018.
[23] Y. Chien, C. Meyer, and M. Bonneville, “γδ T Cells: First Line of Defense and Beyond,” *Annu Rev Immunol*, vol. 32, no. 1, pp. 121–155, Mar. 2014.
[24] M. Ho, H. K. Webster, P. Tongtawe, K. Pattanapanyasat, and W. P. Weidanz, “Increased γδ T cells in acute *Plasmodium falciparum* malaria,” *Immunol Lett*, vol. 25, no. 1, pp. 139–141, Aug. 1990.
[25] E. D. Amir *et al.*, “viSNE enables visualization of high dimensional single-cell data and reveals phenotypic heterogeneity of leukemia,” *Nat Biotech*, vol. 31, no. 6, pp. 545–552, Jun. 2013.
[26] D. L. Barber *et al.*, “Restoring function in exhausted CD8 T cells during chronic viral infection,” *Nature*, vol. 439, no. 7077, pp. 682–687, Feb. 2006.
[27] M. N. Wykes and S. R. Lewin, “Immune checkpoint blockade in infectious diseases,” *Nat Rev Immunol*, vol. 18, no. 2, pp. 91–104, Feb. 2018.
[28] M. S. Davey *et al.*, “Clonal selection in the human Vδ1 T cell repertoire indicates γδ TCR-dependent adaptive immune surveillance,” *Nat Commun*, vol. 8, Mar. 2017.
[29] J. R. Fergusson *et al.*, “CD161 Defines a Transcriptional and Functional Phenotype across Distinct Human T Cell Lineages,” *Cell Reports*, vol. 9, no. 3, pp. 1075–1088, Nov. 2014.
[30] D. Kabelitz and D. Wesch, “Role of gamma delta T-lymphocytes in HIV infection,” *Eur. J. Med. Res.*, vol. 6, no. 4, pp. 169–174, Apr. 2001.
[31] L. Farnault *et al.*, “Clinical evidence implicating gamma-delta T cells in EBV control following cord blood transplantation,” *Bone Marrow Transplant*, vol. 48, no. 11, pp. 1478–1479, Nov. 2013.
[32] S. Hunter *et al.*, “Human liver infiltrating γδ T cells are composed of clonally expanded circulating and tissue-resident populations,” *J Hepatol*, May 2018.
[33] F. Wunderlich, S. Al-Quraishy, and M. A. Dkhil, “Liver-inherent immune system: its role in blood-stage malaria,” *Front Microbiol*, vol. 5, Nov. 2014.
[34] P. Liehl *et al.*, “Host-cell sensors for Plasmodium activate innate immunity against liver-stage infection,” *Nat Med*, vol. 20, no. 1, pp. 47–53, Jan. 2014.
[35] M. S. Davey, C. R. Willcox, A. T. Baker, S. Hunter, and B. E. Willcox, “Recasting Human Vδ1 Lymphocytes in an Adaptive Role,” *Trends Immunol*, Apr. 2018.
[36] A. Bauer *et al.*, “Analysis of the requirement for β2-microglobulin for expression and formation of human CD1 antigens,” *Eur. J. Immunol.*, vol. 27, no. 6, pp. 1366–1373, Dec. 2005.

[37] A. R. Kazen and E. J. Adams, “Evolution of the V, D, and J gene segments used in the primate γδ T-cell receptor reveals a dichotomy of conservation and diversity,” *PNAS*, vol. 108, no. 29, pp. E332–E340, Jul. 2011.
[38] M. Lepore *et al.*, “Functionally diverse human T cells recognize non-microbial antigens presented by MR1,” *eLife*, vol. 6, p. e24476, May 2017.
[39] L. M. Coronado, N. M. Tayler, R. Correa, R. M. Giovani, and C. Spadafora, “Separation of *Plasmodium falciparum* Late Stage-infected Erythrocytes by Magnetic Means,” *J Vis Exp*, no. 73, Mar. 2013.

Chapter 6

General Discussion

Despite being a unicellular organism, *Plasmodium falciparum* has an extremely complex life cycle that is highly adapted to its human and mosquito hosts. An especially striking feature of this adaptation are the intricate strategies the parasite has evolved to avoid recognition by the human immune system [157].

The many interactions between malaria parasite and the human immune system make understanding the human immune response towards malaria a difficult task. This is reflected in the many obstacles that need to be overcome in order to produce an effective malaria vaccine. In this general discussion, I highlight for each manuscript a key finding and its implications for malaria immunology and vaccine development:

6.1. We found expression of IL-4, IL-21 and CD154 in CSP-specific $CD4^+$ T cells upon RTS,S vaccination, highlighting the importance of appropriate T-cell help for effective humoral immunity.

6.2. The immune response towards the PfSPZ vaccine is considerably lower in Tanzanians than US volunteers, emphasizing diversity in the immune response between different human populations.

6.3. The activation of MAIT cells depends on the growth condition of the bacteria that produce the MAIT-cell antigens, highlighting the many interactions between gut microbiome and the human immune system.

6.4. Vδ1 T cells are activated in a personalised response during malaria infection, emphasizing the wide range of T cells that are activated during malaria. In addition, we discovered a functionally expressed TCR Vγ10 gene that might only exist in the African population. These findings points out how the distinct immunogenetic background of individuals and populations can influence the human immune system.

6.1. RTS,S/AS01E Malaria Vaccine Induces Memory and Polyfunctional T cell responses in a Pediatric African Phase III Trial

Understanding the interplay between cellular and humoral immunity is critically important in the context of malaria vaccination, as it has proven difficult to achieve vaccination-induced humoral immunity leading to long-lasting protection [85]. However, the T-cell response towards the malaria vaccine RTS,S remains poorly understood, especially in African children, and so far, most studies have focussed on analysis of cytokine release from T_H1 cells only [89]–[91].

Here, we characterised and compared the CSP- and HBsAg-specific T-cell response of RTS,S-vaccinated children from Tanzania and Mozambique in unprecedented detail. We observed for the first time in a paediatric malaria vaccine trial the T_H2- and T_{FH}-cell-associated cytokines IL-4 and IL-21, respectively. Furthermore, a significant number of CSP-specific T cells expressed CD40 ligand (CD154), contrasting with findings from other studies [158], [159]. This highlights a more complex T-cell functionality than previously appreciated and could have important implications for the interplay between T-cell and B-cell responses towards RTS,S.

IL-21 represents, together with IL-6, the central cytokine inducing T_{FH} commitment, through its potential to increase the expression of BCL-6, the key transcription factor for T_{FH} development [102]. Furthermore, IL-21 can promote B-cell proliferation, generation of plasma cells and isotype switching, indicating its central role in regulating B-cell function [160]. Similarly, CD154 is an important help signal provided by T cells to B cells during the germinal centre response [102]. Therefore, the expression of these effector molecules by CSP-specific T cells might be important for development of an effective B-cell response upon RTS,S vaccination. While we were able to detect IL-4, IL-21 and CD154 on CSP-specific T cells, this holds true for only a minority of volunteers, indicating the personalised nature of the immune response towards RTS,S. Furthermore, IL-21 and CD154 were only detectable in the effector memory (EM) subset, but were completely absent from the central memory (CM) compartment of T cells. Induction of a high frequency of CSP-specific CM T cells might be important for induction of long-term protection, as CM T cells possess high proliferative capacity and functional potency [161]. The low frequency of antigen-specific T cells in the CM compartment could therefore contribute to the short protection observed in this clinical trial and upon RTS,S vaccination in general.

Interestingly, CSP-specific T-cell responses were lower than the ones to HBsAg, both in terms of frequency and polyfunctionality. One possible explanation could be that the children in our cohort should have been previously vaccinated against hepatitis B, and this response might have been boosted by RTS,S. Alternatively, the lower dose of CSP compared to HBsAg could explain the lower immune response, as the RTS,S is formulated at a RTS to S ratio of 1:4 [162]. Furthermore, intrinsic properties of peptides influence their interactions with MHC molecules and thus their immunogenicity [163].

This study was not aimed to include correlational studies with clinical parameters, as children with episodes of malaria during follow-up were excluded from the analysis. It will be interesting to see if the described phenotypes of polyfunctionality, memory phenotype and distinct effector molecules correlate with clinical outcome. Ultimately, a better understanding

of the interactions between vaccine-specific T cells and B cells might lead to improved malaria vaccine design.

6.2. Safety, immunogenicity and protective efficacy against controlled human malaria infection of *Plasmodium falciparum* sporozoite vaccine in Tanzanian adults

The observed vaccine efficacy of 20% in the BSPZV1 clinical trial against homologous CHMI was considerably lower than previously observed in US volunteers (93.4%) [164], but in a similar range as the one observed in a comparable study conducted in Mali (29%) [135]. One confounding parameter when comparing those clinical trials is the different methods that were used to assess vaccine efficacy. In the US, CHMI was performed by mosquito bite; in the BSPZV1 cohort by DVI of 3'200 PfSPZ Challenge; in the Mali study vaccine efficacy was assessed by field exposure.

Additionally, vaccine-induced anti-CSP antibody titres were also lower in our study than observed in US volunteers [164], but higher than the ones observed in Mali [135]. Recently, data from a phase I study in Equatorial Guinea indicated even lower antibody responses than in Tanzania or Mali [134].

Together, these data show convincingly that vaccine efficacy and immunogenicity is considerably lower in sub-Saharan Africans than in US volunteers. The observation that vaccine efficacy varies between different human populations is not new and in fact has been reported for vaccines against many diseases such as tuberculosis, hepatitis B, tetanus, diphtheria or influenza [165]. The reason behind those marked differences between populations in terms of vaccination-induced protection and immunogenicity remain incompletely understood, but most likely, there are many different causes [165].

One effect that has been suggested to influences malaria vaccine efficacy is previous exposure to *Plasmodium* parasites [166]. A possible immunological mechanism might involve exhaustion and decreased functionality of antigen-specific T cells during repeated exposure, leading to altered memory formation [167].

Another mechanism that influences vaccine responsiveness is reported in a study comparing the immune response to yellow fever vaccination between Swiss and Ugandan volunteers [168]. Immunogenicity of the vaccine was significantly lower in the African population, an effect that could not be attributed to neutralising antibodies targeting the vaccine, as no neutralising antibodies were detectable at baseline. Rather, a general state of activation of the

immune system, including innate and adaptive compartments, correlated with low vaccine response [168]. This effect could also explain reports that imply decreased vaccine immunogenicity in people with low socioeconomic status in developing countries as they live in more unsanitary conditions and are supposedly exposed to a wider range of pathogens, leading to a more activated immune state [169]. Attributing these effects to distinct cellular mechanisms is difficult, but inhibitory effects of activated NK cells on T-cell responses have been described in mouse models of viral infection. [170], emphasising the interlinked nature of 'innate' and 'adaptive' immunity.

Another factor influencing vaccine response are infections with pathogens such as helminths (see section 6.3) [171]. Furthermore, human genetic variation, especially in immune-related genes can greatly affect vaccine response (see section 6.4) [172].

Taken together, these effects can partially explain why the malaria vaccine response is lower in sub-Saharan Africans, however they cannot provide a simple solution. Currently, the strategy to overcome the low immunogenicity of malaria vaccines in African volunteers is to increase the dose of vaccine that is administered [137]. However, understanding the factors that are responsible for the differences in vaccine efficacy between populations is crucial. This absolutely requires studying the immune responses towards malaria vaccines in sub-Saharan Africans. Therefore, a key finding of this manuscript is the safety and tolerability of PfSPZ Vaccine and CHMI in healthy, male Tanzanian adults. This is the first time that CHMI was used in Africa to assess malaria vaccine efficacy. The use of a CHMI as opposed to infection by natural exposure is of great value, as it allows for faster and better controlled assessment of vaccine efficacy, ultimately leading to accelerated development of malaria vaccines [151]. Furthermore, it enables us to study the human immune response towards *P. falciparum* in a highly controlled setting in the population at highest risk of malaria.

6.3. Modulation of bacterial metabolism by the microenvironment controls MAIT cell stimulation

The term 'blood-stage' malaria might be misleading, as malaria pathogenesis involves a wide range of human tissues and organs including skin, liver, brain, retina, kidneys, spleen, placenta, lungs and gut [26]. While the connection between the gut, its microbiota and malaria infection might not be an obvious one, there are several studies showing interactions between malaria infection, gut microbiota and integrity of the intestinal barrier. One example involves antibodies that are reactive to the glycan Galα1-3Galβ1-4GlcNAc-R (α-gal) that is expressed

on different pathogens, but not on host cells. Generation of these antibodies depends on the presence of α-gal on the cell wall of gut-resident bacteria, and intriguingly, these antibodies can contribute to protection against *Plasmodium* infection through binding of α-gal on the sporozoite surface [173].

Malaria infection can also alter the intestinal architecture, leading to shortening of villi, detachment of epithelia, increased intestinal permeability, and changes in the gut microbiome composition in mouse models of malaria [174]. Importantly, changes in gastrointestinal permeability have also been observed in humans with *P. falciparum* malaria infection [175], which can be explained by sequestration of infected erythrocytes in gut endothelia, which has been observed in fatal human malaria cases [176]. Moreover, gastrointestinal symptoms such as diarrhoea are common during human malaria infection, and might also influence the gut microbiome [26].

Malaria infection does not only influence the microbiota, but there is also an influence of the microbiota on malaria disease severity. This has been demonstrated in mice, where genetically similar mouse strains exhibited different parasite burden and mortality, and this effect could be transferred to donor mice by faecal transplantation [177]. In humans, associations between microbiome composition and prospective malaria risk have been reported [178]. Thus, there is a bidirectional influence between the gut microbiome and malaria infection [26]. This might also contribute to the differences in terms of vaccine response between sub-Saharan Africans and US volunteers, as the gut microbiome has been shown to be significantly different between these populations [179].

Furthermore, pathogens that infect the human intestine at time of vaccination can influence vaccine responsiveness as demonstrated by reduced vaccination-induced protection in helminth-infected mice receiving BCG vaccination [171]. Similarly, there is evidence that helminth infections can alter the clinical course of malaria disease and might also influence malaria vaccination [180].

Thus, there is an intricate link between malaria, the intestinal microenvironment and the human immune system. We show that MAIT cells provide a link between the gut microbiota and the immune system through their ability to sense microbial metabolites. We demonstrated phenotypic diversity of MAIT cells between peripheral blood and gut tissue. *In vitro* assays indicated that these different activation states can be induced by distinct stimuli that depend on the growth conditions of the bacteria that produce the MAIT-cell antigens. An independent study further suggested that MAIT cells play a role in the maintenance of gut integrity [181]. In *Chapter 5*, we showed that MAIT cells expand and get activated upon CHMI. Whether this

activation is purely cytokine-mediated or antigen-dependent is not known, but the gut microbiota and intestinal integrity could influence MAIT-cell activation. One mechanism might involve malaria-induced changes in the frequency of riboflavin-synthesising versus non-synthesising bacteria in the gut, thereby altering the amount of available MAIT-cell antigens. Additionally, increased gastrointestinal permeability could lead to higher availability of gut-microbiome-derived MAIT-cell antigens in blood and liver, where MAIT cells are especially abundant [182].

Of note, we developed an unbiased analysis pipeline to identify phenotypic differences between gut-resident and peripheral-blood-derived MAIT cells using dimensionality reduction and clustering. This approach is extremely versatile and allows us not only to detect phenotypic differences in different tissues, but also to identify inter-donor or longitudinal differences and to monitor intervention-induced effects. A similar analysis pipeline was used in *Chapter 5* to reveal malaria-vaccination-induced and CHMI-induced phenotypic alterations in MAIT cells and γδ T-cell subsets.

6.4. Unbiased analysis of unconventional T cells in Tanzanian volunteers reveals a personalised Vδ1 T-cell response upon controlled human malaria infection

The immune response during malaria in humans influences a wide range of immune-cell subsets. In the case of unconventional T cells, this has been known for a long time for Vγ9Vδ2 T cells that respond to parasite-derived phosphoantigens [116]. The more recently described MAIT-cell subset has also been shown to dynamically change during the course of malaria infection [121]. Here, we analysed the response of unconventional T cells to PfSPZ vaccination and CHMI in the BSPZV1 cohort using multicolour flow cytometry, followed by an unbiased analysis pipeline of these high-dimensional data. Consistent with previous reports, we found expansion and phenotypic changes in Vγ9Vδ2 T cells upon blood-stage parasitaemia [115]. Unexpectedly, we found Vδ1 T cells and Vδx T cells to show a distinct pattern of activation upon CHMI that is characterised by co-expression of CD38 and PD-1. This contrasts with the absence of PD-1 expression on expanded MAIT cells and Vδ2 T cells and implies a distinct mechanism of activation within Vδ1 T cells and Vδx T cells upon CHMI. Of note, PD-1 has been shown to be enriched on antigen-specific T cells not only in cancer, but also during chronic infections [183], [184]. Thus, we hypothesize that activation of the $CD38^{+}PD\text{-}1^{+}$ T-cell subsets occurred in an antigen-specific, TCR-dependent manner. This hypothesis is supported

by the fact that expansion of this $CD38^+PD\text{-}1^+$ subset was very marked in some volunteers, but almost absent in others, indicating a personalised response that might depend on differences in the Vδ1 TCR repertoire [48]. A similar, personalised Vδ1 T-cell response was recently observed in the context of CMV infection [29].

Interestingly, Vδ1 T cells are abundant in the liver, where they represent around 50% of γδ T cells [185], and also in the intestine, representing around 80% of γδ T cells [186]. Together with the fact that malaria strongly influences the liver and gut [26], this could indicate that the activation of Vδ1 T cells during malaria infection occurs in one of these tissues. Our *in vitro* data based on stimulation of Vδ1 T-cell clones suggest that those cells could be reactive to liver-tissue derived cell lines. It is conceivable that our T-cell clones recognise in a TCR-dependent manner a self-ligand that is particularly abundant on altered hepatocytes. Liver stress-surveillance by Vδ1 T cells could be crucial in pre-erythrocytic protection against malaria and could complement conventional, $CD8^+$ αβ T-cell mediated protection.

Together, these findings show for the first time the distinct activation pattern of Vδ1 T cells during malaria infection, expanding the great diversity of immune cells that are involved in the immune response to malaria. Importantly, this puts further emphasis on the potentially highly personalised nature of the human immune response during malaria.

In addition, we described for the first time the functionality of the human TCR Vγ10 gene, which so far has been thought to be non-functional due to a mutation in the splice donor site [187]. Our TCR-transfer experiment using SKW-3 cells confirms that the TCR Vγ10 gene product is functional and abundantly expressed on the cell surface. A data base search in the 1000 genome project indicated that the functional TCR Vγ10 gene is exclusive to Africans or people of recent African descent [188].

The discovery of a functional T-cell population exclusive to Africans highlights genetic diversity as one of the obstacles when developing a malaria vaccine. Although the influence of $V\gamma10^+$ T cells on malaria vaccination and disease are completely unexplored, the discovery of a functional allele provides an example of the different immunogenetic background between sub-Saharan Africans and Europeans or US-Americans. Hence, not only the malaria pre-exposure status, but also differences in the TCR repertoire could contribute to the variety in vaccine efficacy when evaluating a malaria vaccine such as the PfSPZ Vaccine.

Genetic differences clearly have an impact on vaccine responsiveness [172]. Heritability of common viral vaccines are estimated to be between 40% to 90% [172], indicating that the impact of the genetic background is specific for each vaccine. The most obvious genetic

differences playing a role in immune responsiveness are polymorphisms in the HLA locus, but polymorphisms in PRRs, cytokines and their receptors, and others have been found [172]. This effect is expected to be large in sub-Saharan Africans, who are genetically extremely diverse due to the long evolutionary history of humans in Africa [188]. The example of Vγ10 is a striking case in which a SNP can change the expression of an entire TCR chain, which might lead to the presence or absence of an entire T-cell subset.

An intriguing question is why the functional Vγ10 allele is so strongly enriched in sub-Saharan Africans. One possibility is a genetic bottleneck during human migration or the loss of the allele by genetic drift. Alternatively, there might be an evolutionary selection pressure that selects for the presence of these T cells in sub-Saharan Africans. This could be explained by a protective role of $V\gamma10^+$ T cells in a disease that was especially prevalent in sub-Saharan Africa in recent human evolution. An obvious candidate is malaria that is known to exert a strong influence on the human genome, as indicated by the well-known examples of sickle-cell anaemia or glucose-6-phosphate dehydrogenase (G6PD) deficiency [189]. Another example of how malaria infection shapes the human immune system was highlighted more recently with the discovery of broadly reactive anti-PfRBC antibodies, whose reactivity depends on a LAIR1 insertion [190].

Taken together, our findings in *Chapter 5* highlight the personalised immune response towards malaria infection within the Vδ1 T-cell subset. Furthermore, the first description of a Vγ10-expressing T cell emphasizes how much we can still learn about immunogenetic differences between human populations and individuals, and their potential impact on the immune response during infectious diseases.

Chapter 7

Outlook

With large-scale phase III clinical trials completed, RTS,S is now being rolled out in Ghana, Kenya and Malawi as the first generation malaria vaccine [191]. For this pilot implementation, 750,000 children will be randomized to vaccinated and unvaccinated clusters, with four doses of RTS,S administered in the vaccine testing group. RTS,S will be implemented into the current malaria control strategy as a complementary tool and is not planned to replace the measures already in place. Clearly, RTS,S falls – in its current formulation – short of the recommendation of the malaria technology roadmap claiming the malaria community should develop and license a first-generation malaria vaccine that has a protective efficacy of more than 50 percent against severe disease and lasts longer than one year [192].

Currently, some of the most promising malaria vaccine candidates are based on whole *P. falciparum* sporozoites applied by direct venous inoculation. We are now receiving the first data from clinical trials using the PfSPZ Vaccine in sub-Saharan Africa in Mali [135], Equatorial Guinea [134] and Tanzania (see *Chapter 3*, Jongo et al., manuscript in press). From these initial results, we can expect that immunogenicity and vaccine efficacy will be significantly lower in sub-Saharan Africa than what initial results from malaria-naïve, US volunteers suggested [76]. Other vaccination approaches based on whole-sporozoite approaches are now entering clinical trials. One of these approaches is the attenuation of PfSPZ not by radiation, but through genetic manipulation of the parasite [146], [193]. This has the potential benefit of being able to control the stage at which the parasite arrests, through selection of the genes that are knocked out. If the parasite can progress further in its development within the liver, it should express a wider range and higher load of antigens, which could lead to improved immunogenicity. However, the occurrence of a break-through infection in a clinical trial with genetically attenuated parasite shows the balance between immunogenicity and safety [145]. This has led to the development of a triple-knock-out PfSPZ vaccine that is safe, but arrests early in liver-stage development [147]. Despite this early arrest, it will be interesting to see how this vaccine performs in clinical trials in sub-Saharan Africa.
Another vaccination approach combines the administration of fully infectious PfSPZ to recipients who are taking malaria chemoprophylaxis [140]. This has the advantage of exposing the immune system to the whole range of *P. falciparum* liver-stage antigens and additionally to early blood-stage antigens. The inoculation of PfSPZ by mosquito bites has recently been replaced with administration by needle and syringe of the PfSPZ Challenge during chloroquine administration (PfSPZ-CVac) [142]. This approach is currently under evaluation in Equatorial Guinea and Mali and it will be interesting to see if this approach can overcome the sub-optimal

vaccine efficacy observed in the PfSPZ Vaccine in sub-Saharan Africa. However, one of the limitations with CVac is the requirement to monitor for potential malaria break-through infections during vaccination and the side effects of chloroquine like pruritus [194].
Ultimately, however, all of those approaches might suffer from the same drawback, which is the ability of *P. falciparum* to evade the human immune response [157]. Currently, the strategy to overcome low vaccine efficacy is to increase the dose and alter the dosing schedule [137]. Alternatively, administration of a mixture of different *P. falciparum* strains or *Plasmodium* species might improve immunogenicity and heterologous protection against the diversity of circulating field strains. In fact, a combination of strains administered during prophylaxis has been successfully used for decades in a veterinary vaccination against *Theileria parva*, the causative agent for East Coast fever in cattle [195]. However, administration of several *P. falciparum* strains might complicate the vaccine manufacturing process and could face regulatory difficulties.

Clearly, a main reason for the difficulties in developing an effective malaria vaccine is our incomplete understanding of the interplay between malaria biology and the human immune response in different human populations. However, the current malaria vaccine trials offer a unique opportunity to study exactly those mechanisms in a controlled setting. In *Chapter 5*, this has enabled us to examine the involvement of γδ T cells in the malaria immune response, and allowed us to make interesting observations that are worth following up. For the first time, we found dynamic changes in frequency and phenotype of Vδ1 and Vδx T-cell subsets upon CHMI. A next step could be to examine the TCR repertoire of those cells to confirm that the observed expansion of $CD38^{+}PD\text{-}1^{+}$ cells is indeed a TCR-mediated clonal expansion. Recent technological advances allow the concomitant analysis of surface marker expression and transcriptome on a single-cell level [196], [197]. It would be highly interesting to apply this technology to our sample set, as this could allow us to identify the cells of interest through the surface markers, and simultaneously assess their TCR sequences and possible effector functions by analysing the transcriptome on a single-cell level. Alternatively, the hypothesis that the $CD38^{+}PD\text{-}1^{+}$ cells are clonally expanded populations could be assessed by single-cell sorting of some of the cells and sequencing of their TCR. Or, the TCRδ repertoire could be assessed by bulk sequencing of sorted non-Vγ9Vδ2 γδ T cells pre-vaccination, post-vaccination and post-challenge. If indeed we found clonal expansion, those cells could be isolated and their function assessed using *in vitro* assays. One particularly interesting assay would be co-culture of the isolated Vδ1 T cells with PfSPZ-infected hepatoma cells. This could

give an indication if indeed, those T cells are responsive to *P. falciparum* liver-stage infected hepatocytes.

The study of the newly identified Vγ10$^+$ T cells is currently hampered by the lack of a specific antibody for this TCRγ chain. Thus, although challenging, a first step could be the generation of a Vγ10-specific antibody that would allow for detection of malaria-induced phenotypic alterations of these cells by flow cytometry. Furthermore, this would simplify the task of isolating and propagating additional T cells that bear this TCRγ chain. In the absence of a Vγ10-specific antibody, one would have to establish a wide range of T-cell clones and screen their TCRγ expression by PCR. However, the fact that we already genotyped our cohort for the presence of the TRGV10*novel allele would simplify this task.
Furthermore, it would be especially interesting to study Vδ1 T cells in volunteers from West Africa, as they have a particularly high abundance of Vδ1 T cells in peripheral blood ([119] and our unpublished observations).

Controlled human infections beyond malaria are either well-developed like for influenza virus or are under development like for hookworm infections [198]. The push for controlled human infections is clearly a consequence of the limited extrapolation of results obtained in animal models of infectious disease to the human system (see e.g. [199]). Using these controlled human infection models, the involvement of the Vγ10$^+$ T cells beyond malaria could be explored since we can expect that these cells are not only associated with malaria infections.

In conclusion, the way forward in malaria vaccine development should involve two interdependent strategies. First, the current approaches of whole-sporozoite-based vaccination should be further developed and tested in sub-Saharan Africa as described above. Second, this gives us the unprecedented opportunity to explore the interactions between parasite and the human immune response in a highly controlled environment in different human populations and age groups. We should use this opportunity and learn as much as we can about these interactions using immunological methods that assess a wide range of parameters in an unbiased way. This might finally enable us to develop surrogates and correlates of vaccine-induced protection against malaria. In contrast to the already established vaccines applied during the expanded program on immunization (EPI) on a global scale, the new generation of vaccines against chronic infectious diseases like malaria might need to be more tailored towards different human subpopulations [200].

Chapter 8

References

[1] World Health Organization, *World Malaria Report 2017*. S.l.: World Health Organization, 2017.
[2] A. S. I. Aly, A. M. Vaughan, and S. H. I. Kappe, "Malaria Parasite Development in the Mosquito and Infection of the Mammalian Host," *Annu Rev Microbiol*, vol. 63, no. 1, pp. 195–221, Oct. 2009.
[3] R. Ménard, J. Tavares, I. Cockburn, M. Markus, F. Zavala, and R. Amino, "Looking under the skin: the first steps in malarial infection and immunity," *Nat Rev Micro*, vol. 11, no. 10, pp. 701–712, Oct. 2013.
[4] J. C. Beier, J. R. Davis, J. A. Vaughan, B. H. Noden, and M. S. Beier, "Quantitation of *Plasmodium falciparum* sporozoites transmitted in vitro by experimentally infected Anopheles gambiae and Anopheles stephensi," *Am J Trop Med Hyg*, vol. 44, no. 5, pp. 564–570, May 1991.
[5] P. Gueirard *et al.*, "Development of the malaria parasite in the skin of the mammalian host," *PNAS*, vol. 107, no. 43, pp. 18640–18645, Oct. 2010.
[6] C. Cerami *et al.*, "The basolateral domain of the hepatocyte plasma membrane bears receptors for the circumsporozoite protein of plasmodium falciparum sporozoites," *Cell*, vol. 70, no. 6, pp. 1021–1033, Sep. 1992.
[7] D. Mazier *et al.*, "Complete development of hepatic stages of *Plasmodium falciparum* in vitro," *Science*, vol. 227, no. 4685, pp. 440–442, Jan. 1985.
[8] A. Sturm *et al.*, "Manipulation of Host Hepatocytes by the Malaria Parasite for Delivery into Liver Sinusoids," *Science*, vol. 313, no. 5791, pp. 1287–1290, Sep. 2006.
[9] K. Baer, C. Klotz, S. H. I. Kappe, T. Schnieder, and U. Frevert, "Release of Hepatic *Plasmodium yoelii* Merozoites into the Pulmonary Microvasculature," *PLoS Pathog*, vol. 3, no. 11, p. e171, Nov. 2007.
[10] D. Mazier, L. Rénia, and G. Snounou, "A pre-emptive strike against malaria's stealthy hepatic forms," *Nat Rev Drug Discov*, vol. 8, no. 11, pp. 854–864, Nov. 2009.
[11] M. A. Phillips, J. N. Burrows, C. Manyando, R. H. van Huijsduijnen, W. C. V. Voorhis, and T. N. C. Wells, "Malaria," *Nat Rev Dis Primers*, vol. 3, p. 17050, Aug. 2017.
[12] A. S. Paul, E. S. Egan, and M. T. Duraisingh, "Host–parasite interactions that guide red blood cell invasion by malaria parasites," *Current Opinion in Hematology*, vol. 22, no. 3, pp. 220–226, May 2015.
[13] L. Bannister and G. Mitchell, "The ins, outs and roundabouts of malaria," *Trends Parasitol*, vol. 19, no. 5, pp. 209–213, May 2003.
[14] D. J. Sullivan, I. Y. Gluzman, and D. E. Goldberg, "Plasmodium Hemozoin Formation Mediated by Histidine-Rich Proteins," *Science*, vol. 271, no. 5246, pp. 219–222, Jan. 1996.
[15] B. L. Salmon, A. Oksman, and D. E. Goldberg, "Malaria parasite exit from the host erythrocyte: A two-step process requiring extraerythrocytic proteolysis," *PNAS*, vol. 98, no. 1, pp. 271–276, Jan. 2001.
[16] G. A. Josling and M. Llinás, "Sexual development in Plasmodium parasites: knowing when it's time to commit," *Nat Rev Micro*, vol. 13, no. 9, pp. 573–587, Sep. 2015.
[17] R. Aguilar *et al.*, "Molecular evidence for the localization of *Plasmodium falciparum* immature gametocytes in bone marrow," *Blood*, vol. 123, no. 7, pp. 959–966, Feb. 2014.
[18] R. Joice *et al.*, "*Plasmodium falciparum* transmission stages accumulate in the human bone marrow," *Sci Transl Med*, vol. 6, no. 244, pp. 244re5-244re5, Jul. 2014.
[19] O. Billker *et al.*, "Identification of xanthurenic acid as the putative inducer of malaria development in the mosquito," *Nature*, vol. 392, no. 6673, pp. 289–292, Mar. 1998.

[20] L. A. Baton and L. C. Ranford-Cartwright, “How do malaria ookinetes cross the mosquito midgut wall?,” *Trends in Parasitology*, vol. 21, no. 1, pp. 22–28, Jan. 2005.
[21] A. F. Cowman, J. Healer, D. Marapana, and K. Marsh, “Malaria: Biology and Disease,” *Cell*, vol. 167, no. 3, pp. 610–624, Oct. 2016.
[22] G. N. Jakeman, A. Saul, W. L. Hogarth, and W. E. Collins, “Anaemia of acute malaria infections in non-immune patients primarily results from destruction of uninfected erythrocytes,” *Parasitology*, vol. 119 (Pt 2), pp. 127–133, Aug. 1999.
[23] N. J. White, “Malaria parasite clearance,” *Malar J*, vol. 16, p. 88, Feb. 2017.
[24] X. Y. Yam, M. Niang, K. G. Madnani, and P. R. Preiser, “Three Is a Crowd – New Insights into Rosetting in *Plasmodium falciparum*,” *Trends Parasitol*, vol. 33, no. 4, pp. 309–320, Apr. 2017.
[25] S. Goel *et al.*, “RIFINs are adhesins implicated in severe *Plasmodium falciparum* malaria,” *Nat Med*, vol. 21, no. 4, pp. 314–317, Apr. 2015.
[26] C. Coban, M. S. J. Lee, and K. J. Ishii, “Tissue-specific immunopathology during malaria infection,” *Nat Rev Immunol*, vol. 18, no. 4, pp. 266–278, Apr. 2018.
[27] L. H. Miller, H. C. Ackerman, X. Su, and T. E. Wellems, “Malaria biology and disease pathogenesis: insights for new treatments,” *Nat Med*, vol. 19, no. 2, pp. 156–167, 2013.
[28] D. I. Godfrey, A. P. Uldrich, J. McCluskey, J. Rossjohn, and D. B. Moody, “The burgeoning family of unconventional T cells,” *Nat Immunol*, vol. 16, no. 11, pp. 1114–1123, Nov. 2015.
[29] M. S. Davey *et al.*, “Clonal selection in the human Vδ1 T cell repertoire indicates γδ TCR-dependent adaptive immune surveillance,” *Nat Commun*, vol. 8, Mar. 2017.
[30] M. S. Davey *et al.*, “The human Vδ2 + T-cell compartment comprises distinct innate-like Vγ9 + and adaptive Vγ9 - subsets,” *Nat Commun*, vol. 9, no. 1, p. 1760, May 2018.
[31] H. Saito, D. M. Kranz, Y. Takagaki, A. C. Hayday, H. N. Eisen, and S. Tonegawa, “Complete primary structure of a heterodimeric T-cell receptor deduced from cDNA sequences,” *Nature*, vol. 309, no. 5971, pp. 757–762, Jul. 1984.
[32] Y. Chien, M. Iwashima, K. B. Kaplan, J. F. Elliott, and M. M. Davis, “A new T-cell receptor gene located within the alpha locus and expressed early in T-cell differentiation,” *Nature*, vol. 327, no. 6124, pp. 677–682, Jun. 1987.
[33] P. Vantourout and A. Hayday, “Six-of-the-best: unique contributions of γδ T cells to immunology,” *Nat Rev Immunol*, vol. 13, no. 2, pp. 88–100, Feb. 2013.
[34] E. P. Rock, P. R. Sibbald, M. M. Davis, and Y. H. Chien, “CDR3 length in antigen-specific immune receptors.,” *J Exp Med*, vol. 179, no. 1, pp. 323–328, Jan. 1994.
[35] X. Zeng *et al.*, “γδ T Cells Recognize a Microbial Encoded B Cell Antigen to Initiate a Rapid Antigen-Specific Interleukin-17 Response,” *Immunity*, vol. 37, no. 3, pp. 524–534, Sep. 2012.
[36] A. L. Smith and A. C. Hayday, “An αβ T-cell-independent immunoprotective response towards gut coccidia is supported by γδ cells,” *Immunology*, vol. 101, no. 3, pp. 325–332, Nov. 2000.
[37] D. M. Asarnow, T. Goodman, L. LeFrancois, and J. P. Allison, “Distinct antigen receptor repertoires of two classes of murine epithelium-associated T cells,” *Nature*, vol. 341, no. 6237, pp. 60–62, Sep. 1989.
[38] S. Itohara *et al.*, “Homing of a γδ thymocyte subset with homogeneous T-cell receptors to mucosal epithelia,” *Nature*, vol. 343, no. 6260, pp. 754–757, Feb. 1990.
[39] D. M. Asarnow, W. A. Kuziel, M. Bonyhad, R. E. Tigelaar, P. W. Tucker, and J. P. Allison, “Limited diversity of γδ antigen receptor genes of thy-1+ dendritic epidermal cells,” *Cell*, vol. 55, no. 5, pp. 837–847, Dec. 1988.
[40] R. Di Marco Barros *et al.*, “Epithelia Use Butyrophilin-like Molecules to Shape Organ-Specific γδ T Cell Compartments,” *Cell*, vol. 167, no. 1, pp. 203-218.e17, Sep. 2016.

[41] Y. Tanaka, C. T. Morita, Y. Tanaka, E. Nieves, M. B. Brenner, and B. R. Bloom, "Natural and synthetic non-peptide antigens recognized by human γδ T cells," *Nature*, vol. 375, no. 6527, pp. 155–158, May 1995.
[42] C. T. Morita, C. Jin, G. Sarikonda, and H. Wang, "Nonpeptide antigens, presentation mechanisms, and immunological memory of human Vγ2Vδ2 T cells: discriminating friend from foe through the recognition of prenyl pyrophosphate antigens," *Immunological Reviews*, vol. 215, no. 1, pp. 59–76, Feb. 2007.
[43] M. Hintz *et al.*, "Identification of (E)-4-hydroxy-3-methyl-but-2-enyl pyrophosphate as a major activator for human γδ T cells in Escherichia coli," *FEBS Letters*, vol. 509, no. 2, pp. 317–322, Dec. 2001.
[44] H.-J. Gober, M. Kistowska, L. Angman, P. Jenö, L. Mori, and G. De Libero, "Human T Cell Receptor γδ Cells Recognize Endogenous Mevalonate Metabolites in Tumor Cells," *J Exp Med*, vol. 197, no. 2, pp. 163–168, Jan. 2003.
[45] J. F. Bukowski, C. T. Morita, Y. Tanaka, B. R. Bloom, M. B. Brenner, and H. Band, "V gamma 2V delta 2 TCR-dependent recognition of non-peptide antigens and Daudi cells analyzed by TCR gene transfer.," *J Immunol*, vol. 154, no. 3, pp. 998–1006, Feb. 1995.
[46] A. Sandstrom *et al.*, "The Intracellular B30.2 Domain of Butyrophilin 3A1 Binds Phosphoantigens to Mediate Activation of Human Vγ9Vδ2 T Cells," *Immunity*, vol. 40, no. 4, pp. 490–500, Apr. 2014.
[47] L. Boutin and E. Scotet, "Towards Deciphering the Hidden Mechanisms That Contribute to the Antigenic Activation Process of Human Vγ9Vδ2 T Cells," *Front Immunol*, vol. 9, Apr. 2018.
[48] M. S. Davey, C. R. Willcox, A. T. Baker, S. Hunter, and B. E. Willcox, "Recasting Human Vδ1 Lymphocytes in an Adaptive Role," *Trends Immunol*, Apr. 2018.
[49] A. Alejenef, A. Pachnio, M. Halawi, S. E. Christmas, P. a. H. Moss, and N. Khan, "Cytomegalovirus drives Vδ2neg γδ T cell inflation in many healthy virus carriers with increasing age," *Clin Exp Immunol*, vol. 176, no. 3, pp. 418–428, Feb. 2014.
[50] A. Knight *et al.*, "The role of Vδ2-negative γδ T cells during cytomegalovirus reactivation in recipients of allogeneic stem cell transplantation," *Blood*, vol. 116, no. 12, pp. 2164–2172, Sep. 2010.
[51] F. Halary *et al.*, "Shared reactivity of Vδ2neg γδ T cells against cytomegalovirus-infected cells and tumor intestinal epithelial cells," *J Exp Med*, vol. 201, no. 10, pp. 1567–1578, May 2005.
[52] C. T. Morita, C. M. Parker, M. B. Brenner, and H. Band, "TCR usage and functional capabilities of human γδ T cells at birth," *J Immunol*, vol. 153, no. 9, pp. 3979–3988, Nov. 1994.
[53] K. Deusch, F. Lüling, K. Reich, M. Classen, H. Wagner, and K. Pfeffer, "A major fraction of human intraepithelial lymphocytes simultaneously expresses the γ/δ T cell receptor, the CD8 accessory molecule and preferentially uses the Vδ1 gene segment," *Eur. J. Immunol.*, vol. 21, no. 4, pp. 1053–1059, Apr. 1991.
[54] S. Ravens *et al.*, "Human γδ T cells are quickly reconstituted after stem-cell transplantation and show adaptive clonal expansion in response to viral infection," *Nat Immunol*, vol. 18, no. 4, pp. 393–401, Apr. 2017.
[55] C. R. Willcox *et al.*, "Cytomegalovirus and tumor stress surveillance by binding of a human γδ T cell antigen receptor to endothelial protein C receptor," *Nat Immunol*, vol. 13, no. 9, p. 872, Sep. 2012.
[56] Y. Chien, C. Meyer, and M. Bonneville, "γδ T Cells: First Line of Defense and Beyond," *Annu Rev Immunol*, vol. 32, no. 1, pp. 121–155, Mar. 2014.
[57] O. Patel *et al.*, "Recognition of vitamin B metabolites by mucosal-associated invariant T cells," *Nat Commun*, vol. 4, Jul. 2013.

[58] M. Lepore *et al.*, “Parallel T-cell cloning and deep sequencing of human MAIT cells reveal stable oligoclonal TCRβ repertoire,” *Nat Commun*, vol. 5, May 2014.
[59] F. Tilloy *et al.*, “An Invariant T Cell Receptor α Chain Defines a Novel TAP-independent Major Histocompatibility Complex Class Ib–restricted α/β T Cell Subpopulation in Mammals,” *J Exp Med*, vol. 189, no. 12, pp. 1907–1921, Jun. 1999.
[60] E. Treiner *et al.*, “Selection of evolutionarily conserved mucosal-associated invariant T cells by MR1,” *Nature*, vol. 422, no. 6928, pp. 164–169, Mar. 2003.
[61] L. Kjer-Nielsen *et al.*, “MR1 presents microbial vitamin B metabolites to MAIT cells,” *Nature*, vol. 491, no. 7426, pp. 717–723, Nov. 2012.
[62] A. J. Corbett *et al.*, “T-cell activation by transitory neo-antigens derived from distinct microbial pathways,” *Nature*, vol. 509, no. 7500, pp. 361–365, May 2014.
[63] A. N. Keller *et al.*, “Drugs and drug-like molecules can modulate the function of mucosal-associated invariant T cells,” *Nat Immunol*, vol. 18, no. 4, pp. 402–411, Apr. 2017.
[64] E. W. Meermeier *et al.*, “Human TRAV1-2-negative MR1-restricted T cells detect S. pyogenes and alternatives to MAIT riboflavin-based antigens,” *Nat Commun*, vol. 7, p. 12506, Aug. 2016.
[65] M. Lepore *et al.*, “Functionally diverse human T cells recognize non-microbial antigens presented by MR1,” *eLife*, vol. 6, p. e24476, May 2017.
[66] L. Le Bourhis *et al.*, “Antimicrobial activity of mucosal-associated invariant T cells,” *Nat Immunol*, vol. 11, no. 8, pp. 701–708, Aug. 2010.
[67] J. R. Fergusson *et al.*, “CD161 Defines a Transcriptional and Functional Phenotype across Distinct Human T Cell Lineages,” *Cell Reports*, vol. 9, no. 3, pp. 1075–1088, Nov. 2014.
[68] J. E. Ussher *et al.*, “CD161++CD8+T cells, including the MAIT cell subset, are specifically activated by IL-12+IL-18 in a TCR-independent manner,” *Eur. J. Immunol.*, vol. 44, no. 1, pp. 195–203, 2014.
[69] T. M. Tran *et al.*, “An Intensive Longitudinal Cohort Study of Malian Children and Adults Reveals No Evidence of Acquired Immunity to *Plasmodium falciparum* Infection,” *Clin Infect Dis*, vol. 57, no. 1, pp. 40–47, Jul. 2013.
[70] P. D. Crompton *et al.*, “Malaria Immunity in Man and Mosquito: Insights into Unsolved Mysteries of a Deadly Infectious Disease,” *Annu Rev Immunol*, vol. 32, no. 1, pp. 157–187, 2014.
[71] H. B. da Silva *et al.*, “Early skin immunological disturbance after Plasmodium-infected mosquito bites,” *Cell Immunol*, vol. 277, no. 1, pp. 22–32, May 2012.
[72] I. Usynin, C. Klotz, and U. Frevert, “Malaria circumsporozoite protein inhibits the respiratory burst in Kupffer cells,” *Cell Microbiol*, vol. 9, no. 11, pp. 2610–2628, Nov. 2007.
[73] P. Liehl *et al.*, “Host-cell sensors for Plasmodium activate innate immunity against liver-stage infection,” *Nat Med*, vol. 20, no. 1, pp. 47–53, Jan. 2014.
[74] J. E. Egan *et al.*, “Humoral Immune Responses in Volunteers Immunized with Irradiated *Plasmodium falciparum* Sporozoites,” *Am J Trop Med Hyg*, vol. 49, no. 2, pp. 166–173, Aug. 1993.
[75] D. Herrington *et al.*, “Successful Immunization of Humans with Irradiated Malaria Sporozoites: Humoral and Cellular Responses of the Protected Individuals,” *Am J Trop Med Hyg*, vol. 45, no. 5, pp. 539–547, Nov. 1991.
[76] R. A. Seder *et al.*, “Protection Against Malaria by Intravenous Immunization with a Nonreplicating Sporozoite Vaccine,” *Science*, vol. 341, no. 6152, pp. 1359–1365, Sep. 2013.

[77] L. Schofield, J. Villaquiran, A. Ferreira, H. Schellekens, R. Nussenzweig, and V. Nussenzweig, “γ Interferon, CD8+ T cells and antibodies required for immunity to malaria sporozoites,” *Nature*, vol. 330, no. 6149, pp. 664–666, Dec. 1987.
[78] J. E. Epstein *et al.*, “Live Attenuated Malaria Vaccine Designed to Protect Through Hepatic CD8+ T Cell Immunity,” *Science*, vol. 334, no. 6055, pp. 475–480, Oct. 2011.
[79] S. Chakravarty, I. A. Cockburn, S. Kuk, M. G. Overstreet, J. B. Sacci, and F. Zavala, “CD8+ T lymphocytes protective against malaria liver stages are primed in skin-draining lymph nodes,” *Nat Med*, vol. 13, no. 9, pp. 1035–1041, Sep. 2007.
[80] I. A. Cockburn *et al.*, “Dendritic Cells and Hepatocytes Use Distinct Pathways to Process Protective Antigen from Plasmodium in vivo,” *PLOS Pathogens*, vol. 7, no. 3, p. e1001318, Mar. 2011.
[81] M. M. Mota *et al.*, “Migration of Plasmodium Sporozoites Through Cells Before Infection,” *Science*, vol. 291, no. 5501, pp. 141–144, Jan. 2001.
[82] M. G. Overstreet, I. A. Cockburn, Y.-C. Chen, and F. Zavala, “Protective CD8+ T cells against Plasmodium liver stages: immunobiology of an ‘unnatural’ immune response,” *Immunological Reviews*, vol. 225, no. 1, pp. 272–283, Oct. 2008.
[83] N. W. Schmidt, N. S. Butler, V. P. Badovinac, and J. T. Harty, “Extreme CD8 T Cell Requirements for Anti-Malarial Liver-Stage Immunity following Immunization with Radiation Attenuated Sporozoites,” *PLOS Pathogens*, vol. 6, no. 7, p. e1000998, Jul. 2010.
[84] E. M. Riley and V. A. Stewart, “Immune mechanisms in malaria: new insights in vaccine development,” *Nat Med*, vol. 19, no. 2, pp. 168–178, Feb. 2013.
[85] M. T. White *et al.*, “Immunogenicity of the RTS,S/AS01 malaria vaccine and implications for duration of vaccine efficacy: secondary analysis of data from a phase 3 randomised controlled trial,” *Lancet Infect Dis*, vol. 15, no. 12, pp. 1450–1458, Dec. 2015.
[86] I. J. Amanna, N. E. Carlson, and M. K. Slifka, “Duration of Humoral Immunity to Common Viral and Vaccine Antigens,” *N Engl J Med*, p. 13, Nov. 2007.
[87] J. M. Lumsden *et al.*, “Protective Immunity Induced with the RTS,S/AS Vaccine Is Associated with IL-2 and TNF-α Producing Effector and Central Memory CD4+ T Cells,” *PLOS ONE*, vol. 6, no. 7, p. e20775, Nov. 2011.
[88] P. Sun *et al.*, “Protective Immunity Induced with Malaria Vaccine, RTS,S, Is Linked to *Plasmodium falciparum* Circumsporozoite Protein-Specific CD4+ and CD8+ T Cells Producing IFN-γ,” *J Immunol*, vol. 171, no. 12, pp. 6961–6967, Dec. 2003.
[89] A. Olotu *et al.*, “Circumsporozoite-Specific T Cell Responses in Children Vaccinated with RTS,S/AS01E and Protection against P falciparum Clinical Malaria,” *PLOS ONE*, vol. 6, no. 10, p. e25786, Jun. 2011.
[90] F. M. Ndungu *et al.*, “A Statistical Interaction between Circumsporozoite Protein-Specific T Cell and Antibody Responses and Risk of Clinical Malaria Episodes following Vaccination with RTS,S/AS01E,” *PLOS ONE*, vol. 7, no. 12, p. e52870, Dec. 2012.
[91] A. Barbosa *et al.*, “*Plasmodium falciparum*-Specific Cellular Immune Responses after Immunization with the RTS,S/AS02D Candidate Malaria Vaccine in Infants Living in an Area of High Endemicity in Mozambique,” *Infect. Immun.*, vol. 77, no. 10, pp. 4502–4509, Oct. 2009.
[92] S. A. Plotkin, “Complex Correlates of Protection After Vaccination,” *Clinical Infectious Diseases*, vol. 56, no. 10, pp. 1458–1465, May 2013.
[93] D. Perez-Mazliah and J. Langhorne, “CD4 T-Cell Subsets in Malaria: TH1/TH2 Revisited,” *Front Immunol*, vol. 5, Jan. 2015.

[94] M. Guenot *et al.*, “Phosphoantigen Burst upon *Plasmodium falciparum* Schizont Rupture Can Distantly Activate Vγ9Vδ2 T Cells,” *Infect. Immun.*, vol. 83, no. 10, pp. 3816–3824, Oct. 2015.
[95] K. Marsh and S. Kinyanjui, “Immune effector mechanisms in malaria,” *Parasite Immunol*, vol. 28, no. 1–2, pp. 51–60, Dec. 2005.
[96] K. E. Lyke *et al.*, “Serum Levels of the Proinflammatory Cytokines Interleukin-1 Beta (IL-1β), IL-6, IL-8, IL-10, Tumor Necrosis Factor Alpha, and IL-12(p70) in Malian Children with Severe *Plasmodium falciparum* Malaria and Matched Uncomplicated Malaria or Healthy Controls,” *Infect. Immun.*, vol. 72, no. 10, pp. 5630–5637, Oct. 2004.
[97] M. Walther *et al.*, “Innate Immune Responses to Human Malaria: Heterogeneous Cytokine Responses to Blood-Stage *Plasmodium falciparum* Correlate with Parasitological and Clinical Outcomes,” *J Immunol*, vol. 177, no. 8, pp. 5736–5745, Oct. 2006.
[98] R. T. Gazzinelli, P. Kalantari, K. A. Fitzgerald, and D. T. Golenbock, “Innate sensing of malaria parasites,” *Nat Rev Immunol*, vol. 14, no. 11, pp. 744–757, Nov. 2014.
[99] G. Krishnegowda *et al.*, “Induction of Proinflammatory Responses in Macrophages by the Glycosylphosphatidylinositols of *Plasmodium falciparum*,” *J. Biol. Chem.*, vol. 280, no. 9, pp. 8606–8616, Mar. 2005.
[100] L. Turner *et al.*, “Severe malaria is associated with parasite binding to endothelial protein C receptor,” *Nature*, vol. 498, no. 7455, pp. 502–505, Jun. 2013.
[101] J. Langhorne, S. Gillard, B. Simon, S. Slade, and K. Eichmann, “Frequencies of CD4+ T cells reactive with *Plasmodium chabaudi chabaudi*: distinct response kinetics for cells with Th1 and Th2 characteristics during infection,” *Int. Immunol.*, vol. 1, no. 4, pp. 416–424, 1989.
[102] H. Qi, “T follicular helper cells in space-time,” *Nat Rev Immunol*, vol. 16, no. 10, pp. 612–625, Oktober 2016.
[103] A. Horowitz, K. C. Newman, J. H. Evans, D. S. Korbel, D. M. Davis, and E. M. Riley, “Cross-Talk between T Cells and NK Cells Generates Rapid Effector Responses to *Plasmodium falciparum*-Infected Erythrocytes,” *J Immunol*, vol. 184, no. 11, pp. 6043–6052, Jun. 2010.
[104] D. S. Hansen, M. C. D’Ombrain, and L. Schofield, “The role of leukocytes bearing Natural Killer Complex receptors and Killer Immunoglobulin-like Receptors in the immunology of malaria,” *Curr Opin Immunol*, vol. 19, no. 4, pp. 416–423, Aug. 2007.
[105] M. C. D’Ombrain, D. S. Hansen, K. M. Simpson, and L. Schofield, “γδ-T cells expressing NK receptors predominate over NK cells and conventional T cells in the innate IFN-γ response to *Plasmodium falciparum* malaria,” *Eur. J. Immunol.*, vol. 37, no. 7, pp. 1864–1873, Jul. 2007.
[106] S. Cohen, I. A. McGREGOR, and S. Carrington, “Gamma-Globulin and Acquired Immunity to Human Malaria,” *Nature*, vol. 192, no. 4804, pp. 733–737, Nov. 1961.
[107] A. Scherf, J. J. Lopez-Rubio, and L. Riviere, “Antigenic Variation in *Plasmodium falciparum*,” *Annu Rev Microbiol*, vol. 62, no. 1, pp. 445–470, 2008.
[108] S. Portugal, S. K. Pierce, and P. D. Crompton, “Young Lives Lost as B Cells Falter: What We Are Learning About Antibody Responses in Malaria,” *J Immunol*, vol. 190, no. 7, pp. 3039–3046, Apr. 2013.
[109] I. Zaidi *et al.*, “γδ T Cells Are Required for the Induction of Sterile Immunity during Irradiated Sporozoite Vaccinations,” *J Immunol*, vol. 199, no. 11, pp. 3781–3788, Dec. 2017.

[110] D. I. Stanisic *et al.*, "γδ T cells and CD14+ Monocytes Are Predominant Cellular Sources of Cytokines and Chemokines Associated With Severe Malaria," *J Infect Dis*, vol. 210, no. 2, pp. 295–305, Jul. 2014.
[111] J. L. Miller, B. K. Sack, M. Baldwin, A. M. Vaughan, and S. H. I. Kappe, "Interferon-Mediated Innate Immune Responses against Malaria Parasite Liver Stages," *Cell Reports*, vol. 7, no. 2, pp. 436–447, Apr. 2014.
[112] C. Roussilhon, M. Agrapart, P. Guglielmi, A. Bensussan, P. Brasseur, and J. J. Ballet, "Human TcRγδ+ lymphocyte response on primary exposure to *Plasmodium falciparum*," *Clin Exp Immunol*, vol. 95, no. 1, pp. 91–97, Jan. 1994.
[113] M. Ho *et al.*, "Polyclonal expansion of peripheral gamma delta T cells in human *Plasmodium falciparum* malaria.," *Infect. Immun.*, vol. 62, no. 3, pp. 855–862, Mar. 1994.
[114] P. Jagannathan *et al.*, "Loss and dysfunction of Vδ2+ γδ T cells are associated with clinical tolerance to malaria," *Sci Transl Med*, vol. 6, no. 251, pp. 251ra117-251ra117, Aug. 2014.
[115] C. Behr and P. Dubois, "Preferential expansion of V gamma 9 V delta 2 T cells following stimulation of peripheral blood lymphocytes with extracts of *Plasmodium falciparum*," *Int. Immunol.*, vol. 4, no. 3, pp. 361–366, Mar. 1992.
[116] C. Behr *et al.*, "*Plasmodium falciparum* stimuli for human gammadelta T cells are related to phosphorylated antigens of mycobacteria.," *Infect Immun*, vol. 64, no. 8, pp. 2892–2896, Aug. 1996.
[117] G. Costa *et al.*, "Control of *Plasmodium falciparum* erythrocytic cycle: γδ T cells target the red blood cell–invasive merozoites," *Blood*, vol. 118, no. 26, pp. 6952–6962, Dec. 2011.
[118] D. F. Angelini *et al.*, "FcγRIII discriminates between 2 subsets of Vγ9Vδ2 effector cells with different responses and activation pathways," *Blood*, vol. 104, no. 6, pp. 1801–1807, Sep. 2004.
[119] L. Hviid *et al.*, "High frequency of circulating γδ T cells with dominance of the Vδ1 subset in a healthy population," *Int. Immunol.*, vol. 12, no. 6, pp. 797–805, Jun. 2000.
[120] L. Hviid *et al.*, "Perturbation and Proinflammatory Type Activation of Vδ1+ γδ T Cells in African Children with *Plasmodium falciparum* Malaria," *Infect. Immun.*, vol. 69, no. 5, pp. 3190–3196, May 2001.
[121] M. Mpina *et al.*, "Controlled Human Malaria Infection Leads to Long-Lasting Changes in Innate and Innate-like Lymphocyte Populations," *J Immunol*, vol. 199, no. 1, pp. 107–118, Jul. 2017.
[122] M. Kanehisa and S. Goto, "KEGG: Kyoto Encyclopedia of Genes and Genomes," *Nucleic Acids Res*, vol. 28, no. 1, pp. 27–30, Jan. 2000.
[123] C. H. Coelho, J. Y. A. Doritchamou, I. Zaidi, and P. E. Duffy, "Advances in malaria vaccine development: report from the 2017 malaria vaccine symposium," Nature Publishing Group, Report, Nov. 2017.
[124] R. Gosling and L. von Seidlein, "The Future of the RTS,S/AS01 Malaria Vaccine: An Alternative Development Plan," *PLOS Med*, vol. 13, no. 4, p. e1001994, Dec. 2016.
[125] E. A. Ashley, A. Pyae Phyo, and C. J. Woodrow, "Malaria," *The Lancet*, vol. 391, no. 10130, pp. 1608–1621, Apr. 2018.
[126] J. Cohen, V. Nussenzweig, J. Vekemans, and A. Leach, "From the circumsporozoite protein to the RTS,S/AS candidate vaccine," *Human Vaccines*, vol. 6, no. 1, pp. 90–96, Jan. 2010.
[127] A. M. Didierlaurent, B. Laupèze, A. D. Pasquale, N. Hergli, C. Collignon, and N. Garçon, "Adjuvant system AS01: helping to overcome the challenges of modern vaccines," *Expert Review of Vaccines*, vol. 16, no. 1, pp. 55–63, Jan. 2017.

[128] RTS,S Clinical Trials Partnership, "Efficacy and safety of RTS,S/AS01 malaria vaccine with or without a booster dose in infants and children in Africa: final results of a phase 3, individually randomised, controlled trial," *The Lancet*, vol. 386, no. 9988, pp. 31–45, Jul. 2015.
[129] T. RTS,S Clinical Trials Partnership (2014), "Efficacy and Safety of the RTS,S/AS01 Malaria Vaccine during 18 Months after Vaccination: A Phase 3 Randomized, Controlled Trial in Children and Young Infants at 11 African Sites," *PLOS Med*, vol. 11, no. 7, p. e1001685, Jul. 2014.
[130] K. S. Vannice, G. V. Brown, B. D. Akanmori, and V. S. Moorthy, "MALVAC 2012 scientific forum: accelerating development of second-generation malaria vaccines," *Malar J*, vol. 11, p. 372, Nov. 2012.
[131] D. F. Clyde, H. Most, V. C. McCarthy, and J. P. Vanderberg, "Immunization of man against sporozite-induced falciparum malaria," *Am. J. Med. Sci.*, vol. 266, no. 3, pp. 169–177, Sep. 1973.
[132] K. H. Rieckmann, P. E. Carson, R. L. Beaudoin, J. S. Cassells, and K. W. Sell, "Sporozoite induced immunity in man against an ethiopian strain of *Plasmodium falciparum*," *Trans R Soc Trop Med Hyg*, vol. 68, no. 3, pp. 258–259, Jan. 1974.
[133] S. L. Hoffman *et al.*, "Development of a metabolically active, non-replicating sporozoite vaccine to prevent *Plasmodium falciparum* malaria," *Human Vaccines*, vol. 6, no. 1, pp. 97–106, Jan. 2010.
[134] A. Hamad *et al.*, "Advancing Global Health through Development and Clinical Trials Partnerships: A Randomized, Placebo-Controlled, Double-Blind Assessment of Safety, Tolerability, and Immunogenicity of PfSPZ Vaccine for Malaria in Healthy Equatoguinean Men," *Am J Trop Med Hyg*, vol. 98, no. 1, pp. 308–318, Jan. 2018.
[135] M. S. Sissoko *et al.*, "Safety and efficacy of PfSPZ Vaccine against *Plasmodium falciparum* via direct venous inoculation in healthy malaria-exposed adults in Mali: a randomised, double-blind phase 1 trial," *Lancet Infect Dis*, vol. 17, no. 5, pp. 498–509, May 2017.
[136] N. S. Butler, N. W. Schmidt, A. M. Vaughan, A. S. Aly, S. H. I. Kappe, and J. T. Harty, "Superior Antimalarial Immunity after Vaccination with Late Liver Stage-Arresting Genetically Attenuated Parasites," *Cell Host & Microbe*, vol. 9, no. 6, pp. 451–462, Jun. 2011.
[137] T. L. Richie *et al.*, "Progress with *Plasmodium falciparum* sporozoite (PfSPZ)-based malaria vaccines," *Vaccine*, vol. 33, no. 52, pp. 7452–7461, Dec. 2015.
[138] A. Yayon, J. A. Vande Waa, M. Yayon, T. G. Geary, and J. B. Jensen, "Stage-dependent effects of chloroquine on *Plasmodium falciparum* in vitro," *J. Protozool.*, vol. 30, no. 4, pp. 642–647, Nov. 1983.
[139] R. L. Beaudoin, C. P. A. Strome, F. Mitchell, and T. A. Tubergen, "Plasmodium berghei: Immunization of mice against the ANKA strain using the unaltered sporozoite as an antigen," *Exp Parasitol.*, vol. 42, no. 1, pp. 1–5, Jun. 1977.
[140] M. Roestenberg *et al.*, "Protection against a Malaria Challenge by Sporozoite Inoculation," *N Engl J Med*, vol. 361, no. 5, pp. 468–477, Jul. 2009.
[141] E. M. Bijker *et al.*, "Protection against malaria after immunization by chloroquine prophylaxis and sporozoites is mediated by preerythrocytic immunity," *PNAS*, vol. 110, no. 19, pp. 7862–7867, May 2013.
[142] B. Mordmüller *et al.*, "Sterile protection against human malaria by chemoattenuated PfSPZ vaccine," *Nature*, vol. 542, no. 7642, pp. 445–449, Feb. 2017.
[143] A.-K. Mueller *et al.*, "Plasmodium liver stage developmental arrest by depletion of a protein at the parasite–host interface," *PNAS*, vol. 102, no. 8, pp. 3022–3027, Feb. 2005.

[144] A.-K. Mueller, M. Labaied, S. H. I. Kappe, and K. Matuschewski, “Genetically modified *Plasmodium* parasites as a protective experimental malaria vaccine,” *Nature*, vol. 433, no. 7022, pp. 164–167, Jan. 2005.
[145] M. Spring *et al.*, “First-in-human evaluation of genetically attenuated *Plasmodium falciparum* sporozoites administered by bite of Anopheles mosquitoes to adult volunteers,” *Vaccine*, vol. 31, no. 43, pp. 4975–4983, Oktober 2013.
[146] S. A. Mikolajczak *et al.*, “A Next-generation Genetically Attenuated *Plasmodium falciparum* Parasite Created by Triple Gene Deletion,” *Molecular Therapy*, vol. 22, no. 9, pp. 1707–1715, Sep. 2014.
[147] J. G. Kublin *et al.*, “Complete attenuation of genetically engineered *Plasmodium falciparum* sporozoites in human subjects,” *Sci Transl Med*, vol. 9, no. 371, p. eaad9099, Jan. 2017.
[148] G. Snounou and J.-L. Pérignon, “Chapter Six - Malariotherapy – Insanity at the Service of Malariology,” *Advances in Parasitology*, vol. 81, pp. 223–255, Jan. 2013.
[149] M. B. Nierengarten, “Malariotherapy to treat HIV patients?,” *Lancet Infect Dis*, vol. 3, no. 6, p. 321, Jun. 2003.
[150] D. I. Stanisic, J. S. McCarthy, and M. F. Good, “Controlled Human Malaria Infection: Applications, Advances, and Challenges,” *Infect. Immun.*, vol. 86, no. 1, pp. e00479-17, Jan. 2018.
[151] R. W. Sauerwein, M. Roestenberg, and V. S. Moorthy, “Experimental human challenge infections can accelerate clinical malaria vaccine development,” *Nat Rev Immunol*, vol. 11, no. 1, pp. 57–64, Jan. 2011.
[152] M. Roestenberg *et al.*, “Controlled Human Malaria Infections by Intradermal Injection of Cryopreserved *Plasmodium falciparum* Sporozoites,” *Am J Trop Med Hyg*, vol. 88, no. 1, pp. 5–13, Jan. 2013.
[153] S. H. Sheehy *et al.*, “Optimising Controlled Human Malaria Infection Studies Using Cryopreserved P. falciparum Parasites Administered by Needle and Syringe,” *PLOS ONE*, vol. 8, no. 6, p. e65960, Jun. 2013.
[154] S. Shekalaghe *et al.*, “Controlled Human Malaria Infection of Tanzanians by Intradermal Injection of Aseptic, Purified, Cryopreserved *Plasmodium falciparum* Sporozoites,” *Am J Trop Med Hyg*, vol. 91, no. 3, pp. 471–480, Sep. 2014.
[155] G. P. Gómez-Pérez *et al.*, “Controlled human malaria infection by intramuscular and direct venous inoculation of cryopreserved *Plasmodium falciparum* sporozoites in malaria-naïve volunteers: effect of injection volume and dose on infectivity rates,” *Malar J*, vol. 14, p. 306, Aug. 2015.
[156] B. Mordmüller *et al.*, “Direct venous inoculation of *Plasmodium falciparum* sporozoites for controlled human malaria infection: a dose-finding trial in two centres,” *Malar J*, vol. 14, Mar. 2015.
[157] P. S. Gomes, J. Bhardwaj, J. Rivera-Correa, C. G. Freire-De-Lima, and A. Morrot, “Immune Escape Strategies of Malaria Parasites,” *Front. Microbiol.*, vol. 7, 2016.
[158] D. Ansong *et al.*, “T Cell Responses to the RTS,S/AS01E and RTS,S/AS02D Malaria Candidate Vaccines Administered According to Different Schedules to Ghanaian Children,” *PLOS ONE*, vol. 6, no. 4, p. e18891, Apr. 2011.
[159] S. T. Agnandji *et al.*, “Induction of *Plasmodium falciparum*-Specific CD4+ T Cells and Memory B Cells in Gabonese Children Vaccinated with RTS,S/AS01E and RTS,S/AS02D,” *PLOS ONE*, vol. 6, no. 4, Apr. 2011.
[160] R. Ettinger, S. Kuchen, and P. E. Lipsky, “The role of IL-21 in regulating B-cell function in health and disease,” *Immunol Rev*, vol. 223, no. 1, pp. 60–86, Jul. 2008.

[161] R. A. Seder, P. A. Darrah, and M. Roederer, “T-cell quality in memory and protection: implications for vaccine design,” *Nat Rev Immunol*, vol. 8, no. 4, pp. 247–258, Apr. 2008.
[162] D. G. Heppner *et al.*, “Towards an RTS,S-based, multi-stage, multi-antigen vaccine against falciparum malaria: progress at the Walter Reed Army Institute of Research,” *Vaccine*, vol. 23, no. 17, pp. 2243–2250, Mar. 2005.
[163] J. J. A. Calis *et al.*, “Properties of MHC Class I Presented Peptides That Enhance Immunogenicity,” *PLoS Comput Biol*, vol. 9, no. 10, p. e1003266, Oct. 2013.
[164] J. E. Epstein *et al.*, “Protection against *Plasmodium falciparum* malaria by PfSPZ Vaccine,” *JCI Insight*, vol. 2, no. 1, Jan. 2017.
[165] T. R. Kollmann, “Variation between Populations in the Innate Immune Response to Vaccine Adjuvants,” *Front Immunol*, vol. 4, Apr. 2013.
[166] S. S. Struik and E. M. Riley, “Does malaria suffer from lack of memory?,” *Immunological Reviews*, vol. 201, no. 1, pp. 268–290, Sep. 2004.
[167] J. T. Harty and V. P. Badovinac, “Shaping and reshaping $CD8^+$ T-cell memory,” *Nat Rev Immunol*, vol. 8, no. 2, pp. 107–119, Feb. 2008.
[168] E. Muyanja *et al.*, “Immune activation alters cellular and humoral responses to yellow fever 17D vaccine,” *J Clin Invest*, vol. 124, no. 7, pp. 3147–3158, Jul. 2014.
[169] E. Gotuzzo *et al.*, “Safety, immunogenicity, and excretion pattern of single-dose live oral cholera vaccine CVD 103-HgR in Peruvian adults of high and low socioeconomic levels.,” *Infect. Immun.*, vol. 61, no. 9, pp. 3994–3997, Sep. 1993.
[170] S. N. Waggoner, M. Cornberg, L. K. Selin, and R. M. Welsh, “Natural killer cells act as rheostats modulating antiviral T cells,” *Nature*, vol. 481, no. 7381, pp. 394–398, Jan. 2012.
[171] D. Elias, H. Akuffo, A. Pawlowski, M. Haile, T. Schön, and S. Britton, “Schistosoma mansoni infection reduces the protective efficacy of BCG vaccination against virulent Mycobacterium tuberculosis,” *Vaccine*, vol. 23, no. 11, pp. 1326–1334, Feb. 2005.
[172] I. G. Ovsyannikova and G. A. Poland, “Vaccinomics: Current Findings, Challenges and Novel Approaches for Vaccine Development,” *AAPS J*, vol. 13, no. 3, pp. 438–444, Jun. 2011.
[173] B. Yilmaz *et al.*, “Gut Microbiota Elicits a Protective Immune Response against Malaria Transmission,” *Cell*, vol. 159, no. 6, pp. 1277–1289, Dec. 2014.
[174] T. Taniguchi *et al.*, “*Plasmodium berghei* ANKA causes intestinal malaria associated with dysbiosis,” *Scientific Reports*, vol. 5, p. 15699, Oct. 2015.
[175] P. Wilairatana, J. B. Meddings, M. Ho, S. Vannaphan, and S. Looareesuwan, “Increased gastrointestinal permeability in patients with *Plasmodium falciparum* malaria,” *Clin Infect Dis*, vol. 24, no. 3, pp. 430–435, Mar. 1997.
[176] D. A. Milner *et al.*, “Quantitative Assessment of Multiorgan Sequestration of Parasites in Fatal Pediatric Cerebral Malaria,” *J Infect Dis*, vol. 212, no. 8, pp. 1317–1321, Oct. 2015.
[177] N. F. Villarino *et al.*, “Composition of the gut microbiota modulates the severity of malaria,” *PNAS*, vol. 113, no. 8, pp. 2235–2240, Feb. 2016.
[178] S. Yooseph *et al.*, “Stool microbiota composition is associated with the prospective risk of *Plasmodium falciparum* infection,” *BMC Genom.*, vol. 16, p. 631, Aug. 2015.
[179] T. Yatsunenko *et al.*, “Human gut microbiome viewed across age and geography,” *Nature*, vol. 486, no. 7402, pp. 222–227, Jun. 2012.
[180] F. C. Hartgers and M. Yazdanbakhsh, “Co-infection of helminths and malaria: modulation of the immune responses to malaria,” *Parasite Immunol*, vol. 28, no. 10, pp. 497–506, Jul. 2006.

[181] O. Rouxel *et al.*, “Cytotoxic and regulatory roles of mucosal-associated invariant T cells in type 1 diabetes,” *Nat Immunol*, vol. 18, no. 12, pp. 1321–1331, Dec. 2017.
[182] M. Dusseaux *et al.*, “Human MAIT cells are xenobiotic-resistant, tissue-targeted, CD161hi IL-17–secreting T cells,” *Blood*, vol. 117, no. 4, pp. 1250–1259, Jan. 2011.
[183] D. L. Barber *et al.*, “Restoring function in exhausted CD8 T cells during chronic viral infection,” *Nature*, vol. 439, no. 7077, pp. 682–687, Feb. 2006.
[184] M. N. Wykes and S. R. Lewin, “Immune checkpoint blockade in infectious diseases,” *Nat Rev Immunol*, vol. 18, no. 2, pp. 91–104, Feb. 2018.
[185] S. Hunter *et al.*, “Human liver infiltrating γδ T cells are composed of clonally expanded circulating and tissue-resident populations,” *J Hepatol*, May 2018.
[186] V. Groh, A. Steinle, S. Bauer, and T. Spies, “Recognition of Stress-Induced MHC Molecules by Intestinal Epithelial γδ T Cells,” *Science*, vol. 279, no. 5357, pp. 1737–1740, Mar. 1998.
[187] X.-M. Zhang, C. Tonnelle, M.-P. Lefranc, and S. Huck, “T cell receptor γ cDNA in human fetal liver and thymus: Variable regions of γ chains are restricted to VγI or V9, due to the absence of splicing of the V10 and V11 leader intron,” *Eur. J. Immunol.*, vol. 24, no. 3, pp. 571–578, Mar. 1994.
[188] The 1000 Genomes Project Consortium, “A global reference for human genetic variation,” *Nature*, vol. 526, no. 7571, pp. 68–74, Oct. 2015.
[189] M. G. E. Network *et al.*, “Reappraisal of known malaria resistance loci in a large multicenter study,” *Nat Genet*, vol. 46, no. 11, pp. 1197–1204, Nov. 2014.
[190] J. Tan *et al.*, “A *LAIR1* insertion generates broadly reactive antibodies against malaria variant antigens,” *Nature*, vol. 529, no. 7584, p. 105, Jan. 2016.
[191] WHO, “First malaria vaccine in Africa: A potential new tool for child health and improved malaria control,” p. 4, Apr. 2018.
[192] World Health Organization, “WHO | Malaria vaccine technology roadmap,” *World Health Organization*, Nov-2013. [Online]. Available: http://www.who.int/immunization/topics/malaria/vaccine_roadmap/en/. [Accessed: 09-Jun-2018].
[193] B. C. L. van Schaijk *et al.*, “A genetically attenuated malaria vaccine candidate based on P. falciparum b9/slarp gene-deficient sporozoites,” *eLife*, vol. 3, Nov. 2017.
[194] O. G. Ademowo, O. Sodeinde, and O. Walker, “The disposition of chloroquine and its main metabolite desethylchloroquine in volunteers with and without chloroquine-induced pruritus: Evidence for decreased chloroquine metabolism in volunteers with pruritus,” *Clin Pharmacol Ther*, vol. 67, no. 3, pp. 237–241, Mar. 2000.
[195] D. E. Radley *et al.*, “East coast fever: 1. Chemoprophylactic immunization of cattle against Theileria parva (Muguga) and five theilerial strains,” *Veterinary Parasitology*, vol. 1, no. 1, pp. 35–41, Jun. 1975.
[196] M. Stoeckius *et al.*, “Simultaneous epitope and transcriptome measurement in single cells,” *Nat. Methods*, vol. 14, no. 9, pp. 865–868, Sep. 2017.
[197] V. M. Peterson *et al.*, “Multiplexed quantification of proteins and transcripts in single cells,” *Nature Biotechnology*, vol. 35, no. 10, pp. 936–939, Oct. 2017.
[198] M. Roestenberg, A. Mo, P. G. Kremsner, and M. Yazdanbakhsh, “Controlled human infections: A report from the controlled human infection models workshop, Leiden University Medical Centre 4–6 May 2016,” *Vaccine*, vol. 35, no. 51, pp. 7070–7076, Dec. 2017.
[199] D. F. Warner and V. Mizrahi, “Shortening Treatment for Tuberculosis — Back to Basics,” *N Engl J Med*, Oct. 2014.
[200] G. A. Poland, I. G. Ovsyannikova, and R. B. Kennedy, “Personalized vaccinology: A review,” *Vaccine*, Jul. 2017.